INVESTIGATING PELAGIC FISH LARVAL DISPERSAL AND ECOLOGIC CONNECTIVITY IN THE BLACK SEA USING LAGRANGIAN DRIFTER MODELING

A THESIS SUBMITTED TO
THE INSTITUTE OF MARINE SCIENCES
OF
MIDDLE EAST TECHNICAL UNIVERSITY

BY

BULUT ÇAĞDAŞ

IN PARTIAL FULFILLMENT OF THE REQUIREMENTS
FOR
THE DEGREE OF MASTER OF SCIENCE
IN
OCEANOGRAPHY

SEPTEMBER 2019

Approval of the thesis:

INVESTIGATING PELAGIC FISH LARVAL DISPERSAL AND ECOLOGIC CONNECTIVITY IN THE BLACK SEA USING LAGRANGIAN DRIFTER MODELING

Submitted by Bulut Çağdaş in partial fulfillment of the requirements for the degree of **Master of Science in Oceanography Department, Middle East Technical University** by,

Assoc. Prof. Dr. Bariş Salihoğlu
Director, **Institute of Marine Sciences** _____

Prof. Dr. Süleyman Tuğrul
Head of Department, **Oceanography, METU** _____

Assoc. Prof. Dr. Bettina Fach Salihoğlu
Supervisor, **Oceanography, METU** _____

Examining Committee Members:

Assoc. Prof. Dr. Bettina Fach Salihoğlu
Oceanography, METU _____

Assist. Prof. Dr. Ekin Akoğlu
Marine Biology and Fisheries, METU _____

Prof. Dr. Şükrü Beşiktepe
Oceanography, DEU _____

Date: 02.09.2019

I hereby declare that all information in this document has been obtained and presented in accordance with academic rules and ethical conduct. I also declare that, as required by these rules and conduct, I have fully cited and referenced all material and results that are not original to this work.

Name, Surname : Bulut Çağdaş

Signature:

ABSTRACT

INVESTIGATING PELAGIC FISH LARVAL DISPERSAL AND ECOLOGIC CONNECTIVITY IN THE BLACK SEA USING LAGRANGIAN DRIFTER MODELING

Çağdaş, Bulut
Master of Science, Oceanography
Supervisor: Assoc. Prof. Dr. Bettina Fach Salihoğlu

September 2019, 166 pages

In order to understand fish population dynamics, understanding the physical interaction of the current systems with pelagic fish larvae is necessary. Using a Black Sea circulation model output to undertake Lagrangian drifter studies embedded with a Lagrangian Flow Network the connectivity metrics; onshore transport, offshore transport, local retention and self recruitment are calculated for six different commercially important fish species in the Black Sea: anchovy (*Engraulis encrasicolus ponticus*), sprat (*Sprattus sprattus*), red mullet (*Mullus barbatus*), horse mackerel (*Trachurus mediterraneus ponticus*), bluefish (*Pomatomus saltatrix*) and turbot (*Scophthalmus maeoticus*). Simulations are taking interannual and seasonal variations as well as pelagic larval durations and spawning times of the target fish species into account. Results show that offshore transport is inversely proportional to local retention and self recruitment and that longer pelagic larval duration times effected local retention negatively. Winter season shows the lowest retention values and highest offshore transport followed closely by autumn while spring shows the highest local retention followed closely by summer with both seasons exhibiting the lowest offshore transport values. The northern part of the north western shelf, the south eastern coast of Turkey and the entrance of the Azov Sea show retention in all seasons. The eastern and western gyres show potential retention sites for spring and summer while the remaining areas were susceptible to strong transport facilitated by the rim current that is dependent on seasonal and interannual variations of the Black Sea circulation.

Keywords: Black Sea, Pelagic Larval Duration, Local Retention, Offshore Transport

ÖZ

KARADENIZDE LAGRANC PARÇACIK MODELLEMESI KULLANARAK PELAJIK BALIK LARVA DAĞILIMI VE EKOLOJIK BAĞLILIK ARAŞTIRMASI

Çağdaş, Bulut
Yüksek Lisans, Oşinografi
Tez Danışmanı: Prof. Dr. Bettina Fach Salihoğlu

Eylül 2019, 166 sayfa

Balık popülasyonu dinamiklerini anlamak için öncelikle pelajik balık larvalarının akıntı sistemleriyle olan etkileşimlerini anlamak gerekmektedir. Lagranç Akıntı Ağı'na sahip Karadeniz akıntı modeli çıktısı Lagranç parçacık çalışmaları için kullanılıp, bağlılık ölçütleri olan kıyıya doğru taşınma, açığa doğru taşınma, yerel muhafaza ve öz stoklanma, Karadeniz'in ekonomik öneme sahip altı balık türü hamsi (*Engraulis encrasicolus ponticus*), çaça (*Sprattus sprattus*), barbun (*Mullus barbatus*), istavrit (*Trachurus mediterraneus ponticus*), lüfer (*Pomatomus saltatrix*) ve kalkan (*Scophthalmus maeoticus*) için hesaplanmıştır. Yapılan simülasyonlarda yıllar farklılıklar, mevsimler arası farklılıklar ve de hedef türlerin pelajik larval süreleri ve üreme süreleri hesaba katılmıştır. Sonuçlar, açığa doğru taşınmanın yerel muhafaza ve öz stoklanma ile ters orantılı olduğunu, ve yerel muhafaza ve öz stoklanmanın daha uzun pelajik larval sürelerden olumsuz etkilendiğini göstermektedir. Kış mevsimi en düşük muhafaza değerleri ve en yüksek açığa taşınma değerlerini gösterip sonbahar değerli tarafından yakından takip edilmektedir diğer yandan bahar en yüksek yerel muhafaza değerlerini göstermekte olup yaz tarafından takip edilmektedir, bahar ve yaz mevsiminin ikisi de en düşük açığa taşıma değerlerine sahiptir. Kuzey batı kıyı bölgesinin kuzey tarafı, Türkiye'nin güneydoğu kıyısı ve Azov Denizi'nin giriş bölgesi bütün mevsimlerde muhafaza ihtimali gösterirken doğu ve batı deveranları bahar ve yaz mevsimlerinde muhafaza ihtimali göstermektedir, geriye kalan bölgeler güçlü rim aktıntısına maruz kaldığından Karadeniz'in dolaşımının mevsimsel farklılıklarına bağlı kalmaktadır.

Anahtar Kelimeler: Karadeniz, Pelajik Larva Süresi, Yerel Muhafaza, Kıyıdan Açığa Taşınma

Dedicated to my mother Deniz Çağdaş and father Hasan Çağdaş.

ACKNOWLEDGMENTS

I would like to thank my supervisor Bettina Fach Salihoğlu for her guidance and support all throughout this study, Sinan Hüsrevoğlu and Hasan Çağdaş for helping me with their coding experience and finally the people of Setüstü for their joyful friendship.

Table of Contents

Abstract vii

Öz ix

Acknowledgements xiii

Table of Contents xv

List of Tables xvii

List of Figures xix

1. Introduction 1

1.1 Physical Properties of the Black Sea 2

1.2 Commercially Important Fish Species of the Black Sea 6

1.3 Larval Dispersal and Connectivity 11

1.4 Lagrangian Flow Networks 12

2. Methods 13

2.1 Circulation Model 13

2.2 Lagrangian Particle Tracking 14

2.3 Lagrangian Flow Network 15

2.4 Statistical Analysis 17

3. Results 19

3.1 Onshore and Offshore Transport Probabilities 19

3.1.1 The Impact of Different Pelagic Larval Durations 19

3.1.2 Seasonal Variability 23

3.1.3 Interannual Variability 27

3.2 Local Retention and Self Recruitment 38

3.2.1 The Impact of Different Pelagic Larval Durations 38

3.2.2 Seasonal Variability 41

3.2.3 Interannual Variability 45

4. Discussion 61
4.1 General Transport Patterns 61
4.2 Seasonal Variability 63
4.3 Interannual Variability 66
4.4 Consequences for Fish Species 69
4.5 Modeling Studies of Marine Life in Different Seas 70
4.6 Future Work 72
5. Conclusion 73
References 77
Appendix 87
Section A: Offshore Transport Probability 87
Section B: Onshore Transport Probability 105
Section C: Local Retention 128
Section D: Self Recruitment 144

List of Tables

Table 1 Pelagic larval duration of commercially important fish in the Black Sea 11

Table 2 List of simulations undertaken in this study 15

Table 3 OFTP of 10 years and 4 seasons averaged at 5 different PLD's.....20

Table 4 OFTP of 10 years averaged for 4 seasons at 35 day PLD 24

Table 5 OFTP of 10 years averaged for 4 seasons at 70 day PLD 27

Table 6 OFTP of 10 years for January at 35 day PLD.....28

Table 7 OFTP of 10 years for January at 70 day PLD 29

Table 8 OFTP of 10 years for July at 35 day PLD 33

Table 9 OFTP of 10 years for July at 70 day PLD 34

Table 10 LR of 10 years and 4 seasons averaged at 5 different PLD's 41

Table 11 LR of 10 years averaged for 4 seasons at 35 day PLD 43

Table 12 LR of 10 years averaged for 4 seasons at 70 day PLD 44

Table 13 LR of 10 years for January at 35 day PLD 45

Table 14 LR of 10 years for January at 70 day PLD 48

Table 15 LR of 10 years for April at 35 day PLD 50

Table 16 LR of 10 years for April at 70 day PLD 51

Table 17 LR of 10 years for July at 35 day PLD.....54

Table 18 LR of 10 years for July at 70 day PLD.....55

List of Figures

Figure 1 The main features of the surface layer circulation in the Black Sea.....3

Figure 2 Anchovy spawning, feeding and wintering areas and routes 7

Figure 3 Sprat spawning, feeding and wintering areas and routes 8

Figure 4 Red mullet spawning, feeding and wintering areas and routes 9

Figure 5 Horse mackerel spawning, feeding and wintering areas and routes 10

Figure 6 Offshore Transport Probability averaged over 10 years and 4 seasons depending on different pelagic larval durations 21

Figure 7 Onshore Transport Probability averaged over 10 years and 4 seasons depending on different pelagic larval durations 22

Figure 8 Offshore Transport Probability averaged over 10 years depending on different seasons at 35 day pelagic larval duration.....25

Figure 9 Offshore Transport Probability averaged over 10 years depending on different seasons at 70 day pelagic larval duration.....26

Figure 10 January Offshore Transport Probability of 10 years at 35 day pelagic larval duration 30

Figure 11 January Offshore Transport Probability of 10 years at 70 day pelagic larval duration 31

Figure 12 July Offshore Transport Probability of 10 years at 35 day pelagic larval duration 32

Figure 13 July Offshore Transport Probability of 10 years at 70 day pelagic larval duration 36

Figure 14 Box-Whisker plots of Interannual Offshore Transport Probabilities of January and July of 10 years at 35 and 70 day pelagic larval duration 37

Figure 15 Local Retention averaged over 10 years and 4 seasons depending on different pelagic larval durations.....39

Figure 16 Self Recruitment averaged over 10 years and 4 seasons depending on different pelagic larval durations.....40

Figure 17 Local Retention averaged over 10 years depending on different seasons at 35 day pelagic larval duration 42

Figure 18 Local Retention averaged over 10 years depending on different seasons at 70 day pelagic larval duration 42

Figure 19 January Local Retention of 10 years at 35 day pelagic larval duration 46

Figure 20 January Local Retention of 10 years at 70 day pelagic larval duration 49

Figure 21 April Local Retention of 10 years at 35 day pelagic larval duration 52

Figure 22 April Local Retention of 10 years at 70 day pelagic larval duration 53

Figure 23 July Local Retention of 10 years at 35 day pelagic larval duration..... 56

Figure 24 July Local Retention of 10 years at 70 day pelagic larval duration..... 57

Figure 25 Box-Whisker plots of Local Retention of January, April and July of 10 years at 35 and 70 day pelagic larval duration 58

Figure 26 Circulation velocity fields averaged over 10 years and 4 seasons 61

Figure 27 Circulation velocity fields averaged over 10 years depending on different seasons 63

Figure 28 Pressure differences of NAO and EA-WR over 10 years 68

CHAPTER 1

INTRODUCTION

In order to understand marine ecosystems, the interactions between the physical environment and biological processes need to be taken into account. Unlike on land, where the landscape with which biology interacts changes on large time scales, the seascape is fluid and the constantly changing currents are always interacting with biology, the water is continuously transported, mixed and rearranged by the currents and thus the timescale of these interactions are significantly shorter than on land (Levy et al., 2012, Woodson and Litvin, 2015, McGillicuddy Jr, 2016, Lehahn et al., 2017).

Fine scale processes like fronts and eddies are important for redistribution of physical properties, however the horizontal stirring process that spreads physical properties creates long and convoluted water filaments that make observation of such fine scale process difficult for the human eye (Baudena, 2018). With the advent of satellite tracking since the 1990's it has become possible to accurately acquire the horizontal velocity information of the surface currents which in turn raised the adoption rate of the Lagrangian Flow Network (LFN) implementations that allow for accurate physical flow assessment between neighbouring nodes on the network (Baudena, 2018).

The wind driven circulation of the Black Sea that consists of a cyclonic rim current is thought to act as a biochemical barrier for the exchange between onshore, nutrient rich waters and open ocean waters (Oguz et al, 1994) and may hence also influence fish distribution. However, the rim current exhibits meanders and cross-stream jets and these together with mesoscale eddies associated with the flow may facilitate exchange across this front (Oguz et al., 1994, Oguz 2017).

The unique water column structure of the Black Sea with strong stratification traps oxygen in the approximately 150 m deep surface layer, while the deeper layers are anoxic. This leads fish in the Black Sea to live and spawn in this surface layer whereas in other seas they may be found over a much wider depth range. Many of the commercially important Black Sea fish spawn on the north western shelf (STECF, 2017), the large, shallow shelf area in the north west of the Black Sea where also the large rivers Danube, Dniestr and Dnieper enter onto.

This study aims to investigate the interaction between the unique physical current system of the Black Sea and the life cycle of commercially important fish species using their pelagic larval duration. Specifically, to analyze the seasonal and interannual variability of across-shelf transport and local retention of six different commercial fish species in the entire Black Sea.

For that purpose Lagrangian drifter simulations are undertaken considering the different life history traits and connectivity metrics such as Local Retention (LR), Self Recruitment (SR) and Offshore/Onshore Transport Probability (OFTP and ONTP) are calculated from the results. While there have been many studies that are aimed on quantifying transport and connectivity patterns of larvae in different parts of the world oceans such as the Carribean Sea (Cowen et al., 2006), the Mediterranean Sea (Rossi et al., 2014), North Sea (Erftemeijer et al., 2009) or Australia (Condie et al., 2011; 2011; Roughan et al, 2015) to name a few, to date only few studies have focused on the Black Sea (Fach, 2014, Ozturk et al., 2017, Guraslan et al., 2017). However, these studies in the Black Sea have considered only the dispersion and migration of one species, anchovy, from their known spawning grounds (Fach, 2014, Guraslan et al, 2017) and did not look into across-shelf transport or retention mechanisms and other fish species. The current study fills this gap.

This thesis is structured as follows. The introduction section contains information regarding the unique physical system of the Black Sea, the information on commercially important fish species of the Black Sea and their behavioural patterns and lastly information regarding the concepts of Lagrangian Flow Networks and connectivity. The thesis continues with information on the Lagrangian particle tracking method used in this study, details the results of the simulations undertaken and after a discussion of the results concludes with a summary and conclusions section.

1.1 Physical Properties of the Black Sea

The Black Sea is located between latitudes 41° N and 47° N, longitudes 27° E and 42° E, covers an area of 423000 km^2 and has a maximum depth of 2200 m (Oguz et al., 2004). It is connected to the Marmara Sea through the Bosphorous Strait to the south west and thereby connected to the Mediterranean Sea by way of the Dardanelles Strait and the Aegean Sea, while to the north another connection exists to the Azov

Sea via Kerch Strait (Oguz et al., 2004). The only major shelf structure exists in the north west of the Black Sea and makes up 20% of the total area, the remaining shelf areas are narrow and steep. Three of Europe's largest rivers discharge into the north western shelf, the Danube, Dnester and Dnieper. While in the south Sakarya, Kızılırmak and Yeşilırmak are notable rivers that flow into the Black Sea.

There are three layers present in the water column; the deep water below the thermocline at 100 to 150 m is vertically homogenous down to the abyssal plane featuring temperatures of approximately 9 C°. A cold intermediate layer of water resides roughly around the 80 m depth during spring, summer and autumn then disappears due to winter mixing. The surface layer continues down approximately 50 m with salinity of 18.5 to 18.8 and temperature around 25 C° (Oguz et al, 1994, Oguz et al., 2004).

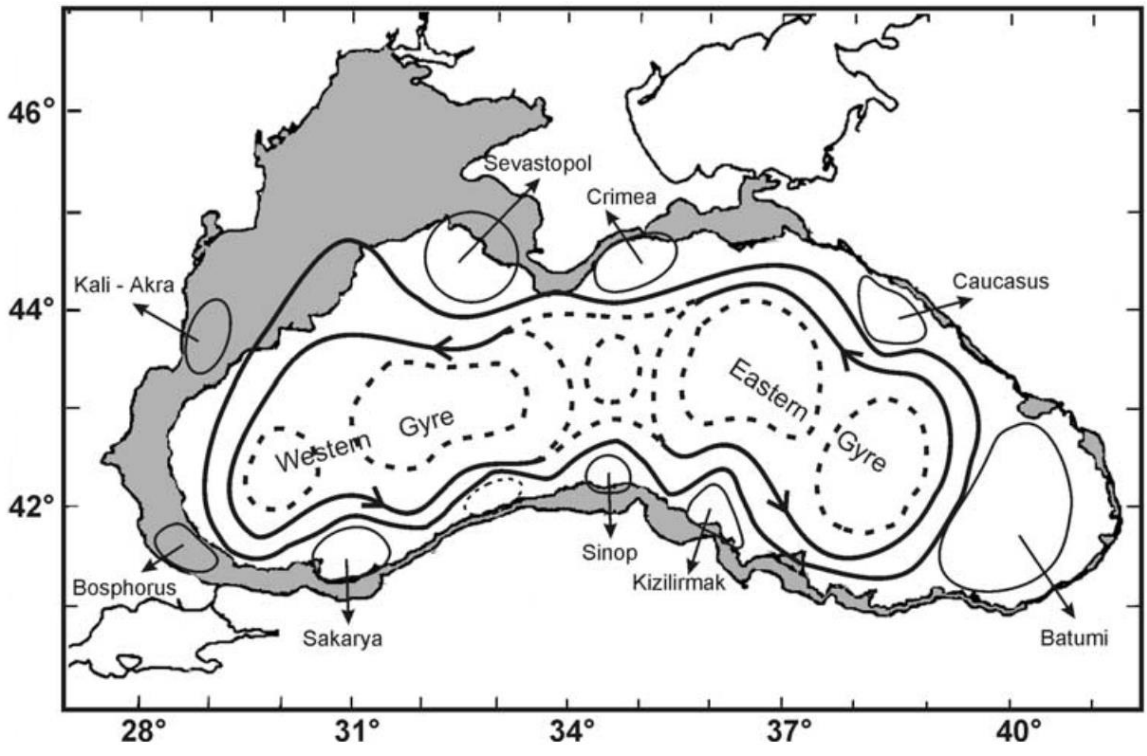

Figure 1: The main features of the surface layer circulation in the Black Sea derived using the hydrographic studies before 1990. Originally made by Oguz et al., 1993, reproduced by Korotaev et al., 2003 and taken from Korotaev et al., 2003.

The Black Sea surface circulation is primarily driven by wind forcing and stirred by the bottom topography, which creates a complicated system dominated by a fast flowing rim current and eddies that interact with one another and the two sub basin-scale gyres of the rim current and associated features (Korotaev et al., 2003). The most notable permanent and semi permanent features of this circulation system are the basin wide cyclonic rim current which circulates the entire basin apart from the north western shelf and the Georgian coast and its periphery (Figure 1), the cyclonic western and eastern gyres located inside the rim current, and the quasi-permanent anti-cyclonic Bosphorus, Sakarya, Sinop, Kizilirmak eddies along the Turkish coast, Batumi eddy on the Georgian coast, Caucasus eddy on the Caucasian coast, Crimea and Sevastapol eddy on the Crimean coast and the Kaliakra eddy on the Romanian and Bulgarian coast (Oguz et al., 1994).

The general winter circulation features from January until March shows the two inner gyres separated from one another approximately around 33° E to 34° E, the borders of the eastern gyre extends towards the south east until the eastern coast as its size reaches twice the size of the western gyre and the points where the two gyres meet at the northern and southern coasts leads to the basin wide rim current system (Korotaev et al., 2003). The severity of the winter weather is what drives the intensity of the circulation system, the years with intense winter weather create a strong cyclonic rim current which in turn leads to strong anti-cyclonic eddies along the coast whereas years with weaker winter weather tend to create broader, weaker general circulation (Korotaev et al., 2003).

Spring conditions from April until June shows the two distinct inner gyres weaken and transform into a single basin wide cyclonic cell creating a broader and weaker rim current while the Batumi eddy (Figure 1) starts forming along the Georgian coast of the Black Sea (Korotaev et al., 2003).

During summer from July to September the inner gyres are further weakened and they break down into small cyclonic eddies around typically 100 km, since these small eddies are what effects the rim current, the general circulation during the summer season is more susceptible to mesoscale variations and interannual variations from year to year are more frequently observed for summer (Besiktepe et al., 2001, Korotaev et al., 2003).

The trend of weakening of the interior cells from summer continues into the autumn season, from October to about 15 days into December the interior of the basin continues to weaken, creating smaller scaled cyclonic eddies as it reaches the most disorganized form of the entire year, the Batumi eddy weakens and the entire basin is susceptible to horizontal variability (Korotaev et al., 2003). As winter approaches, the circulation system starts to stabilize and the eddy dominated nature of the autumn and summer seasons disappear as the circulation turns into an organized and intense structure starting at the second half of December (Korotaev et al., 2003).

The eddy structures located along the southern coast of the Black Sea (Figure 1) consist of semi-permanent Bosphorus and Batumi eddies and the non-permanent Sakarya, Sinop and Kizilirmak eddies. The Bosphorus eddy is present almost year-round while the Batumi eddy starts forming around February, grows and expands towards the interior cell during spring and finally disappears in October with 1 to 2 week shifts annually (Korotaev et al., 2003). While the Sakarya, Sinop and Kizilirmak eddies may form one or two times a year for the duration of a season, if both Sinop and Kizilirmak eddies reach a sufficiently large size they can combine to create one large eddy. The existence of these three eddies depends entirely on the meanders created by the propagation of the rim current (Korotaev et al., 2003). Along the Caucasian cost the rim current flows further away from the coast and this allows for a much broader zone for the, almost always present, Caucasian eddy (Figure 1) to arise (Korotaev et al., 2003). The Crimean coast to the north features two semi-permanent Sevastapol and Crimean eddies (Figure 1). The rim current meandering controls the formation of the Sevastapol eddy, one path located near the south western side tip of the Crimea and another path located on the western Crimean coast at the northern fork of the rim current (Korotaev et al., 2003). The circulation inside the north western shelf is governed by the discharges of the rivers Danube, Dniepr and Dniestr and their interactions with the rim current, while the outer zone of the shelf is driven by the interaction inner shelf current and the rim current. The Kaliakra eddy (Figure 1) located near the Romanian and Bulgarian coast starts to emerge during the end of the summer season and the beginning of autumn and is driven by the coastal currents by high discharges (Korotaev et al., 2003).

1.2 Commercially Important Fish Species of the Black Sea

The Black Sea hosts a number of commercially important fish species for the riparian countries (see Table 1). The most important fishery in the Black Sea is anchovy (*Engraulis encrasicolus*) with total landings of 157,462 tons in 2014 while sprat is the second most important commercial fish with total landings of 58,380 tons in 2014 (STECF-15-16, 2015). Following these species red mullet (*Mullus barbatus*), turbot (*Scophthalmus maeoticus*), Bluefish (*Pomatomus saltatrix*) and horse mackerel (*Trachurus mediterraneus)* are of importance. All of these fish species are known to spawn preferably in shelf areas of the Black Sea, but differ significantly in their life history traits such as their spawning times and pelagic larval stages, which are considered in the simulations of this study.

Two subspecies of anchovy exist in the basin, first is the Black Sea anchovy (*Engraulis encrasicolus ponticus*) and the second is the Azov Sea anchovy (*Engraulis encrasicolus maeticus*) (Ivanova et al., 2013). The Azov Sea anchovy feeds and breeds in the Azov Sea then travels down to the Crimean and Caucasian coasts of the Black Sea, while the Black Sea anchovy travels to wintering grounds located to the south, along the Turkish and Caucasian coasts (Figure 2) around October and November (Ivanov and Beverton, 1985, Chashchin 1996, Chashchin et al., 2015) where they stay until March and form dense hibernating concentrations during which they are subjected to intense fishing (STECF-17-14, 2017). The Black Sea anchovy is known to spawn in the north western shelf and open waters with temperatures higher than 20 C° during the months of June and August with a pelagic larval duration (PLD), the time required for the larvae to obtain the ability to swim on their own without relying on the whim of oceanic currents, of about 36 days (Niermann et al., 1994, Lisovenko and Adrianov, 1996, Sorokin, 2002, Dulcic, 1997). This study focuses on the Black Sea anchovy.

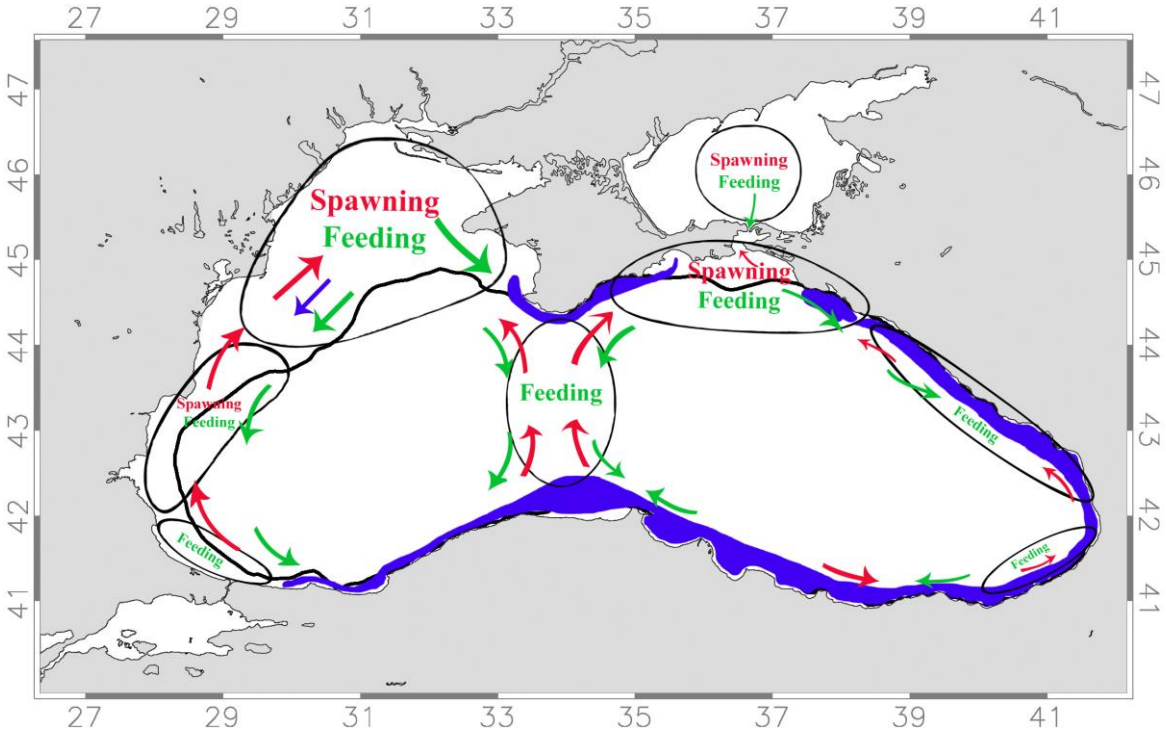

Figure 2: Black Sea anchovy (Engraulis encrasicolus ponticus) and Azov Sea anchovy (Engraulis encrasicolus maeticus) spawning (red), feeding (green) and wintering (blue) areas and migration routes to them. Redrawn from STECF-17-14 (2017).

Sprat (*Sprattus sprattus*) is another important fish species of the Black Sea. Fishing of this species is executed on the north western shelf from April until October and fishing along the rivers of Kizilirmak and Yesilirmak on the southern shelf became common around the 2000's (STECF-17-14, 2017). The Turkish catch of sprat is used as fish food and for oil industry in the country (Knudsen and Zengin, 2006). Sprat prefers spawning inshore areas of the Black Sea about 100 km away from the coast and near river deltas (Figure 3) between autumn and spring, preferably in winter, and has a PLD of about 70 days (Ojaveer, 1981, Houde, 1989, Ivanov and Beverton, 1985).

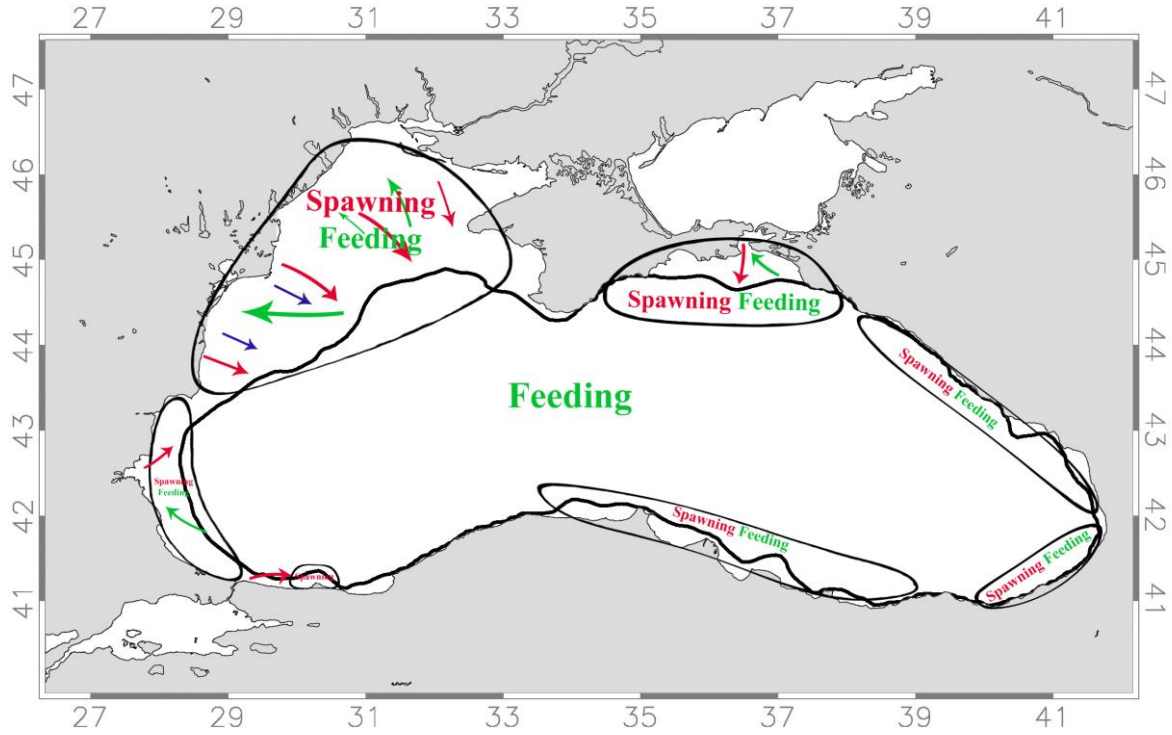

Figure 3: Sprat (Sprattus sprattus) spawning (red), feeding (green) and wintering (blue) areas and migration routes to them, redrawn from STECF-17-14 (2017). Note that feeding areas for sprat are all located onshore of the rim current.

In the northern and eastern parts of the Black Sea, near the Crimean and Caucasian coasts, two different forms of red mullet (*Mullus barbatus*) exist and can be identified as settled and migratory forms (STECF-17-14, 2017). The migratory red mullet travels to the regions of Azov Sea and Kerch Strait in spring time for feeding and spawning and returns to Crimean coasts for wintering (Figure 4), while the settled form does not take part in this migration behaviour to the Azov Sea (STECF-17-14, 2017). Along the western coasts of the Black Sea, the coasts of Romania and Bulgaria, the red mullet migrates down to the Turkish waters south east and the Marmara Sea for wintering between the months of September and November (Figure 4) (STECF-17-14, 2017). Red mullet is known to spawn in the north western shelf and near the Kerch Strait during the summer season and has a PLD of 28 to 35 days (Satilmis et al., 2003, Macpherson and Raventos, 2006, Galarza et al., 2009, STECF-15-16, 2015).

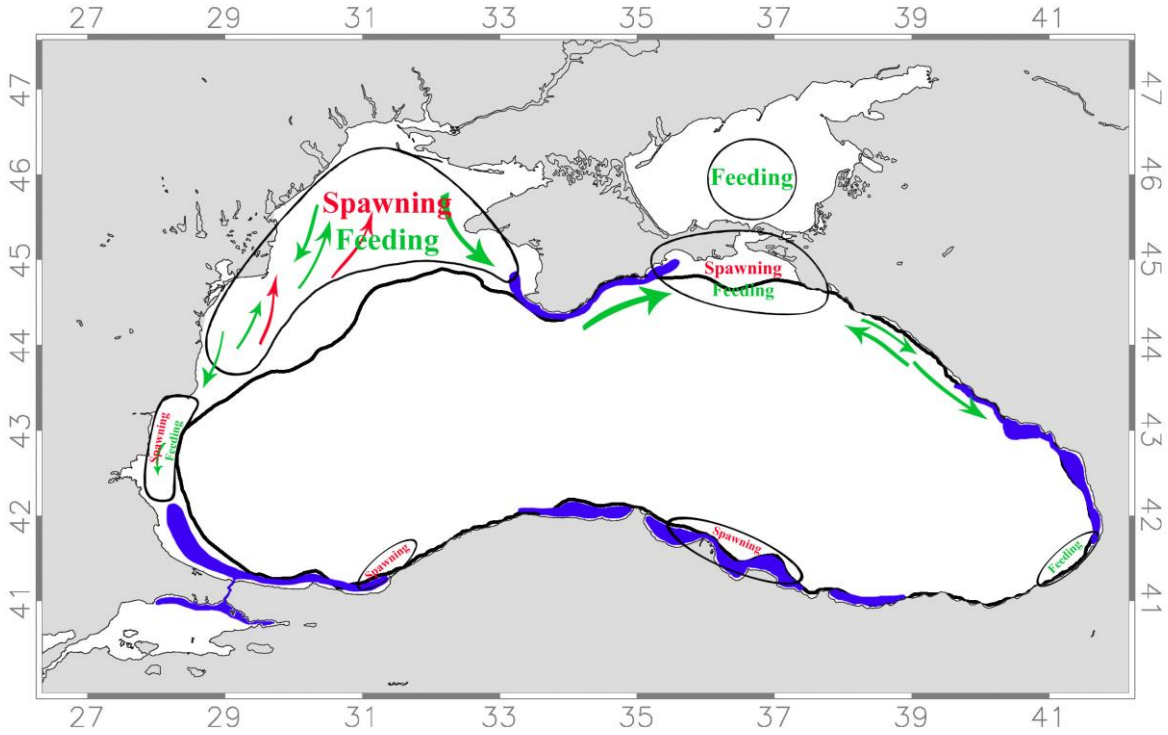

Figure 4: Red mullet (Mullus barbatus) spawning (red), feeding (green) and wintering (blue) areas and migration routes to them. Redrawn from STECF-17-14 (2017).

The Black Sea horse mackerel (*Trachurus mediterraneus ponticus*) exists as a subspecies of the Mediterranean horse mackerel (*Trachurus mediterraneus*) (STECF-17-14, 2017). This species spawns mostly near the north western shelf and the Kerch Strait and travels to the Crimean coast and the Marmara Sea for wintering (Figure 5). The PLD for the red mullet is believed to be between 28 to 35 days (Satilmis et al., 2003, Macpherson and Raventos, 2006, Galarza et al., STECF-15-16, 2015).

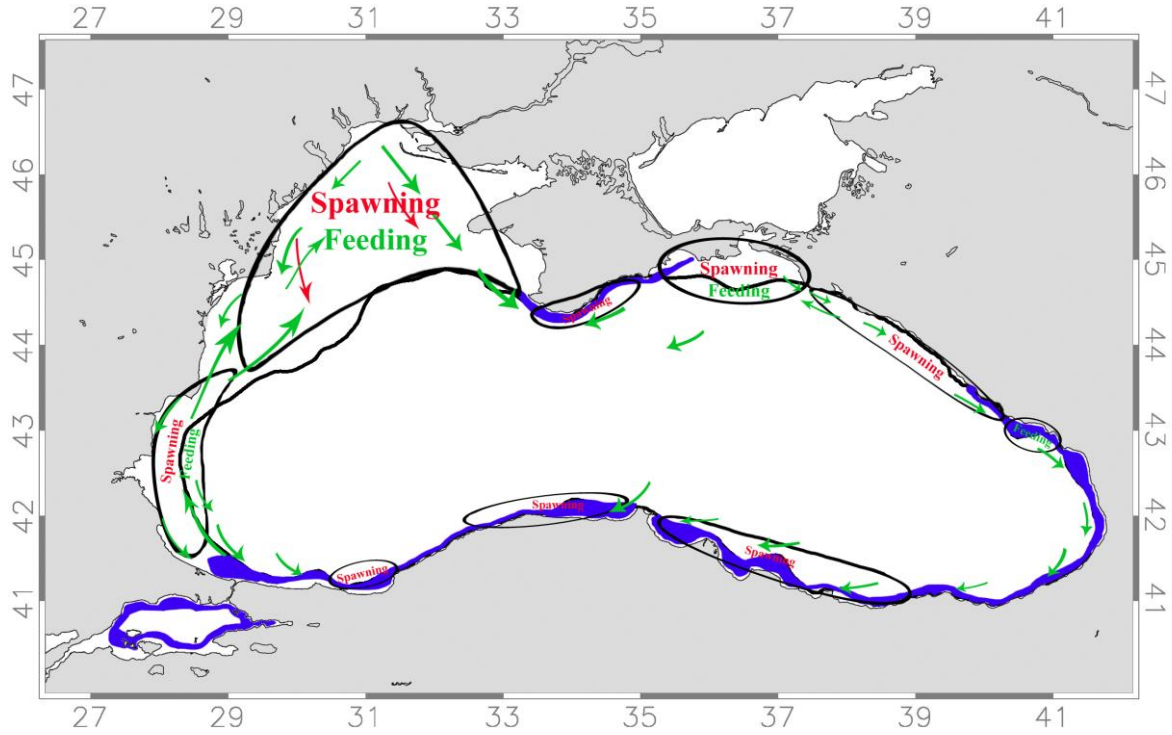

Figure 5: Horse mackerel (Trachurus mediterraneus ponticus) spawning (red), feeding (green) and wintering (blue) areas and migration routes to them. Redrawn from STECF-17-14 (2017).

In addition, Bluefish (*Pomatomus saltatrix*) and Turbot (*Scophthalmus maeoticus*) are important commercially in the Black Sea. Both species spawn in spring, with Bluefish spawning in coastal regions along the Turkish, Ukrainian, and Bulgarian coasts and larvae experiencing a pelagic larval duration of 18-25 days (Table 1) (Gordina and Klimova, 1996, Hare and Cowen, 1997, Satilmis et al., 2003, Satilmis et al., 2014, Ceyhan et al., 2007). Turbot larvae experience larval durations of 29-39 days (Haynes et al., 2011, Satilmis et al., 2014).

Table 1. Important commercial fish species with pelagic larval stages in the Black Sea used as target species in this study.

Species	**Spawning Time**	**Spawning Area**	**PLD**	**Reference**
Anchovy *(Engraulis encrasicolus ponticus)*	June-August	North-western shelf and open water > 20°C	~36 days	Niermann et al. (1994), Lisovenko and Adrianov (1996), Sorokin (2002), Dulcic (1997)
Sprat *(Sprattus sprattus)*	autumn-spring	Inshore areas of Black Sea until ~100 km offshore, river deltas	~70 days	Ojaveer (1981), Houde (1989), Ivanov and Beverton (1985)
Red mullet *(Mullus barbatus ponticus)*	Summer (after May)	North-western shelf and off Kerch Strait	28-35 days	Satilmis et al. (2003), Macpherson and Raventós (2006), Galarza et al. (2009), STECF-15-16, (2015)
Bluefish *(Pomatomus saltatrix)*	Spring - summer	Coastal regions (Turkish, Ukrainian, Bulgarian coasts)	18-25 days	Satilmis et al. (2003; 2014), Ceyhan et al.(2007), Gordina and Klimova (1996), Hare and Cowen (1997)
Turbot *(Scophthalmus maeoticus)*	Spring - summer		29-39 days	Satilmis et al. (2014), Haynes et al. (2011)
Horse mackerel *(Trachurus mediterraneus ponticus)*	summer	Coastal areas	~25 days	Satilmis et al. (2003, 2014)

1.3 Larval Dispersal and Connectivity

Larval exchange between marine environments is crucial to understanding population dynamics and spawning sites of marine fish. However it is unrealistic to expect an experimental way of tracking fish larvae especially for fish with long PLD's (Cowen et al., 2006). In order to accurately study the interaction of larvae with physical

systems the aid of a computer models with an embedded particle tracking system is a very useful tool.

1.4 Lagrangian Flow Networks

A technique employed in this study is the Lagrangian flow network (LFN), which essentially divides the entire Black Sea into a network of nodes connected with one another via directed links. This network of nodes or grids helps represent water transfer between different regions of the ocean, where every link between nodes simulates mass transport between the two nodes regulated by physical currents in a given model time step (Monroy et al., 2017). This technique allows the study of particles interacting with the simulated current system in a variety of different ways in order to gain insight about the transfer of the fish larvae. It is possible to test transport in different seasons, past years or future predictions, extreme events, or testing different regions of the sea for potential zones of spawning not studied in situ. Testing and studying most of these scenarios can be too costly or very impractical and sometimes both using a research vessel, thus use of a LFN is a realistic option for such studies including fish larvae or any particle like object with very limited mobility.

The accuracy of the larval transport simulation depends on the number of particles used in the model, the depth where these particles are tracked and finally the duration of the particle tracking (Monroy et al, 2017). Higher number of particles in the model helps increase the accuracy of the tracking analysis.

CHAPTER 2

METHODS

In this chapter, the three-dimensional circulation model used in this model to obtain the Black Sea circulation field is briefly described. The details of the Lagrangian drifter simulations used to simulate pelagic larvae connectivity within the Black Sea is detailed, as well as the statistical analysis used for investigating different aspects of this connectivity.

2.1 Circulation Model

The Black Sea circulation was modelled using the Stony Brook Parallel Princeton Ocean Model (sbPOM) which itself is a parallel version of the Princeton Ocean Model (POM) and which has been used in previous studies (Salihoglu et al., 2017). The model was used to provide the circulation field of the Black Sea required to be able to calculate the drifter paths in this study. This model spans the entirety of the Black Sea, excluding the Sea of Azov, with a 4x4 km resolution horizontal and 35 layers of terrain following sigma coordinate vertical grids. The turbulence parameterization was done using Mellor-Yamada 2.5 turbulence parameterization (Blumberg and Mellor, 1987). The model includes the water flux of the Bosphorus and the nine largest rivers of the Black Sea. Using the World Ocean Atlas fields (Locarini et al., 2013, Zweng et al., 2013) monthly climatology as initial conditions the model was spun up for 5 years and run for 21 years from 1990 to 2010 (Salihoglu et al., 2017).

In previous studies the circulation model was validated extensively comparing temperature, salinity to in situ observations from the Black Sea - Temperature and salinity observation collection V2 (Black Sea, 2015, Simoncelli et al., 2015) using univariate metrics such as root mean square error, bias, unbiased root mean square error and Pearson Correlation Coefficient. In addition, the reliability of reproducing observable parameters were checked by comparing model results to satellite data of Sea Surface Temperature and satellite derived Sea Level Anomalies were used to validate the model produced circulation fields. The model was found to resolve the Black Sea circulation with its rim current and anti-cyclonic eddies, as well as

interannual variability in the current field well (Allen et al., 2013, Salihoglu et al., 2017).

2.2 Lagrangian Particle Tracking

To undertake Lagrangian drifter analysis, in the entirety of the Black Sea virtual drifters were positioned in the surface circulation at 10 m depth of the Black Sea at 1 km spacing in both latitudinal and longitudinal direction. With this choice it is assumed that larvae are to be homogeneously distributed tin he surface mixed layer. In this study any vertical movements of larvae is ignored, which has been shown to be a reasonable assumption because most particles remain in the selected layer over short time-scales ($\leq$ 2 months) since horizontal velocities are several orders of magnitude higher than vertical ones (Dovidio et al., 2004).

Making use of a land-sea mask the coastal grids did not have any drifters placed on top of the land portions. In the end a total of 410478 drifters were placed in the entirety of the Black Sea. Drifters were advected using a first-order accurate Lagrangian particle tracking scheme in which the 2D velocity field is interpolated to the particles position and then carries the particle to a new position with each time step (Fach, 2014). However, it is a common problem that processes smaller than the grid-spacing of the model cannot be resolved by such velocity fields. Hence it was necessary to add the effect of sub-grid scale turbulence via a numerical technique. This was achieved using a random walk process described and tested in detail in Xue et al. (2008) and Roughan et al. (2011). It scales the simulated turbulent diffusion terms with a Gaussian random process that has a mean of 0 and a standard deviation of 1 between subsequent random events, resulting in a diffusivity coefficient of ca. $5*10^5$ cm^2s^{-1}.

These 410478 drifters are released each year from 2001 to 2010, at the 15th of January, April, July and September representing different seasons (Table 2). In each of these simulations drifters are used to simulate pelagic fish larvae of commercially important fish species detailed above and are tracked for their different pelagic larval durations (20-70 days). That means that in total 200 simulations with 410478 drifters each were undertaken for this study (Table 2). Each drifter was individually tracked, recording its position as latitude and longitude information every hour of every day along with velocity, temperature, diffusion and other model specific parameters.

Table 2. List of simulations undertaken in this study. A total of 200 simulations were undertaken, each with 410478 drifters.

Simulations	**Parameters changed**				
Pelagic larval durations	20 days	30 days	35 days	40 days	70 days
Spawning times	Spring	Summer	Fall	Winter	
Years	2001 - 2010				
TOTAL	**200**				

2.3 Lagrangian Flow Network

To investigate connectivity within the Black Sea in detail, a Lagrangian Flow Network (Ser-Giacomi et al., 2015, Monroy et al., 2017) was established by dividing the entire Black Sea into 10x10 km grids, or nodes, each containing 100 Lagrangian drifters at 1 km spacing. A total of 7735 nodes were established this way, however it should be noted that coastal nodes may contain less than 100 drifters depending on the location in the Black Sea.

Using the position information alongside the grid system it was possible to calculate metrics defining the probability for drifters experiencing across-shelf transport, particularly Onshore Transport Probability (ONTP) and Offshore Transport probability (OFTP), as well as Local Retention (LR) and Self Recruitment (SR) in certain areas, which are good indicators of larval connectivity (Monroy et al, 2017, Condie et al., 2011)

In order to calculate the probability of particles originating anywhere in the Black Sea to be transported into waters shallower or deeper than a specified depth within a specified timeframe corresponding to respective PLDs were calculated. This is a measure of larvae that may get transported on-shelf or off-shelf from their respective spawning sites during their pelagic larval duration times. The specified depth here was chosen to be 200 m as this is a good indicator of the shelf edge. Using the bathymetry information provided from the model each grid cell's average bathymetry was calculated and any cell deeper than 200 m was labelled as offshore. Onshore grids which had transported drifters to any offshore grid were considered to have made an offshore transport, if the drifter remained in an onshore grid then it was considered to have made an onshore transport. The opposite is also true for offshore

grids, any transport made to an onshore grid is considered an onshore transport and if the drifter remains in an offshore grid then it is considered as an offshore transport. Tracking all of the drifters for the desired PLD we are able to obtain the total onshore transport count (ONTC) and offshore transport count (OFTC) for every grid in our flow network. ONTP and OFTP are then calculated for every grid as follows.

$$ONTP = \frac{ONTC}{OFTC+ONTC} \quad (1) \qquad OFTP = \frac{OFTC}{OFTC+ONTC} \quad (2)$$

Other connectivity metrics, such as Local Retention (LR) and Self Recruitment (SR) are also calculated with the LFN. Here LR is the percentage of larvae that is able to stay in the same grid area that they start initially on a grid by grid basis. It refers to the ability of the local population to stay in the same zone. SR is the percentage of larvae that stays in the same grid area that they started initially versus the overall larvae inside this grid on a per grid basis, it is essentially the percentage of the original population remaining in the grid while taking into account the migrations into the grid from other grid sources via currents.

SR and LR are calculated similarly by tracking every drifter for the desired PLD following Ser-Giacomi et al. (2015) and Monroy et al. (2017). For each grid the number of drifters that start initially inside (n_i), the number of drifters that are inside the same cell at the end of the desired PLD (n_f), and the number of drifters that are retained in this cell (n_r) are tracked. LR is the ratio of n_r over n_i, representing the ratio of larvae remaining in the given grid at the end of the PLD to those that originated in the grid at the start of the PLD. The final metric is SR, which is the ratio of n_r over n_f, representing the ratio of original larvae of the grid retained there over the total population of the grid at the end of the PLD with migrations from other grids.

$$LR = \frac{n_r}{n_i} \quad (3) \qquad SR = \frac{n_r}{n_f} \quad (4)$$

All of these metrics are then categorized and plotted for the different simulations (Table 2).

2.4 Statistical Analysis

To reduce the uncertainties associated with the dispersal calculations detailed above and to account for the fact that many of the commercial marine fishes are multiple spawners, dispersal probability (or across-shelf transport, Local Retention and Self Recruitment), is calculated based on a larger number of drifters created by an ensemble run. This means that not only the probability of 410478 drifters released at the beginning of each season and year are considered, but the probability distribution of all drifters during the entire simulation time (90 days) are calculated from day 1 of the simulation to day T, then from day 2 to day T+1, etc. until reaching the last day of each 90-day simulation, thereby creating an ensemble of probabilities (Condie et al., 2011). These probabilities are further averaged to give the probability distribution of each season (averaged over the 90-day period), each year (averaged over 365 days), or over the entire time (averaged across all years) or subsets thereof.

CHAPTER 3

RESULTS

In this chapter the results of different connectivity measurements are presented, starting with ONTP, OFTP, LR and then SR. In all sections the impact of different larval durations and spawning times are assessed and interannual variability described.

3.1 Onshore and Offshore Transport Probabilities

Lagrangian drifter results are analysed to account for variation of Pelagic Larval Durations (PLD's), interannual variation, seasonal variation and years with distinct distributions. In order to present the data easier the Black Sea has been separated into 13 different regions as follows: the Sevastapol Eddy; the north western shelf coast; center of the north western shelf; the Kaliakra eddy; the western coast: coasts from Romania to Bulgaria; south western coast: coasts from Kırklareli to Istanbul; southern coast: coasts from Sakarya to Sinop; south eastern coast: coasts from Samsun to Rize; coasts of Georgia; eastern coast: coasts of the Caucasus; northern coast: the Azov Sea entrance; the Eastern Gyre and the Western Gyre.

3.1.1 The Impact of Different Pelagic Larval Durations

The effect of different PLD's on ONTP and OFTP are best observed when simulation results are averaged over all 10 years and all 4 seasons (Figure 6, Table 3). Averaging simulations over the entire time frame gives the most robust results. The general pattern of these simulation results shows that OFTP in shallow areas less than 200 m depth are low, increasing towards the shelf break and being high in areas deeper than 200 m depth. ONTP values are the inverse of OFTP.

Starting with the Sevastapol Eddy region OFTP increases in the eddy as simulations change from 20 day PLD (Figure 6A) to 70 day PLD (Figure 6D). OFTP values average around 0.35 at 20 days (Figure 6A), increase to an average of 0.4 at 30 (Figure 6B) and 35 days (Figure 6C) then reach 0.55 at 40 (Figure 6D) and 70 days (Figure 6E). Conversely ONTP in the region decreases from 20 day PLD (Figure 7A) to 70 day PLD (Figure 7E). Looking at the ONTP values in the Sevastapol region

starting at 20 days (Figure 7A) the average is around 0.65 then decreases to about 0.6 for 30 (Figure 7B) and 35 days (Figure 7C), finally reaches 0.45 at 40 (Figure 7D) and 70 day PLDs (Figure 7E, Table 3). This symmetry in values is due to the way ONTP and OFTP are calculated. Since the total transport is the sum of ONTP and OFTP as they are calculated, the ONTP and OFTP plots end up becoming inversely coloured versions of one another. From this point on we will only focus on OFTP plots for convenience, the ONTP plots can be found in the Appendix Section B.

The coastal and central regions of the north western shelf stand out for having the lowest OFTP values for all PLD's (Figure 6, Table 3). The Kaliakra eddy, the western coasts from Romania to Bulgaria, south eastern coast of Turkey and the entrance to the Azov Sea located at the northern coast of the Black Sea are all regions with lower OFTP values than the rest of the Black Sea even with PLD increases are taken into account (Table 3). The general OFTP patterns show that as the PLD increases from 20 days to 70 days (Figure 6) the OFTP values in the shallow regions start increasing while the OFTP values in the deep regions start decreasing. The OFTP decrease in the deep regions can be observed in the inner gyres and the steep coastal regions that are close to the rim current periphery like the Georgian coast and the Caucasus coasts (Table 3).

Table 3. Offshore Transport Probability (OFTP) averages of different regions for different Pelagic Larval Durations (PLD) deduced from simulation results of 10 years (2001-2010) and 4 seasons averaged.

2001-2010 4 Seasons OFTP Averages	**20 days**	**30 days**	**35 days**	**40 days**	**70 days**
Sevastapol Eddy	0.35	0.4	0.4	0.55	0.55
NW Shelf Coast	0.1	0.1	0.1	0.1	0.2
NW Shelf Center	0.15	0.2	0.2	0.3	0.35
Kaliakra Eddy	0.1	0.2	0.2	0.2	0.25
W Coast	0.2	0.3	0.3	0.3	0.4
SW Coast	0.2	0.3	0.3	0.3	0.4
S Coast	0.85	0.7	0.7	0.7	0.55
SE Coast	0.2	0.2	0.2	0.2	0.2
Georgian Coast	0.8	0.7	0.7	0.7	0.6
E Coast	0.8	0.8	0.7	0.7	0.6
N Coast	0.35	0.35	0.4	0.45	0.6
West Gyre	0.95	0.95	0.95	0.95	0.85
East Gyre	0.95	0.95	0.95	0.95	0.85

As the 35 days PLD is representing anchovy and the 70 days PLD is representative of sprat, which are two of the most economically important fish species in the Black Sea, from now on all comparisons will be made between 35 day and 70 day PLD's. PLD's from 20 to 40 are relatively close to one another the average differences between them are small (Table 3), hence the choice of 35 days is a good representative of represent the 20, 30, and 40 day simulation results.

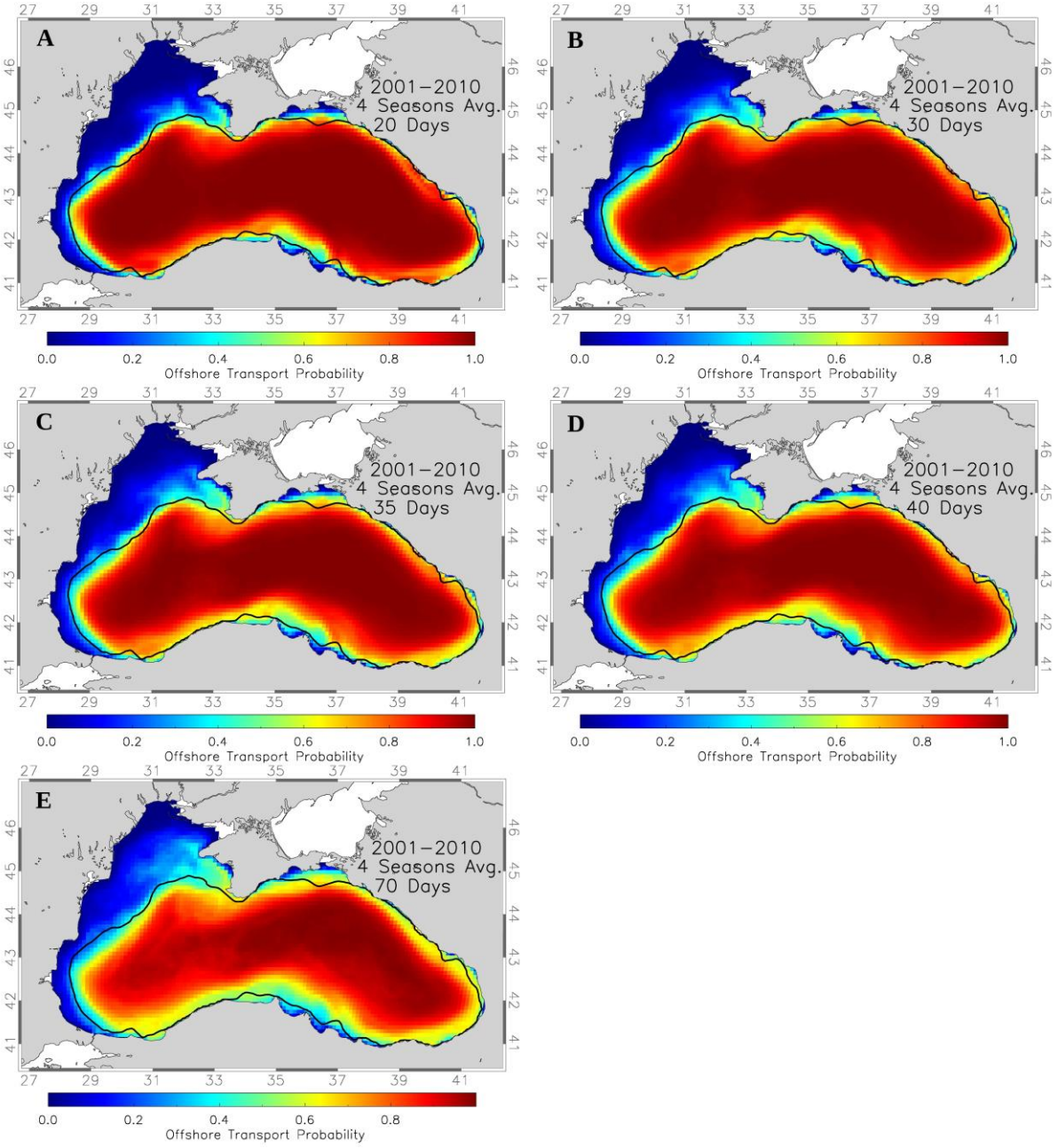

Figure 6: Simulation results of 10 years (2001-2010) and four seasons averaged to calculate the Offshore Transport Probability (OFTP) depending on different Pelagic Larval Durations (PLD). A: 20 day PLD, B: 30 day PLD, C: 35 day PLD, D: 40 day PLD, and E: 70 day PLD.

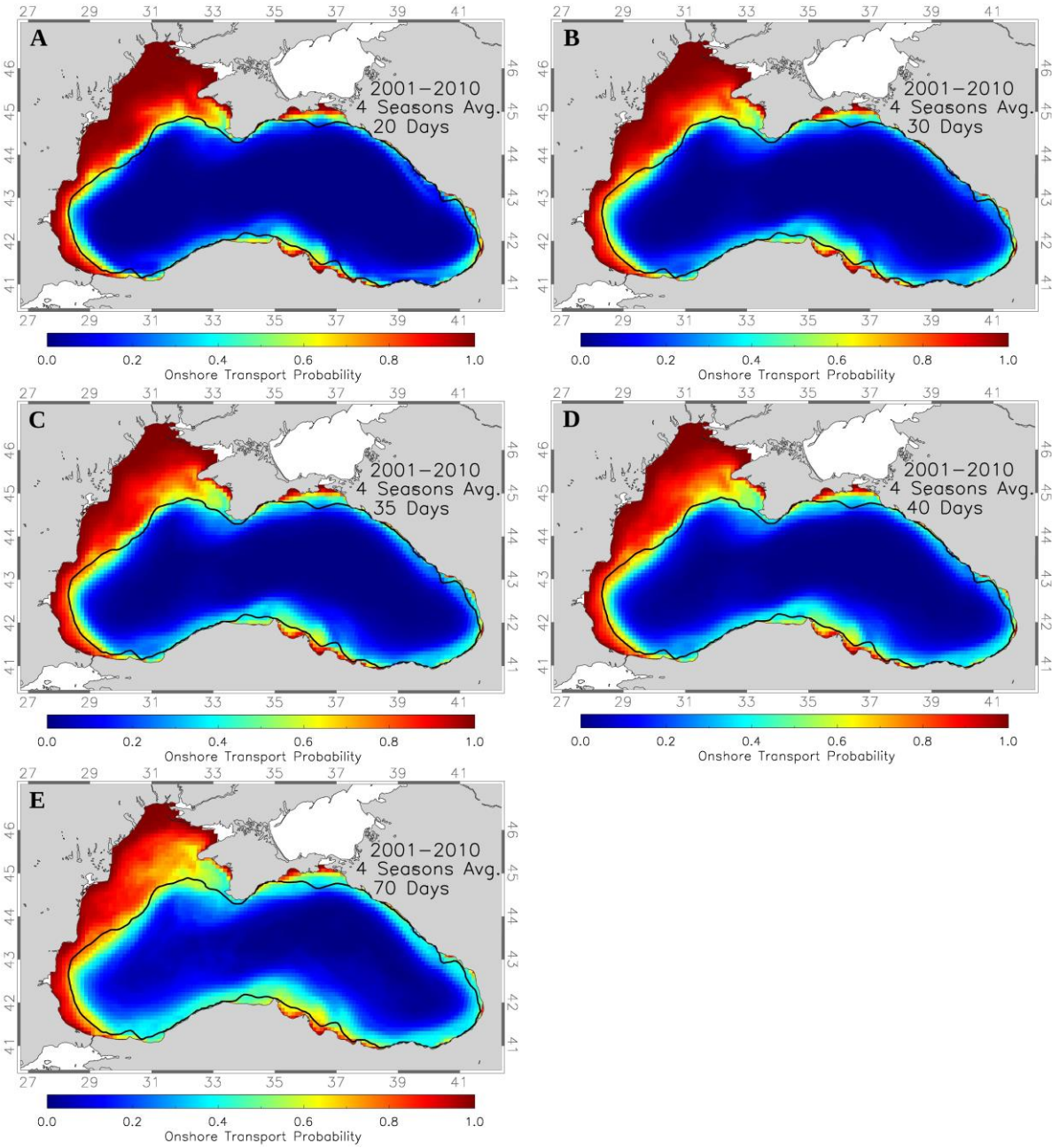

Figure 7: Simulation results of 10 years (2001-2010) and four seasons averaged to calculate the Onshore Transport Probability (ONTP) depending on different Pelagic Larval Durations (PLD). A: 20 day PLD, B: 30 day PLD, C: 35 day PLD, D: 40 day PLD, and E: 70 day PLD.

3.1.2 Seasonal Variability

Seasonal variability in the Lagrangian drifter simulations are investigated by averaging 10 years of simulation results for each of the four seasons. In these simulations January appears to have the highest overall OFTP values in shallow areas and has lower values in deep areas with October very similar to January while April and January have the lowest OFTP values in shallow areas and the highest values in deep areas.

A detailed look at the OFTP values for 35 days (Figure 8, Table 4) shows the previously mentioned areas of low OFTP like the north western shelf, western coast, south eastern coast of Turkey, remain the same for all seasons. Season to season variation (Figure 8, Table 4) shows that for shallow areas January tends to have the highest OFTP values followed closely by October then by a significant decrease with April and finally with the lowest values in July. The deep areas close to the steep coastal regions effected by the rim current like the southern coast of Turkey, Georgian coast and the Caucasus coast have minimum OFTP values in January, OFTP values reach maximum in April and second highest values are seen in July and October. This however is not the case for the inner Gyres which are also considered to be a deep region, they are at maximum values in January and October and reach their minimum values in April and July (Table 4), similar to the shallow regions.

The 35 day PLD shows that OFTP values for January and October tend to be similar and April and July also tend to be similar as well (Table 4). In general OFTP starts at maximum values in January then decreases in April and reaches minimum values in July then increases back to maximum values in October.

Table 4. Offshore Transport Probability (OFTP) averages of different regions for each season deduced from simulation results of 10 years (2001-2010) averaged at 35 day Pelagic Larval Duration (PLD).

2001-2010 35 Day PLD OFTP Averages	January	April	July	October
Sevastapol Eddy	0.55	0.35	0.4	0.55
NW Shelf Coast	0.1	0.0	0.0	0.1
NW Shelf Center	0.4	0.25	0.25	0.4
Kaliakra Eddy	0.35	0.0	0.0	0.35
W Coast	0.3	0.25	0.25	0.3
SW Coast	0.35	0.25	0.25	0.35
S Coast	0.5	0.9	0.7	0.7
SE Coast	0.45	0.45	0.45	0.45
Georgian Coast	0.6	0.75	0.55	0.6
E Coast	0.7	0.8	0.7	0.7
N Coast	0.65	0.55	0.65	0.65
West Gyre	0.95	0.8	0.8	0.95
East Gyre	0.95	0.8	0.8	0.95

OFTP overall is lower in coastal areas and higher inside the inner gyres with the coastal values decreasing from the maximum values of January until July and increasing again in October while the inner gyre has the maximum values during April and July and decreases until January and reaches the minimum values. The north western shelf coast shows almost no OFTP regardless of the season. The southern coast has the maximum and minimum values inverted for the seasons, January has the minimum OFTP while April has the maximum which then it decreases in July and October. OFTP in the south eastern coast of Turkey seems to be not effected by the seasonal changes.

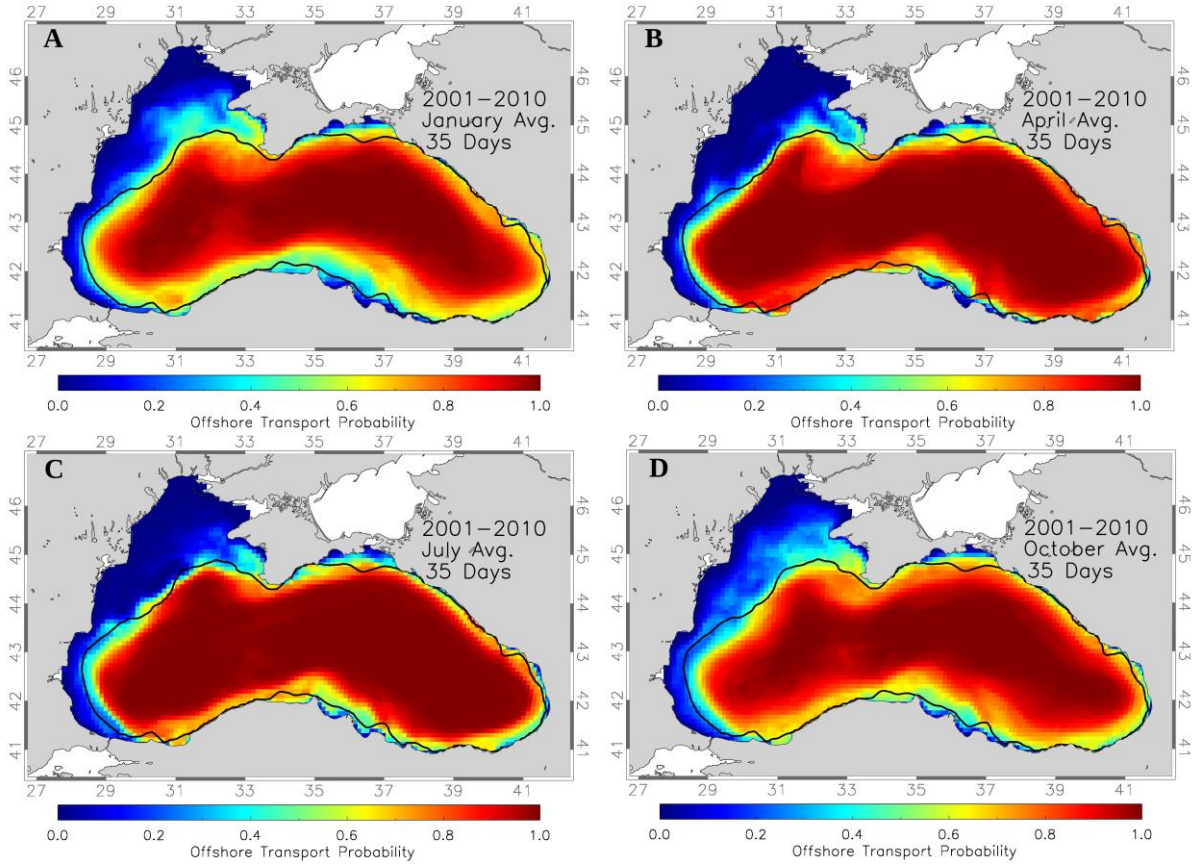

Figure 8: Simulation results averaged over 10 years (2001-2010) for four seasons at 35 day pelagic larval duration (PLD) to calculate the Offshore Transport Probability (OFTP). A: January, B: April, C: July, D: October.

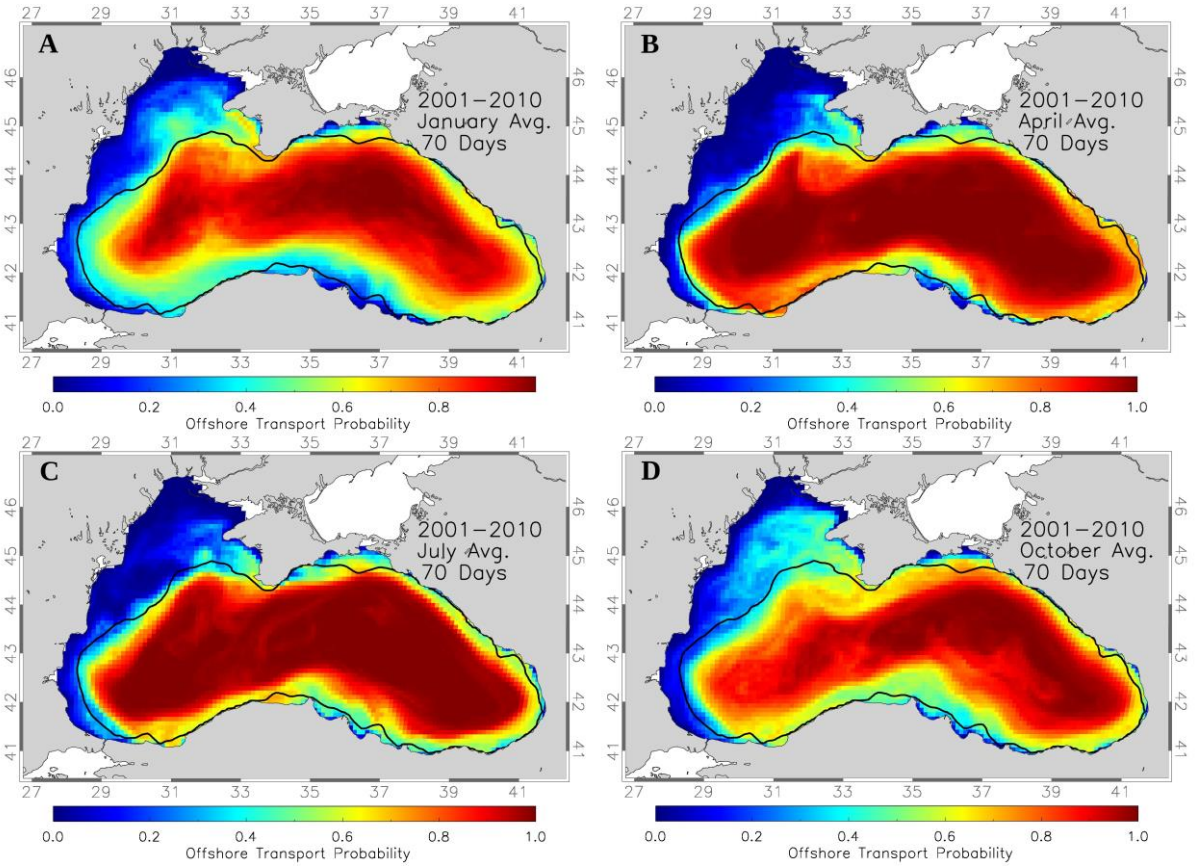

Figure 9: Simulation results averaged over 10 years (2001-2010) for four seasons at 70 day pelagic larval duration (PLD) to calculate the Offshore Transport Probability (OFTP). A: January, B: April, C: July, D: October.

The same simulations using 70 day PLD show overall the same spatial patterns (Figure 9) as the 35 day simulations (Figure 8) in the different seasons investigated here. The main difference is that regions at the shelf edge, where the rim current is located show wider bands of low OFTP indicating higher chances of transport onshore due to the longer transport times. Regions on the north western shelf show a slight increase in OFTP, indicating that these regions have a higher probability of offshore transport (Table 5).

The seasonal 70 day simulations (Figure 9) show the north western shelf starts with the highest OFTP values in January, which decrease in April, reach minimum values in July and finally increases to higher values in October. The rim current OFTP values are the lowest around the coasts in January, increase to maximum values and area covered by April then decrease in July and finally reach minimum values in October. In all seasons OFTP values in the south eastern coast from

Samsun to Rize and the northern coast at the Azov Sea entrance do not significantly change from season to season. Overall OFTP values shows that January and October are similar to one another and April and July seem to be similar to each other as well (Table 4, Table 5).

Table 5. Offshore Transport Probability (OFTP) averages of different regions for each season deduced from simulation results of 10 years (2001-2010) averaged at 70 day Pelagic Larval Duration (PLD).

2001-2010 70 Day PLD OFTP Averages	January	April	July	October
Sevastapol Eddy	0.55	0.45	0.4	0.5
NW Shelf Coast	0.2	0.1	0.1	0.2
NW Shelf Center	0.4	0.2	0.2	0.4
Kaliakra Eddy	0.3	0.1	0.1	0.4
W Coast	0.4	0.6	0.4	0.3
SW Coast	0.4	0.6	0.4	0.4
S Coast	0.5	0.8	0.7	0.6
SE Coast	0.3	0.4	0.5	0.4
Georgian Coast	0.6	0.7	0.6	0.6
E Coast	0.6	0.65	0.55	0.65
N Coast	0.55	0.5	0.55	0.7
West Gyre	0.8	0.9	0.9	0.8
East Gyre	0.8	0.9	0.9	0.8

3.1.3 Interannual Variability

January and July are the two opposite extreme examples of our data as found above in section 3.1.2. In addition, the 10-year averaged April simulations show similar features to the averaged July simulations while the averaged October simulations show similar features to the averaged January simulations. Because the commercially important Black Sea fish species anchovy spawns in summer, while sprat spawns in winter, the January and July simulations will be the main focus from here on to investigate interannual variability.

Table 6. Offshore Transport Probability (OFTP) averages of January for different regions from years 2001 to 2010 with Pelagic Larval Duration (PLD) average of 35 days.

January 35 Day PLD OFTP Averages	2001	2002	2003	2004	2005	2006	2007	2008	2009	2010
Sevastapol Eddy	0.7	0.4	0.8	0.65	0.2	0.4	0.4	0.8	0.7	0.4
NW Shelf Coast	0.1	0.1	0.1	0.1	0.1	0.1	0.1	0.1	0.1	0.1
NW Shelf Center	0.4	0.1	0.55	0.5	0.1	0.4	0.1	0.5	0.55	0.5
Kaliakra Eddy	0.2	0.2	0.2	0.2	0.2	0.3	0.2	0.2	0.2	0.3
W Coast	0.2	0.2	0.3	0.3	0.2	0.2	0.1	0.4	0.3	0.4
SW Coast	0.2	0.2	0.2	0.3	0.4	0.5	0.5	0.3	0.3	0.4
S Coast	0.5	0.5	0.5	0.6	0.7	0.6	0.6	0.5	0.5	0.7
SE Coast	0.1	0.2	0.1	0.1	0.1	0.1	0.1	0.2	0.2	0.1
Georgian Coast	0.5	0.5	0.6	0.6	0.7	0.6	0.6	0.5	0.7	0.7
E Coast	0.6	0.7	0.8	0.8	0.6	0.7	0.6	0.7	0.9	0.8
N Coast	0.6	0.5	0.5	0.7	0.4	0.5	0.5	0.7	0.7	0.5
West Gyre	0.8	0.9	0.9	0.8	0.8	0.8	0.9	0.7	0.8	0.8
East Gyre	0.8	0.8	0.8	0.8	0.8	0.8	0.7	0.8	0.9	0.9

Simulation results for individual years that are also separated for individual seasons represent the most variable picture of onshore and offshore transport dynamics. Even when comparing the same season with the same PLD some years can differ quite significantly from other years as the circulation patterns between years and seasons vary. Here are some examples of the broad differences the different circulation patterns create and some of the outliers in the simulations: the years 2002, 2005 and 2007 for January spawning and 35 day PLD (Table 6) have 0.1 to 0.2 OFTP for the entirety north western shelf, lower than the rest of the years which have between 0.4 to 0.8 OFTP (Figure 10), the 70 day data likewise shows a similar result with 2002, 2005 and 2007 at 0.1 to 0.2 and the rest of the years between 0.4 to 0.8 (Figure 11). In 2008 January 35 days the Western Gyre's outer cells have lower values between the 0.4 to 0.9 range and the Gyre is less pronounced at south west compared to the rest of the years with values between 0.6 and 0.9 (Figure 10).

Table 7. Offshore Transport Probability (OFTP) averages of January for different regions from years 2001 to 2010 with Pelagic Larval Duration (PLD) average of 70 days.

January 70 Day PLD OFTP Averages	2001	2002	2003	2004	2005	2006	2007	2008	2009	2010
Sevastapol Eddy	0.6	0.4	0.8	0.9	0.2	0.6	0.4	0.7	0.7	0.6
NW Shelf Coast	0.2	0.1	0.2	0.2	0.1	0.1	0.1	0.2	0.2	0.1
NW Shelf Center	0.5	0.3	0.6	0.6	0.2	0.4	0.2	0.6	0.6	0.5
Kaliakra Eddy	0.2	0.2	0.3	0.2	0.1	0.2	0.1	0.3	0.2	0.3
W Coast	0.3	0.2	0.3	0.2	0.3	0.2	0.2	0.3	0.3	0.4
SW Coast	0.3	0.3	0.3	0.4	0.4	0.3	0.4	0.3	0.3	0.4
S Coast	0.4	0.4	0.4	0.5	0.5	0.4	0.5	0.4	0.6	0.6
SE Coast	0.1	0.3	0.1	0.1	0.1	0.1	0.1	0.1	0.1	0.2
Georgian Coast	0.5	0.5	0.6	0.5	0.5	0.6	0.5	0.6	0.7	0.7
E Coast	0.5	0.6	0.7	0.7	0.4	0.5	0.4	0.7	0.7	0.7
N Coast	0.5	0.5	0.6	0.7	0.4	0.4	0.3	0.7	0.8	0.5
West Gyre	0.6	0.7	0.6	0.6	0.7	0.6	0.7	0.6	0.7	0.6
East Gyre	0.8	0.6	0.7	0.8	0.8	0.8	0.7	0.8	0.9	0.9

The January simulation with 70 days represents the maximum OFTP values of the entire dataset (Figure 11, Table 7). The increase of PLD to 70 days in January (Table 7) shows an increase in OFTP values in the shallow areas compared to January 35 days (Table 6) while the years 2002 (Figure 11B), 2005 (Figure 11E) and 2007 (Figure 11G) remain outliers with their lower OFTP values in the north western shelf region. In addition the inner gyres start showing meandering patterns not present in 35 days.

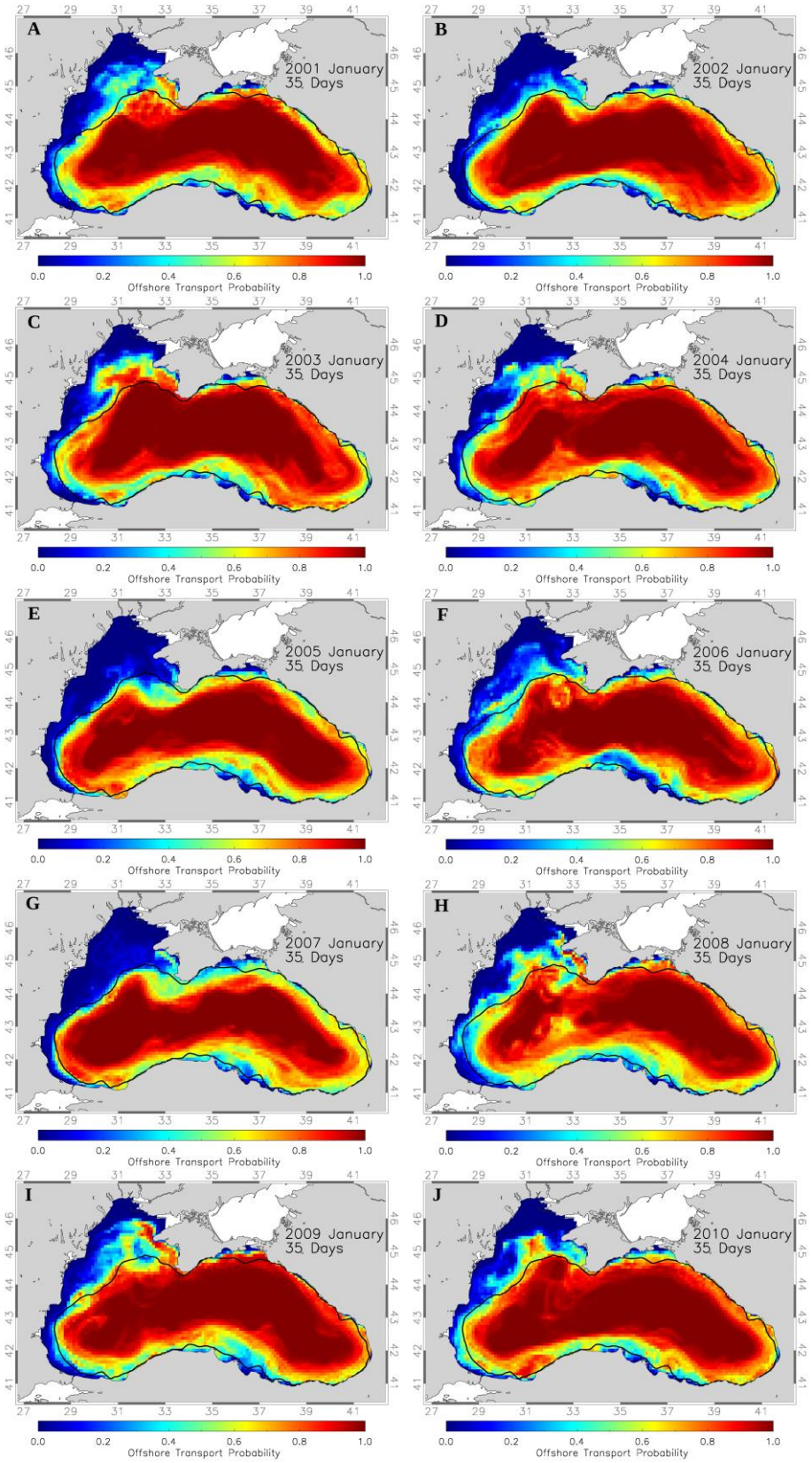

Figure 10: Simulation results of Offshore Transport Probability (OFTP) for simulations with January spawning times and 35 day Pelagic Larval Duration for A-J: 2001-2010.

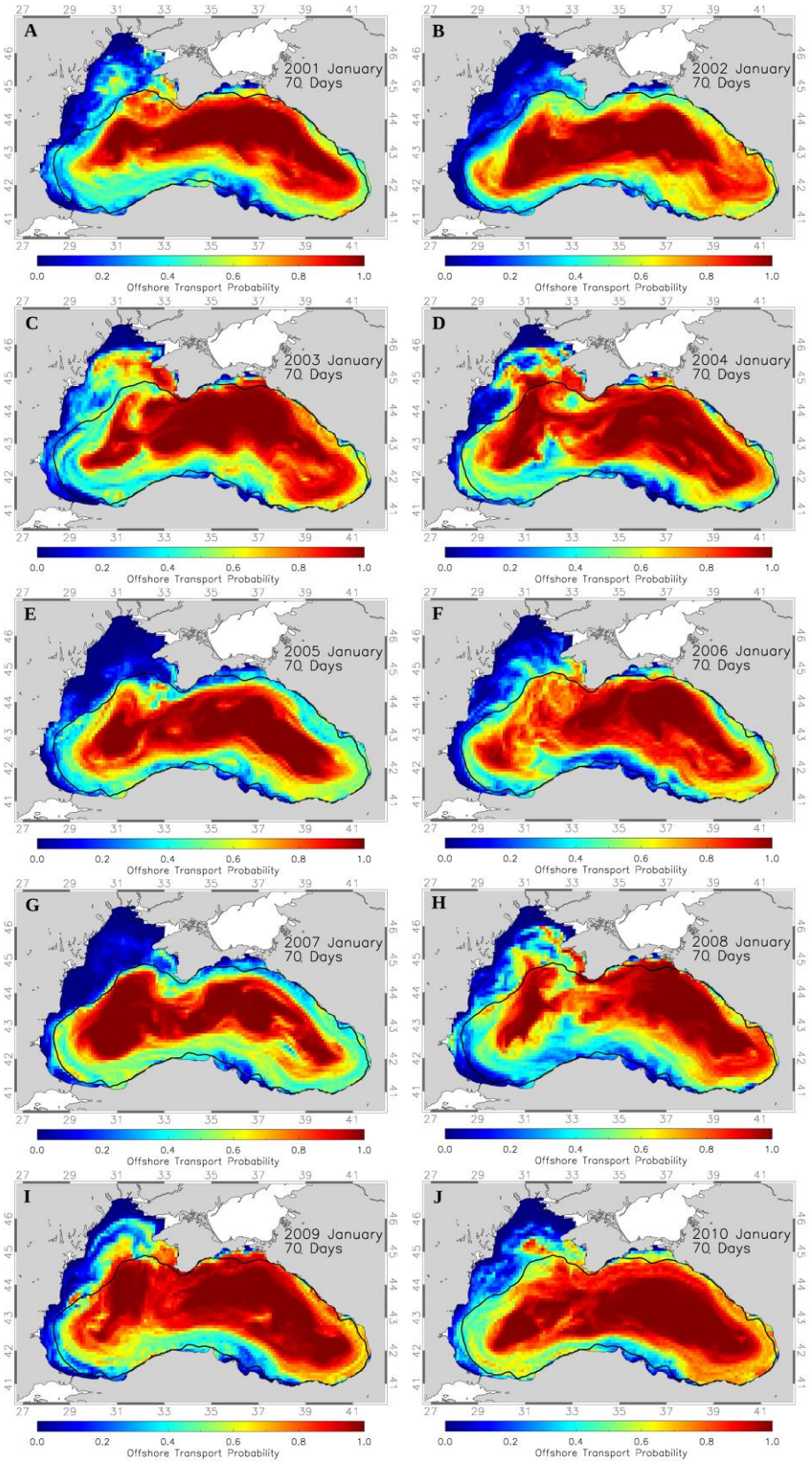

Figure 11: Simulation results of Offshore Transport Probability (OFTP) for simulations with January spawning times and 70 day Pelagic Larval Duration for A-J: 2001-2010.

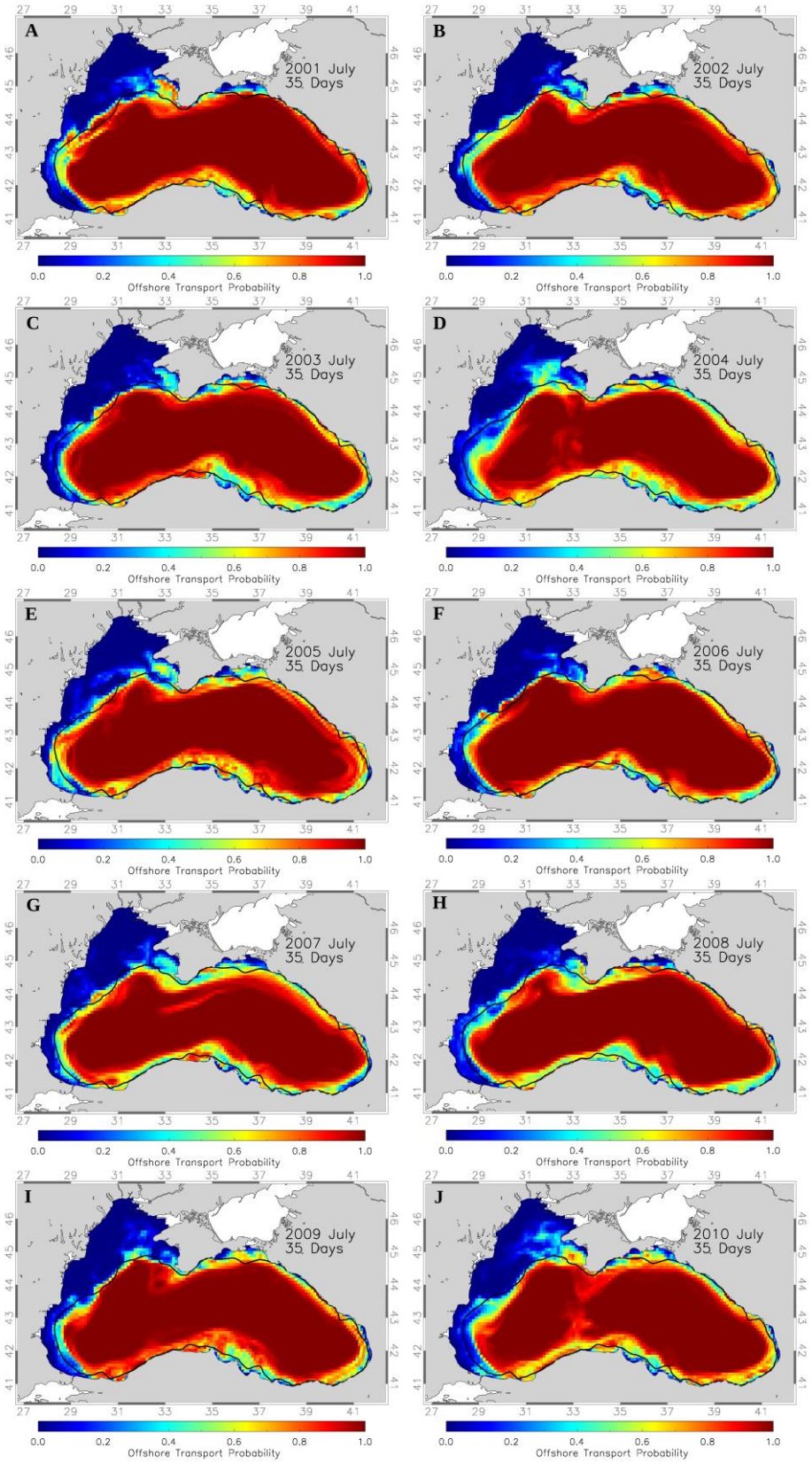

Figure 12: Simulation results of Offshore Transport Probability (OFTP) for simulations with July spawning times and 35 day Pelagic Larval Duration for A-J: 2001-2010.

The July simulation with 35 days (Figure 12) results in contrast to the January simulation with 70 days (Figure 11) represents the lowest overall OFTP values for all seasons. The 35 day July results (Figure 12) show that areas of low retention previously mentioned, such as the north western shelf, and south eastern coast of Turkey still remain. The remaining areas show a reduction in overall values compared to January.

Table 8. Offshore Transport Probability (OFTP) averages of July for different regions from years 2001 to 2010 with Pelagic Larval Duration (PLD) average of 35 days.

July 35 Day PLD OFTP Averages	2001	2002	2003	2004	2005	2006	2007	2008	2009	2010
Sevastapol Eddy	0.7	0.4	0.4	0.3	0.5	0.2	0.4	0.5	0.2	0.7
NW Shelf Coast	0.1	0.1	0.1	0.1	0.1	0.1	0.1	0.1	0.1	0.2
NW Shelf Center	0.2	0.2	0.1	0.4	0.3	0.1	0.1	0.1	0.2	0.3
Kaliakra Eddy	0.1	0.1	0.1	0.1	0.2	0.1	0.2	0.1	0.1	0.1
W Coast	0.3	0.3	0.2	0.2	0.3	0.2	0.1	0.2	0.3	0.3
SW Coast	0.1	0.2	0.2	0.4	0.4	0.1	0.4	0.2	0.2	0.4
S Coast	0.8	0.9	0.9	0.8	0.8	0.7	0.5	0.5	0.9	0.7
SE Coast	0.4	0.3	0.3	0.4	0.4	0.3	0.4	0.4	0.4	0.4
Georgian Coast	0.6	0.7	0.4	0.6	0.5	0.5	0.4	0.4	0.7	0.7
E Coast	0.8	0.7	0.6	0.5	0.8	0.7	0.6	0.8	0.6	0.6
N Coast	0.3	0.3	0.3	0.3	0.5	0.7	0.3	0.3	0.6	0.7
West Gyre	0.9	0.8	0.8	0.7	0.8	0.9	0.9	0.9	0.9	0.8
East Gyre	0.9	0.9	0.9	0.9	0.9	0.9	0.8	0.8	0.8	0.8

At first glance going from July 35 day to 70 day results show a continuation of the specific features in a given region for that year for example the high OFTP values in the Sevastapol region for 2001 at 35 days (Figure 11A) become more pronounced at 70 days (Figure 13A) with high OFTP spreading towards the north western shelf. Unique features for July are the high OFTP protrusions around the north western shelf and the Sevastapol eddy at 2001 (Figure 13A), 2004 (Figure 13D) and 2006 (Figure 13F), the unique lower OFTP of the rim current periphery, causing almost bending

shapes of the inner gyre, for 2004 (Figure 13D) compared to all other years, the high western coast OFTP values only present in 2005 (Figure 13E) and the higher OFTP values at the Azov Sea entrance in 2005 (Figure 13E), 2009 (Figure 13I), 2010 (Figure 13J) compared to remaining years.

Table 9. Offshore Transport Probability (OFTP) averages of July for different regions from years 2001 to 2010 with Pelagic Larval Duration (PLD) average of 70 days.

July 70 Day PLD OFTP Averages	2001	2002	2003	2004	2005	2006	2007	2008	2009	2010
Sevastapol Eddy	0.8	0.4	0.3	0.3	0.5	0.5	0.4	0.7	0.4	0.5
NW Shelf Coast	0.2	0.2	0.1	0.2	0.1	0.1	0.1	0.1	0.2	0.3
NW Shelf Center	0.4	0.3	0.2	0.5	0.4	0.4	0.3	0.4	0.2	0.4
Kaliakra Eddy	0.3	0.1	0.1	0.3	0.2	0.1	0.1	0.2	0.1	0.3
W Coast	0.5	0.4	0.2	0.3	0.5	0.4	0.3	0.2	0.2	0.2
SW Coast	0.3	0.2	0.3	0.4	0.6	0.2	0.4	0.2	0.2	0.5
S Coast	0.6	0.5	0.7	0.5	0.6	0.7	0.7	0.5	0.8	0.7
SE Coast	0.5	0.3	0.4	0.4	0.5	0.3	0.3	0.3	0.5	0.5
Georgian Coast	0.6	0.6	0.6	0.5	0.7	0.6	0.5	0.7	0.5	0.5
E Coast	0.8	0.5	0.7	0.5	0.6	0.5	0.5	0.5	0.6	0.7
N Coast	0.5	0.4	0.5	0.5	0.7	0.5	0.3	0.4	0.6	0.7
West Gyre	0.7	0.7	0.8	0.6	0.7	0.8	0.8	0.7	0.7	0.6
East Gyre	0.8	0.7	0.7	0.7	0.7	0.8	0.7	0.8	0.8	0.7

The Western Gyre in the 35 day simulation consistently shows a flat distribution of cells ranging from 0.5 to 0.8 at the coasts and 0.8 to 1.0 at the center of the Gyre (Figure 12). The years 2004 and 2010 show cells of 0.8 OFTP almost connecting with one another forming a circular structure, while 2009 has a small eddy shaped structure just south of the Sevastapol region in the Western Gyre that is made up of cells averaging at 0.8 OFTP. During the 70 day simulations a meandering structure of cells protrude from the outer coast of the gyre with lower OFTP values between 0.3 and 0.5 these features are more visible on years 2004, and 2010 (Figure 13). In general these aforementioned years have these lower valued cells and meandering structures in the

inner cell as well. Cells just south of the Sevastapol region see a decrease in OFTP down to 0.4 and 0.5 in 2002 and 2004. Also the eddy like structure is present in the years 2002, 2004, 2006 and 2008. The Eastern Gyre in the 35 day PLD simulations sees a mostly consistent 0.9 to 1.0 OFTP distribution at the center and the coasts. 2007 shows a band of cells north west of the gyre with an average value of 0.8. In the 70 day PLD simulation on the other hand the Eastern Gyre sees a decrease of OFTP in the outer cells of the Gyre, more notably to the south, averaging around 0.5 and 0.6 OFTP values, the band structure is present at 0.8 value north and east of the gyre in 2004, north and east center of the gyre at an average of 0.7 in 2007 and with an average of 0.6 east of the gyre in 2010.

Simulated OFTP values in July (Figure 12, Figure 13) compared to January (Figure 10, Figure 11) appear lower in overall and shallow areas of high OFTP in January results appear to have withdrawn in July results. At the same time the deep areas of low OFTP in January appear to have enlarged with higher values towards the coasts. Apart from 2004 (Figure 13D) and 2010 (Figure 13J) the July results appear more similar to each other with these two years having an inner gyre structure and rim current periphery at lower OFTP values.

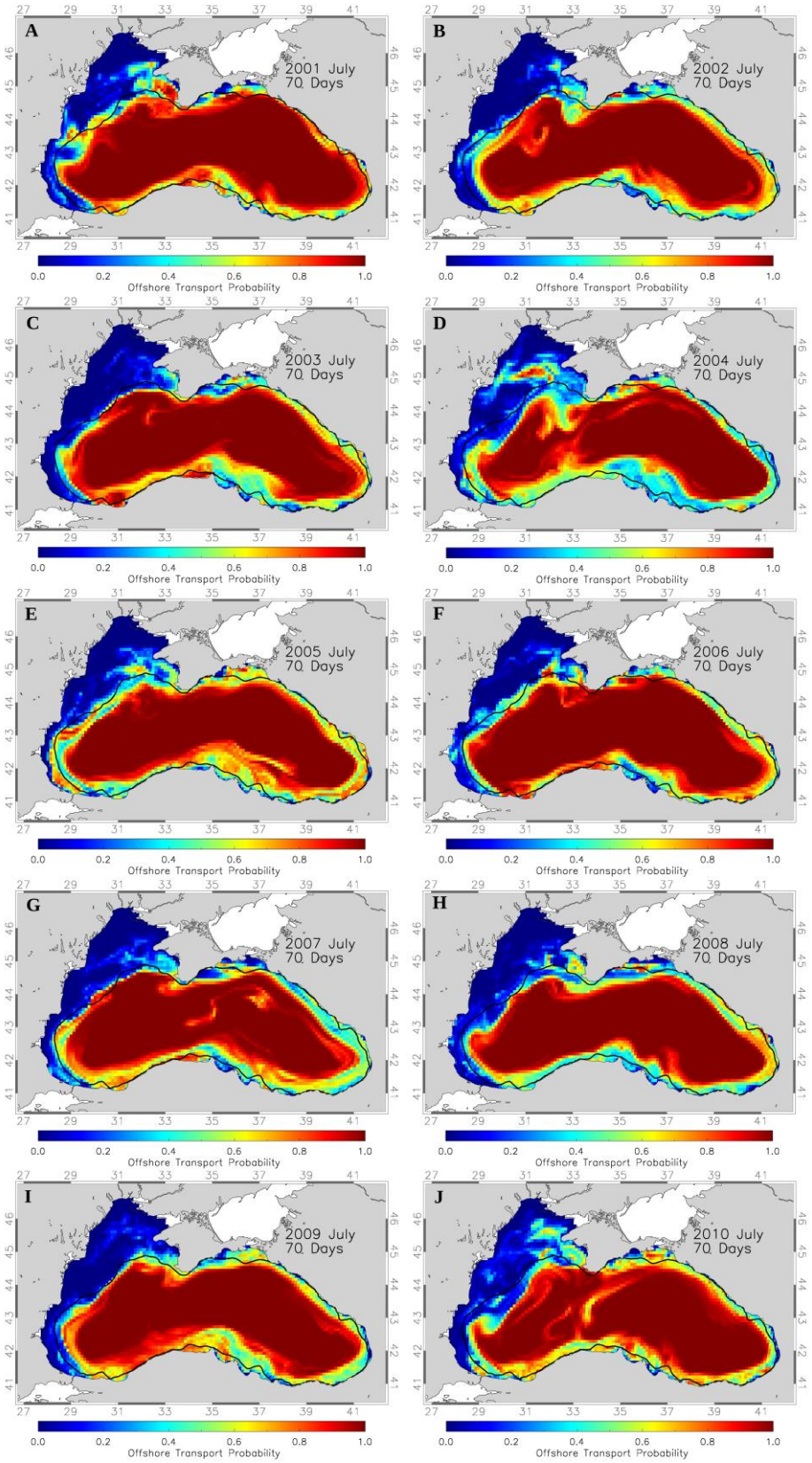

Figure 13: Simulation results of Offshore Transport Probability (OFTP) for simulations with July spawning times and 70 days Pelagic Larval Duration for A-J: 2001-2010.

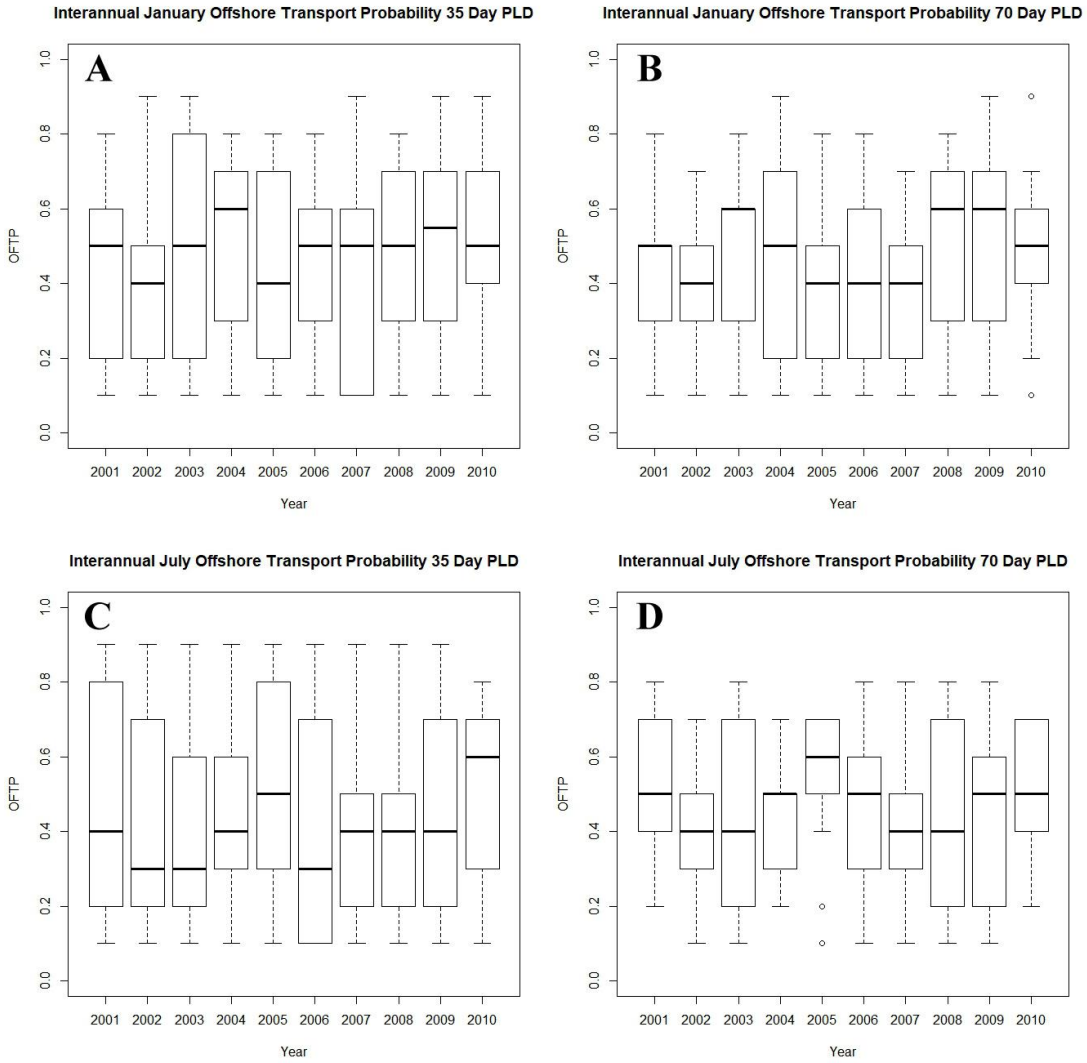

Figure 14: Box-Whisker plots of Interannual Offshore Transport Probabilities derived from Table 6, Table 7, Table 8 and Table 9. A: January 35 day PLD, B: January 70 day PLD, C: July 35 day PLD, D: July 70 day PLD. The circles denote extreme values outside the range of the average.

The box-whisker plots of the interannual OFTP simulation results (Figure 14) displays the average values and variation between the different years. The average OFTP is 0.46 for the January simulations with 35 days (Figure 10) and 0.44 for the 70 day (Figure 11) simulation, while it is 0.45 for the July simulation with 35 days (Figure 12) and 0.46 for the 70 day (Figure 13) simulation. However the range of different values for each year appears to be big, some 70 day PLD cases like January 2001 (Figure 11A), 2002 (Figure 11B) or July 2002 (Figure 13B), 2005 (Figure 13E) show closer grouped values.

3.2 Local Retention and Self Recruitment

LR and SR data are analyzed similarly to the ONTP and OFTP results, accounting for PLD variability, seasonal changes and interannual differences. The 13 regions previously established are also used in this section. It should also be noted that the majority of results for LR and SR data are distributed between 0.0 and 0.001 range, therefore in order to make plotting more coherent a logarithmic distribution is used for the plots rather than a linear distribution.

3.2.1 Impact of Different Larval Durations

Comparison of the effect of PLD on the respective LR (Figure 15) and SR (Figure 16) distribution show almost near identical plots for both analysis. In general, both show higher values in the 20 day simulation than in the 70 day simulation, highest values are located on the north western shelf and coastal areas near the Azov Sea entrance. In the location of the rim current no Local Retention or Self Recruitment is found. The similarities between the two analyses are due to the fact that SR is a) derived from LR and b) probabilities have been averaged over 10 years and all 4 seasons. SR only starts to deviate from LR in longer PLD's with no averaging of the data. Due to the almost imperceptible difference, only LR data is discussed in this section. The calculations for LR and SR (section 2) both use the number of retained particles while SR uses the final number of particles in the grid cell as opposed to the initial number of particles for LR on top of this the metrics are then logarithmically scaled losing the resolution in the higher ranges. The end results shows very similar plots for both metrics, with about 1 to 5 grid cells with different values comparing LR and SR.

In general the high LR values (Figure 16) are concentrated in the Sevastapol eddy, the north western shelf, western coast, the Sakarya eddy, south eastern coast of Turkey and the entrance to the Azov Sea. Increase in PLD sees the LR values drop overall but the areas that have high LR remain the same.

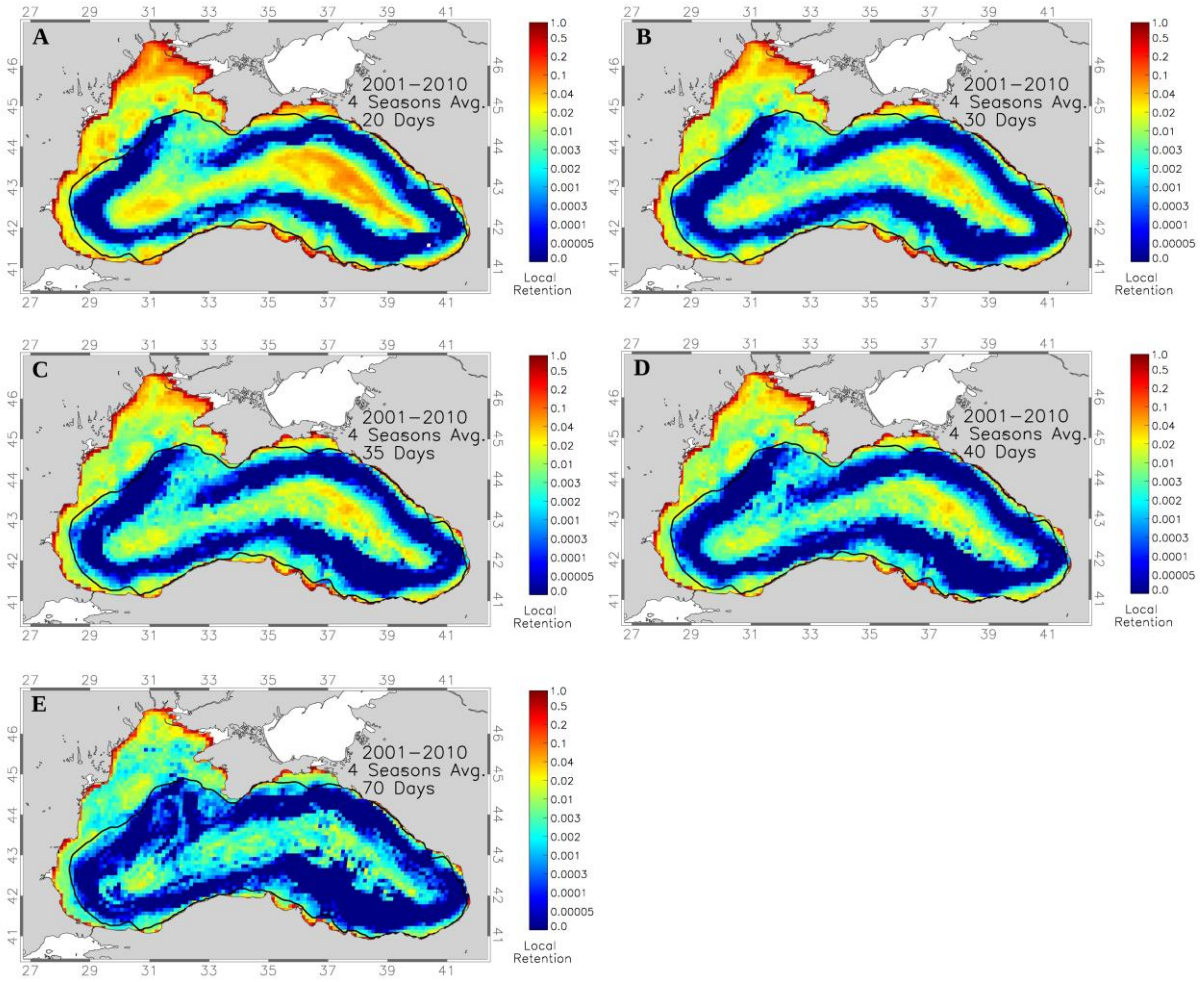

Figure 15: Simulation results of 10 years (2001-2010) and four seasons averaged to calculate the Local Retention (LR) depending on different Pelagic Larval Durations (PLD). A: 20 day PLD, B: 30 day PLD, C: 35 day PLD, D: 40 day PLD, and E: 70 day PLD.

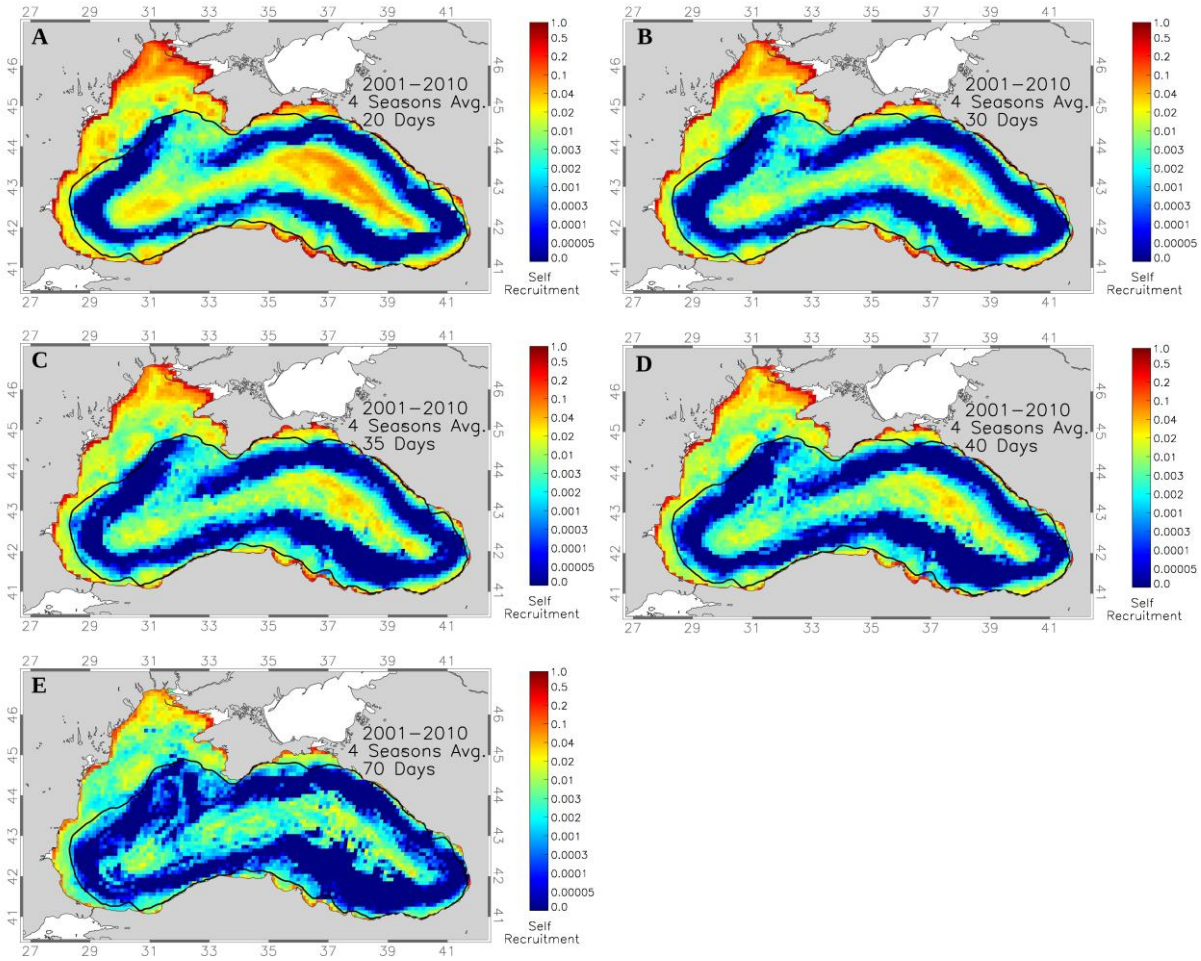

Figure 16: Simulation results of 10 years (2001-2010) and four seasons averaged to calculate the Self Recruitment (SR) depending on different Pelagic Larval Durations (PLD). A: 20 day PLD, B: 30 day PLD, C: 35 day PLD, D: 40 day PLD, and E: 70 day PLD.

The effect of PLD length on LR can be seen in Figure 15 and average values are listed in Table 10. The LR values show a sharp decrease in 70 days compared to the rest while the LR values for 30, 35 and 40 days tend to be very similar to one another. The inner gyres also show moderate to high LR values with the exception of 70 day PLD (Table 10).

Table 10. Local Retention (LR) averages of different regions for different Pelagic Larval Durations (PLD) deduced from simulation results of 10 years (2001-2010) and 4 seasons averaged.

2001-2010 4 Seasons Local Retention Averages	20 days	30 days	35 days	40 days	70 days
Sevastapol Eddy	0.04	0.02	0.02	0.02	0.01
NW Shelf Coast	0.2	0.1	0.1	0.04	0.02
NW Shelf Center	0.02	0.02	0.01	0.01	0.003
Kaliakra Eddy	0.04	0.02	0.02	0.02	0.003
W Coast	0.04	0.02	0.02	0.02	0.01
SW Coast	0.02	0.01	0.01	0.01	0.003
S Coast	0.02	0.02	0.01	0.01	0.002
SE Coast	0.2	0.2	0.2	0.2	0.1
Georgian Coast	0.02	0.02	0.02	0.02	0.002
E Coast	0.02	0.003	0.003	0.003	0.001
N Coast	0.04	0.04	0.04	0.04	0.01
West Gyre	0.02	0.01	0.01	0.01	0.002
East Gyre	0.04	0.02	0.02	0.02	0.003

The spatial distribution shows highest values are located on the north western shelf and coastal areas of the Kerch Strait region. In the location of the rim current no or minimal Local Retention is found. Some regions like the Azov Sea are less effected by the increase of PLD until the 70 day PLD simulation. Nearly all coasts, excluding the Caucasus coast, have high LR values in the range of 0.5 to 1.0 at all PLD values including 70 days.

3.2.2 Seasonal Variability

In order to compare the LR seasonal differences, results from 2001 to 2010 are averaged within their respective seasons. Only the 35 day (Figure 17) and 70 day (Figure 18) results are compared as the commercially important fish species have these PLD's and 35 day results can reasonably represent 20, 30 and 40 days. Also the change from 35 days to 70 days provides contrast between high and low retention areas.

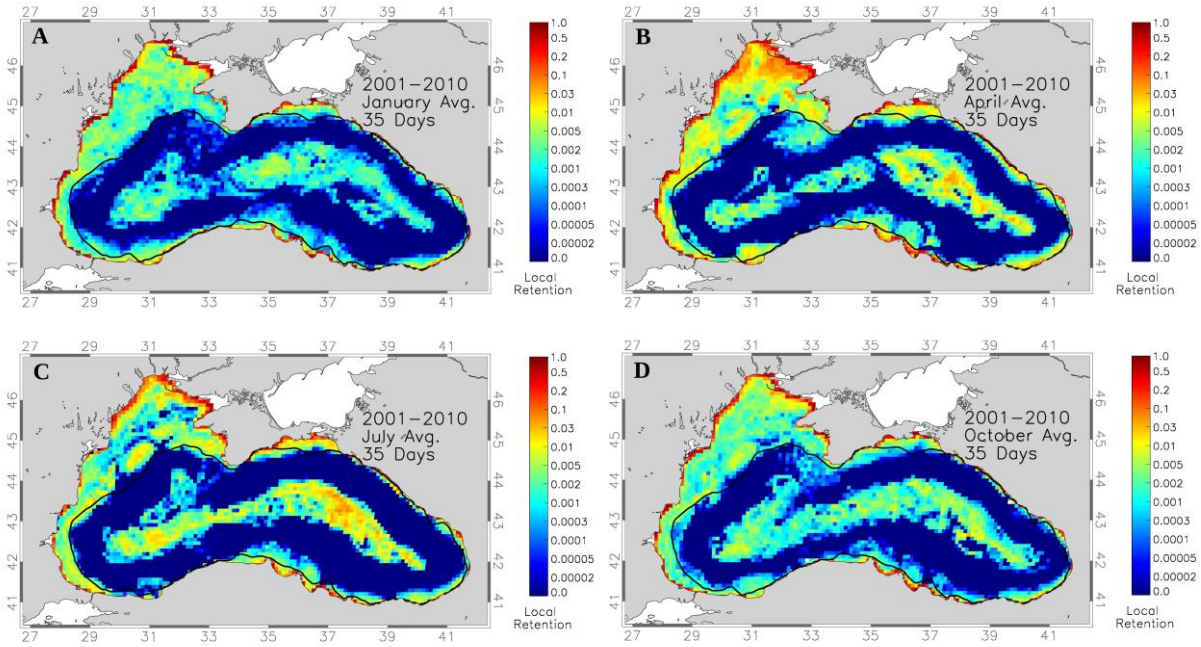

Figure 17: Simulation results of 10 years (2001-2010) averaged at 35 day Pelagic Larval Duration (PLD) to calculate the Local Retention (LR) for all seasonal averages. A: January average, B: April average, C: July average and D: October average.

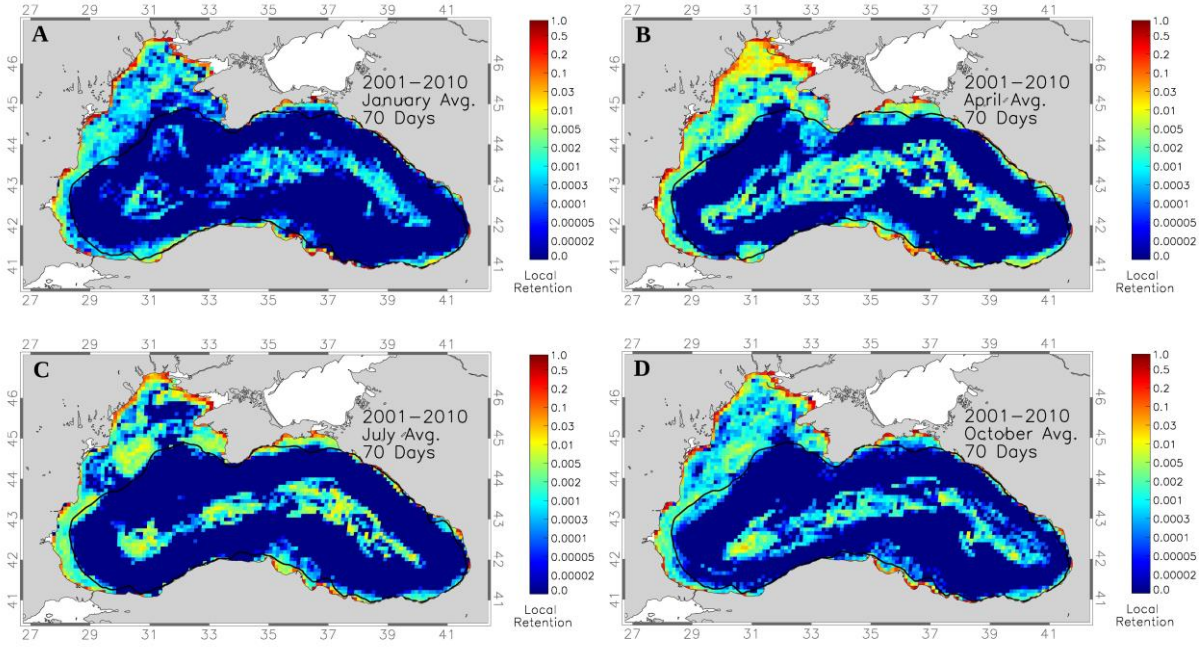

Figure 18: Simulation results of 10 years (2001-2010) averaged at 70 day Pelagic Larval Duration (PLD) to calculate the Local Retention (LR) for all seasonal averages. A: January average, B: April average, C: July average and D: October average.

The 35 day PLD (Table 11) in January simulation result (Figure 17A) starts with the lowest LR values, reaches the highest values in April (Figure 17B) especially in the north western shelf. In July (Figure 17C) the LR values start to decrease then in October (Figure 17D) decrease to the point of almost matching January values. High LR areas are the north western shelf, western coast, south eastern coast of Turkey and the entrance to the Azov Sea for all seasons. The Sakarya eddy exhibits high LR in January and April, Sevastapol eddy in April, July and October, Georgian coast in April and finally the inner gyres in April and July with April covering a wider area.

Table 11. Local Retention (LR) averages of different regions for each season deduced from simulation results of 10 years (2001-2010) averaged at 35 day Pelagic Larval Duration (PLD).

2001-2010 35 Day Local Retention Averages	January	April	July	October
Sevastapol Eddy	0.002	0.01	0.01	0.002
NW Shelf Coast	0.01	0.03	0.01	0.01
NW Shelf Center	0.005	0.01	0.01	0.005
Kaliakra Eddy	0.005	0.01	0.01	0.005
W Coast	0.002	0.01	0.005	0.002
SW Coast	0.002	0.005	0.01	0.001
S Coast	0.001	0.002	0.0003	0.001
SE Coast	0.01	0.1	0.01	0.03
Georgian Coast	0.002	0.03	0.01	0.002
E Coast	0.0001	0.01	0.0001	0.0001
N Coast	0.005	0.01	0.01	0.005
West Gyre	0.001	0.001	0.01	0.01
East Gyre	0.001	0.01	0.03	0.01

At 70 day PLD (Figure 18) the seasons behave similar to 35 days, in January LR is minimum next in April reach maximum then in July decreasing finally in October almost reaching the minimum values of January.

Regional features are similar to 35 days with LR cells with values of 0.0 or very close to 0.0 increase in areas covered in almost all regions at 70 days. However the south eastern coast seems to be an exception as in both PLD's the coast retains a high LR average.

Table 12. Local Retention (LR) averages of different regions for each season deduced from simulation results of 10 years (2001-2010) averaged at 70 day Pelagic Larval Duration (PLD).

2001-2010 70 Day Local Retention Averages	January	April	July	October
Sevastapol Eddy	0.0003	0.005	0.005	0.002
NW Shelf Coast	0.001	0.1	0.01	0.005
NW Shelf Center	0.002	0.005	0.001	0.002
Kaliakra Eddy	0.002	0.005	0.005	0.002
W Coast	0.001	0.002	0.002	0.002
SW Coast	0.0003	0.001	0.002	0.001
S Coast	0.001	0.0003	0.00002	0.00005
SE Coast	0.01	0.03	0.01	0.03
Georgian Coast	0.002	0.005	0.001	0.001
E Coast	0.0001	0.001	0.0003	0.0001
N Coast	0.002	0.005	0.005	0.002
West Gyre	0.0003	0.002	0.002	0.002
East Gyre	0.001	0.005	0.005	0.001

3.2.3 Interannual Variability

January and April are included in the section as they contain the minimum and maximum LR values respectively and July is included as anchovy spawn in that season, October is omitted as it resembles January and it is available in the appendix. The PLD's are 35 and 70 days for anchovy and sprat.

Table 13. Local Retention (LR) averages of January for different regions from years 2001 to 2010 with Pelagic Larval Duration (PLD) average of 35 days.

January 35 Day PLD LR Averages	2001	2002	2003	2004	2005	2006	2007	2008	2009	2010
Sevastapol Eddy	0.001	0.005	0.002	0.001	0.002	0.002	0.002	0.0001	0.0001	0.01
NW Shelf Coast	0.1	0.1	0.05	0.05	0.1	0.1	0.1	0.2	0.1	0.1
NW Shelf Center	0.005	0.02	0.001	0.002	0.02	0.01	0.02	0.01	0.002	0.05
Kaliakra Eddy	0.002	0.01	0.05	0.01	0.001	0.002	0.002	0.002	0.002	0.01
W Coast	0.005	0.01	0.005	0.01	0.001	0.002	0.001	0.005	0.005	0.01
SW Coast	0.002	0.005	0.005	0.002	0.001	0.001	0.001	0.002	0.005	0.01
S Coast	0.002	0.002	0.002	0.002	0.0005	0.001	0.002	0.002	0.001	0.005
SE Coast	0.05	0.05	0.05	0.05	0.05	0.05	0.05	0.05	0.02	0.05
Georgian Coast	0.01	0.005	0.01	0.005	0.002	0.002	0.002	0.002	0.002	0.002
E Coast	0.0005	0.0005	0.0005	0.0005	0.0005	0.0005	0.0005	0.0005	0.0005	0.0005
N Coast	0.002	0.005	0.005	0.005	0.002	0.002	0.002	0.002	0.001	0.02
West Gyre	0.001	0.002	0.002	0.002	0.001	0.002	0.002	0.005	0.002	0.005
East Gyre	0.005	0.005	0.005	0.005	0.005	0.005	0.005	0.005	0.005	0.005

The January 35 day LR values (Table 13, Figure 19) shows generally low LR values in the Black Sea. Regions with higher LR values are the north western shelf, western coast, south eastern coast of Turkey and in some years the Kaliakra eddy (Figure 19C) and the entrance to the Azov Sea (Figure 19J).

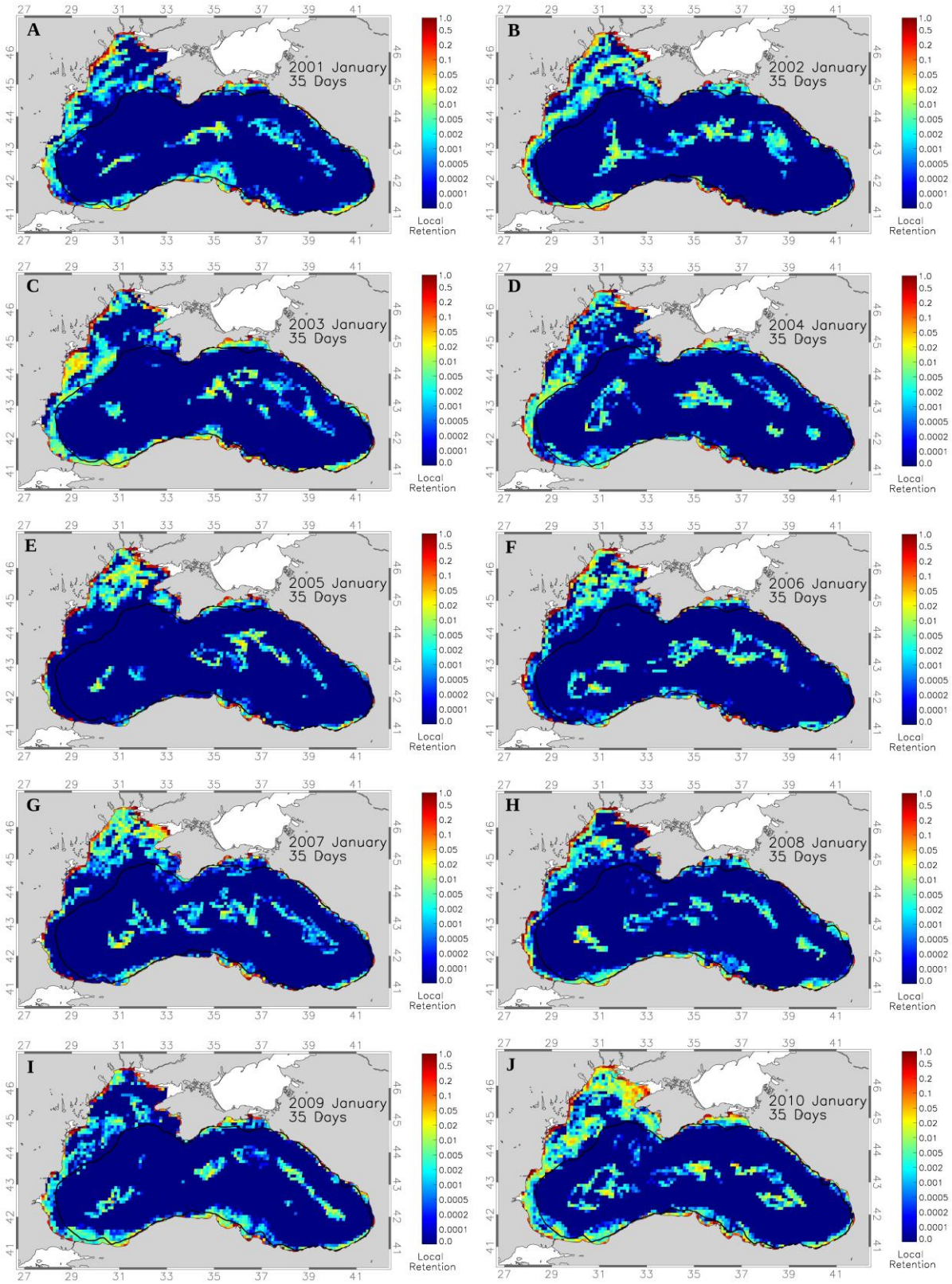

Figure 19: Simulation results of Local Retention (LR) using January spawning times and 35 day Pelagic Larval Duration (PLD) for A-J: 2001-2010.

The south eastern coast has high LR averages at the coastal cells for both 35 (Figure 19) and 70 (Figure 20) day PLD's ranging from 0.1 to 1.0 however the number of offshore cells with 0.0 LR is increased at 70 days (Table 14). Georgian coast LR averages between 0.002 and 0.002 near the coast for 35 days (Figure 19) and for 70 days (Figure 20) LR average drops close to 0.0. The eastern coast for both 35 and 70 day PLD's averages close to 0.0 apart from some coastal cells close to 1.0. Northern coast at 35 day PLD the Azov Sea entrance averages between 0.005 and 0.01 with some coastal cells between 0.1 and 1.0, with 70 day PLD the LR average drops near 0.0005. The western gyre at 35 day (Figure 19) PLD has cells scattered around ranging from 0.002 to 0.02, at 70 days (Figure 20) there is almost no LR, notable exceptions are 2004 (Figure 20D) with an LR average of 0.002 and 2010 (Figure 20J) 0.02. The eastern gyre at 35 days (Figure 19) LR averages 0.002 and 0.02 with pockets of cells scattered in the region, at 70 days (Figure 20) the average LR decreases close to 0.0 with very few cells around 0.001 and 0.002 LR.

The LR results of the January simulation with 70 day PLD (Figure 20, Table 14) exhibit the lowest LR values. The entire Black Sea has almost no retention apart from a few coastal cells. Even the previously mentioned areas of high retention show a significant decrease of LR value at this PLD. The western coast (Figure 20) appears as the only semi consistent in all years that has moderate LR values.

Table 14. Local Retention (LR) averages of January for different regions from years 2001 to 2010 with Pelagic Larval Duration (PLD) average of 70 days.

January 70 Day PLD LR Averages	2001	2002	2003	2004	2005	2006	2007	2008	2009	2010
Sevastapol Eddy	0.0001	0.0002	0.0002	0.0001	0.0005	0.0005	0.0005	0.0001	0.0001	0.001
NW Shelf Coast	0.01	0.02	0.01	0.005	0.01	0.01	0.005	0.005	0.005	0.02
NW Shelf Center	0.002	0.01	0.001	0.0001	0.002	0.002	0.0001	0.0001	0.0001	0.001
Kaliakra Eddy	0.001	0.001	0.002	0.005	0.0001	0.0001	0.0001	0.0001	0.002	0.0005
W Coast	0.001	0.005	0.001	0.005	0.0001	0.005	0.0001	0.0005	0.002	0.002
SW Coast	0.001	0.001	0.002	0.002	0.0001	0.001	0.0001	0.001	0.002	0.002
S Coast	0.0001	0.0001	0.0001	0.0001	0.0001	0.0001	0.0001	0.0001	0.0001	0.0001
SE Coast	0.01	0.01	0.01	0.01	0.01	0.01	0.01	0.01	0.01	0.01
Georgian Coast	0.001	0.001	0.001	0.001	0.001	0.001	0.001	0.001	0.001	0.001
E Coast	0.001	0.001	0.001	0.001	0.001	0.001	0.001	0.001	0.001	0.001
N Coast	0.001	0.001	0.001	0.001	0.001	0.001	0.001	0.001	0.002	0.002
West Gyre	0.0001	0.0001	0.0001	0.002	0.0001	0.0001	0.0001	0.0001	0.001	0.002
East Gyre	0.001	0.001	0.001	0.001	0.001	0.001	0.001	0.001	0.001	0.001

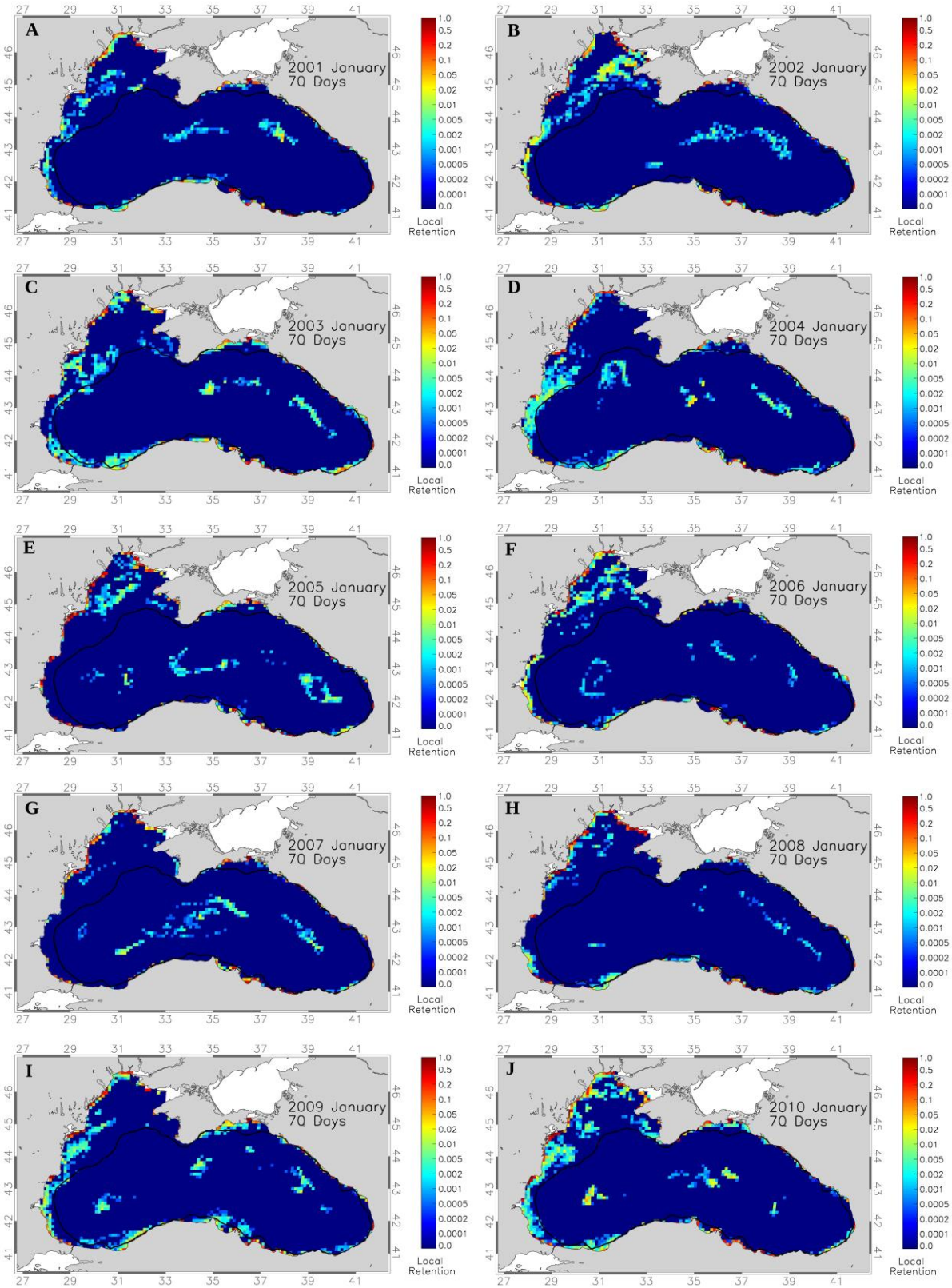

Figure 20: Simulation results of Local Retention (LR) using January spawning times and 70 day Pelagic Larval Duration (PLD) for A-J: 2001-2010.

The April 35 day LR values (Table 15) representing the highest values create a sharp contrast to January. The high LR areas are Sevastapol eddy, the north western shelf, western coast, south eastern coast of Turkey, Georgian coast and the entrance to the Azov Sea for all years, Sakarya eddy in all years except for 2005 (Figure 21E) and 2007 (Figure 21G) and finally the coasts of the Caucasus in all years except for 2001 (Figure 21A) and 2002 (Figure 21B). Compared to January the overall LR values in April are increased and they cover much larger areas, they are also the highest values compared to all other seasons.

Table 15. Local Retention (LR) averages of April for different regions from years 2001 to 2010 with Pelagic Larval Duration (PLD) average of 35 days.

April 35 Day PLD LR Averages	**2001**	**2002**	**2003**	**2004**	**2005**	**2006**	**2007**	**2008**	**2009**	**2010**
Sevastapol Eddy	0.01	0.01	0.01	0.02	0.01	0.01	0.05	0.05	0.01	0.05
NW Shelf Coast	0.1	0.05	0.05	0.1	0.1	0.1	0.1	0.1	0.1	0.1
NW Shelf Center	0.005	0.005	0.005	0.005	0.01	0.01	0.005	0.005	0.01	0.005
Kaliakra Eddy	0.01	0.005	0.005	0.002	0.005	0.002	0.002	0.005	0.01	0.01
W Coast	0.02	0.01	0.005	0.005	0.005	0.01	0.02	0.02	0.01	0.005
SW Coast	0.005	0.005	0.001	0.01	0.001	0.005	0.001	0.001	0.001	0.02
S Coast	0.0001	0.0001	0.0001	0.0001	0.0001	0.0001	0.0001	0.0001	0.0001	0.0001
SE Coast	0.1	0.1	0.1	0.1	0.1	0.1	0.1	0.1	0.1	0.1
Georgian Coast	0.01	0.005	0.005	0005	0.002	0.005	0.005	0.01	0.01	0.005
E Coast	0.005	0.001	0.005	0.01	0.005	0.005	0.005	0.01	0.005	0.005
N Coast	0.01	0.01	0.01	0.01	0.01	0.01	0.01	0.01	0.01	0.01
West Gyre	0.005	0.005	0.005	0.005	0.005	0.005	0.005	0.005	0.005	0.005
East Gyre	0.005	0.05	0.05	0.02	0.02	0.05	0.005	0.02	0.005	0.005

The results of the 70 day PLD simulation (Table 16) starting in April shows the expected decrease in LR values, however compared to the rest of the seasons April at 70 days shows a less sharp decrease from 35 to 70 days as retention is still visibly seen in non-coastal areas. Years 2006 (Figure 22F) and 2010 (Figure 22J) stand out with very high LR values and area coverage of the north western shelf. The effect of the Sakarya eddy is almost gone with the exception of 2004 (Figure 22D).

Table 16. Local Retention (LR) averages of April for different regions from years 2001 to 2010 with Pelagic Larval Duration (PLD) average of 70 days.

April 70 Day PLD LR Averages	**2001**	**2002**	**2003**	**2004**	**2005**	**2006**	**2007**	**2008**	**2009**	**2010**
Sevastapol Eddy	0.001	0.002	0.001	0.01	0.005	0.005	0.001	0.001	0.001	0.005
NW Shelf Coast	0.1	0.05	0.05	0.1	0.1	0.1	0.1	0.1	0.1	0.1
NW Shelf Center	0.001	0.002	0.005	0.002	0.002	0.01	0.001	0.001	0.001	0.005
Kaliakra Eddy	0.005	0.005	0.005	0.001	0.001	0.0001	0.0001	0.0001	0.005	0.01
W Coast	0.005	0.005	0.002	0.001	0.001	0.001	0.001	0.005	0.005	0.001
SW Coast	0.0001	0.0001	0.0001	0.005	0.0001	0.0001	0.0001	0.0001	0.0001	0.0001
S Coast	0.0001	0.0001	0.0001	0.0001	0.0001	0.0001	0.0001	0.0001	0.0001	0.0001
SE Coast	0.02	0.02	0.02	0.005	0.05	0.005	0.005	0.005	0.02	0.05
Georgian Coast	0.002	0.001	0.002	0.002	0.001	0.001	0.002	0.001	0.002	0.001
E Coast	0.001	0.001	0.001	0.001	0.001	0.001	0.001	0.001	0.001	0.001
N Coast	0.005	0.005	0.001	0.005	0.002	0.002	0.002	0.005	0.002	0.001
West Gyre	0.0001	0.0001	0.005	0.005	0.002	0.0001	0.0001	0.005	0.001	0.005
East Gyre	0.002	0.002	0.001	0.001	0.002	0.002	0.002	0.0001	0.0001	0.005

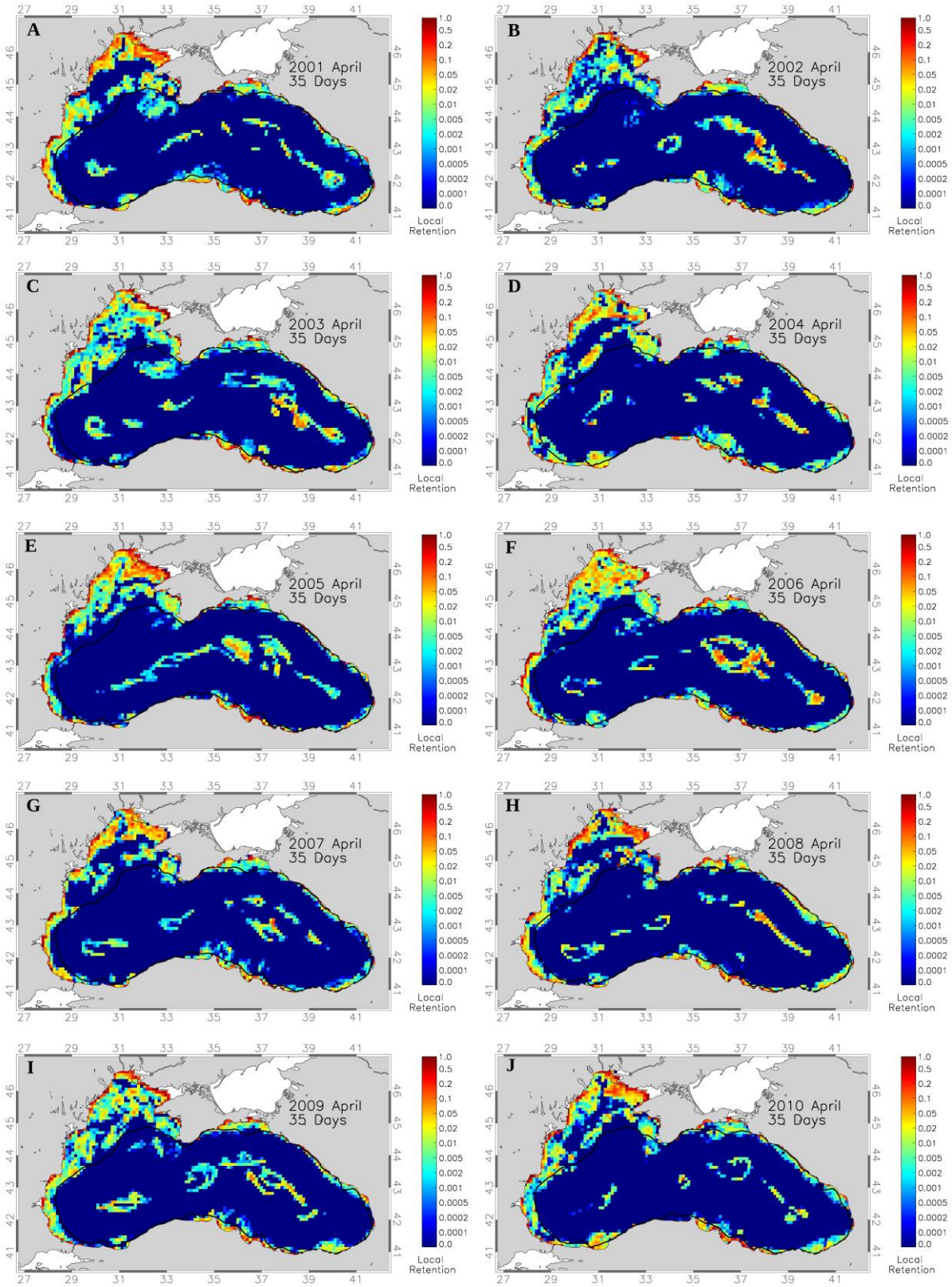

Figure 21: Simulation results of Local Retention (LR) using April spawning times and 35 day Pelagic Larval Duration (PLD) for A-J: 2001-2010.

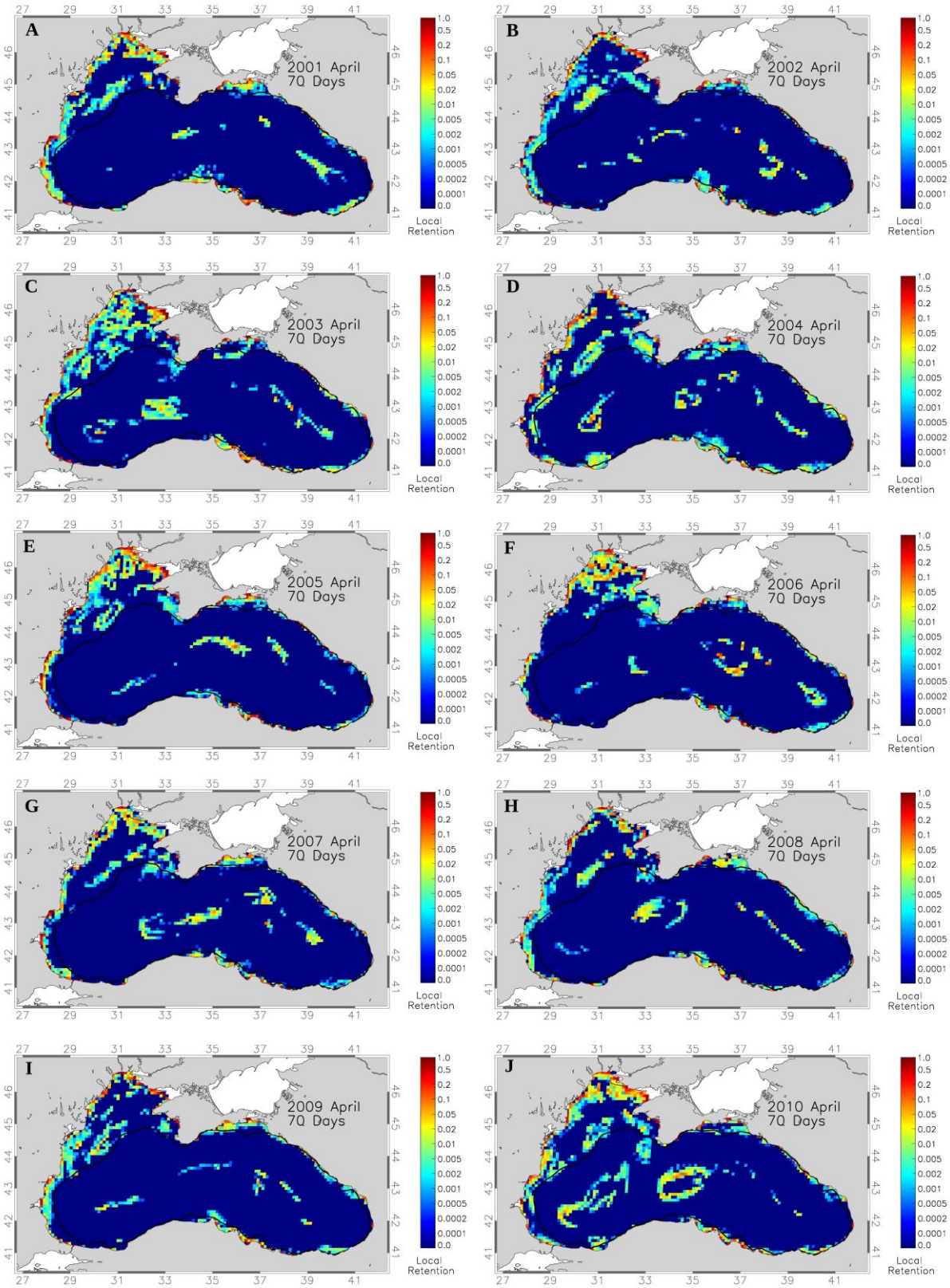

Figure 22: Simulation results of Local Retention (LR) using April spawning times and 70 day Pelagic Larval Duration (PLD) for A-J: 2001-2010.

July 35 day (Table 17) results appear similar to April 35 day (Table 15) results but with lower LR values and area coverage. Some areas such as the Sevastapol region disappears in all years except for 2010 (Figure 23J). All years feature the high LR areas of the Sevastapol eddy, north western shelf, the south eastern coast of Turkey and the entrance to the Azov Sea, the LR areas at the Caucasus coast shrink down considerably compared to April. Band like LR structures in the inner gyres start showing up and cover more area than April.

Table 17. Local Retention (LR) averages of July for different regions from years 2001 to 2010 with Pelagic Larval Duration (PLD) average of 35 days.

July 35 Day PLD LR Averages	2001	2002	2003	2004	2005	2006	2007	2008	2009	2010
Sevastapol Eddy	0.01	0.005	0.02	0.002	0.005	0.02	0.01	0.002	0.02	0.005
NW Shelf Coast	0.05	0.05	0.02	0.01	0.05	0.05	0.05	0.05	0.02	0.02
NW Shelf Center	0.005	0.001	0.005	0.001	0.005	0.001	0.005	0.001	0.02	0.001
Kaliakra Eddy	0.002	0.001	0.01	0.001	0.002	0.001	0.005	0.005	0.002	0.001
W Coast	0.005	0.002	0.005	0.002	0.002	0.001	0.005	0.005	0.001	0.002
SW Coast	0.001	0.001	0.001	0.001	0.001	0.001	0.001	0.001	0.001	0.001
S Coast	0.0001	0.0001	0.0001	0.0001	0.0001	0.0001	0.0001	0.0001	0.0001	0.0001
SE Coast	0.02	0.01	0.01	0.01	0.02	0.01	0.01	0.01	0.02	0.02
Georgian Coast	0.002	0.002	0.001	0.002	0.002	0.001	0.001	0.001	0.002	0.002
E Coast	0.001	0.001	0.001	0.001	0.001	0.001	0.001	0.001	0.001	0.001
N Coast	0.02	0.02	0.02	0.02	0.02	0.01	0.01	0.02	0.01	0.005
West Gyre	0.02	0.005	0.01	0.005	0.005	0.02	0.002	0.005	0.005	0.005
East Gyre	0.01	0.01	0.01	0.05	0.01	0.05	0.005	0.01	0.01	0.005

July 70 days (Table 18) show a sharp decrease in overall LR values compared to 35 days (Table 17). The July 35 to 70 day decrease appears higher than the April 35 to 70 day PLD decrease.

Table 18. Local Retention (LR) averages of July for different regions from years 2001 to 2010 with Pelagic Larval Duration (PLD) average of 70 days.

July 70 Day PLD LR Averages	2001	2002	2003	2004	2005	2006	2007	2008	2009	2010
Sevastapol Eddy	0.001	0.002	0.001	0.002	0.001	0.001	0.002	0.001	0.02	0.001
NW Shelf Coast	0.02	0.02	0.005	0.002	0.02	0.02	0.02	0.02	0.002	0.002
NW Shelf Center	0.001	0.002	0.002	0.002	0.005	0.002	0.005	0.002	0.005	0.005
Kaliakra Eddy	0.001	0.001	0.001	0.001	0.002	0.001	0.002	0.001	0.002	0.001
W Coast	0.002	0.001	0.005	0.001	0.001	0.002	0.002	0.001	0.002	0.001
SW Coast	0.0001	0.0001	0.0001	0.0001	0.0001	0.0001	0.0001	0.0001	0.0001	0.0001
S Coast	0.0001	0.0001	0.0001	0.0001	0.0001	0.0001	0.0001	0.0001	0.0001	0.0001
SE Coast	0.005	0.002	0.005	0.005	0.02	0.005	0.005	0.005	0.005	0.005
Georgian Coast	0.001	0.001	0.001	0.001	0.001	0.001	0.001	0.001	0.001	0.001
E Coast	0.001	0.001	0.001	0.001	0.001	0.001	0.001	0.001	0.001	0.001
N Coast	0.01	0.005	0.005	0.001	0.002	0.005	0.005	0.005	0.001	0.001
West Gyre	0.0001	0.001	0.001	0.001	0.0001	0.001	0.001	0.001	0.001	0.005
East Gyre	0.001	0.001	0.001	0.005	0.002	0.005	0.005	0.002	0.002	0.001

The July simulation results with 70 days resembles the 70 days January simulation rather than April simulation. The coastal areas are the only consistent retention areas that remain. While the area coverage of LR grid cells decreases compared to April, the non 0.0 values still remain high, especially for 35 day PLD, therefore July still retains high LR value averages. The stand out feature of July then becomes the inner gyres which show high LR values in both 35 day and 70 day cases, years such as 2002, 2006 and 2010 show the high LR values and area coverage.

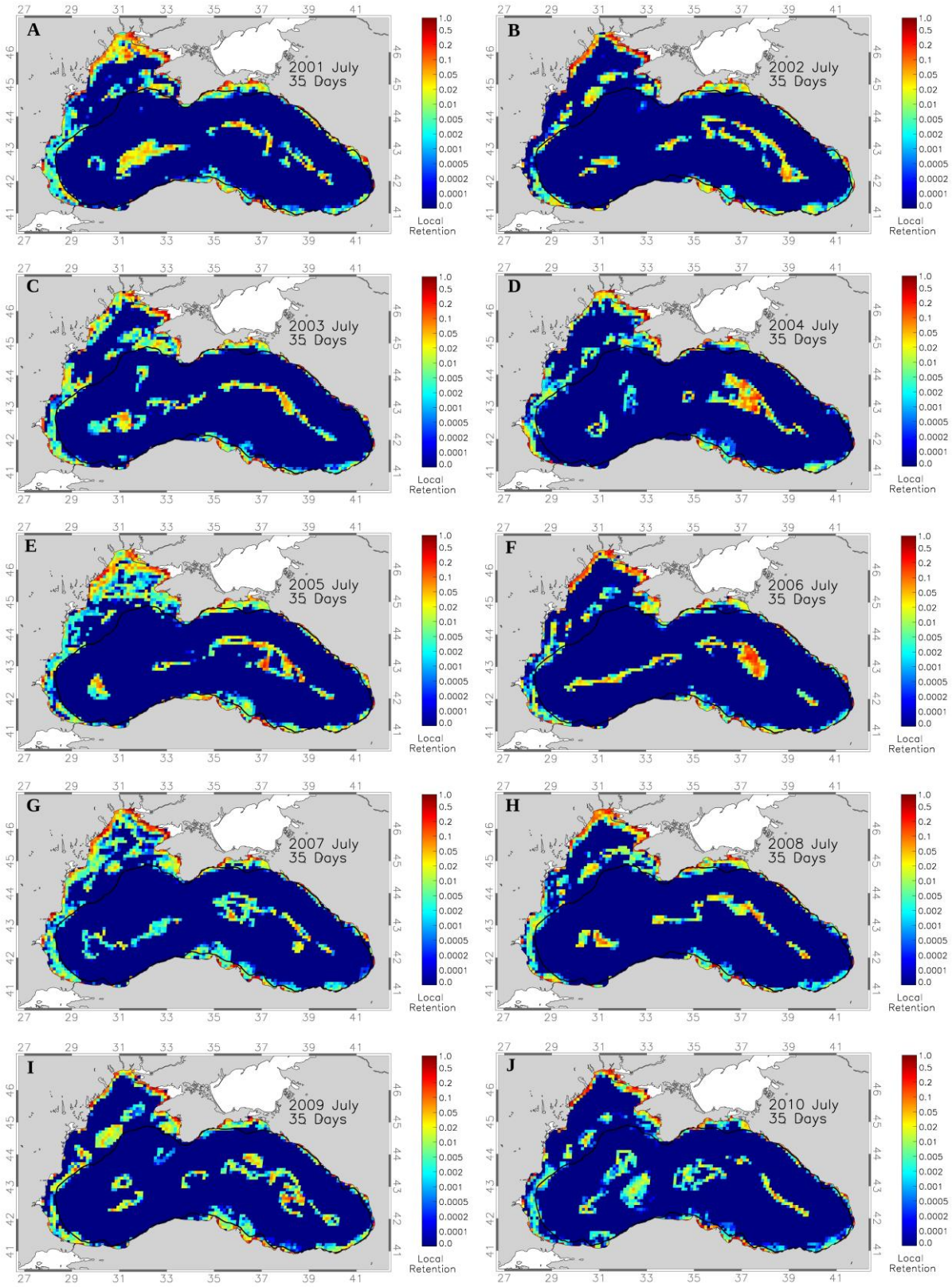

Figure 23: Simulation results of Local Retention (LR) using July spawning times and 35 day Pelagic Larval Duration (PLD) for A-J: 2001-2010.

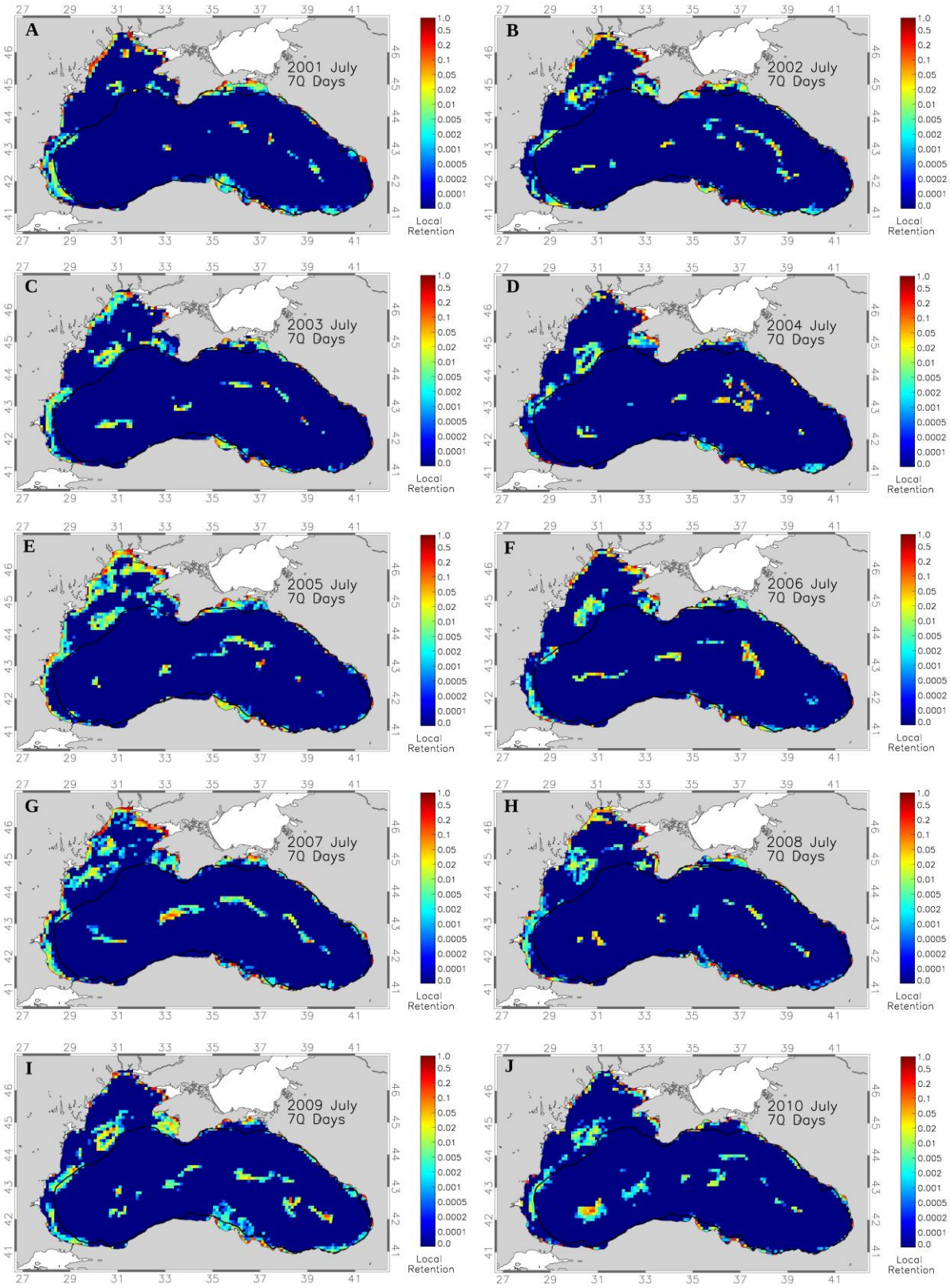

Figure 24: Simulation results of Local Retention (LR) using July spawning times and 70 day Pelagic Larval Duration (PLD) for A-J: 2001-2010.

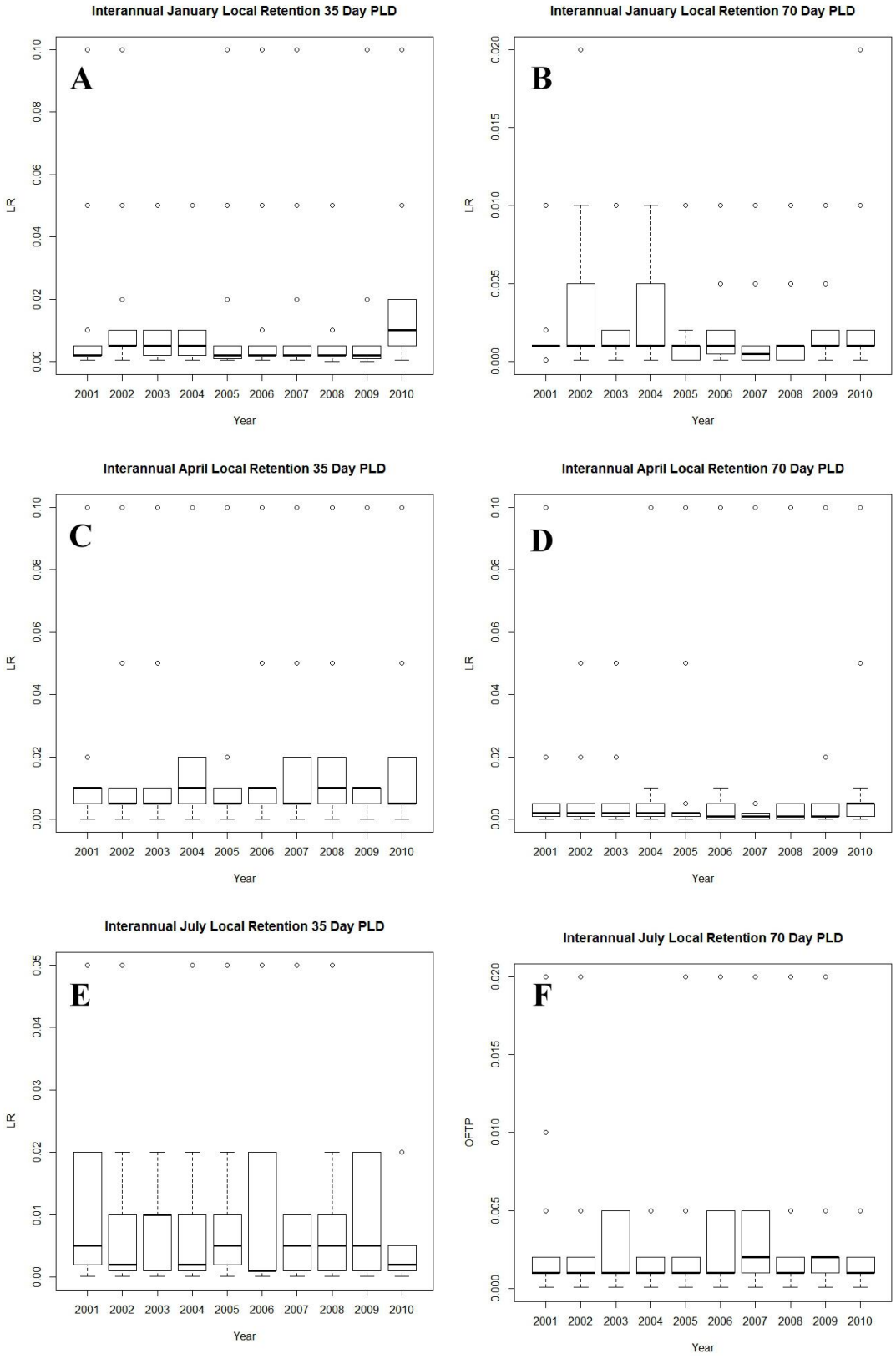

Figure 25: Box-Whisker plots of Interannual Local Retention derived from Table 13, Table 14, Table 15, Table 16, Table 17 and Table 18. A: January 35 day PLD, B: January 70 day PLD, C: April 35 day PLD, D: April 70 day PLD, E: July 35 day PLD, F: July 70 day PLD, The circles denote extreme values outside the range of the average.

Overall, January starts with the lowest LR values and area coverage of the year, followed up by April increasing the LR values and area coverage to the yearly maximum followed by a slight decrease in July and finally in January the values and area coverage decrease back down to minimum.

The box-whisker plots for LR (Figure 25) have the maximum LR value on the y-axis set manually to lower values in order to make the data easier to view. The maximum values, denoted by the circles, are picked as the most extreme ends from the tables. January 35 day results average at 0.015 and 70 day results average at 0.002 meanwhile the April results average at 0.061 for 35 days and 0.010 for 70 days and finally July 35 day results average at 0.009 and 70 day results average at 0.003

CHAPTER 4

DISCUSSION

In this section the simulation results are discussed using the circulation velocity field data of the model, the known established circulation of the Black Sea in section 1.1 and the target fish spawning reports also given in section 1.2. In addition, it will be discussed here what the results found above imply for the target fish species.

4.1 General transport patterns

While the 10 year (2001 to 2010) and 4 seasons averaged simulation result (Figure 6, Figure 7, Figure 15, Figure 16) is too broad to give specifics about connectivity metrics of any region, comparing the broad metrics to the 10 year (2001-2010) averaged circulation velocity fields (Figure 26) establishes a general idea of how the circulation system effects the metrics.

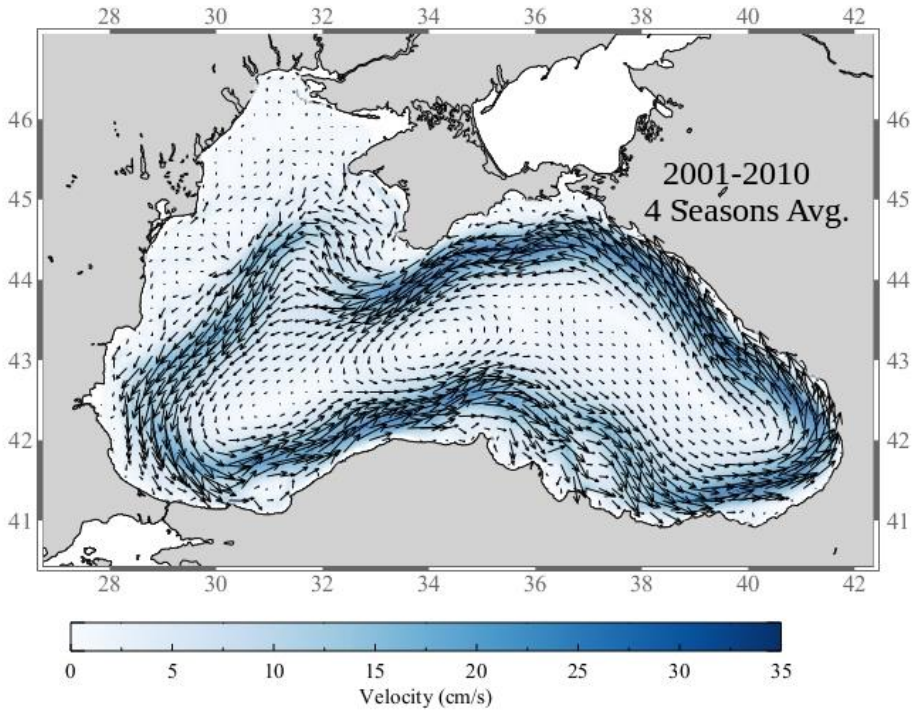

Figure 26: Simulation results of 10 years (2001-2010) and four seasons averaged circulation velocity fields.

The 10 year averaged offshore transport pattern (Figure 6) appears to be related to the magnitude of the velocity fields in the region in shallow areas (less than 200 m depth). The north western shelf, western coast and south western coast has the lowest velocity field magnitudes (Figure 26) and the lowest OFTP (Figure 6) values in the region while the regions close to the rim current like southern coast, Georgian coast, eastern coast and northern coast boasts the highest velocity magnitudes (Figure 26) and the highest OFTP (Figure 6) values as well. The deep areas (more than 200 m depth) show the highest OFTP values as they are pass the threshold thus commenting about the circulation and OFTP in deep areas become difficult. However the 70 day PLD (Figure 6E) case shows decreasing of values at the rim current, almost an erosion like pattern compared to 20 day PLD (Figure 6A) case, and meandering shapes appear in both gyres and the middle region where they meet all regions with relatively moderate velocity magnitudes (Figure 26). LR (Figure 15) and SR (Figure 16) are inversely related to the velocity field magnitudes (Figure 26) showing the highest values in the north western shelf, western coast, south eastern coast and also inside the western and eastern gyres, as there is no depth threshold for LR and SR. On the other hand LR (Figure 15) and SR (Figure 16) is practically 0.0 on top of the rim current itself which has the highest velocity magnitude (Figure 26) in the basin, indicating that the rim current serves as a strong transport mechanism as can be expected.

Another reason for LR (Figure 15) and SR (Figure 16) values being almost identical, previously discussed at the start of section 3.1, could be related to the Black Sea circulation dynamics, almost the entire basin is subjected either directly or indirectly through meandering to the very strong rim current. This makes it highly unlikely for neighbouring cells to receive migration from each other as the rim current evenly distributes what particles it comes across through the region in a circle, as there does not appear to be a particular area where these particles accumulate. In the regions like the north western shelf that are not subjected to the rim current directly, the grid cells are again unlikely to receive migration from neighbouring cells due to the low velocity magnitude in these areas, therefore in either case the final number and initial number of particles in a given cell is likely going to be very similar to one another, combining this with the logarithmic scaling of the data, the end result is LR and SR data that look almost identical.

4.2 Seasonal Variability

Comparing the 10 year (2001 to 2010) averaged seasonal connectivity metrics (Figure 8, Figure 9, Figure 17, Figure 18) with the 10 year averaged seasonal circulation velocity fields (Figure 27) yields more detailed conclusions on a region basis.

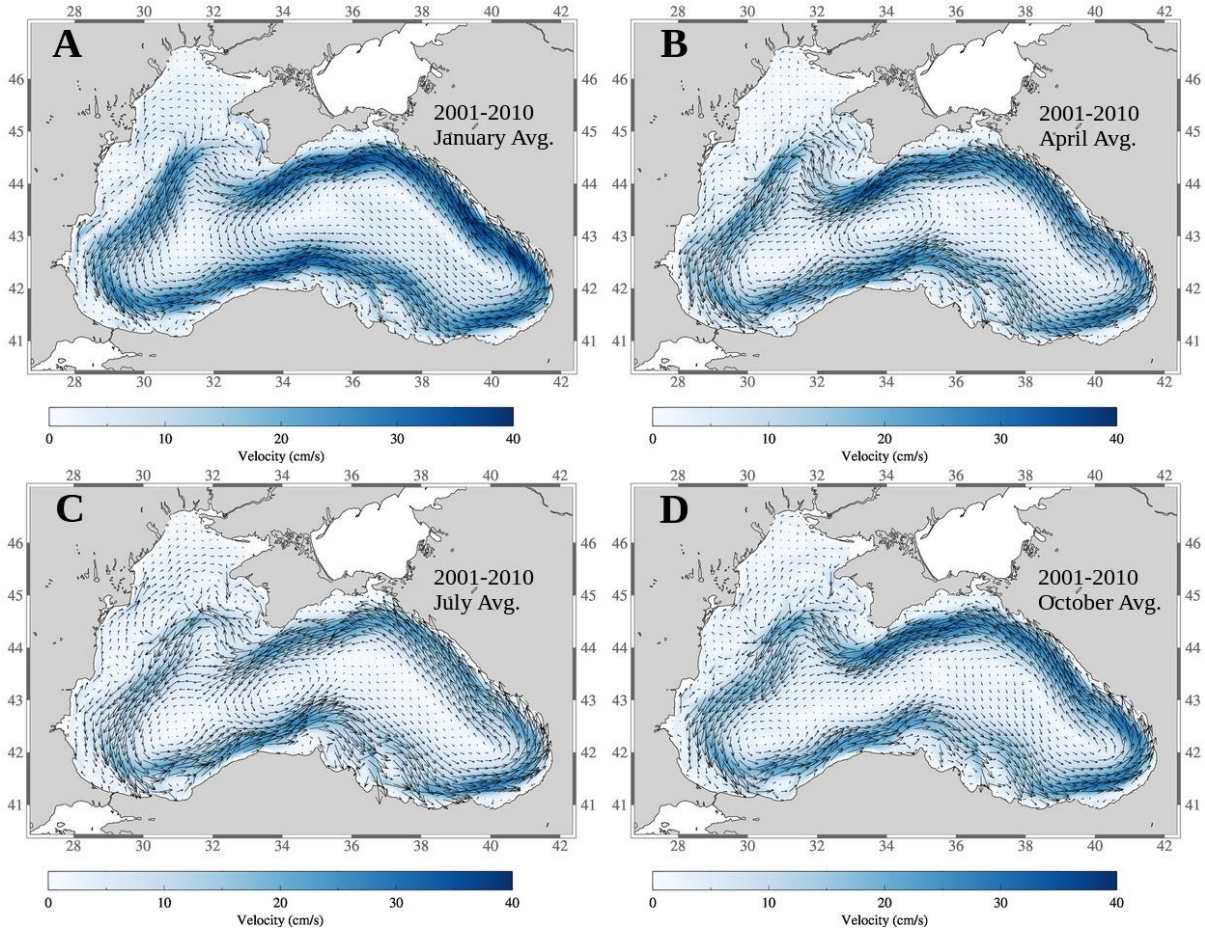

Figure 27: Simulation results of 10 years (2001-2010) averaged circulation velocity fields for all seasonal averages. A: January average, B: April average, C: July average and D: October average. Provided by A. Bettina Fach for this study.

The winter circulation velocity (Figure 27A) features the two inner gyres separated around 33°E previously mentioned in section 1.1 (Korotaev et al., 2003). Winter OFTP values (Figure 8A, Figure 9A) for the north western shelf are at their highest compared to other seasons except for October (Figure 8D, Figure 9D), which has roughly the same values, while the OFTP values on the periphery of the rim current appear to be lower compared to other seasons. These results are likely due to the

magnitude of the winter rim current velocity as it is the highest of all seasons (Figure 27), particles located on the shelf are more likely to be transported offshore due to the increased meandering while particles on the rim current periphery are more likely to end of onshore. Winter LR values shows for 35 day PLD (Figure 17A) the only regions capable of maintaining their larvae are the coastal edges of the north western shelf, western coast and the coasts close to the Azov Sea entrance and if possible the western and eastern inner gyres. 70 day PLD (Figure 18A) on the other hand shows that there is almost no retention anywhere apart from a few coastal cells scattered around. Sprat is the only target species that spawns during winter season, with their long 70 day PLD the only few feasible grid cells for the larvae to be retained (Figure 18A) during the harsh winter circulation are located at the coastal edges of the north western shelf, western coastal edges, mouth of the, the Sakarya eddy, the south eastern coastal edges of Turkey and the entrance of the Azov Sea.

While the OFTP results for April and July are similar (Figure 8B, Figure 8C), they are considerably different for LR (Figure 17B, Figure 17C) which shows April to be higher than July. This is likely caused by the weaker circulation of the summer which is more susceptible to interannual variations resulting in lower values in more cases than spring (Korotaev et al., 2003). April shows generally the highest LR values for all PLD's (Figure 17B, Figure 18B) in all regions of the Black Sea. The circulation velocity field for April (Figure 27B) when combined with the 35 day LR values (Figure 17B) shows the formation of the anticyclonic eddies like Sevastapol eddy, Kaliakra eddy, Sakarya eddy, Sinop eddy, Kizilirmak eddy, Yesilirmak eddy, mentioned in section 1.1 (Figure 1), which host the high LR values. In general the grid cells with moderate to high LR values like 0.5 to 1.0 cover a lot more space in April (Figure 17B) results compared to July (Figure 17C). Sprat spawning ends around April, comparing the spawning areas (Figure 3) with the 70 LR values (Figure 18B) shows that coastal and inner north western shelf, the western coasts, the south eastern Turkish coasts and the entrance of the Azov Sea have the highest retention of larvae while the Georgian coast and the coasts of the Caucasus have moderate retention rates. Anchovy larvae that spawn late spring, close to the end of May, would be retained with moderate to high values of LR (0.1 to 1.0) in the Sevastapol eddy, the north western shelf coast and center, the Kaliakra eddy, western coasts and the Azov Sea entrance comparing the spawning sites (Figure 2) and the 35 day PLD results (Figure 17B).

Mentioned in the paragraph above the July OFTP values are very similar to April results. The target fish species anchovy, red mullet and horse mackerel are all assumed to spawn during summer with PLD's ranging from 25 to 36 days as mentioned in section 1.2, thus the 35 day July results (Figure 17C) are able to represent retention for all these species. The anchovy spawning sites (Figure 2) in the Sevastapol eddy, the nortwestern shelf coast, the western coast and the Azov Sea entrance all have moderate to high LR values with the north western shelf and the Sevastapol eddy region having the highest probabilities for retention. For red mullet the spawning sites (Figure 4) are the same as anchovy with the addition of the very high retention region of the south eastern coast of Turkey and the low to moderate retention Sakarya eddy. The inconsistent average of the Sakarya eddy can be explained with the high interannual variability of the summer season. Finally last of the target species, horse mackerel, has the same spawning sites as the red mullet with the further additions (Figure 5) of the southern coast tip of Turkey, the north eastern coasts of the Caucasus and the northern Crimean coast between the Sevastapol eddy and the entrance of the Azov Sea. LR values are typically low (Figure 17C) for the Crimean coast and the Caucasian coast, except for the occasional coastal grid cell on the Caucasian coast with moderate retention, while the southern coast tip of Turkey fares a better with generally moderate values however none of them are comparable to the high values of north western shelf or the south eastern coast of Turkey.

October results are similar to winter results in all connectivity metrics (Figure 8D, Figure 9D, Figure 17D, Figure 18D). It is possible to see the weakened interior cell structure mentioned in section 1.1 (Korotaev et al., 2003) on the October circulation velocity field (Figure 27D). Sprat is reported to spawn from October until April mentioned in section 1.2, comparing the spawn areas (Figure 3) with the 70 day October LR results (Figure 18D) shows possibility of sprat spawning October and retained until early December in the coastal regions of the north western shelf, the western coast, south eastern coasts of Turkey, the entrance of the Azov Sea and some scattered areas within the inner gyres (Figure 18D), although the inner gyres are not reported as spawning areas. It should be noted that the October LR (Figure 18D) values are only slightly better than January LR (Figure 18A) values and the Sakarya gyre is not yet formed in October.

A special mention of the inner western and eastern gyres should be made. While none of the target fish species are reported to spawn inside the gyre (section 1.2), even in the lowest retention results of January 70 day PLD (Figure 18A) there are grid cell patches present inside the gyre with retention values ranging from commonly around 0.001 to occasionally around 0.01 just enough to be relevant. For sprat January 70 day (Figure 18A) results mentioned appear mostly in the eastern gyre and the middle of both gyres with smaller areas present in the western gyre, the October 70 day (Figure 18D) results show higher average LR spread roughly in the same areas with the western gyre having the highest values around 0.1. April 70 day LR (Figure 18B) results have the highest values and are concentrated in the middle of the two gyres, although both gyres have retention present inside as well. The remaining fish species; anchovy, red mullet and horse mackerel can be discussed using the 35 day July LR (Figure 17C) results which shows moderate retention from 0.002 to 0.03 mostly concentrated in the eastern gyre then at the western gyre and finally at the intersection of the of the gyres. In theory sprat is most likely to be retained at the both gyres and the intersection of both gyres at April and the western gyre at October. While the remaining species anchovy, red mullet and horse mackerel are most likely to be retained in the eastern gyre. The retention of the gyres should not be written off as back in the 1980's an increase of anchovy spawning in the southern Black Sea was reported and a considerable amount of anchovy eggs were found recently by cruises in the Turkish coasts and all over the southern Black Sea in general (Gucu et al., 2016).

4.3 Interannual Variability

Putting interannual connectivity results side by side for onshore areas the OFTP and LR results are inversely proportionate with each other. Areas with high LR tend to have low OFTP while areas with low LR tend to have high OFTP.

The interannual January 70 day PLD LR (Figure 20) results along with January 70 day OFTP (Figure 11) combined with sprat spawning sites (Figure 3), shows the viable spawning sites for the following years: 2002 (Figure 20B) at the north western shelf and Bulgarian coast, 2003 (Figure 20C) at the Sakarya eddy and Georgian coast, 2004 (Figure 20D) at Kaliakra eddy and Bulgarian coast, 2005 (Figure 20E) at the north western shelf and the western coast with few almost 1.0 LR cells, 2006 (Figure

20F) at the north western shelf and Bulgarian coast, 2008 (Figure 20H) at the Sakarya eddy, 2009 (Figure 20I) at the western coast and Sakarya eddy and 2010 (Figure 20J) at the north western shelf. South eastern Turkish coast always has high LR between 0.2 and 1.0 in few but consistent coastal grid cells through all the years (Figure 20) making the area always viable for spawning.

The 70 day interannual April LR (Figure 22) results for sprat spawning sites are as follows: the north western shelf in all years, especially larger areas in 2003 (Figure 22C), 2005 (Figure 22E), 2006 (Figure 22F) and 2010 (Figure 22J), western coast in all years but less so in 2004 (Figure 22D), 2005 (Figure 22E) and 2006 (Figure 22F), Sakarya eddy in 2004 (Figure 22D) and 2010 (Figure 22J), south eastern coast of Turkey in all years with high LR, Georgian coast and the Caucasus coast with low LR values in small areas in all years and the Azov Sea entrance with moderate to high LR values in all years.

July 35 day LR (Figure 23) interannual results and viable spawning sites for the target fish species anchovy, red mullet and horse mackerel through the years are as follows: north western shelf and Sevastapol eddy at all years with high LR values, with larger areas in 2001 (Figure 23A), 2005 (Figure 23E) and 2007 (Figure 23G), for all three species, low to moderate LR at the western coast for all years for all three species, Sakarya eddy in 2010 (Figure 23J) with low LR for red mullet and horse mackerel, southern coast of Turkey in 2001 (Figure 23A), 2005 (Figure 23E), 2006 (Figure 23F) and 2007 (Figure 23G) with low to moderate LR for horse mackerel, south eastern coast of Turkey in all years with high LR for red mullet and horse mackerel, north eastern Caucasus coast with low to moderate LR for a handful of grid cells in all years for horse mackerel and finally the entrance of the Azov Sea between moderate to high LR in all years for all three species.

The Black Sea in the 1980's and 1990's was subject to strong climate variability associated with changes in the North Atlantic Oscillation (NAO) (Oguz, 2005). The positive pressure difference periods of NAO is known to correspond with to colder and harsher years in general as evidenced by the drop in sea surface temperature, CIL temperature and mean basin wide temperature while the inverse, warmer years, can also be inferred from the negative pressure difference (Oguz, 2005). This oscillation is weather phenomenon mainly observed in winter in the North Atlantic that is also

known to influence other regions in Europe and the Black Sea. It is caused by pressure differences between the Icelandic Low and the Azores high, that can be measured (Figure 28). Similarly, the East Atlantic – West Russia (EA-WR) teleconnection influences temperature and precipitation distributions over Eurasia throughout the year. Among other things the EA-WR has a strong influence over the precipitation in the Mediterranean region (Krichak et al, 2002; Krichak and Alpert, 2005) with extreme wet (dry) winter months being characterized by anomaly patterns in the negative (positive) phase of EAWR. The Black Sea has been shown to be influenced by this index as well (Akpinar, 2016).

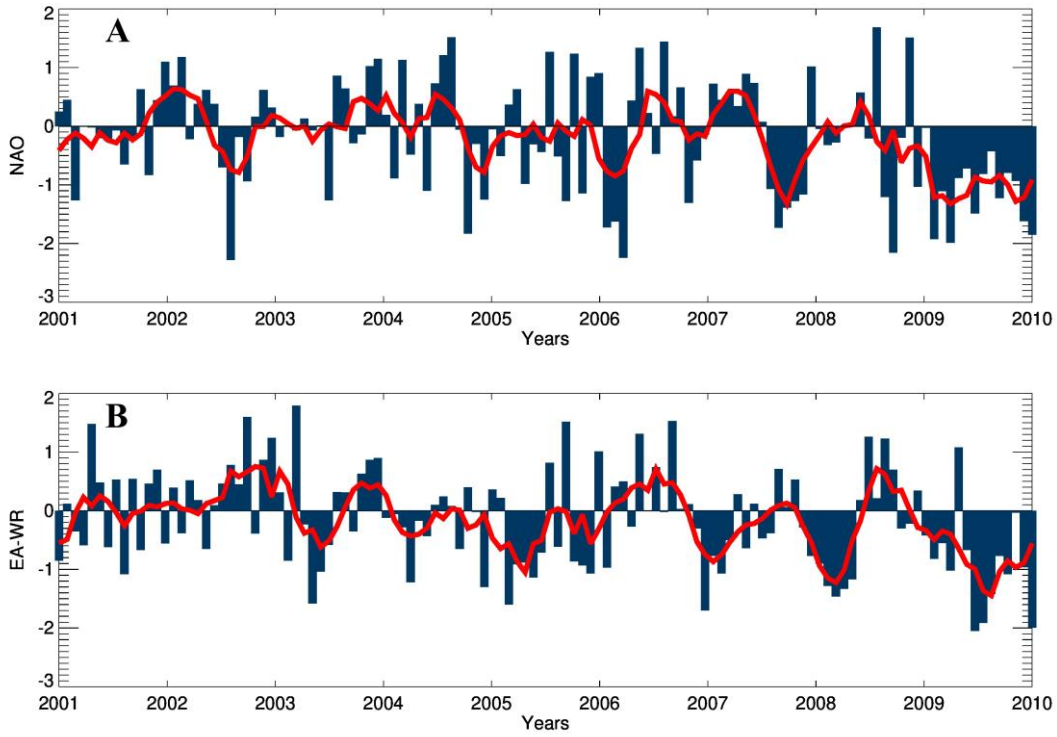

Figure 28: Time series of A: North Atlantic Oscillation (NAO), B: East Atlantic - West Russia (EA-WR) from 2001 to 2010. Data is taken from National Oceanic and Atmospheric Administration (NOAA).

For the current study the variability of both the NAO and EA-WR indices (Figure 28) are compared to the simulated results of the study The negative pressure difference period for both NAO and EA-WR from 2009 to 2010 (Figure 28) appears to correlate with the higher than average LR values for January 2010 (Figure 19J). Comparing the OFTP at the north western shelf at January 35 day days (Figure 10) with the pressure differences (Figure 28) shows that the high OFTP in 2003 (Figure 10C) correlate with

the positive pressure difference of EA-WR (Figure 28B), moderate to high OFTP in 2004 (Figure 10D) correlate with the positive pressure difference of both NAO (Figure 28A) and EA-WR (Figure 28B), the low OFTP in 2005 (Figure 10E) correlates with the negative pressure difference of NAO (Figure 28A) and EA-WR (Figure 28B) together, 2007 (Figure 10G) correlate with EA-WR negative (Figure 28B) pressure difference with low OFTP. Years not mentioned do not show an apparent correlation with the pressure difference.

4.4 Consequences for Fish Species

The finding presented in this study show the high probability of dispersal for any of the commercial fish in the Black Sea considered in this study. Local retention is surprisingly low, even on the north western shelf which is generally considered a spawning and nursery area for fish. Thereby offshore transport probability from shallow areas increases as the PLD times of fish increase. The reverse is true for onshore transport. In addition, transport probabilities are higher in autumn and winter than in spring or summer and consequently local retention is lower in autumn and winter than in spring or summer. This is due to the seasonal variability of the basin wide circulation in the Black Sea as has been detailed above. Only certain areas promise high retention rates in the Black Sea, at all times of the year and regardless of the season and PLD. These are the coastal parts of north western shelf, the south eastern coast of Turkey and the entrance of the Azov Sea.

For the fish species considered in this study, which all spawn in coastal regions and predominantly the north western shelf, this means that they may not at all be able stay in the area but will be transported offshore. Thereby fish with long PLDs (such as sprat) have significantly higher offshore transport probabilities after spawning than those with low PLDs (such as bluefish) and may therefore not recruit back to the area where they were spawned. In addition, fish spawning in fall or winter (e.g. sprat) have larger risk of offshore transport than those spawning in summer (e.g. anchovy or red mullet).

It should be noted that all the target fish species of this study have different attributes regarding their eggs and larvae, such as shape, size and density. This fact is not taken into consideration as the simulation runs assume all larvae to be weightless

and to be always floating at 10 m depth. This means that different larvae for different species may be located at different depths like sprat, which can differ between 30 and 80 meters (Ivanov and Beverton, 1985) opposed to anchovy which ??? and hence may be exposed to slightly different current speeds and directions. Factoring different larval densities and sizes for different fish species could therefore change the results as larvae would sink or float at different depths, therefore this should be considered as a limitation of the study as this is just a theoretical work. Vertical migration is also a possible movement larvae can make but is not considered to be a part of this study. These factors may introduce slight variations in the drifter paths and hence change the results.

The LR and OFTP data presented in this study may be useful during efforts to calculate spawning stock biomass and recruitment power over time, as these results can give insight into how retention and dispersal in different regions of the Black Sea develop interannually.

4.5 Modeling Studies of Marine Life in Different Seas

This type of particle tracking of fish larvae using an Lagrangian Flow Network in the Black Sea has not been done before, however similar studies in similar have been conducted in different seas and on different marine species. The finding presented in this study fit well within the results of other particle tracking studies.

Cowen et al. (2006) studied larval dispersal and exchange of marine populations in the Caribbean region and reports that dispersal ranges for reef fish species are in a scale of 10 to 100 km and the sustainability of most populations are dependent both on self recruitment and outside larval import. However the study also points out populations isolated in some regions unable to reach other populations limited by their larval dispersal range (Cowen et al., 2006).

Another study, on the Australian continent and its major current systems (Condie et al., 2011) also investigated local retention rates of pelagic fish larvae and larval transport between shelf and offshore areas. The study results suggest a barrier effect for onshore transport caused by East Australian Current which also supports offshore transport by entraining shelf waters. The blue mackerel (*Scomber australasicus*) benefits from the offshore transport of the East Australian current by increasing its

dispersal of eggs and larvae, while the Australian anchovy (*Engraulis australis*) and sardine (*Sardinops sagax*) may be able to benefit from the high coastal retention rate scaused by the Leuuwin Current system during the summer season (Condie et al., 2011). The impact of the East Australian Current on larval transport was in addition studied by Roughan et al. (2011) using a Lagrangian particle tracking model for larvae of 5 fish species are analyzed for seasonal and interannual variability. Dispersal of larvae was found to be varying with release latitude, distance to shore and the total time larvae spends floating. The East Australian Current was again found acting as a barrier for onshore transport, keeping offshore particles away while trapping the particles inside the current system impacting coastal connectivity (Roughan et al., 2011).

In studies modeling the effects of coastal reclamation on fish larvae in the North Sea very small differences in the larval dispersal, arrival time to nursing grounds and the rate of transport success was found between simulations with coastal reclamation versus no coastal reclamation yielded thus the effects of coastal reclamation was deemed negligible on larval transport success (Erftemeijer et al., 2009). In addition, it was determined that the year class strength of Downs herring is associated with local retention instead of dispersal of the larvae and delivery of the larvae to spawning sites. And plaice larvae was found to be susceptible to seasonal and interannual variability of the North Sea hydrodynamics (Bolle et al., 2009).

Rossi et al. (2014) investigates potentially viable marine protected areas in the Mediterranean basin using a LFN model similar to the one employed in the current study. The larval dispersal results are then used to identify boundaries which contains the dispersal and the study suggest potential marine protected areas using these regions and illustrates the usefulness of this technique in a variety of research questions.

Lagrangian particle tracking has also been applied to study the connectivity of lobster (*Homarus americanus*) population in the Gulf of Maine using a model with particle tracking and biophysical features like temperature dependent larval growth (Xue et al., 2008). The study exposes areas of high larval accumulation such as along the western coast of Maine while taking interannual variability into account.

4.6 Future Work

This study can be further improved in the future by exploring in detail the cause for the self recruitment metrics to be so similar to local retention metrics and perhaps finding a better way to represent self recruitment. As this study does not keep track of where the advected fish end up exactly, connectivity matrix for the different Black Sea nodes will be of interest for future studies to get a high resolution impression of the connectivity within the Black Sea. Furthermore vertical movement of fish larvae and different buoyancy parameters for each target fish species can be implemented for more detailed simulation analyses. While the model does not include the Azov Sea, the current system near the entrance of the Azov Sea is still represented, and since the particles tracked in the model can represent any larvae, analyses of Azov Sea anchovy and Black Sea anchovy can be made separately, and a combined system using LR and regional connectivity matrix can be used to analyze potential larval exchange between the two anchovy species.

CHAPTER 5

CONCLUSION

In this thesis a multitude of Lagrangian drifter simulations were undertaken using the surface circulation fields created by the sb-POM circulation model set up for the Black Sea. Using the method of Lagrangian Flow Networks several connectivity metrics on onshore and offshore transport, local retention and self recruitment were calculated for ten different years (2001 to 2010), four different seasons (spring to winter) and five different pelagic larval durations corresponding to economically important target fish species such as anchovy, sprat, red mullet, blue fish, turbot and horse mackerel (20, 30, 35, 40 and 70 days).

In general it was observed that offshore transport probability from shallow areas increased as the PLD times increased while in deep areas the onshore transport probability increased as PLD times increased. Both, local retention and self recruitment are inversely related to PLD length, showing lower retention probabilities in general for fish species with increasing PLD times. At the same time local retention and self recruitment values for shallow areas were inversely related to offshore transport probabilities. It was found that local retention and self recruitment calculations gave very similar results and hence self recruitment was deemed not a useful metrics for this study, as the dispersal probabilities in the Black Sea are very high.

Seasonally averaged simulations showed that offshore transport probabilities for January and October are similar to each other with the highest offshore transport for all seasons in shallow areas and lowest values for deep areas. At the same time April and July probabilities are also similar with lowest values for offshore transport in shallow areas for April and slightly higher values in July. Finally for deep areas both seasons are similar enough to say they have the highest values in all 4 seasons. Local retention is lowest in January, reaches the highest values in April, slightly decrease in July and again reach low values in. Since all fish species considered in this study spawn in coastal regions and the north western shelf, this means that fish with long PLDs (such as sprat) than those with low PLDs (such as bluefish) have significantly higher offshore transport probabilities after spawning and may therefore not recruit back to the area where they were spawned. In addition, fish spawning in fall or winter (e.g.

sprat) have larger risk of offshore transport than those spawning in summer (e.g. anchovy or red mullet).

The coastal parts of north western shelf, the south eastern coast of Turkey and the entrance of the Azov Sea consistently have high local retention values regardless of the season and PLD. The Sevastapol eddy in January and October can be observed some years with low to moderate local retention and disappears completely in other years while April and July consistently feature this eddy with moderate to high LR. The Sakarya eddy is seen in January, April and October with low to moderate LR values and disappears almost completely in July. The Kaliakra eddy consistently shows moderate LR during April and not in other seasons. The western coast consistently has LR in all seasons with January and October from low to moderate and in April and July usually from moderate to high LR values. The southern coast from Sakarya to Sinop has almost no local retention regardless of the season. The Georgian coast consistently shows low to moderate LR smaller in size during January and October while slightly larger during April and July. The Caucasian coast has moderate local retention in all seasons. The inner western and eastern gyres consistently have low to moderate LR in all seasons with highest values during April and July, slightly lower values in October and lowest in January.

Overall, simulations showed that local retention is surprisingly low, even on the north western shelf which is generally considered a spawning and nursery area for fish. Fish spawned on the shelf may not at all be able stay in the area but be transported offshore. Where they exactly get transported to offshore has not been analysed within the scope of this study. Taking the spawning sites and PLD times in consideration together for the target fish species the best areas for each species to be retained after spawning are found. For sprat spawning in winter the northernmost coastal areas of the north western shelf, the western coast, Sakarya eddy, south eastern coast of Turkey and the entrance of the Azov Sea appear to be the best areas for retention. During fall spawning the same areas provide retention, however without the Sakarya eddy region while the Georgian coast and the coasts of the Caucasus become feasible. For anchovy, red mullet and horse mackerel when spawning in summer the Sevastapol eddy, the inner parts of the north western shelf, the western coast and the entrance of the Azov Sea are areas that may provide high retention rates, while the south eastern coast of

Turkey is feasible for red mullet and horse mackerel retention and the coast of Caucasus may retain horse mackerel.

References

Akpinar, A. (2016). Seasonal to decadal variability in the physical and biological properties of the Black Sea and Levantine Basin as inferred from satellite remote sensing. Middle East Technical University (Mersin).

Allen, I., Arkin, S., Cossarini, G., Butenschoen, M., Ciavatti, S., Christensen, A., Libralato, S., Salihoglu, B., Triantafyllou, G., Tsiaras, K., Wan, Z. (2013). D2.6: Report on reanalysis hindcast skill. OPEC Report, pp 66.

Baudena, A. (2018). How do marine mid trophic levels respond to fine scale processes*?*. Pierre and Marie Curie University.

Besiktepe, S, Lozano, C. J., & Robinson, A. R. (2001). On the summer mesoscale variability of the Black Sea. *Journal of Marine Research, 59*(4), 475-515. doi:10.1357/002224001762842163

Black Sea (2015) - Temperature and salinity observation collection V2. https://doi.org/10.12770/227e9f7b-ddfc-4004-b0e5-f4785d36d43f

Blumberg, A. F., and Mellor, G. L. (1987). "A description of a three-dimensional coastal ocean model," in Three Dimensional Coastal Ocean Models, ed N. S.Heaps (Washington, DC: American Geophysical Union), 1–16.

Bolle, L. J., Dickey-Collas, M., van Beek, J. K. L., Erftemeijer, P. L. A., Witte, J. IJ., van der Veer, H. W., & Rijnsdorp, A. D. (2009). Variability in transport of fish eggs and larvae. III. Effects of hydrodynamics and larval behaviour on recruitment in plaice. *Marine Ecology Progress Series, 390*, 195-211. doi:10.3354/meps08177

Ceyhan, T., Akyol, O., Ayaz, A., & Juanes, F. (2007). Age, growth, and reproductive season of bluefish (Pomatomus saltatrix) in the Marmara region, Turkey. *ICES Journal of Marine Science, 64*(3), 531-536. doi:10.1093/icesjms/fsm026

Chashchin, A. K. (1996). The Black Sea populations of anchovy. *Scientia Marina*, 60, 219–225.

Chashchin, A., Shlyakhov, V. A., Dubovik, V. E., & Negoda, S. (2015). Stock Assessment of Anchovy (Engraulis encrasicolus L) in Northern Black Sea and Sea of Azov. *Advances in Environmental Engineering and Green Technologies Progressive Engineering Practices in Marine Resource Management*, 209-243. doi:10.4018/978-1-4666-8333-4.ch006

Condie, S. A., Mansbridge, J. V., & Cahill, M. L. (2011). Contrasting local retention and cross-shore transports of the East Australian Current and the Leeuwin Current and their relative influences on the life histories of small pelagic fishes. *Deep Sea Research Part II: Topical Studies in Oceanography, 58*(5), 606-615. doi:10.1016/j.dsr2.2010.06.003

Cowen, R. K., Paris, C. B., & Srinivasan, A. (2006). Scaling of Connectivity in Marine Populations. *Science, 311*(5760), 522-527. doi:10.1126/science.1122039

Dickey-Collas, M., Bolle, L. J., van Beek, J. K. L., & Erftemeijer, P. L. A. (2009). Variability in transport of fish eggs and larvae. II. Effects of hydrodynamics on the transport of Downs herring larvae. *Marine Ecology Progress Series, 390*, 183-194. doi:10.3354/meps08172

Dovidio, F., Fernández, V., Hernández-García, E., & López, C. (2004). Mixing structures in the Mediterranean Sea from finite-size Lyapunov exponents. *Geophysical Research Letters*, *31*(17). doi: 10.1029/2004gl020328

Dulcic, J. (1997). Growth of anchovy, Engraulis encrasicolus (L.), larvae in the Northern Adriatic Sea. *Fisheries Research, 31*(3), 189-195. doi:10.1016/s0165-7836(97)00030-1

Erftemeijer, P. L. A., van Beek, J. K. L., Bolle, L. J., Dickey-Collas, M., & Los, H. F. J. (2009). Variability in transport of fish eggs and larvae. I. Modelling the effects of coastal reclamation. *Marine Ecology Progress Series, 390*, 167-181. doi:10.3354/meps08173

Fach, B. A. (2014). *Turkish Journal of Fisheries and Aquatic Sciences, 14*(2). doi:10.4194/1303-2712-v14_2_06

Galarza J. A., Boulay R., Cerdá, X., Doums, C., Federici, P., Magalon, H., Monnin, T., & Rico, C. (2009). Development of single sequence repeat markers for the ant Aphaenogaster senilis and cross-species amplification in A. iberica, A. gibbosa, A. subterranea and Messor maroccanus. *Conservation Genetics, 10*, 519-521. doi:10.1007/s10592-008-9554-9

Gordina, A. D., & Klimova, T. N. (1996). On Bluefish (Pomatomus saltatrix L.) Spawning in the Black Sea. *Marine and Freshwater Research, 47*(2), 315. doi:10.1071/mf9960315

Gucu, A. C., Genc, Y., Dagtekin, M., Sakinan, S., Ak, O., Ok, M., & Aydin, I. (2017). On Black Sea Anchovy and Its Fishery. *Reviews in Fisheries Science & Aquaculture, 25*(3), 230-244. doi:10.1080/23308249.2016.1276152

Guraslan, C., Fach, B. A., & Oguz, T. (2017). Understanding the Impact of Environmental Variability on Anchovy Overwintering Migration in the Black Sea and its Implications for the Fishing Industry. *Frontiers in Marine Science, 4*. doi:10.3389/fmars.2017.00275

Hare, J. A., & Cowen, R. K. (1997). Size, Growth, Development, and Survival of The Planktonic Larvae Ofpomatomus Saltatrix (Pisces: Pomatomidae). *Ecology, 78*(8), 2415-2431. doi:10.1890/0012-9658(1997)078[2415:sgdaso]2.0.co;2

Haynes, P. S., Brophy, D., & Mcgrath, D. (2011). The early life history of turbot (Psetta maxima L.) on nursery grounds along the west coast of Ireland: 2007–2009, as described by otolith microstructure. *Fisheries Research, 110*(3), 478-482. doi:10.1016/j.fishres.2011.05.014

Houde, E. D. (1989). Comparative Growth, Mortality, and Energetics of Marine Fish Larvae –Temperature and Implied Latitudinal Effects. *Fishery Bulletin, 87*(3), 471-495.

Ivanov, L. S., & Beverton, R. J. H. (1985). The fisheries resources of the Mediterranean. Part two: Black Sea. *FAO Studies and reviews.* 60-135.

Ivanova, P. P., Dobrovolov I. S., Bat, L., Kideys, A. E., Nikolsky, V. N., Yuneva T. V., Shchepkina A. M., & Shulman. G. E. (2013). Application of esterase polymorphism to specify population genetic structure of Engraulis encrasicolus (Pisces: Engraulidae) in the Black and Azov Seas. *Marine Ecologial Journal, 12,* 45–52.

Knudsen, S., & Zengin, M. (2006). Multidisciplinary Modeling of Black Sea Fisheries: A Case Study From Samsun. Turkey. Black Sea Ecosystem 2005 and Beyond, 1st Biannual Scientific Conference, BSERP/BSC, 8-10 May 2006, Istanbul Turkey.

Korotaev, G., Oguz, T., Nikiforov, A., & Koblinsky, C. (2003). Seasonal, interannual, and mesoscale variability of the Black Sea upper layer circulation derived from

altimeter data. *Journal of Geophysical Research, 108*(C4). doi:10.1029/2002JC001508

Krichak, S. O., Kishcha, P., & Alpert, P. (2002). Decadal trends of main Eurasian oscillations and the Eastern Mediterranean precipitation. *Theoretical and Applied Climatology*, *72*(3-4), 209–220. doi: 10.1007/s007040200021

Krichak, S. O., & Alpert, P. (2005). Decadal trends in the east Atlantic-west Russia pattern and Mediterranean precipitation. *International Journal of Climatology*, *25*(2), 183–192. doi: 10.1002/joc.1124

Lehahn, Y., Dovidio, F., & Koren, I. (2018). A Satellite-Based Lagrangian View on Phytoplankton Dynamics. *Annual Review of Marine Science, 10*(1), 99-119. doi:10.1146/annurev-marine-121916-063204

Levy, M., Ferrari, R., Franks, P. J., Martin, A. P., & Riviere, P. (2012). Bringing physics to life at the submesoscale. *Geophysical Research Letters, 39*(14). doi:10.1029/2012gl052756

Lisovenko, L. A., & Andrianov, D. P. (1996). Reproductive biology of anchovy (Engraulis encrasicoluspontics Alexandrov 1927) in the Black Sea. *Scientia Marina,* 60, 209–218.

Locarnini, R. A., Mishonov, A. V., Antonov, J. I., Boyer, T. P., Garcia, H.E., Baranova, O. K., et al. (2013). "World Ocean Atlas 2013, Volume 1:temperature," in NOAA Atlas NESDIS73, eds S. Levitus and A. Mishonov (Sliver Spring, MD: National Oceanographic Data Center), 40.

Macpherson, E., & Raventos, N. (2006). Relationship between pelagic larval duration and geographic distribution of Mediterranean littoral fishes. *Marine Ecology Progress Series, 327,* 257-265. doi:10.3354/meps327257

Mcgillicuddy Jr, D. J. (2016). Mechanisms of Physical-Biological-Biogeochemical Interaction at the Oceanic Mesoscale. *Annual Review of Marine Science, 8*(1), 125-159. doi:10.1146/annurev-marine-010814-015606

Monroy, P., Rossi, V., Ser-Giacomi, E., Lopez, C., & Hernández-Garcia, E. (2017). Sensitivity and robustness of larval connectivity diagnostics obtained from Lagrangian Flow Networks. *ICES Journal of Marine Science, 74*(6), 1763-1779. doi:10.1093/icesjms/fsw235

National Oceanic and Atmospheric Administration. (n.d.). Retrieved from https://www.noaa.gov/

Niermann, U., Bingel, F., Gorban, A., Gordina, A. D., Gucu, A. C., Kideys, A. E., Konsulov, A., Radu, G., Subbotin A. A., & Zaika V. E. (1994). Distribution of anchovy eggs and larvae (Engraulis encrasicolus Cuv.) in the Black Sea in 1991-1992. *ICES Journal of Marine Science*, *51*(4), 395-406. doi:10.1006/jmsc.1994.1041

Oguz, T. (2005). Black Sea Ecosystem Response to Climatic Teleconnections. *Oceanography*, *18*(2), 122–133. doi: 10.5670/oceanog.2005.47

Oguz, T. (2017). Controls of Multiple Stressors on the Black Sea Fishery. *Frontiers in Marine Science, 4*. doi:10.3389/fmars.2017.00110

Oguz, T., Aubrey, D. G., Latun, V. S., Demirov, E., Koveshnikov, L., Sur, H. I., Diaconu, V., Besiktepe, S., Duman, M., Limeburner, R., & Eremeev, V. (1994). Mesoscale circulation and thermohaline structure of the Black Sea observed during

HydroBlack 91. *Deep Sea Research Part I: Oceanographic Research Papers, 41*(4), 603-628. doi:10.1016/0967-0637(94)90045-0

Oguz, T., Suleyman, T., Kideys, A. E., Ediger, V., & Kubilay, N. (2004). Pyhsical and Biogeochemical Charactheristics of the Black Sea.

Ojaveer E. A. (1981). The Effect of Temperature and Salnitiy on The Embryonic-Development of The Baltic Herring Clupea-Harengus Membras L. *Biologiya Morya-Marine Biology,* 5, 39-48.

Ozturk, B., Fach, B. A., Keskin, C, Arkin, S., Topaloglu, B., & Ozturk, A. A. (2017). Prospects for Marine Protected Areas in the Turkish Black Sea. *Management of Marine Protected Areas,* 247-262. doi:10.1002/9781119075806.ch13

Pearce, A., Slawinski, D., Feng, M., Hutchins, B., & Fearns, P. (2011). Modelling the potential transport of tropical fish larvae in the Leeuwin Current. *Continental Shelf Research, 31*(19-20), 2018-2040. doi:10.1016/j.csr.2011.10.006

Rossi, V., Ser-Giacomi, E., Lopez, C., & Hernández-Garcia, E. (2014). Hydrodynamic provinces and oceanic connectivity from a transport network help designing marine reserves. *Geophysical Research Letters, 41*(8), 2883-2891. doi:10.1002/2014gl059540

Roughan, M., Macdonald, H. S., Baird, M. E., & Glasby, T. M. (2011). Modelling coastal connectivity in a Western Boundary Current: Seasonal and inter-annual variability. *Deep Sea Research Part II: Topical Studies in Oceanography, 58*(5), 628-644. doi:10.1016/j.dsr2.2010.06.004

Salihoglu, B., Arkin, S. S., Akoglu, E., & Fach, B. A. (2017). Evolution of Future Black Sea Fish Stocks under Changing Environmental and Climatic Conditions. *Frontiers in Marine Science, 4*. doi:10.3389/fmars.2017.00339

Satilmis, H. H., Gordina, A. D., Bat, L., Bircan, R., Culha, M., Akbulut, M., & Kideys, A. E. (2003). Seasonal distribution of fish eggs and larvae off sinop (the southern Black Sea) in 1999-2000. *Acta Oecologica, 24.* doi:10.1016/s1146-609x(03)00022-5

Satilmis, H. H., Sumer, C., Ozdemir, S., & Bayrakli, B. (2014). Length-weight relationships of the three most abundant pelagic fish species caught by mid-water trawls and purse seine in the Black Sea. *Cahiers De Biologie Marine, 55*(2), 259-265.

Scientific, Technical and Economic Committee for Fisheries (STECF). (2015) Black Sea assessments (STECF-15-16). 2015. Publications Office of the European Union, Luxembourg, EUR 27517EN, JRC 98095, 284, doi:10.2788/29417

Scientific, Technical and Economic Committee for Fisheries (STECF). (2017). Stock assessments in the Black Sea (STECF-17-14). Publications Office of the European Union, Luxembourg, 2017, ISBN 978-92-79-67486-0, doi:10.2760/881421

Ser-Giacomi, E., Rossi, V., López, C., & Hernández-García, E. (2015). Flow networks: A characterization of geophysical fluid transport. *Chaos: An Interdisciplinary Journal of Nonlinear Science, 25*(3), 036404. doi:10.1063/1.4908231

Simoncelli S., Coatanoan C., Myroshnychenko V., Sagen H., Bäck Ö., Scory S., Grandi A., Schlitzer R., Fichaut M. (2015). Second release of the SeaDataNet aggregated data sets products. WP10 Fourth Year Report - DELIVERABLE D10.4. http://doi.org/10.13155/50382

Sorokin, Y. I. (2002). Black Sea Ecology and Oceanography. *Amsterdam: Backhuys Publishers,* 621.

Woodson, C. B., & Litvin, S. Y. (2015). Ocean fronts drive marine fishery production and biogeochemical cycling. *Proceedings of the National Academy of Sciences, 112*(6), 1710-1715. doi:10.1073/pnas.1417143112

Xue, H., Incze, L., Xu, D., Wolff, N., & Pettigrew, N. (2008). Connectivity of lobster populations in the coastal Gulf of Maine Part I: Circulation and larval transport potential. *Ecological Modelling*, *210*(1-2), 193-211. doi:10.1016/j.ecolmodel.2007.07.024

Zweng, M. M., Reagan, J. R., Antonov, J. I., Locarnini, R. A., Mishonov, A. V., Boyer, T. P., et al. (2013). "World Ocean Atlas 2013,Volume 2: Salinity," in NOAA Atlas NESDIS, eds S. Levitus and A. Mishonov, 74.

Appendix

Section A: Offshore Transport Probability

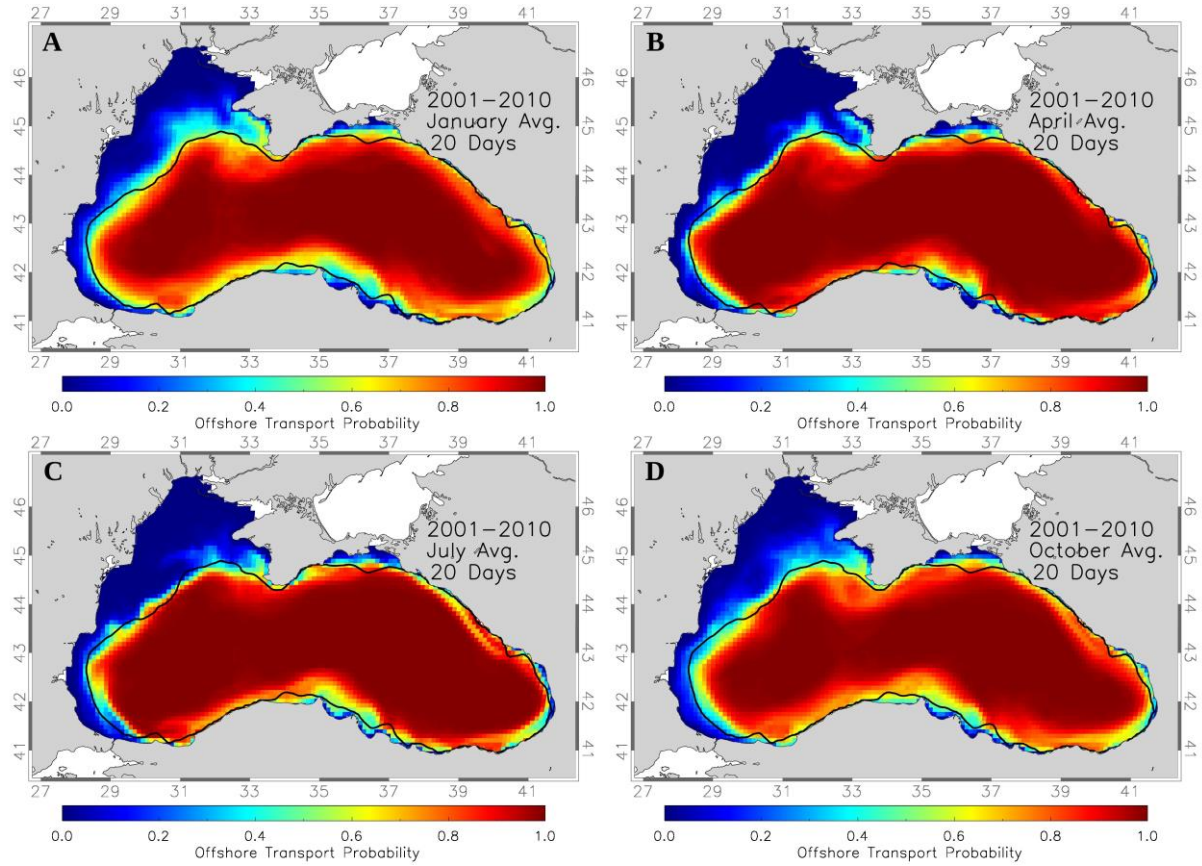

Appendix A 1: Simulation results averaged over 10 years (2001-2010) for four seasons at 20 day pelagic larval duration (PLD) to calculate the Offshore Transport Probability (OFTP). A: January, B: April, C: July, D: October.

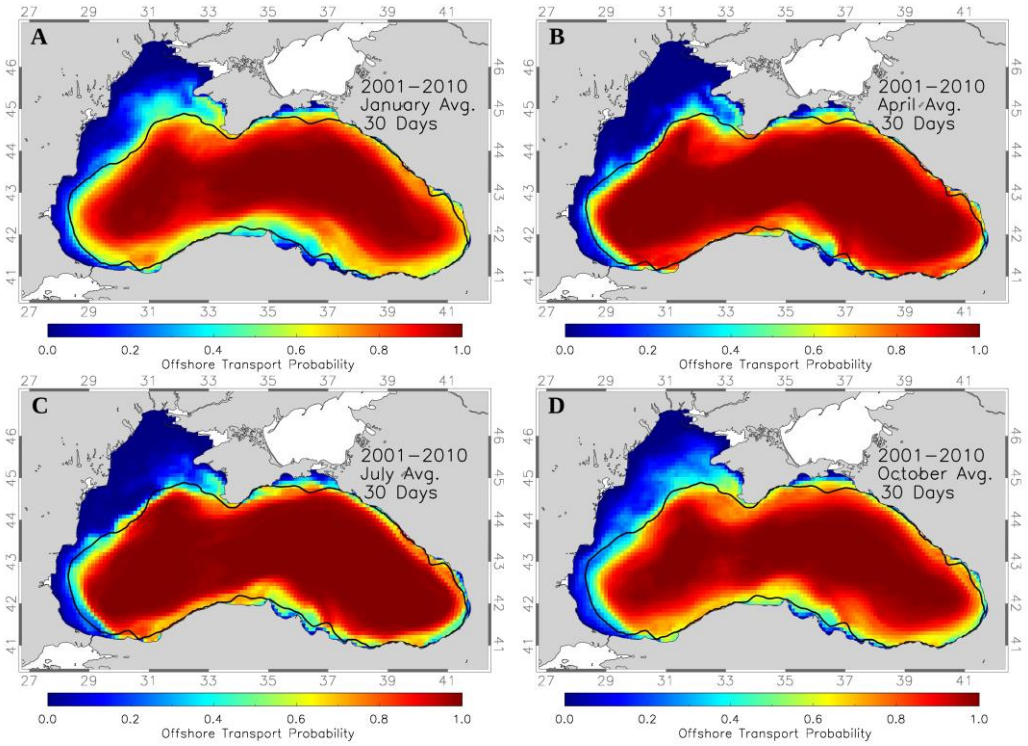

Appendix A 2: Simulation results averaged over 10 years (2001-2010) for four seasons at 30 day pelagic larval duration (PLD) to calculate the Offshore Transport Probability (OFTP). A: January, B: April, C: July, D: October.

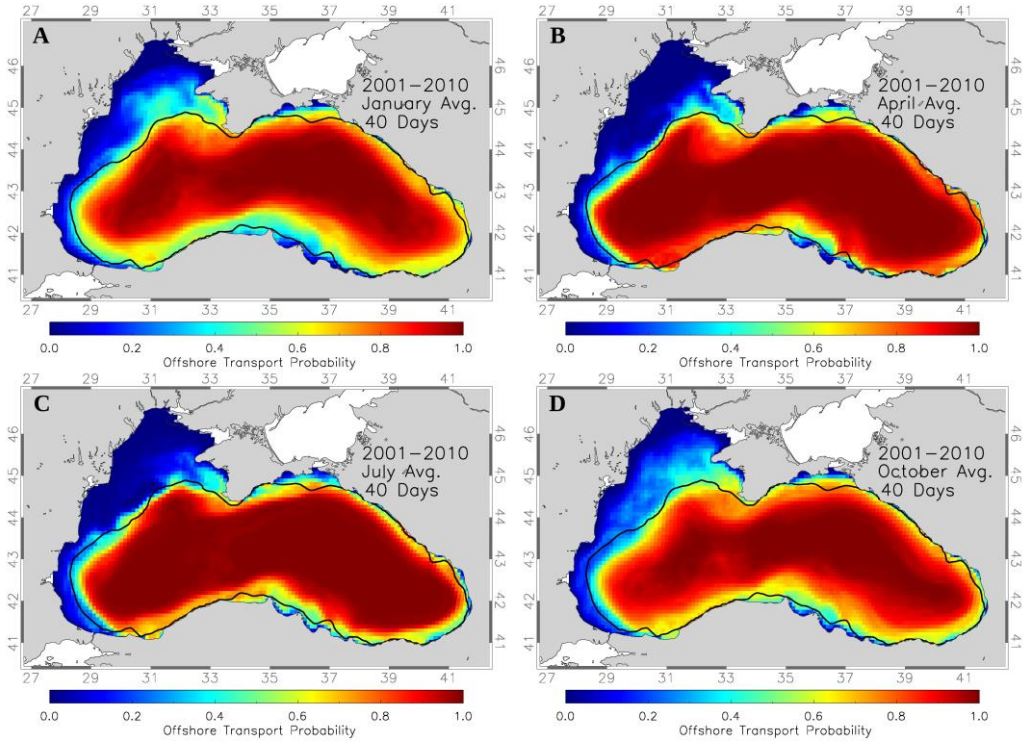

Appendix A 3: Simulation results averaged over 10 years (2001-2010) for four seasons at 40 day pelagic larval duration (PLD) to calculate the Offshore Transport Probability (OFTP). A: January, B: April, C: July, D: October.

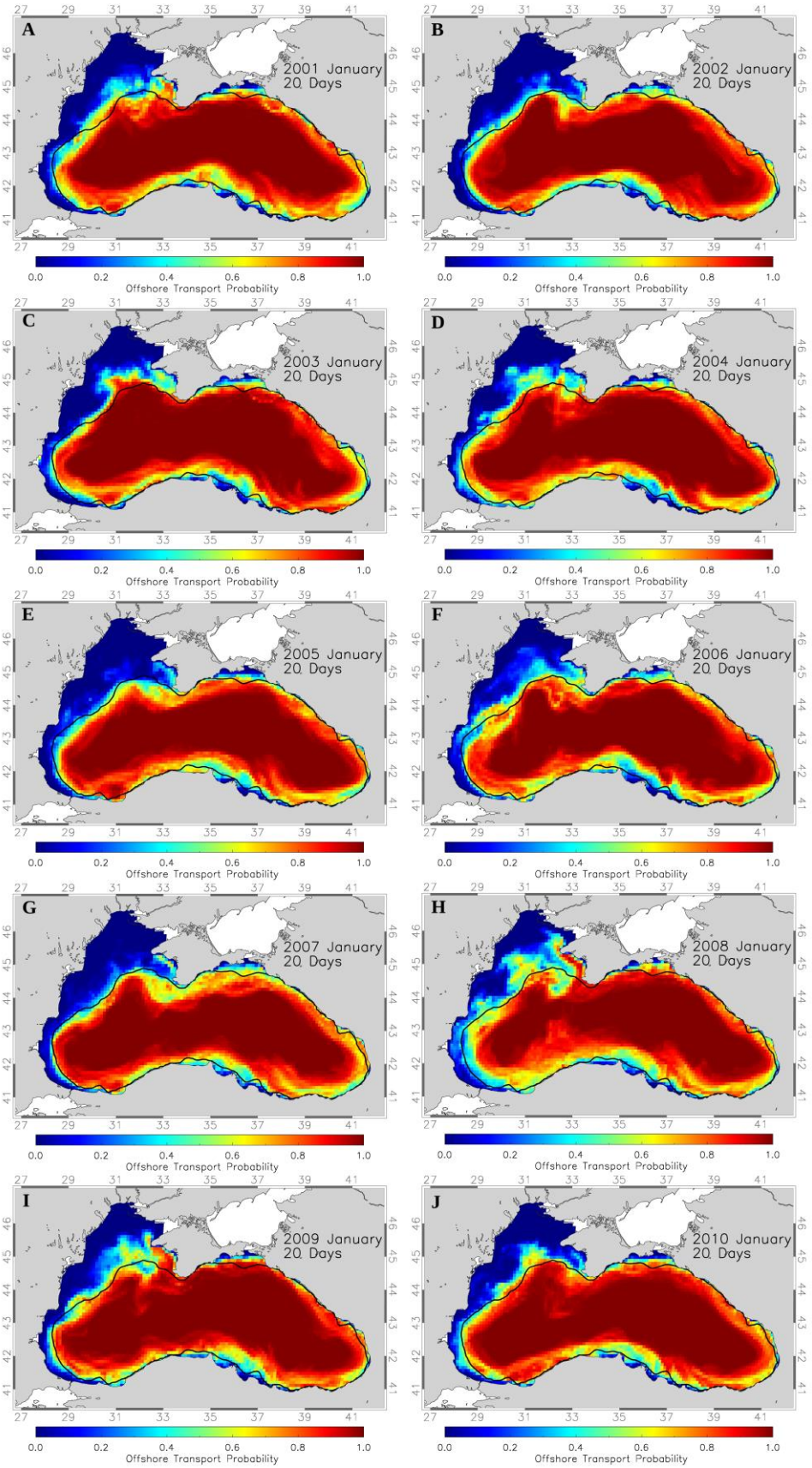

Appendix A 4: Simulation results of Offshore Transport Probability (OFTP) for simulations with January spawning times and 20 day Pelagic Larval Duration for A-J: 2001-2010.

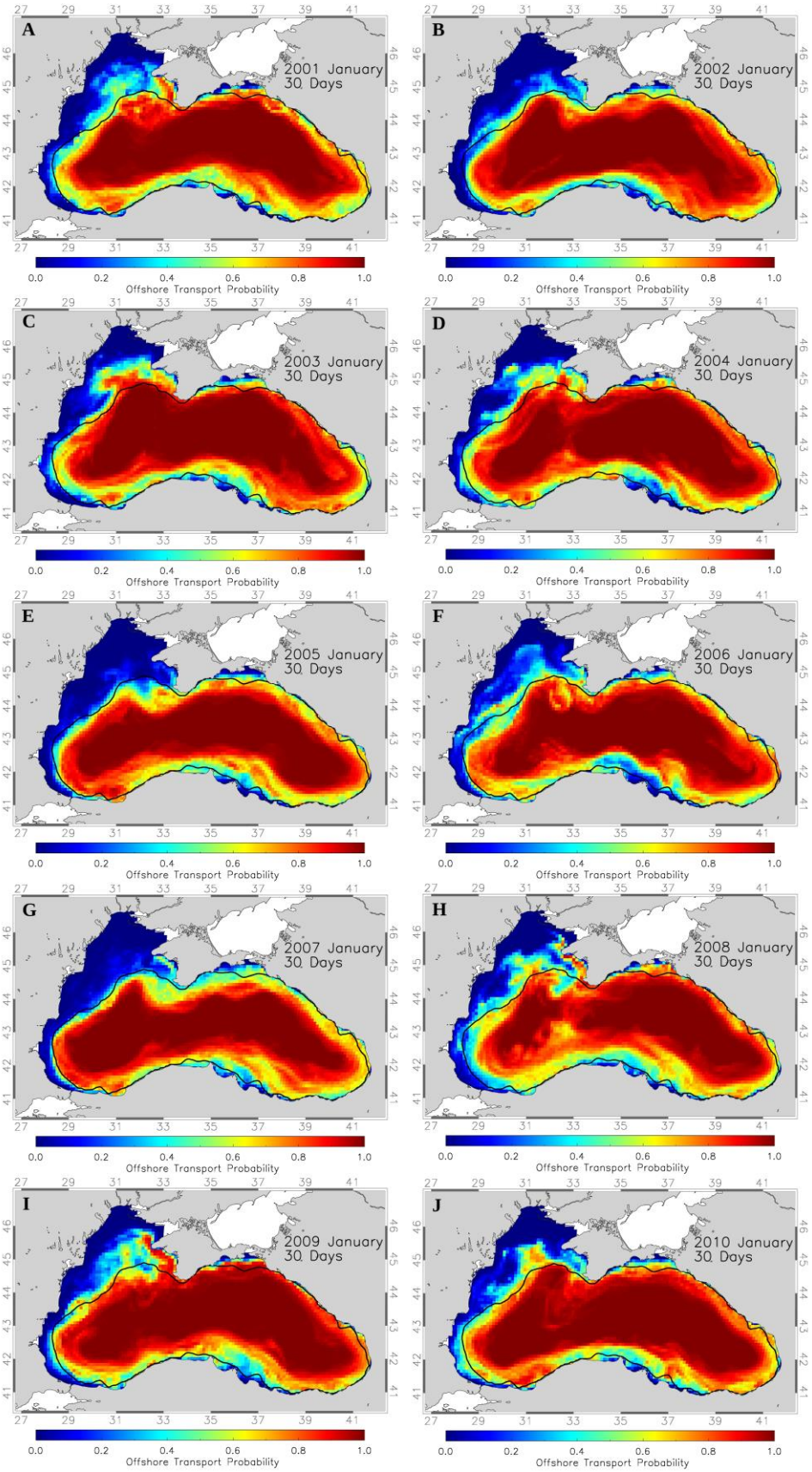

Appendix A 5: Simulation results of Offshore Transport Probability (OFTP) for simulations with January spawning times and 30 day Pelagic Larval Duration for A-J: 2001-2010.

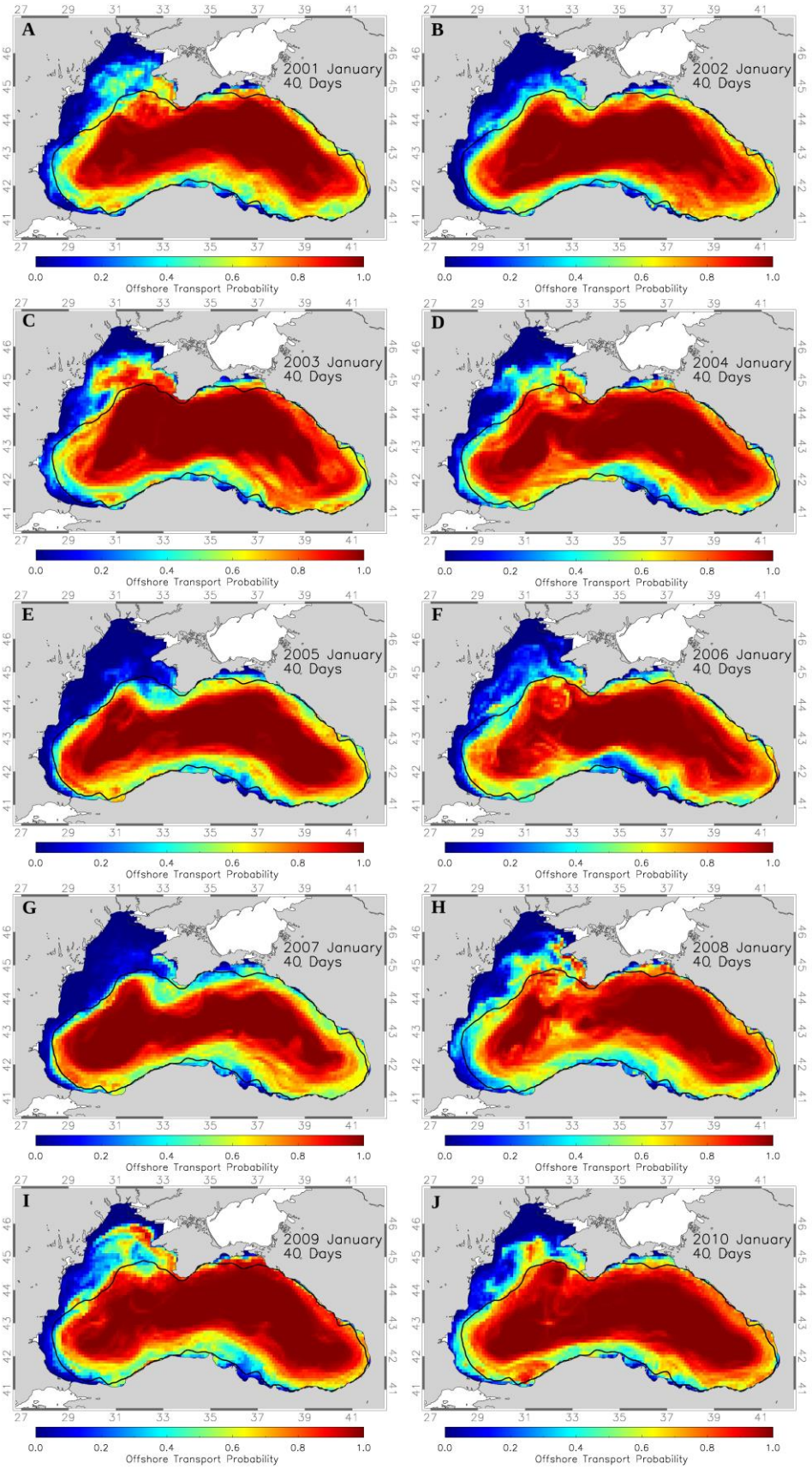

Appendix A 6: Simulation results of Offshore Transport Probability (OFTP) for simulations with January spawning times and 40 day Pelagic Larval Duration for A-J: 2001-2010.

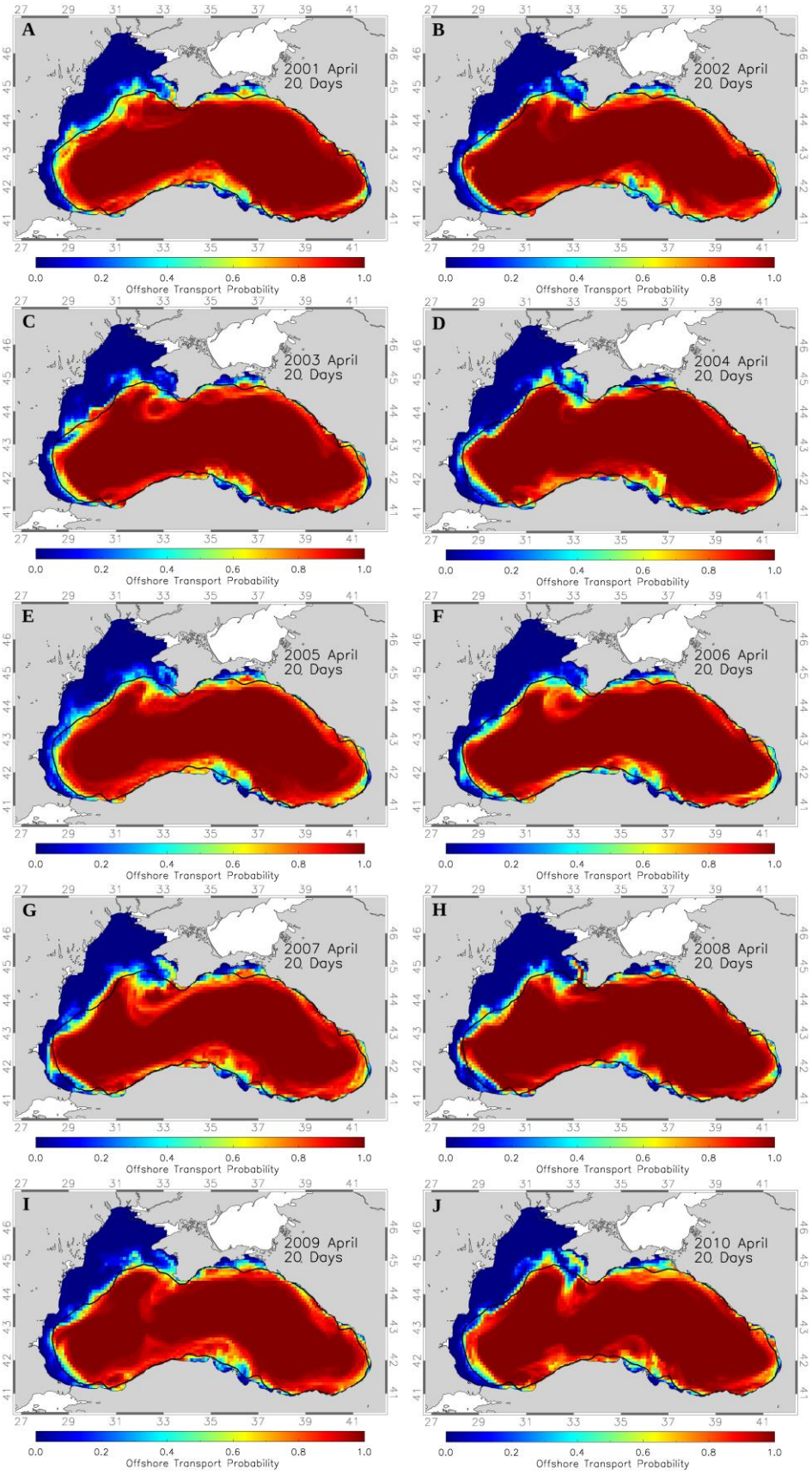

Appendix A 7: Simulation results of Offshore Transport Probability (OFTP) for simulations with April spawning times and 20 day Pelagic Larval Duration for A-J: 2001-2010.

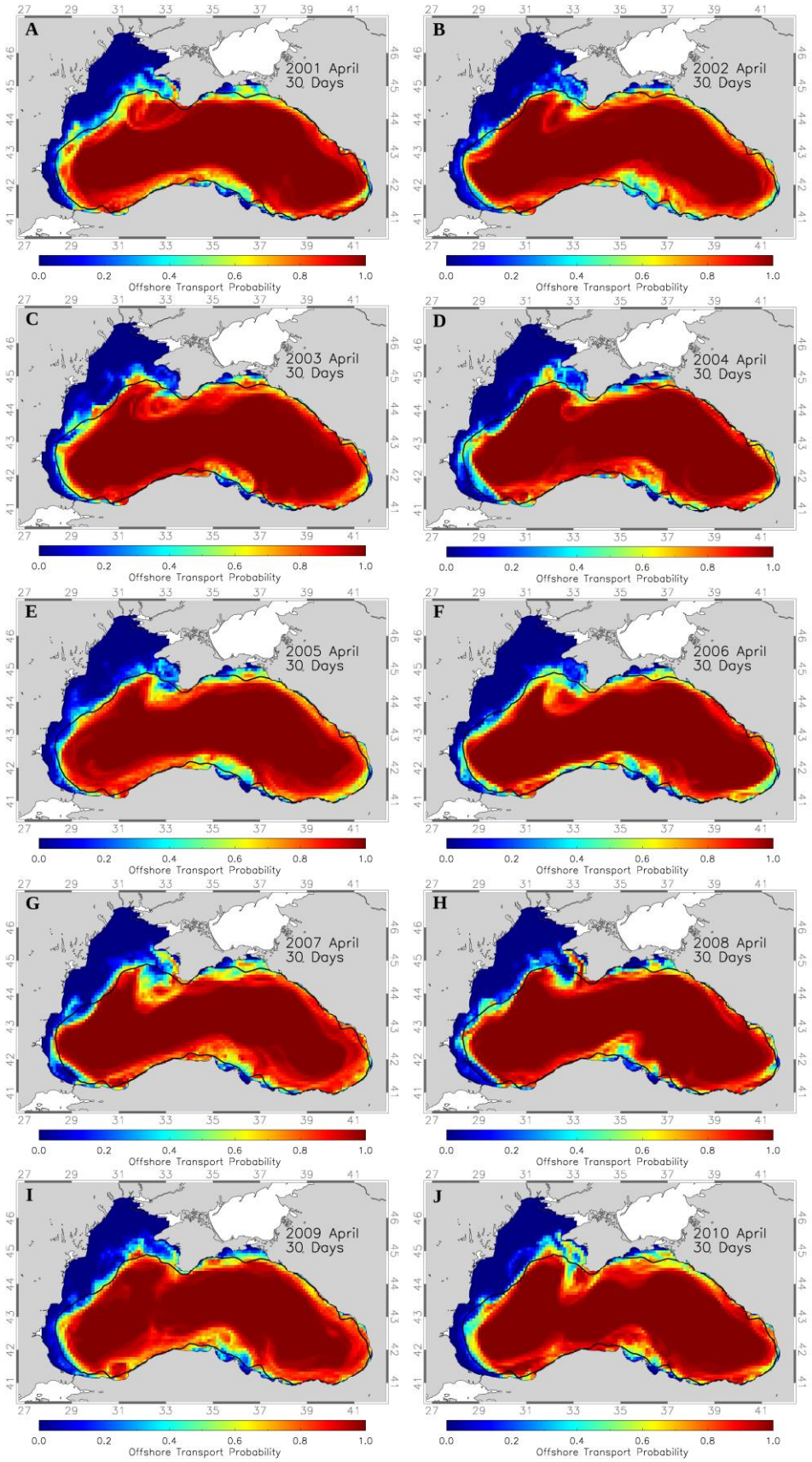

Appendix A 8: Simulation results of Offshore Transport Probability (OFTP) for simulations with April spawning times and 30 day Pelagic Larval Duration for A-J: 2001-2010.

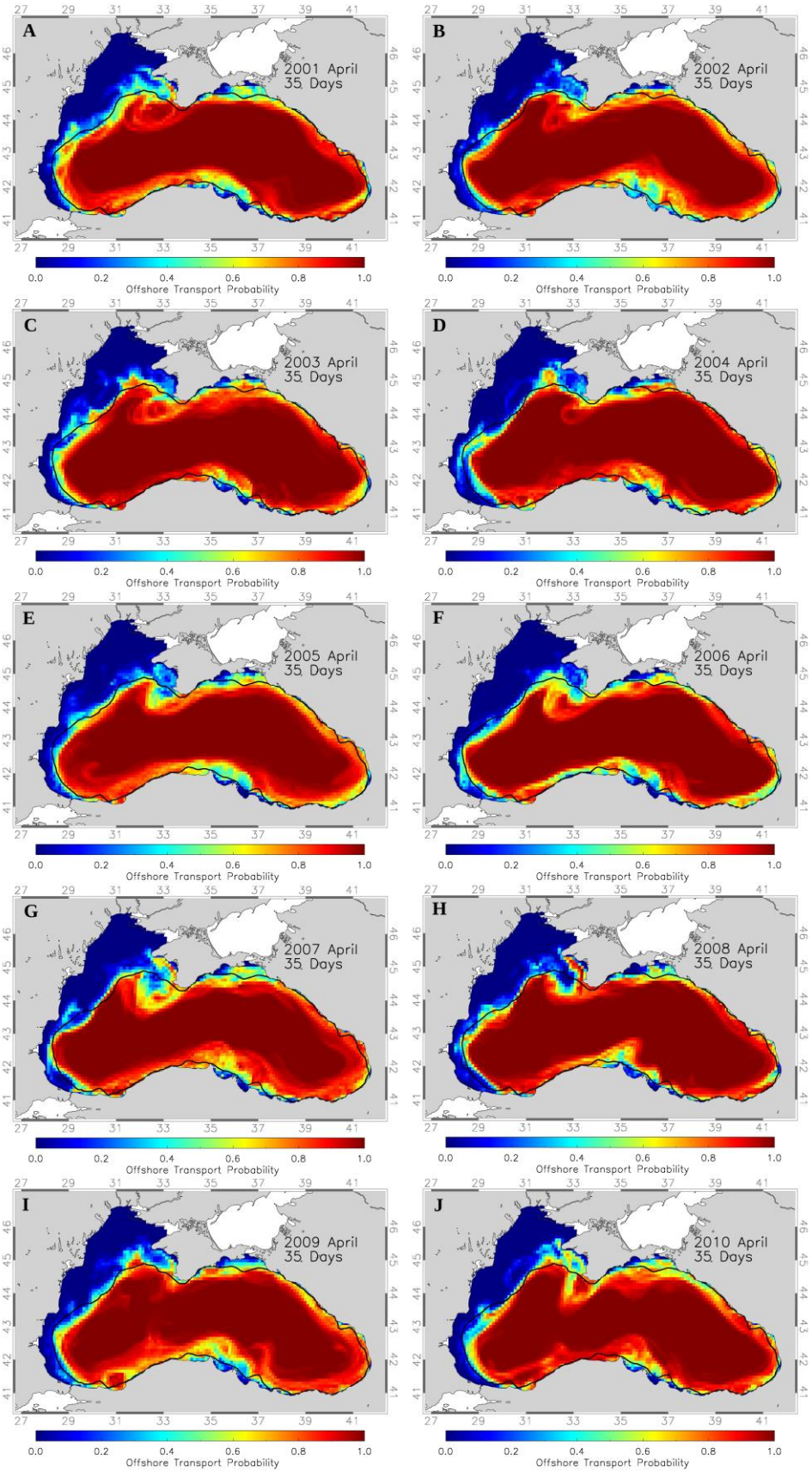

Appendix A 9: Simulation results of Offshore Transport Probability (OFTP) for simulations with April spawning times and 35 day Pelagic Larval Duration for A-J: 2001-2010.

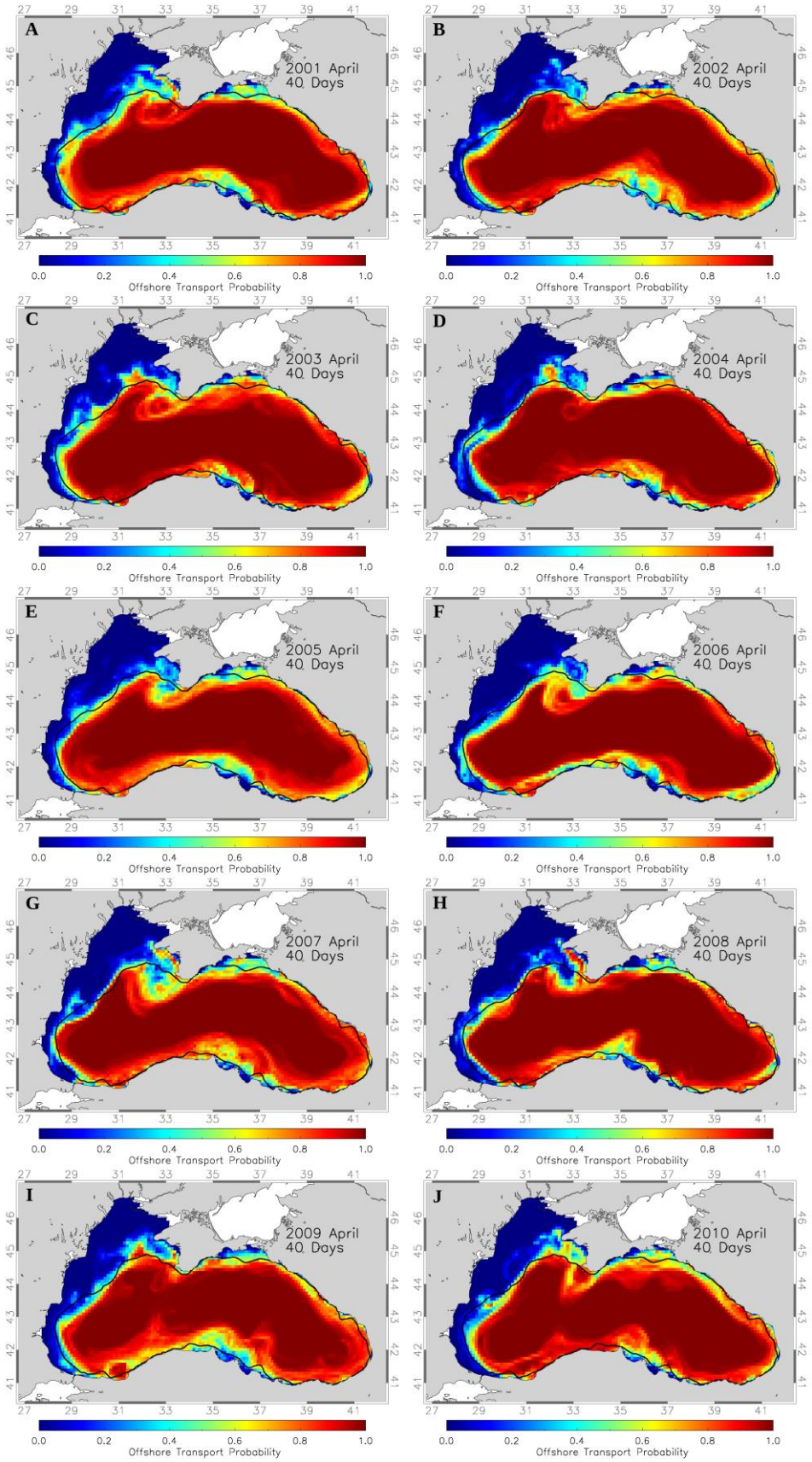

Appendix A 10: Simulation results of Offshore Transport Probability (OFTP) for simulations with April spawning times and 40 day Pelagic Larval Duration for A-J: 2001-2010.

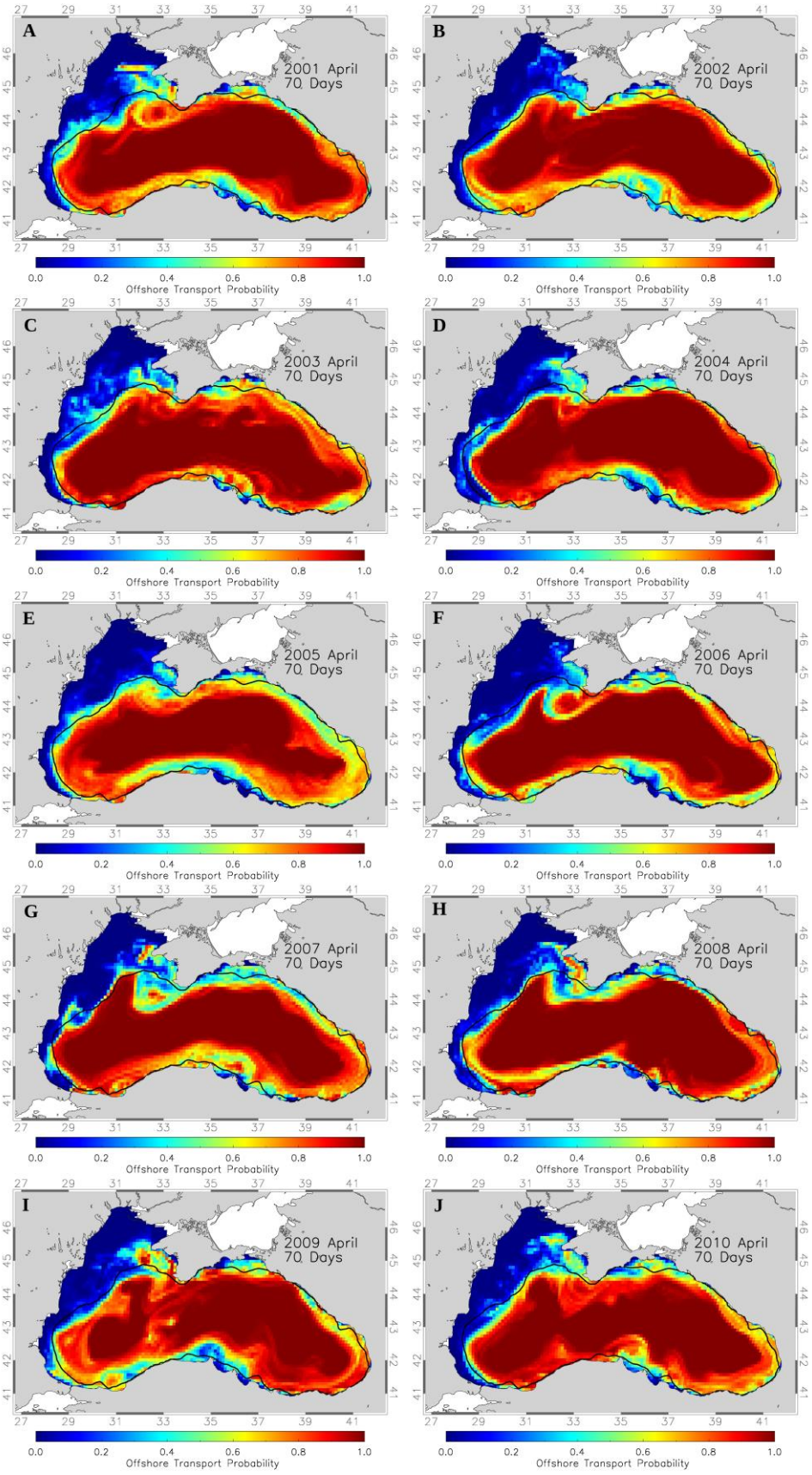

Appendix A 11: Simulation results of Offshore Transport Probability (OFTP) for simulations with April spawning times and 70 day Pelagic Larval Duration for A-J: 2001-2010.

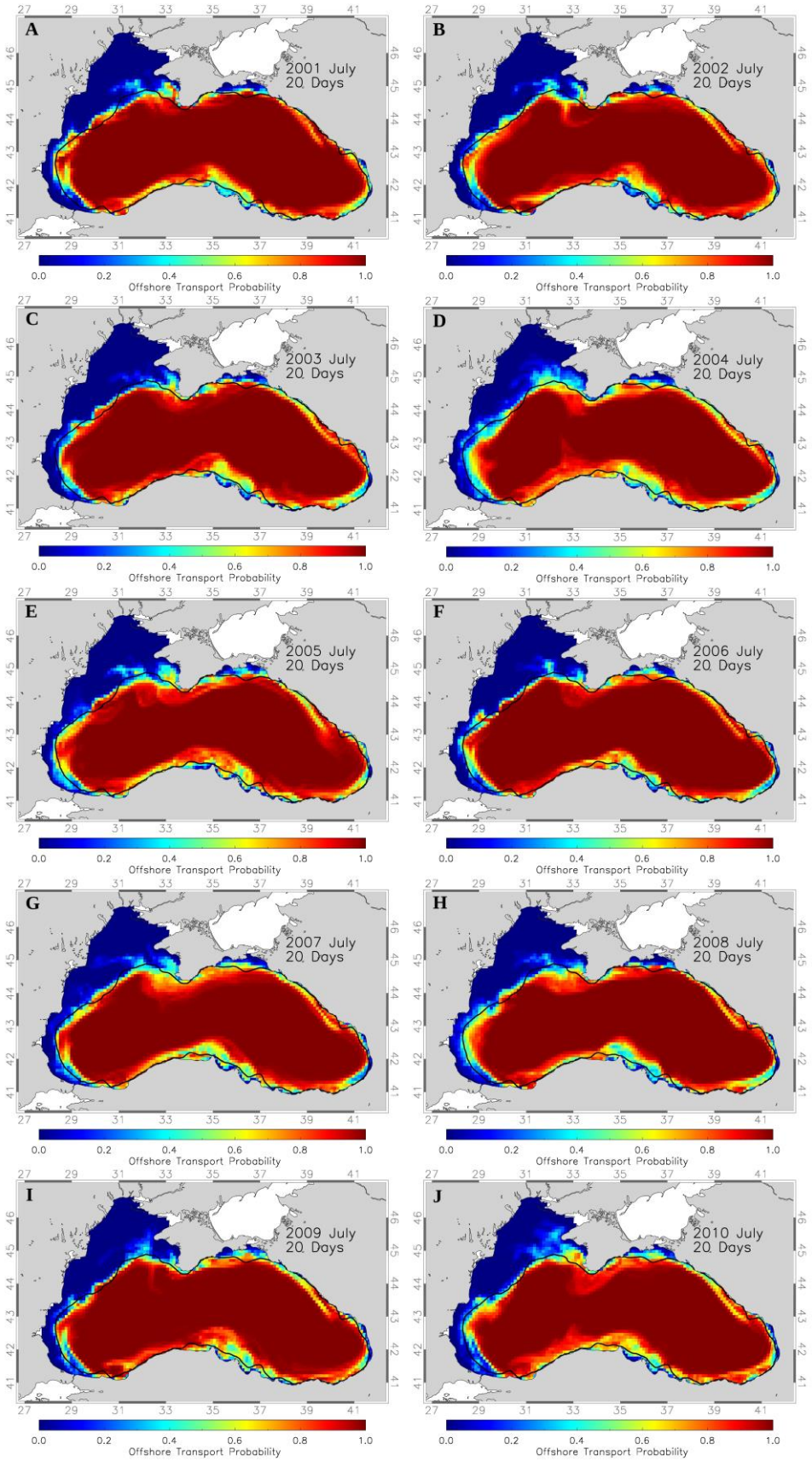

Appendix A 12: Simulation results of Offshore Transport Probability (OFTP) for simulations with July spawning times and 20 day Pelagic Larval Duration for A-J: 2001-2010.

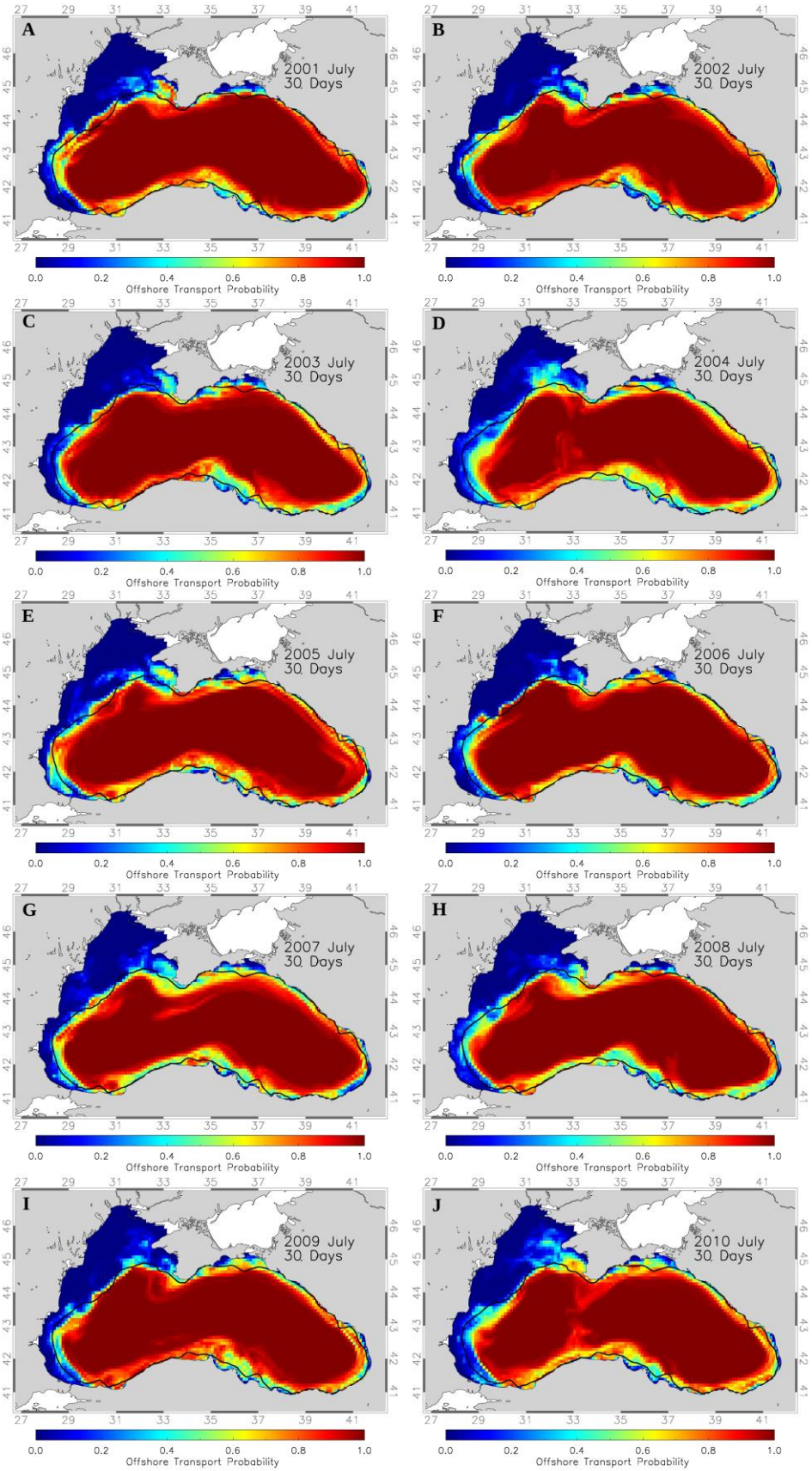

Appendix A 13: Simulation results of Offshore Transport Probability (OFTP) for simulations with July spawning times and 30 day Pelagic Larval Duration for A-J: 2001-2010.

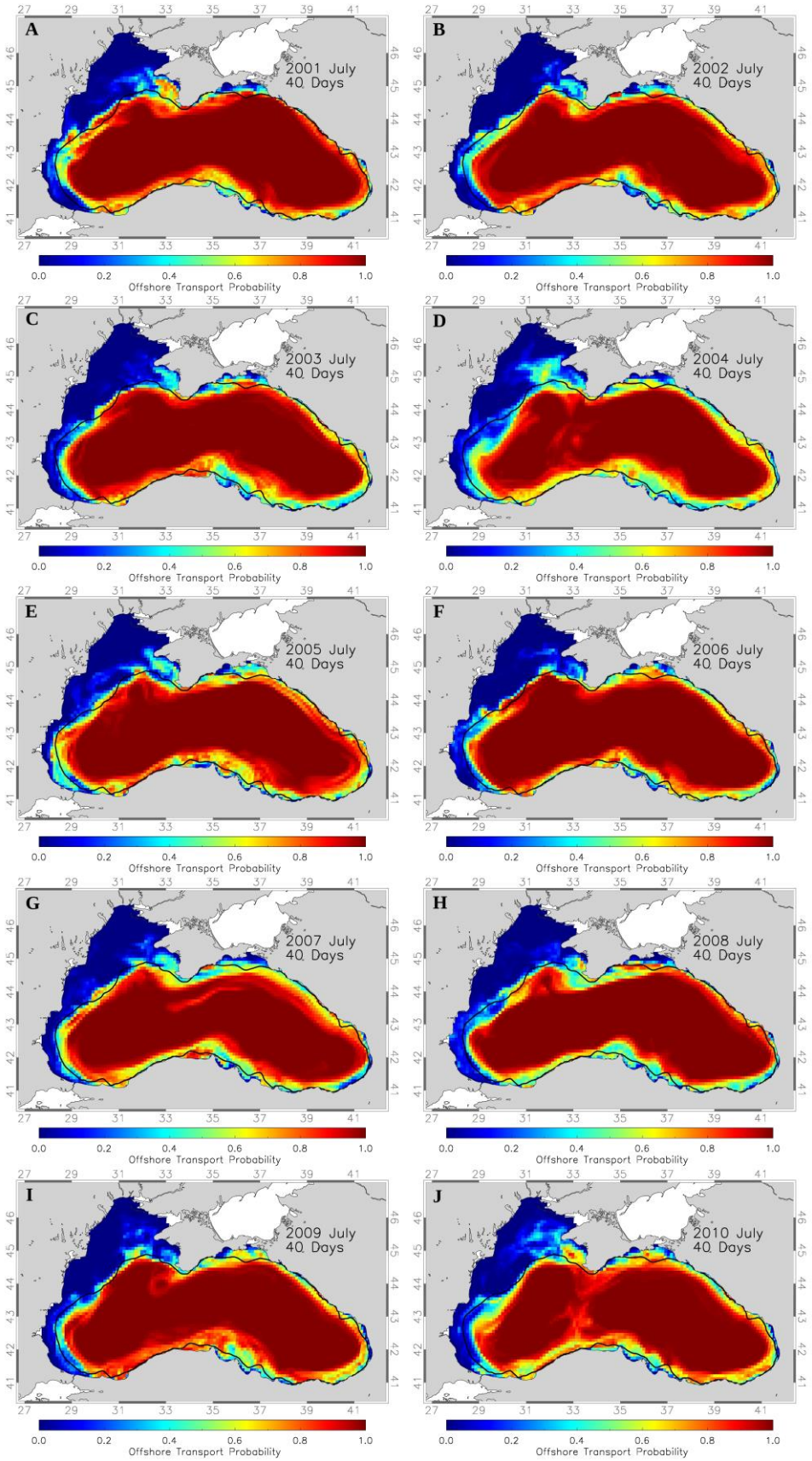

Appendix A 14: Simulation results of Offshore Transport Probability (OFTP) for simulations with July spawning times and 40 day Pelagic Larval Duration for A-J: 2001-2010.

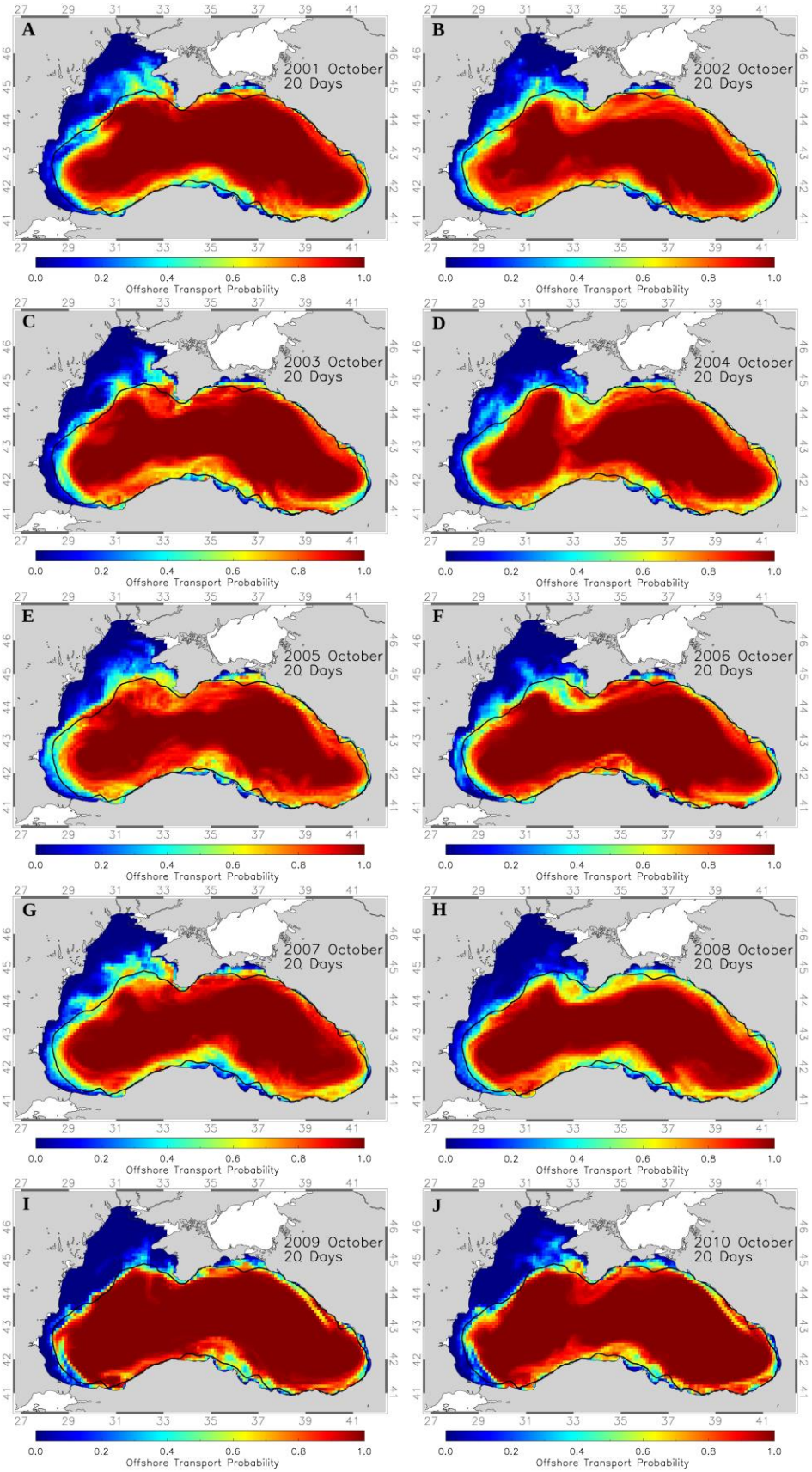

Appendix A 15: Simulation results of Offshore Transport Probability (OFTP) for simulations with October spawning times and 20 day Pelagic Larval Duration for A-J: 2001-2010.

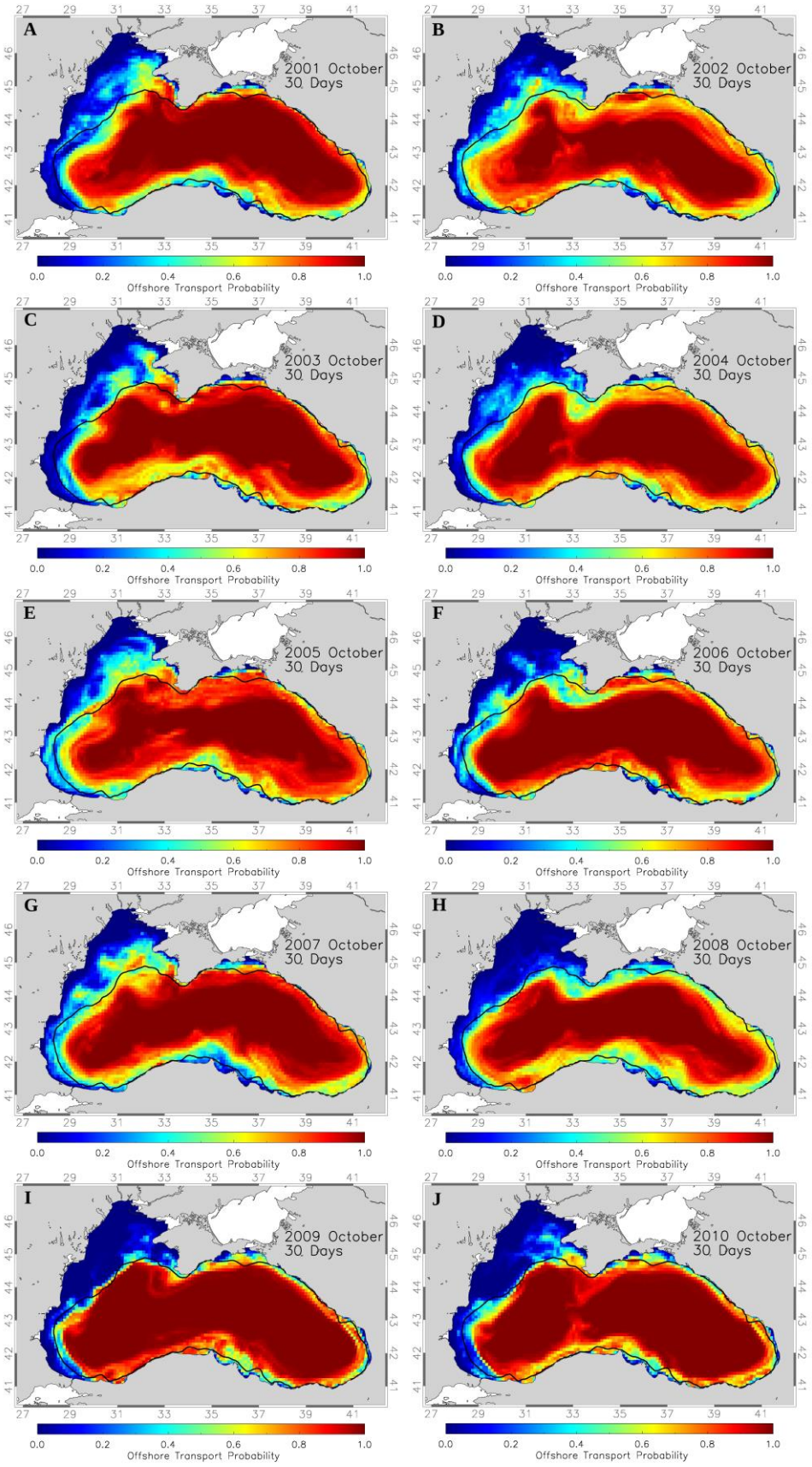

Appendix A 16: Simulation results of Offshore Transport Probability (OFTP) for simulations with October spawning times and 30 day Pelagic Larval Duration for A-J: 2001-2010

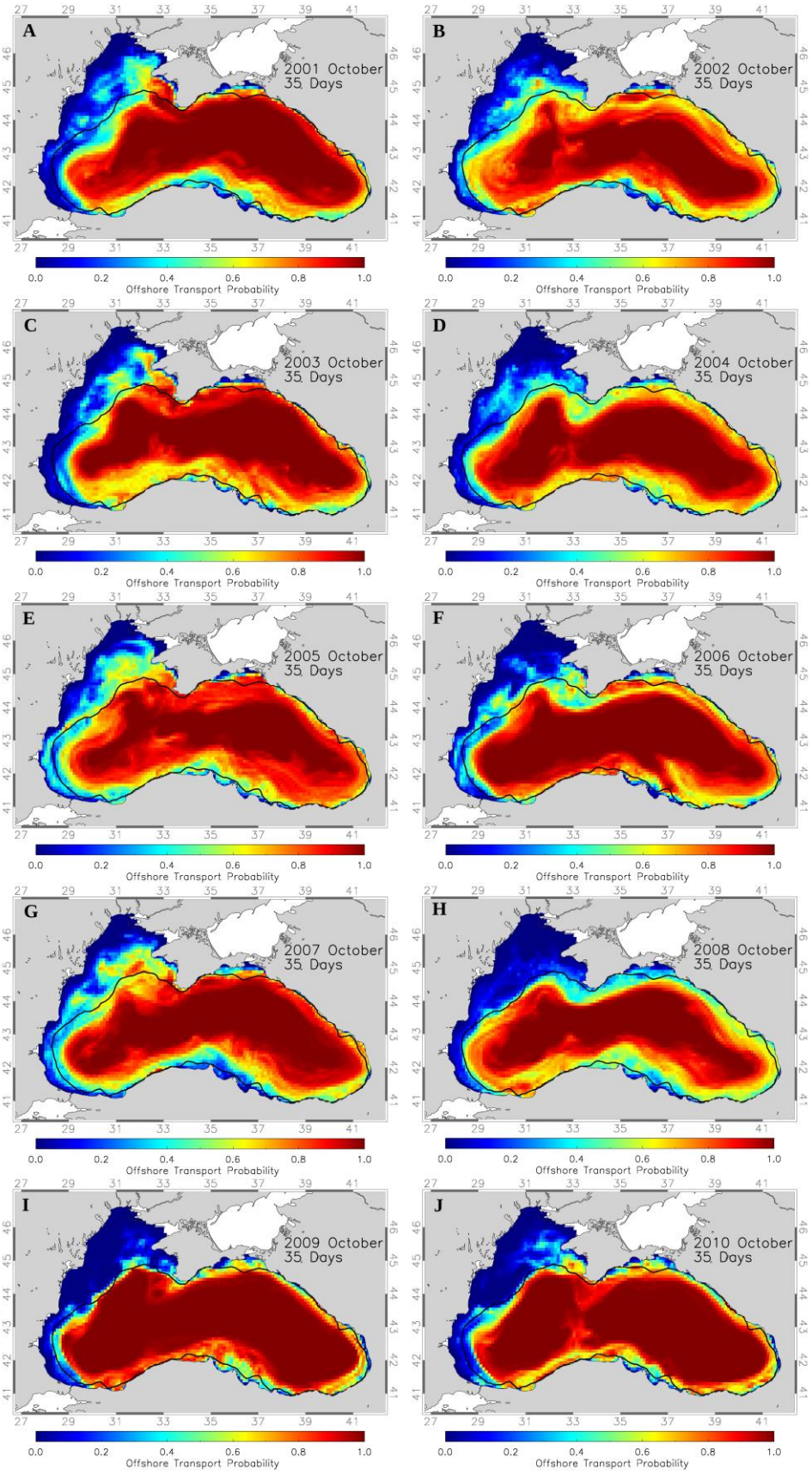

Appendix A 17: Simulation results of Offshore Transport Probability (OFTP) for simulations with October spawning times and 35 day Pelagic Larval Duration for A-J: 2001-2010.

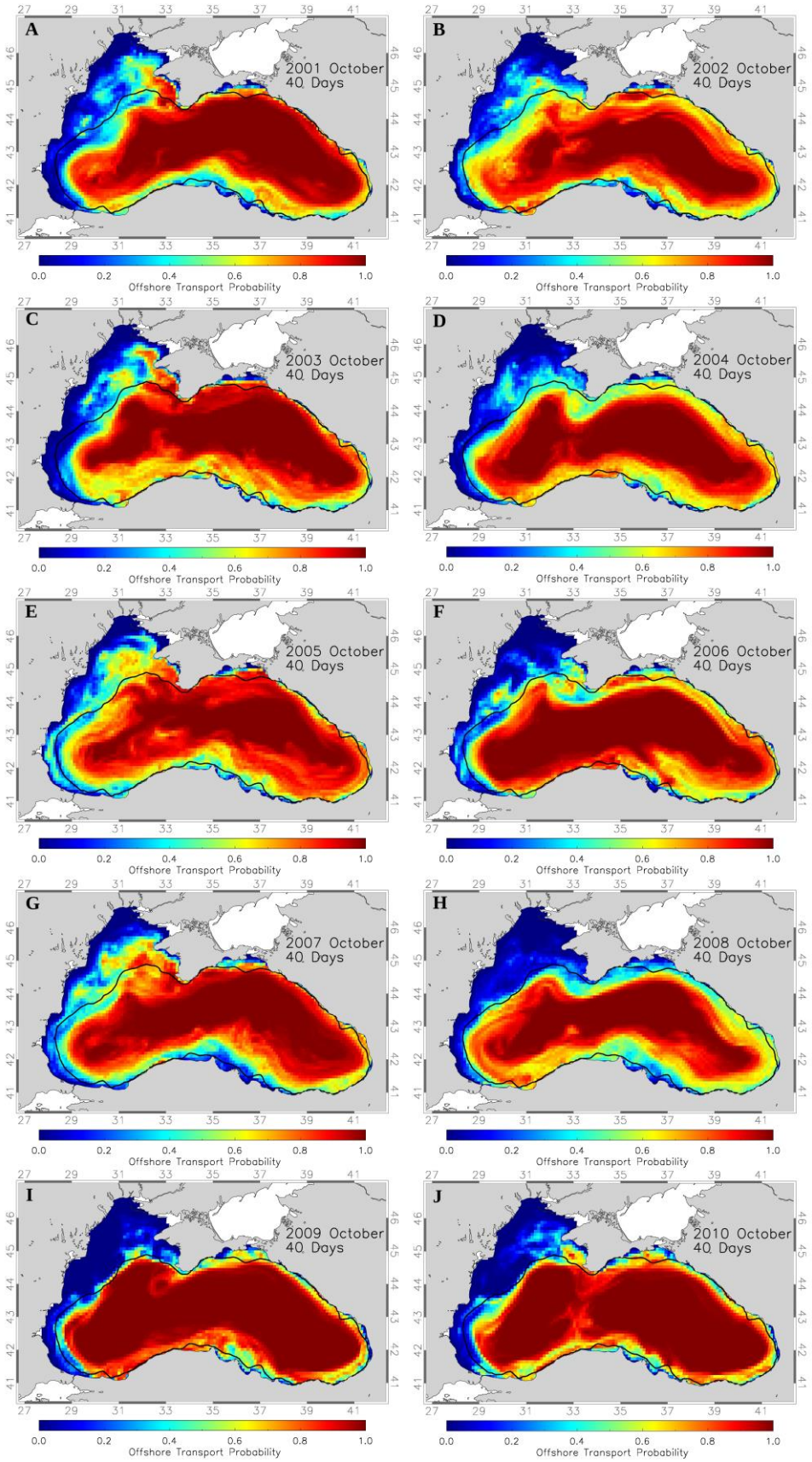

Appendix A 18: Simulation results of Offshore Transport Probability (OFTP) for simulations with October spawning times and 40 day Pelagic Larval Duration for A-J: 2001-2010.

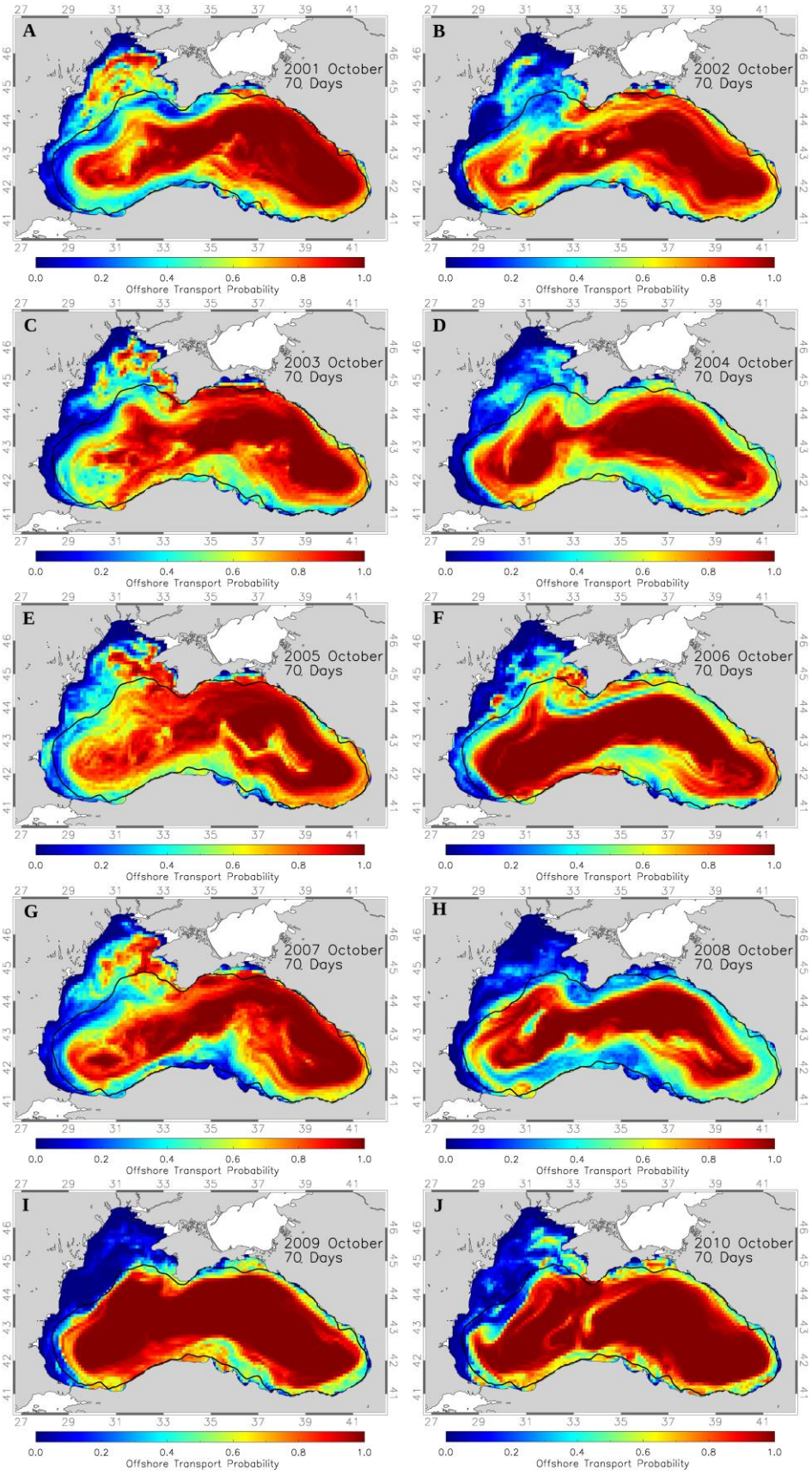

Appendix A 19: Simulation results of Offshore Transport Probability (OFTP) for simulations with October spawning times and 70 day Pelagic Larval Duration for A-J: 2001-2010.

Section B: Onshore Transport Probability

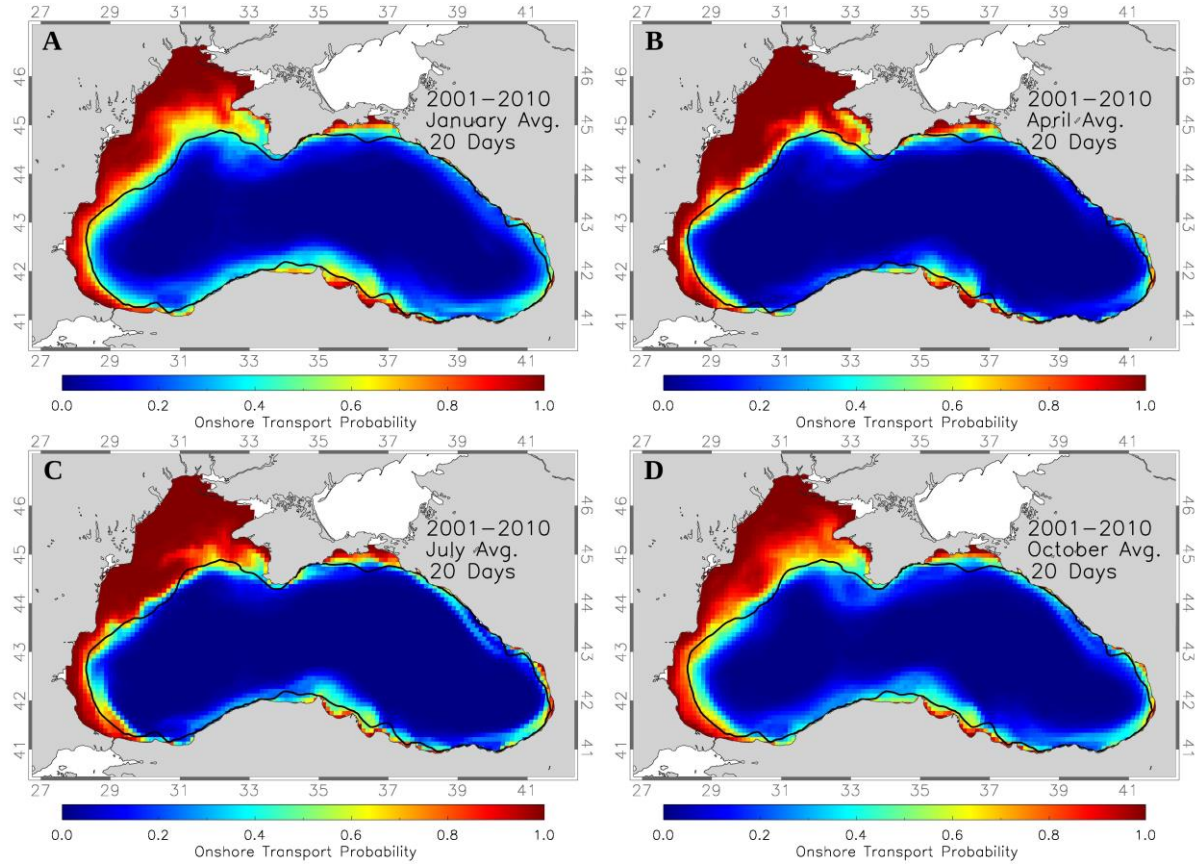

Appendix B 1: Simulation results averaged over 10 years (2001-2010) for four seasons at 20 day pelagic larval duration (PLD) to calculate the Onshore Transport Probability (ONTP). A: January, B: April, C: July, D: October.

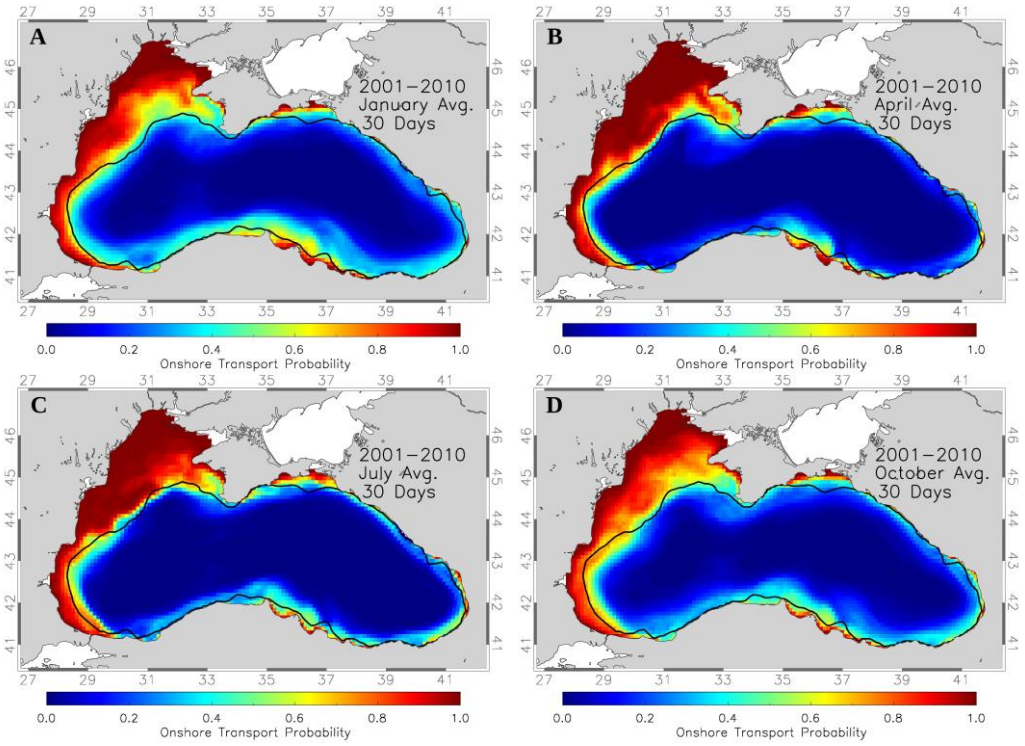

Appendix B 2: Simulation results averaged over 10 years (2001-2010) for four seasons at 30 day pelagic larval duration (PLD) to calculate the Onshore Transport Probability (ONTP). A: January, B: April, C: July, D: October.

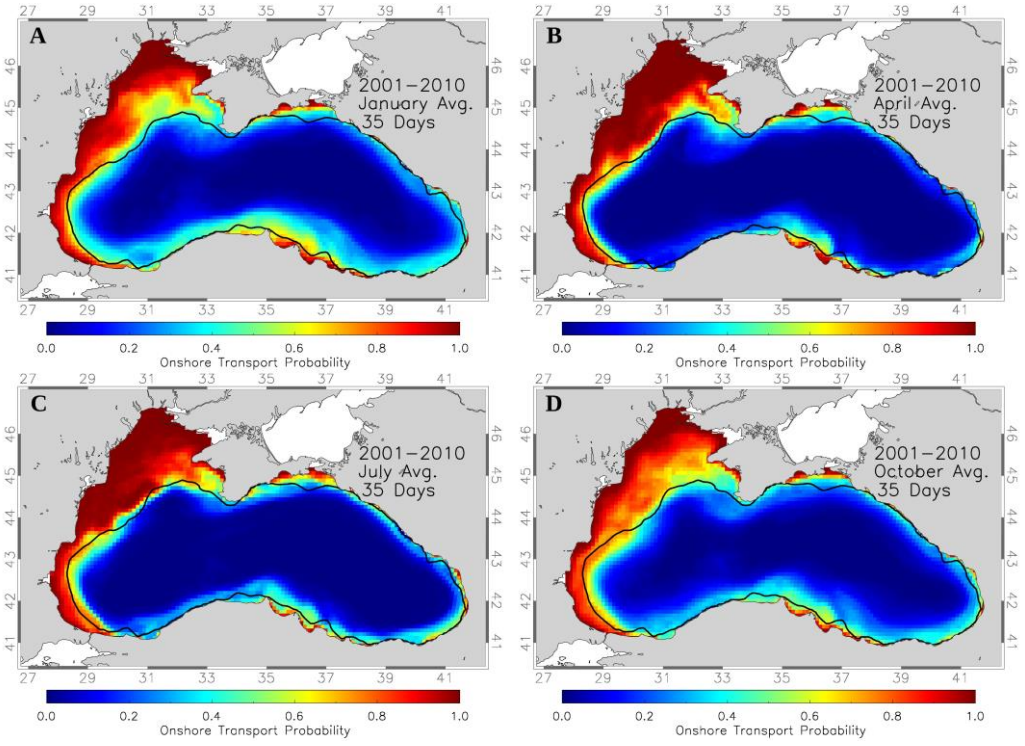

Appendix B 3: Simulation results averaged over 10 years (2001-2010) for four seasons at 35 day pelagic larval duration (PLD) to calculate the Onshore Transport Probability (ONTP). A: January, B: April, C: July, D: October.

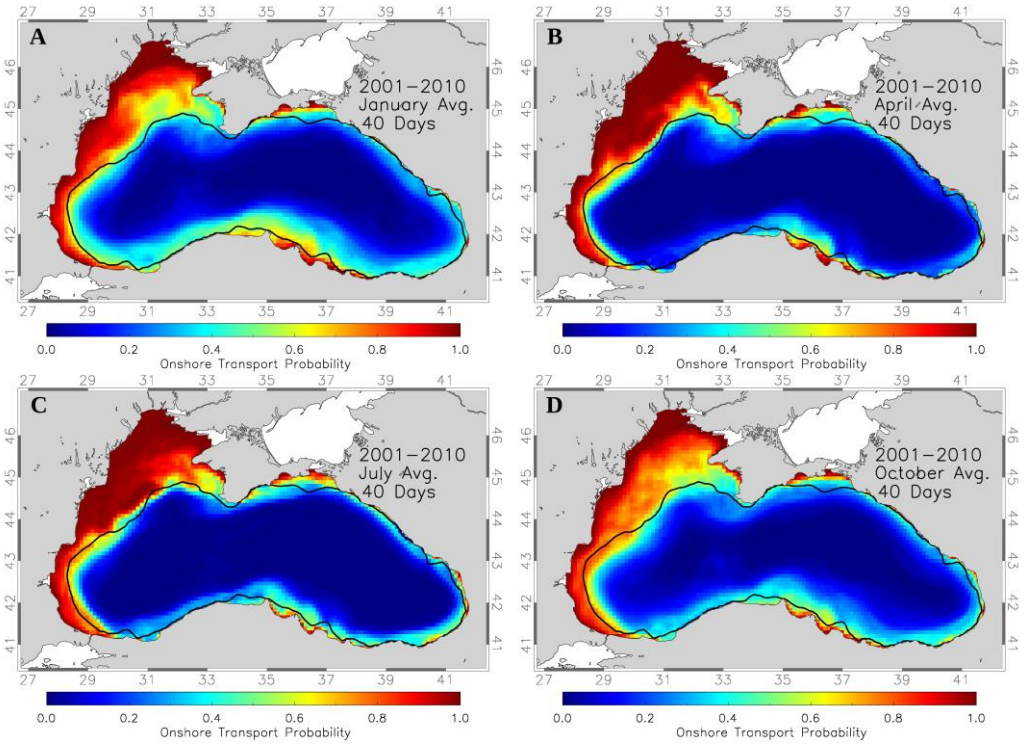

Appendix B 4: Simulation results averaged over 10 years (2001-2010) for four seasons at 40 day pelagic larval duration (PLD) to calculate the Onshore Transport Probability (ONTP). A: January, B: April, C: July, D: October.

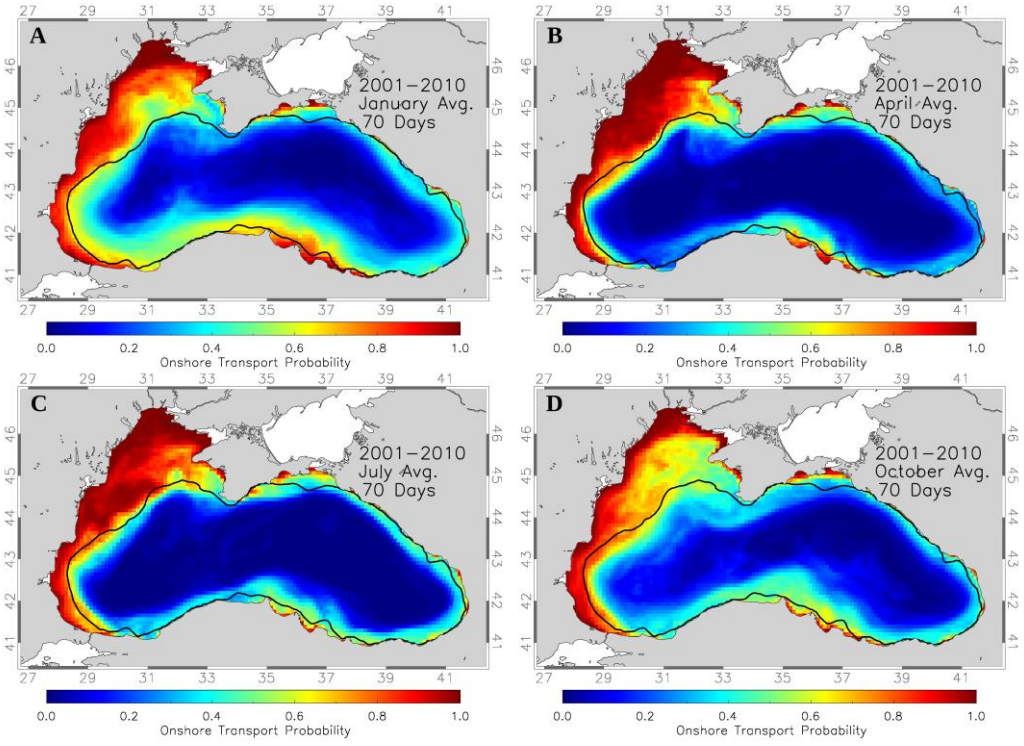

Appendix B 5: Simulation results averaged over 10 years (2001-2010) for four seasons at 70 day pelagic larval duration (PLD) to calculate the Onshore Transport Probability (ONTP). A: January, B: April, C: July, D: October.

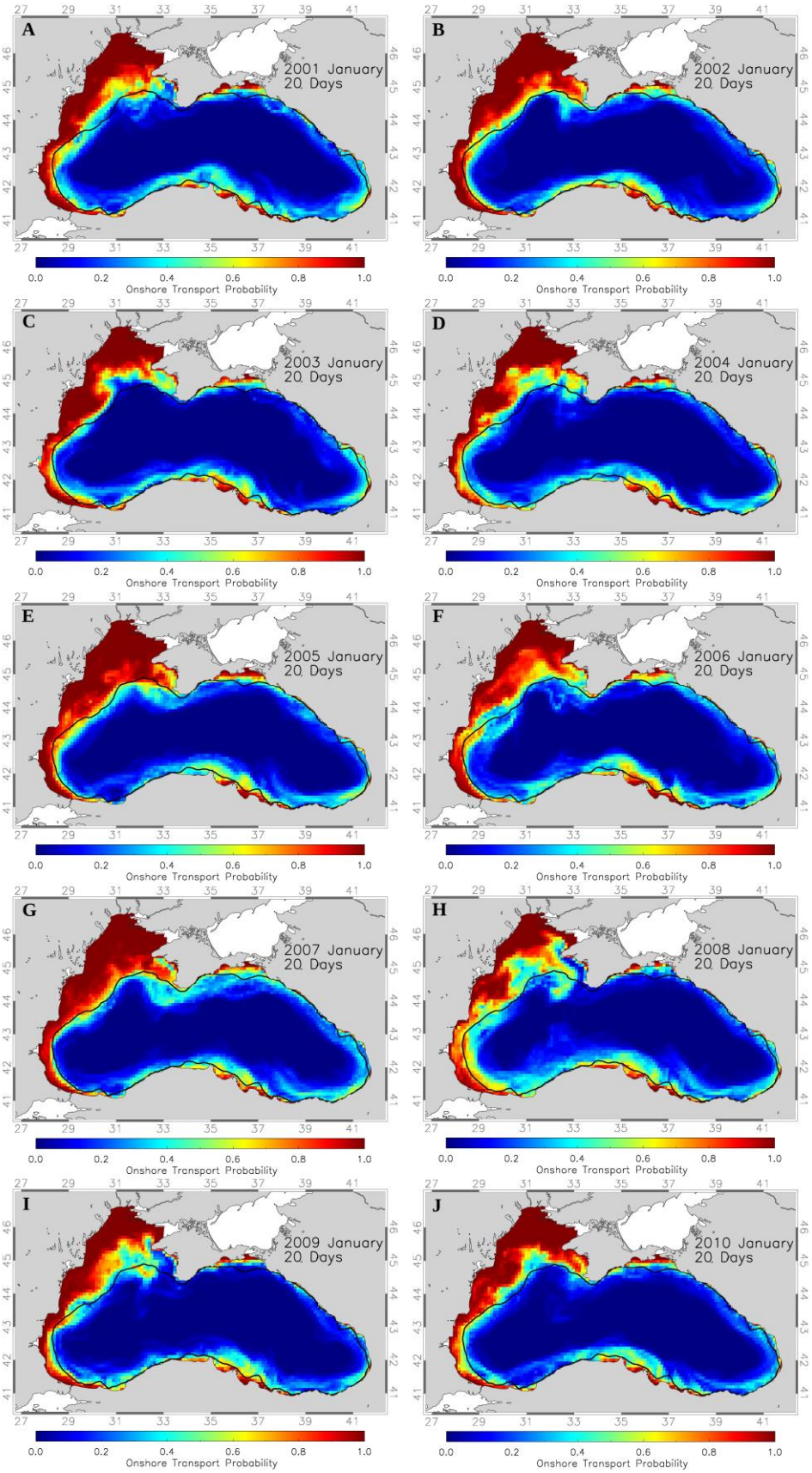

Appendix B 6: Simulation results of Onshore Transport Probability (ONTP) for simulations with January spawning times and 20 day Pelagic Larval Duration for A-J: 2001-2010.

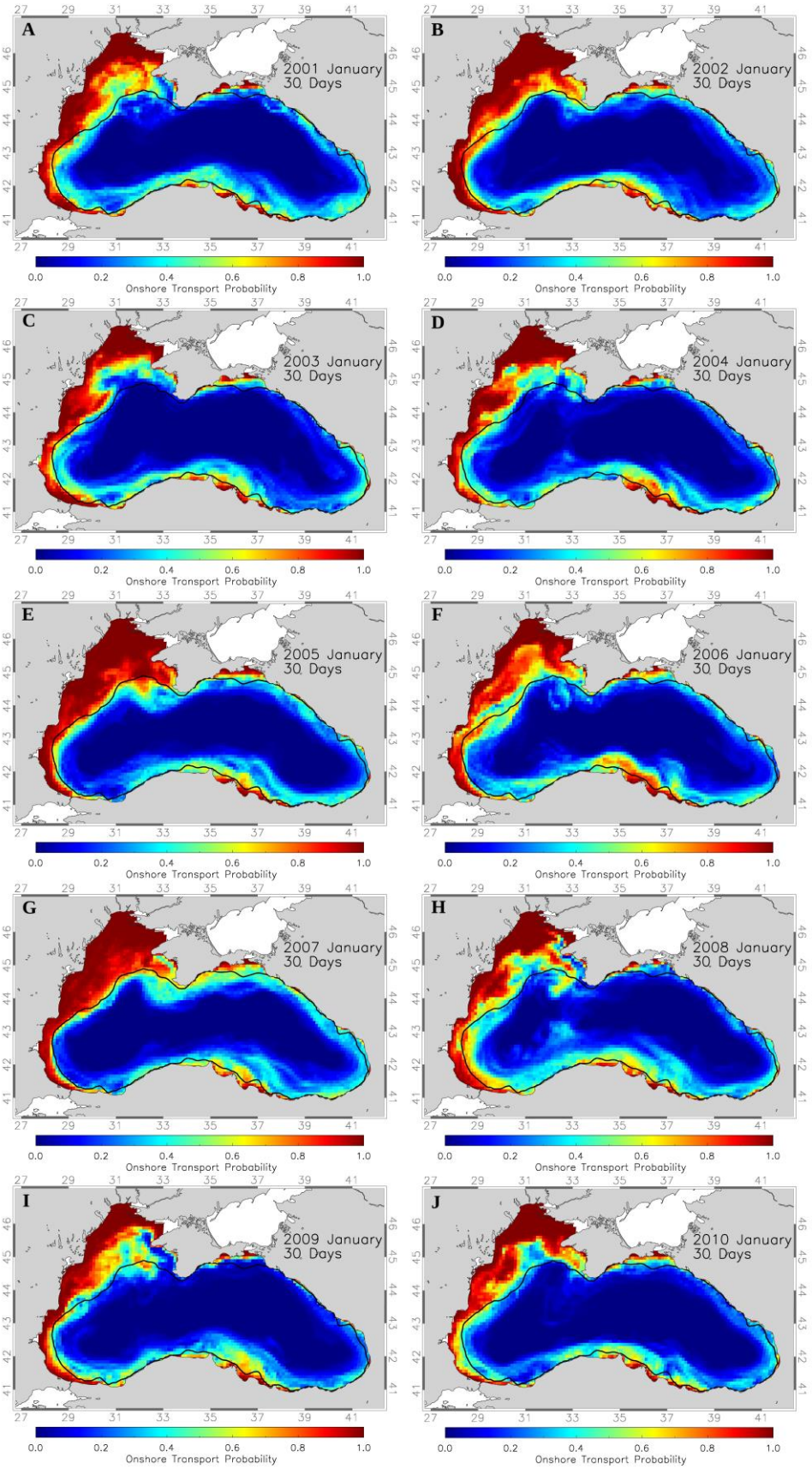

Appendix B 7: Simulation results of Onshore Transport Probability (ONTP) for simulations with January spawning times and 30 day Pelagic Larval Duration for A-J: 2001-2010.

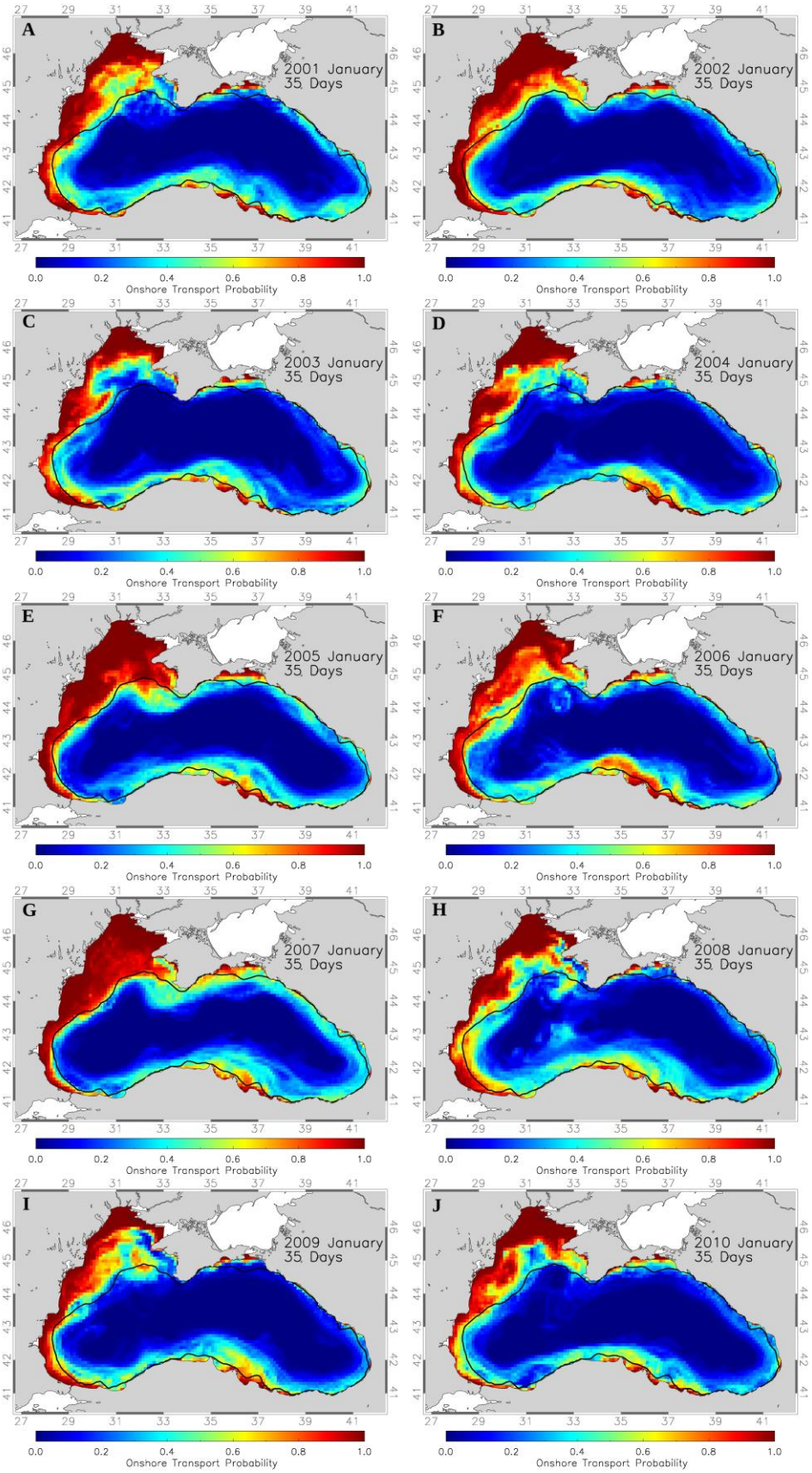

Appendix B 8: Simulation results of Onshore Transport Probability (ONTP) for simulations with January spawning times and 35 day Pelagic Larval Duration for A-J: 2001-2010.

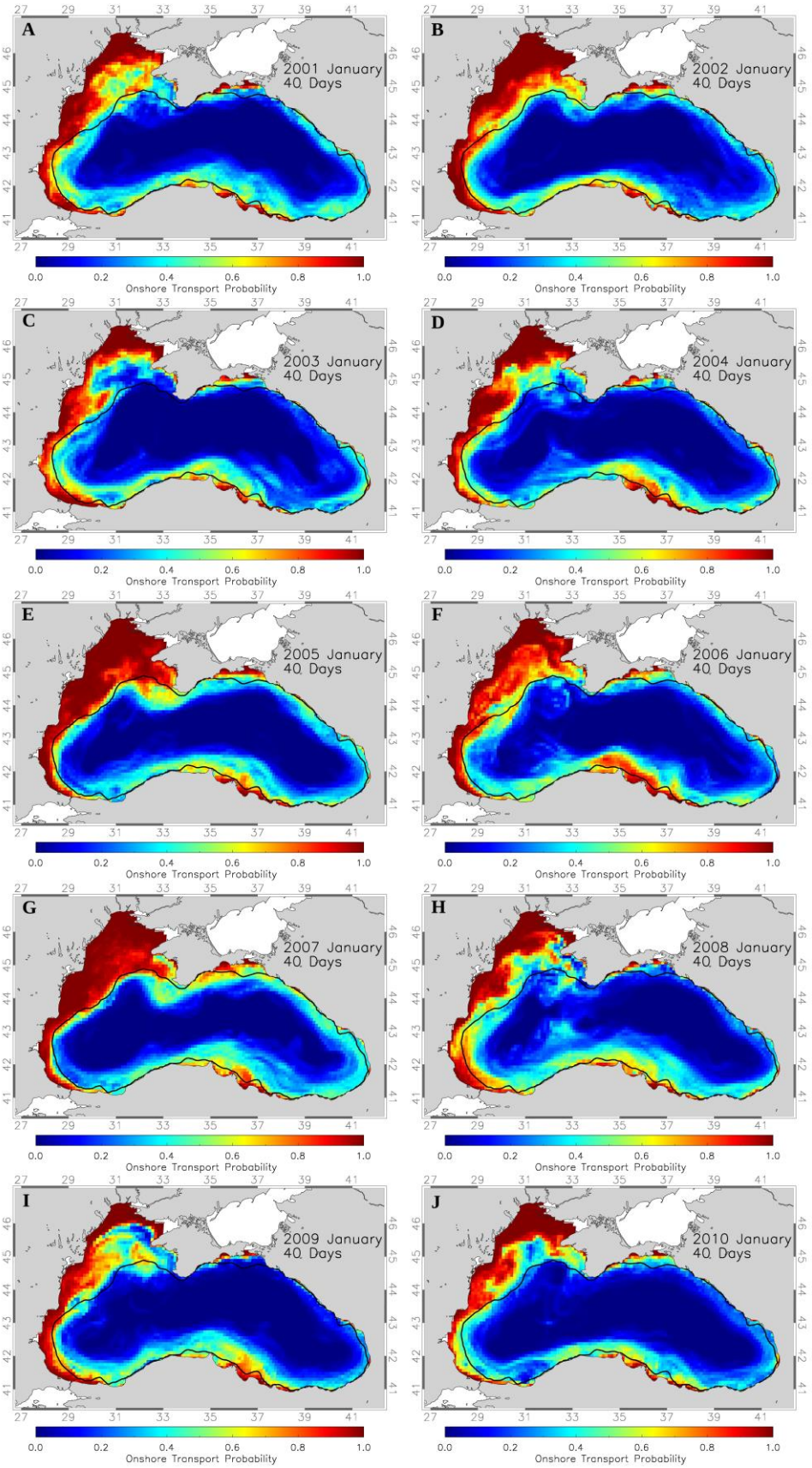

Appendix B 9: Simulation results of Onshore Transport Probability (ONTP) for simulations with January spawning times and 40 day Pelagic Larval Duration for A-J: 2001-2010.

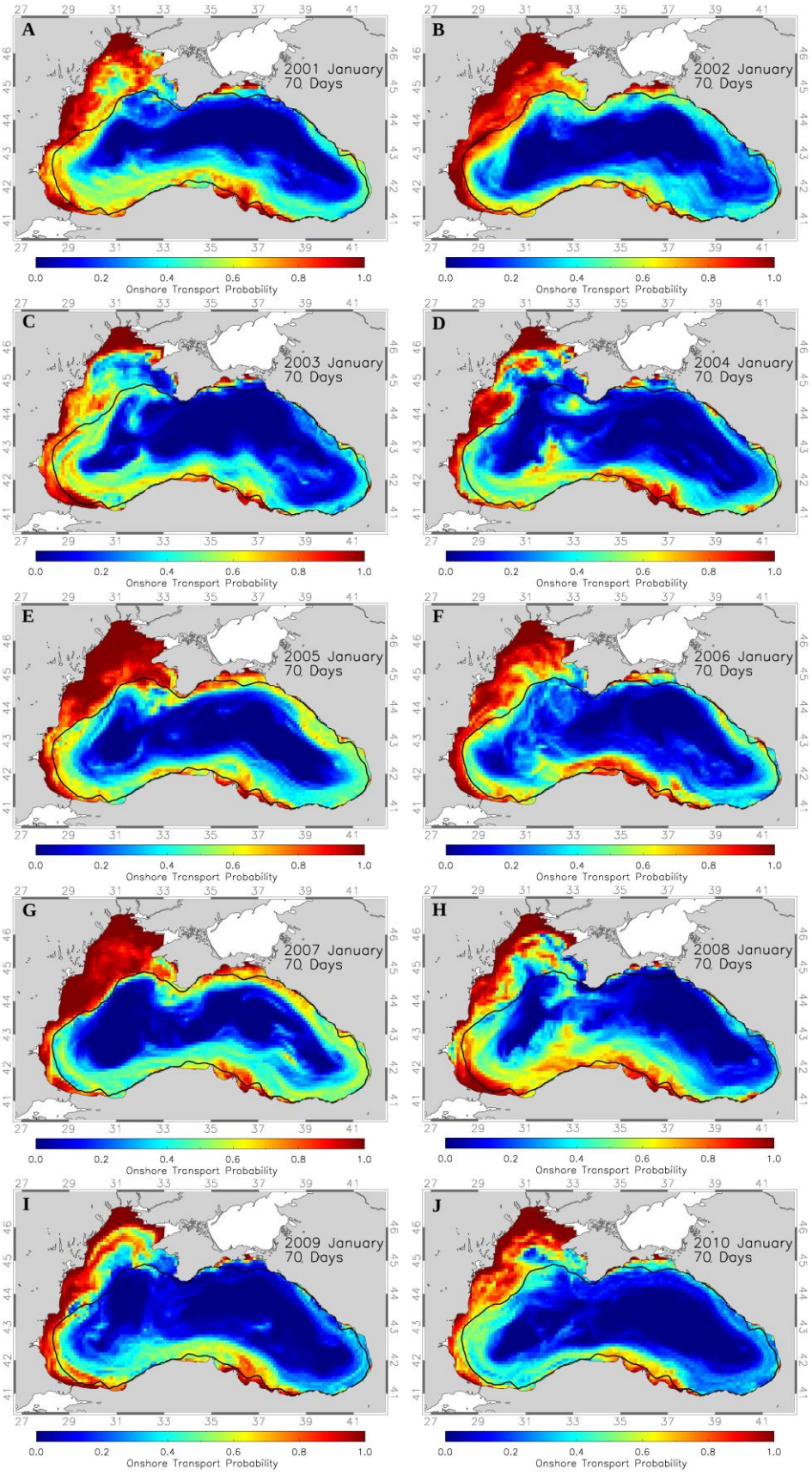

Appendix B 10: Simulation results of Onshore Transport Probability (ONTP) for simulations with January spawning times and 70 day Pelagic Larval Duration for A-J: 2001-2010.

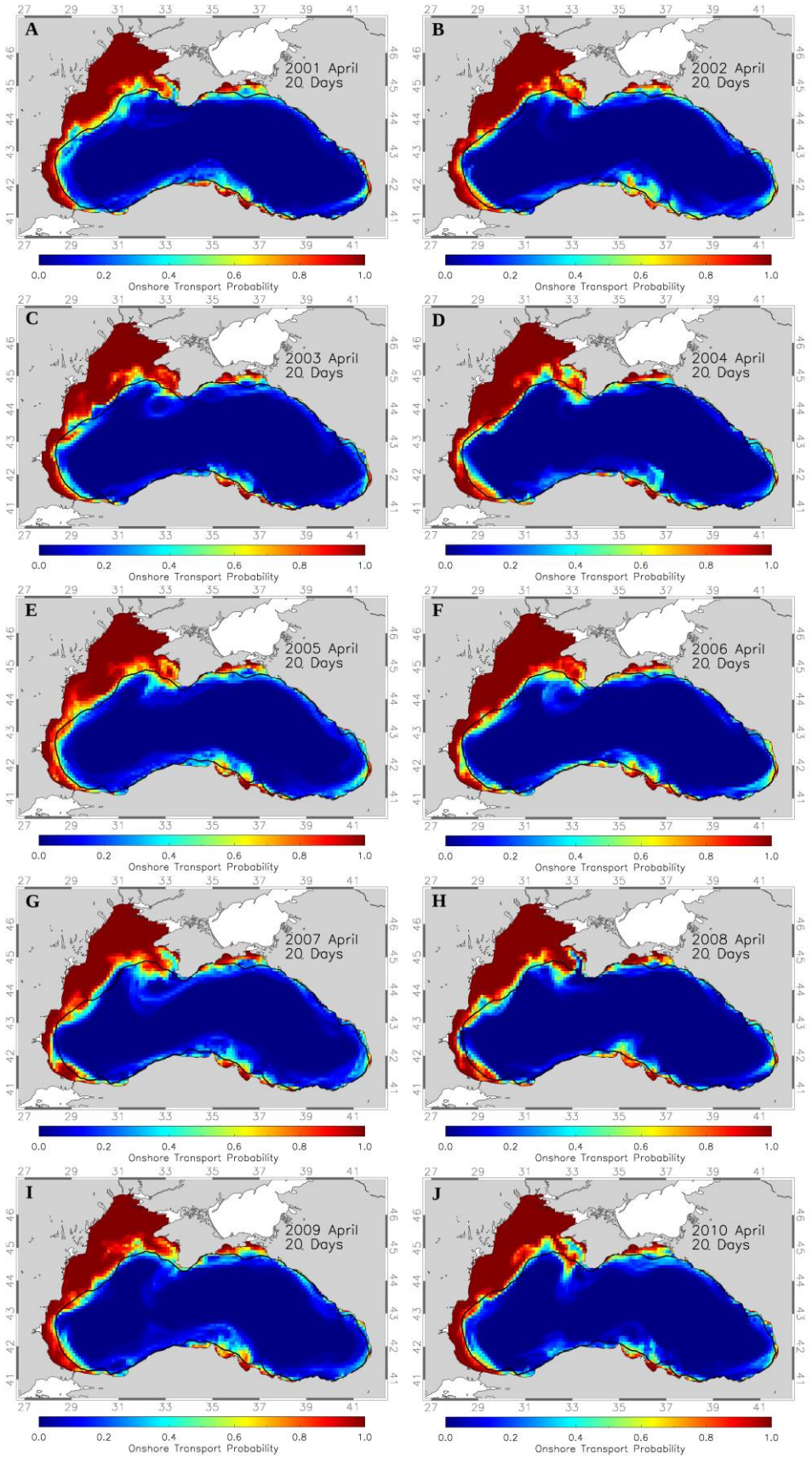

Appendix B 11: Simulation results of Onshore Transport Probability (ONTP) for simulations with April spawning times and 20 day Pelagic Larval Duration for A-J: 2001-2010.

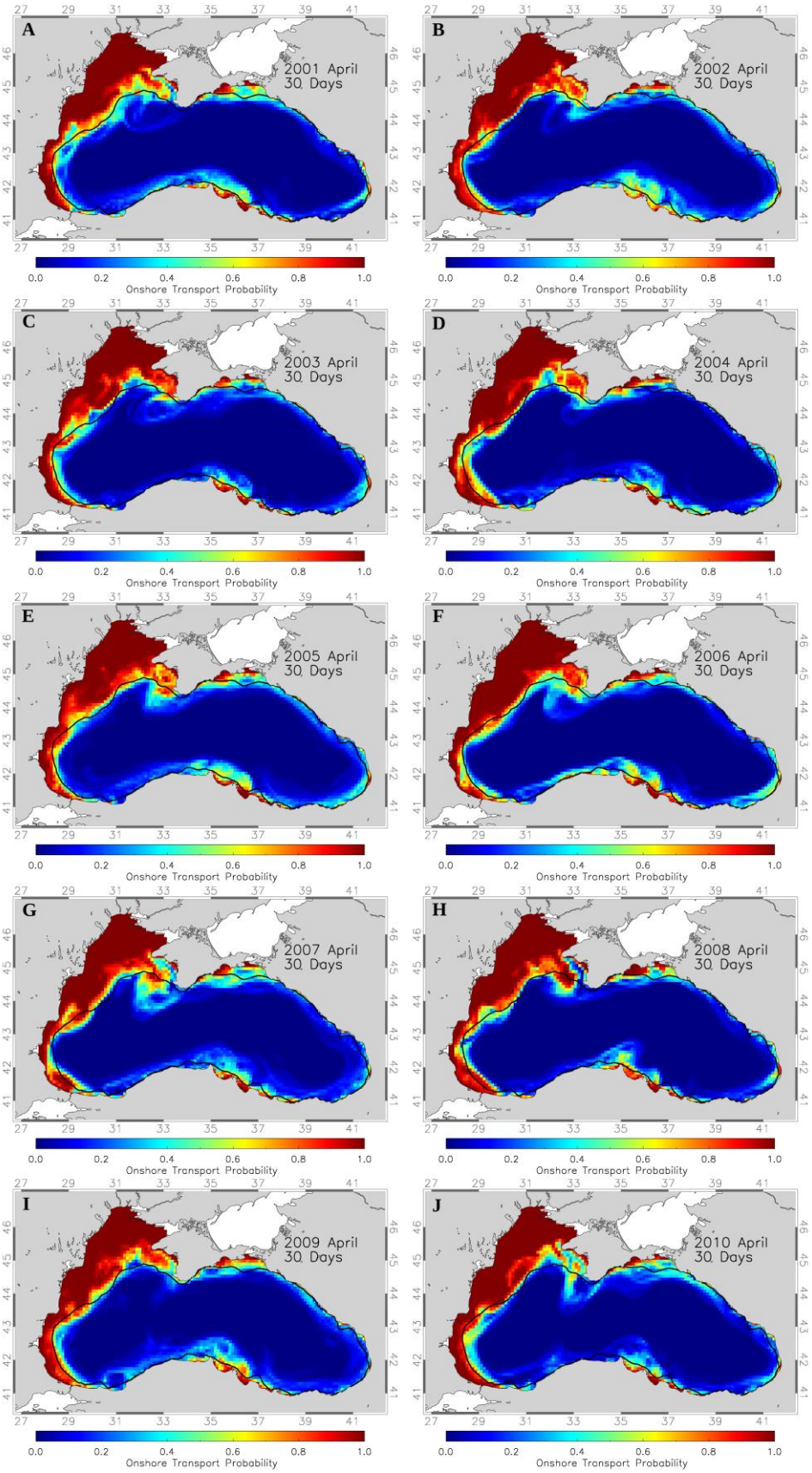

Appendix B 12: Simulation results of Onshore Transport Probability (ONTP) for simulations with April spawning times and 30 day Pelagic Larval Duration for A-J: 2001-2010.

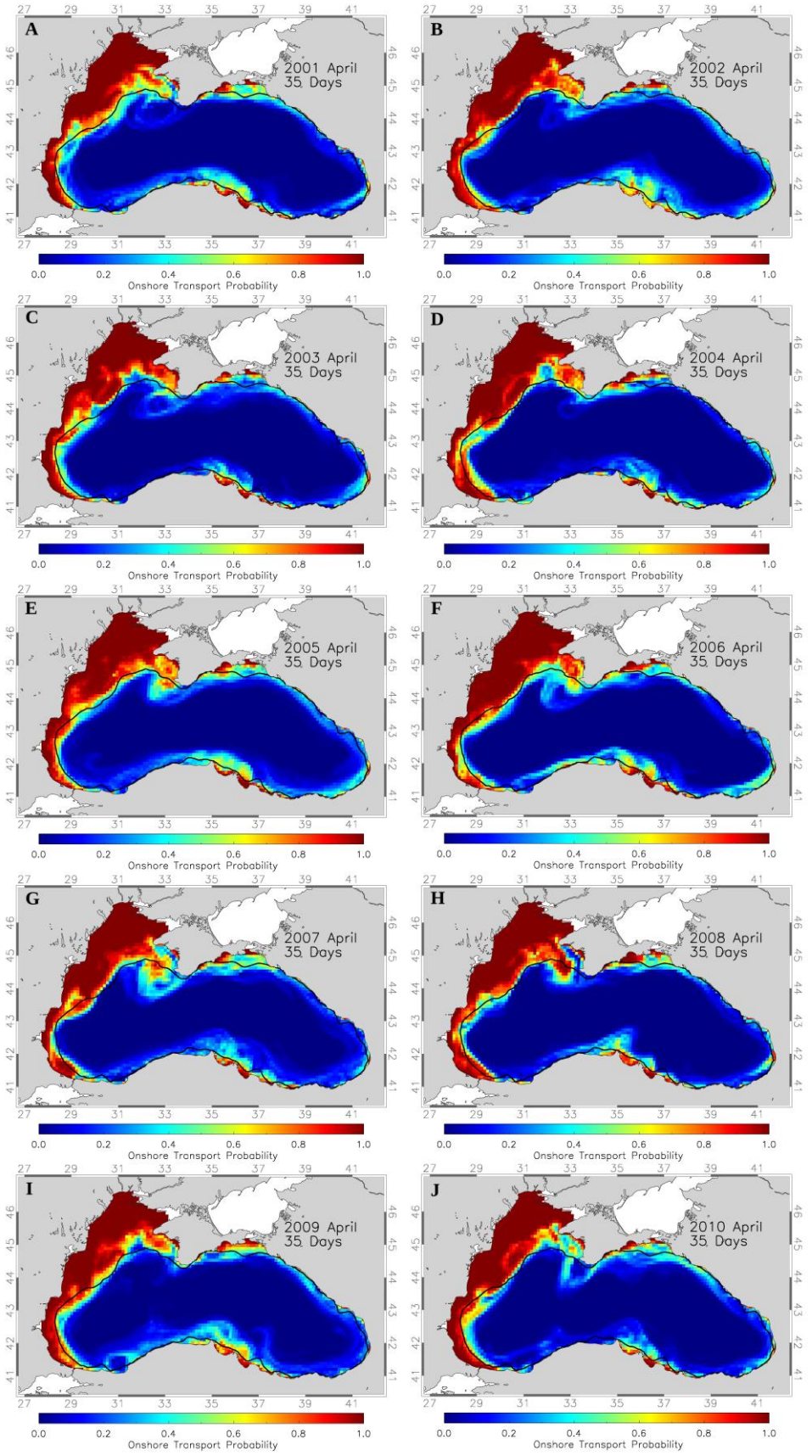

Appendix B 13: Simulation results of Onshore Transport Probability (ONTP) for simulations with April spawning times and 35 day Pelagic Larval Duration for A-J: 2001-2010.

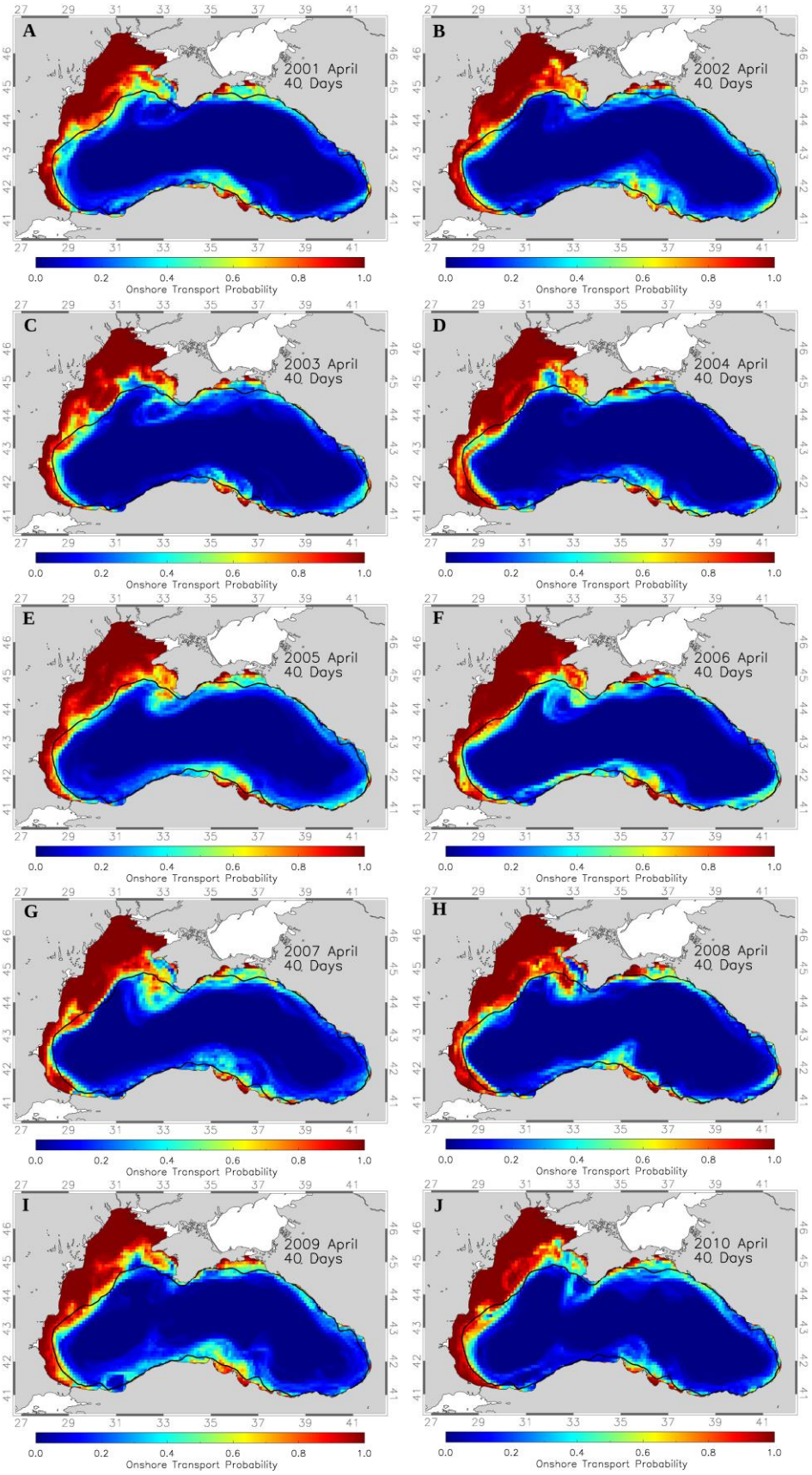

Appendix B 14: Simulation results of Onshore Transport Probability (ONTP) for simulations with April spawning times and 40 day Pelagic Larval Duration for A-J: 2001-2010.

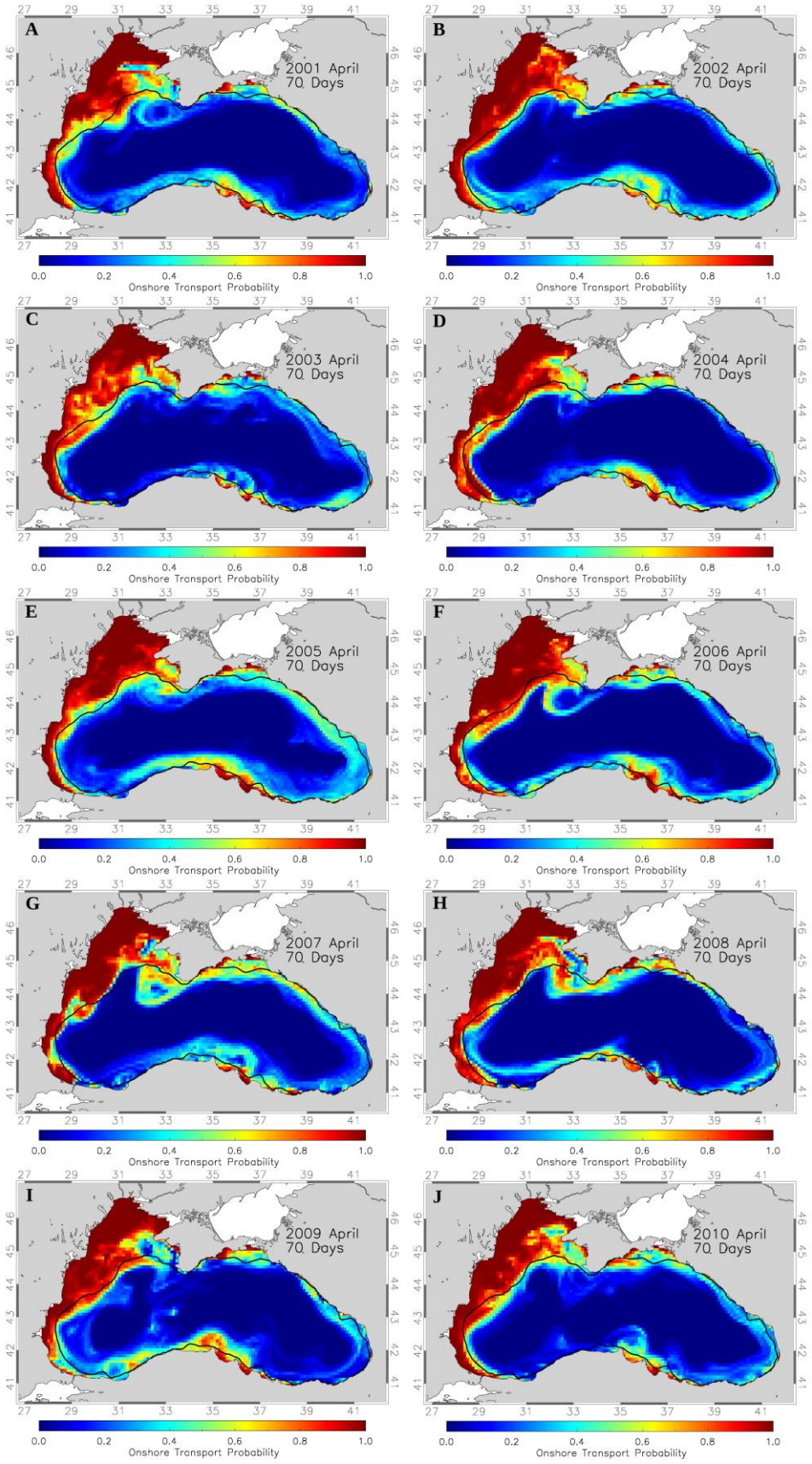

Appendix B 15: Simulation results of Onshore Transport Probability (ONTP) for simulations with April spawning times and 70 day Pelagic Larval Duration for A-J: 2001-2010.

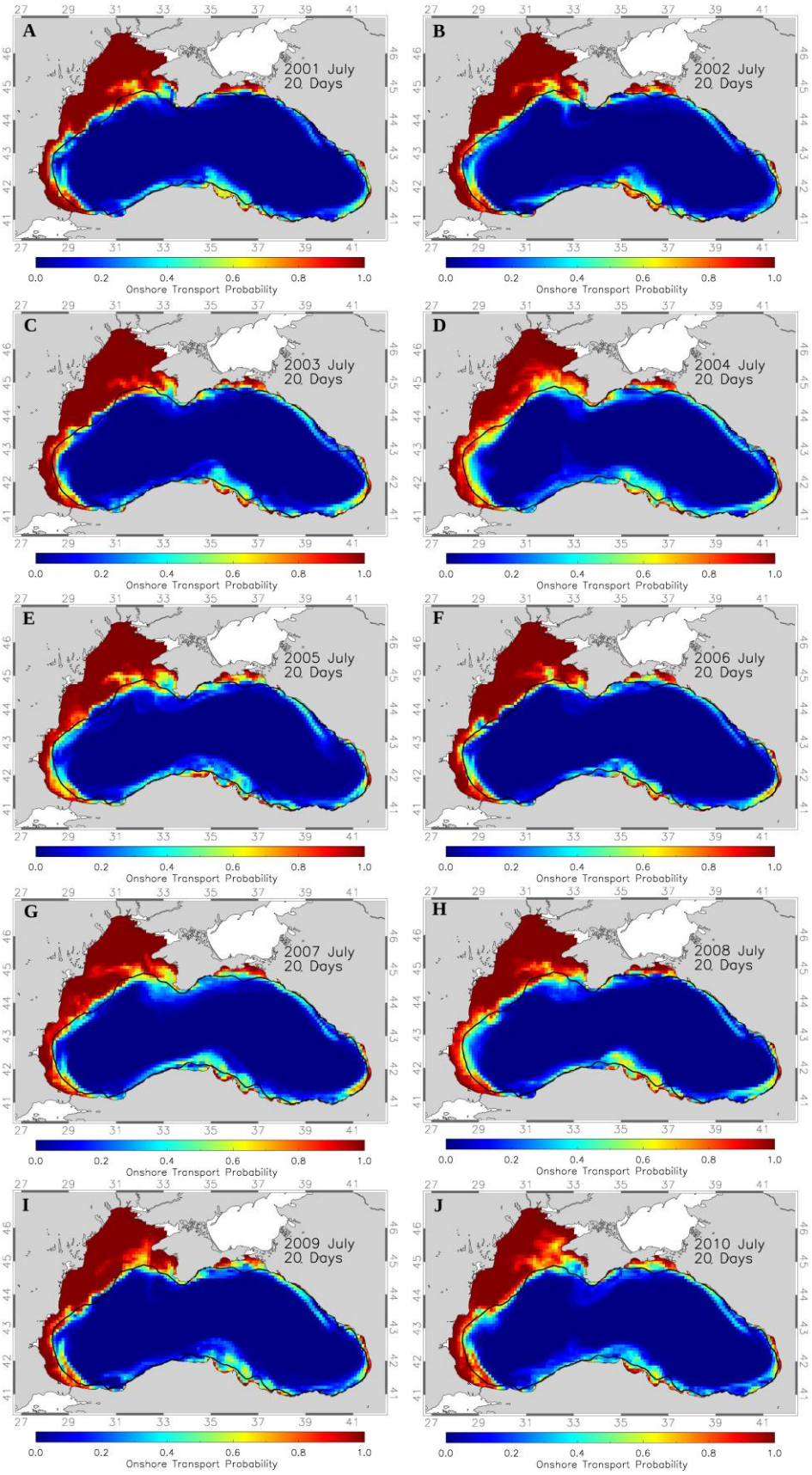

Appendix B 16: Simulation results of Onshore Transport Probability (ONTP) for simulations with July spawning times and 20 day Pelagic Larval Duration for A-J: 2001-2010.

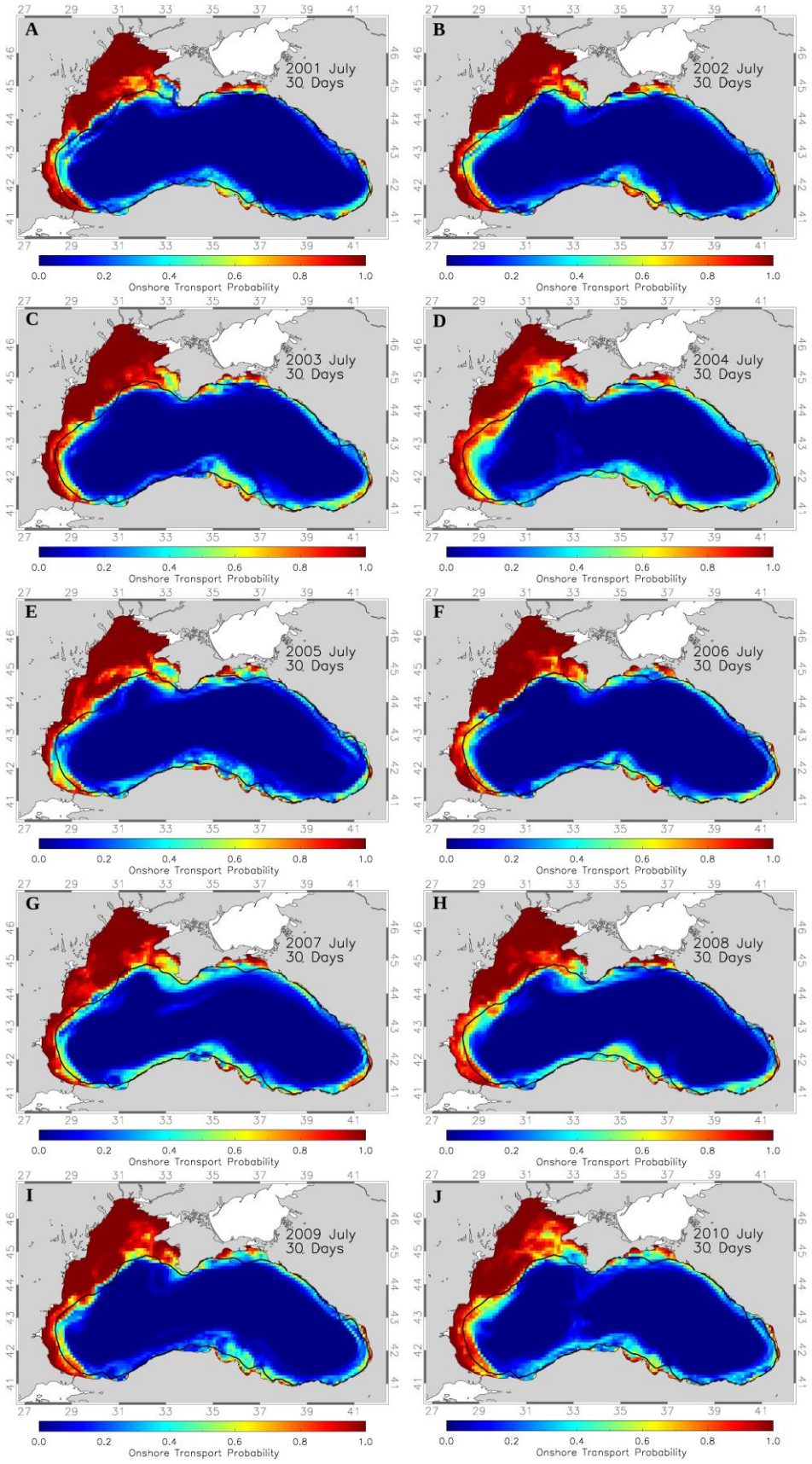

Appendix B 17: Simulation results of Onshore Transport Probability (ONTP) for simulations with July spawning times and 30 day Pelagic Larval Duration for A-J: 2001-2010.

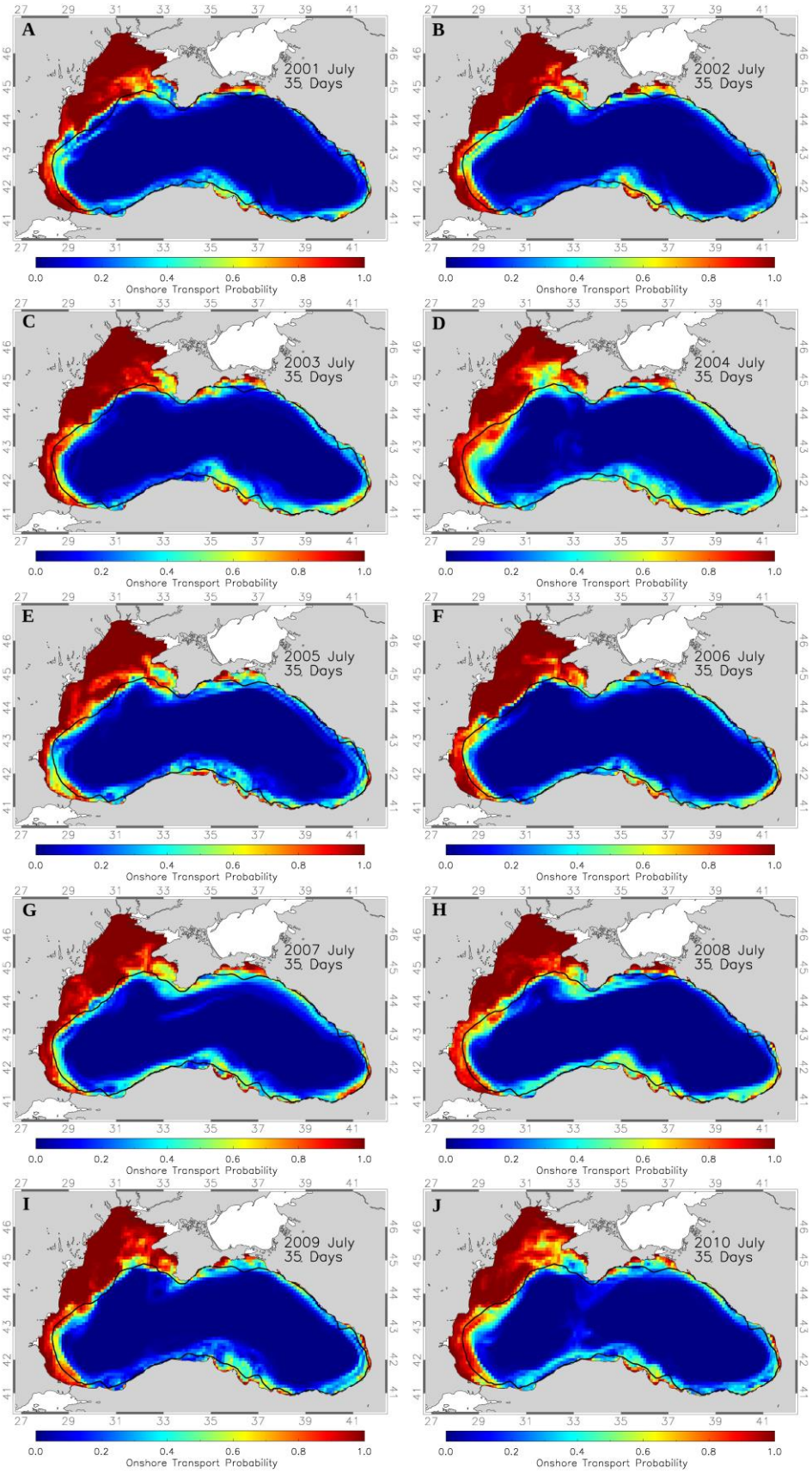

Appendix B 18: Simulation results of Onshore Transport Probability (ONTP) for simulations with July spawning times and 35 day Pelagic Larval Duration for A-J: 2001-2010.

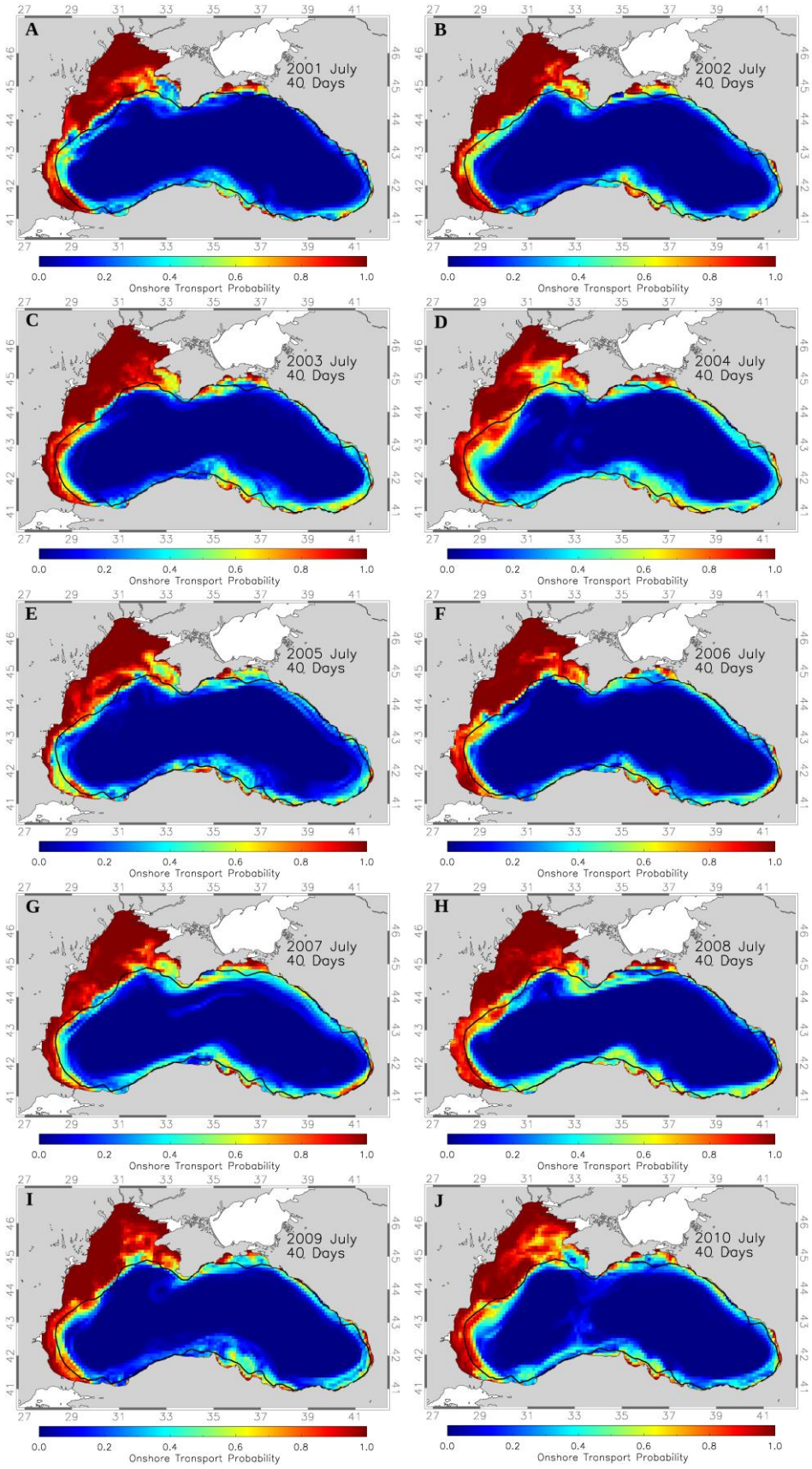

Appendix B 19: Simulation results of Onshore Transport Probability (ONTP) for simulations with July spawning times and 40 day Pelagic Larval Duration for A-J: 2001-2010.

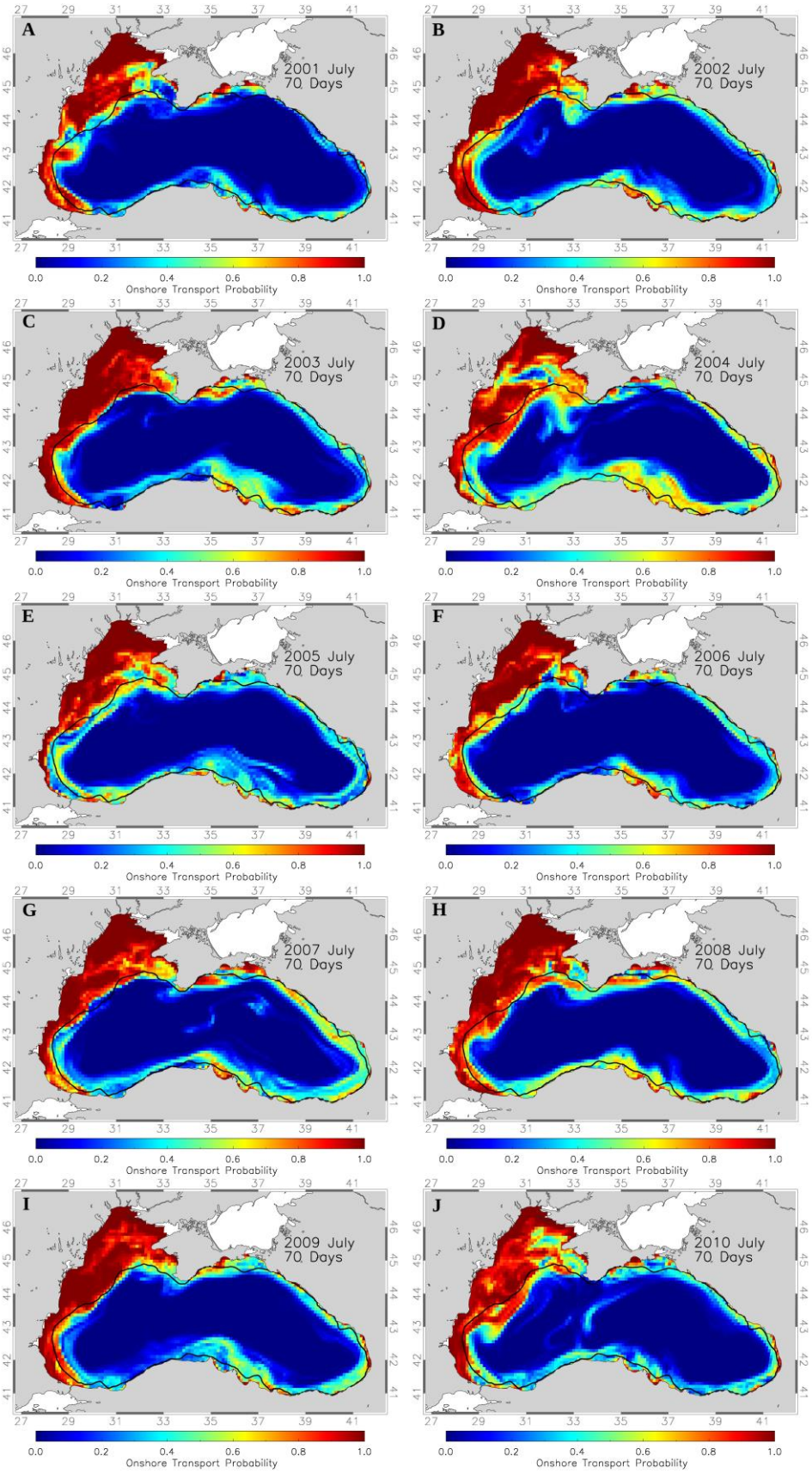

Appendix B 20: Simulation results of Onshore Transport Probability (ONTP) for simulations with July spawning times and 70 day Pelagic Larval Duration for A-J: 2001-2010.

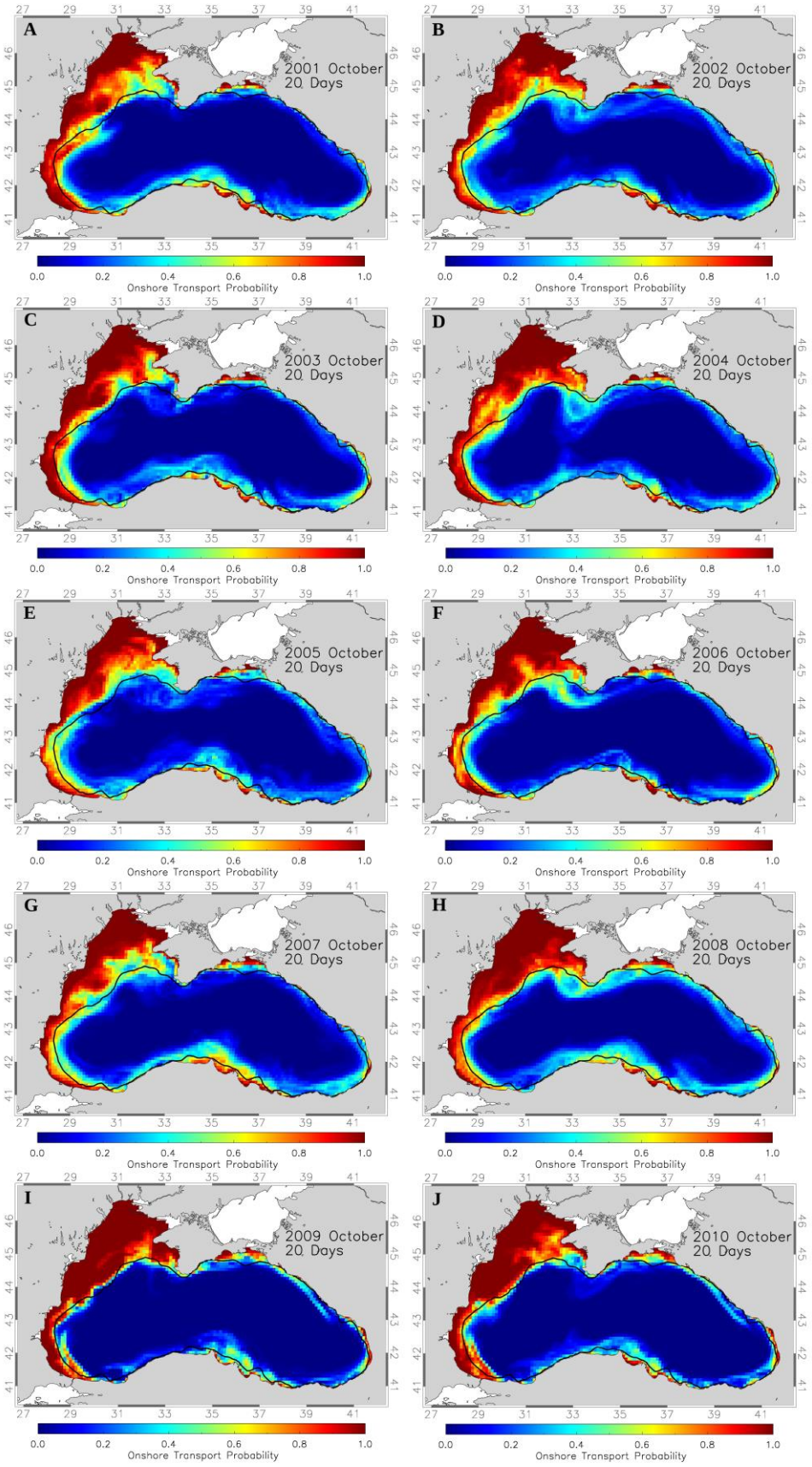

Appendix B 21: Simulation results of Onshore Transport Probability (ONTP) for simulations with October spawning times and 20 day Pelagic Larval Duration for A-J: 2001-2010.

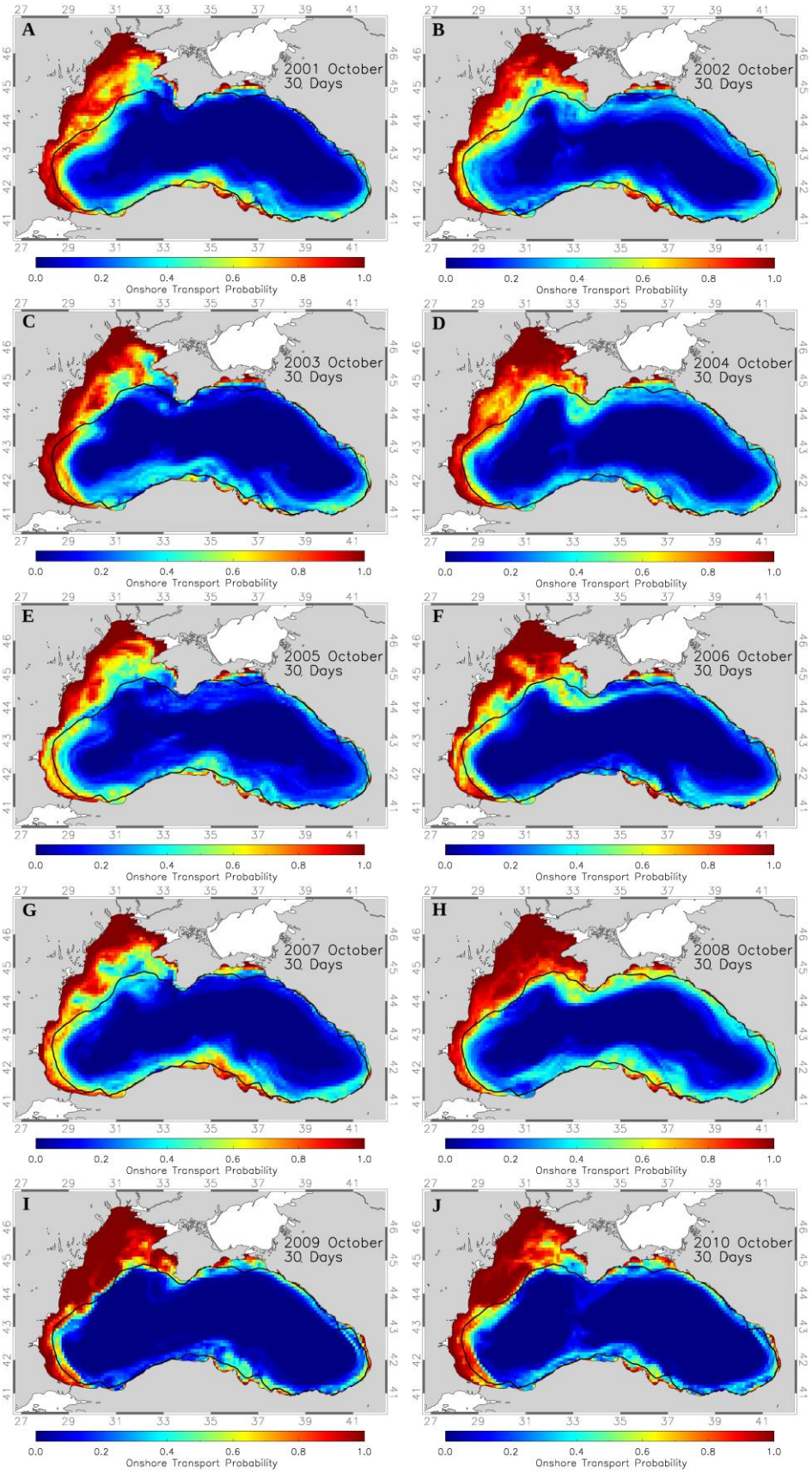

Appendix B 22: Simulation results of Onshore Transport Probability (ONTP) for simulations with October spawning times and 30 day Pelagic Larval Duration for A-J: 2001-2010.

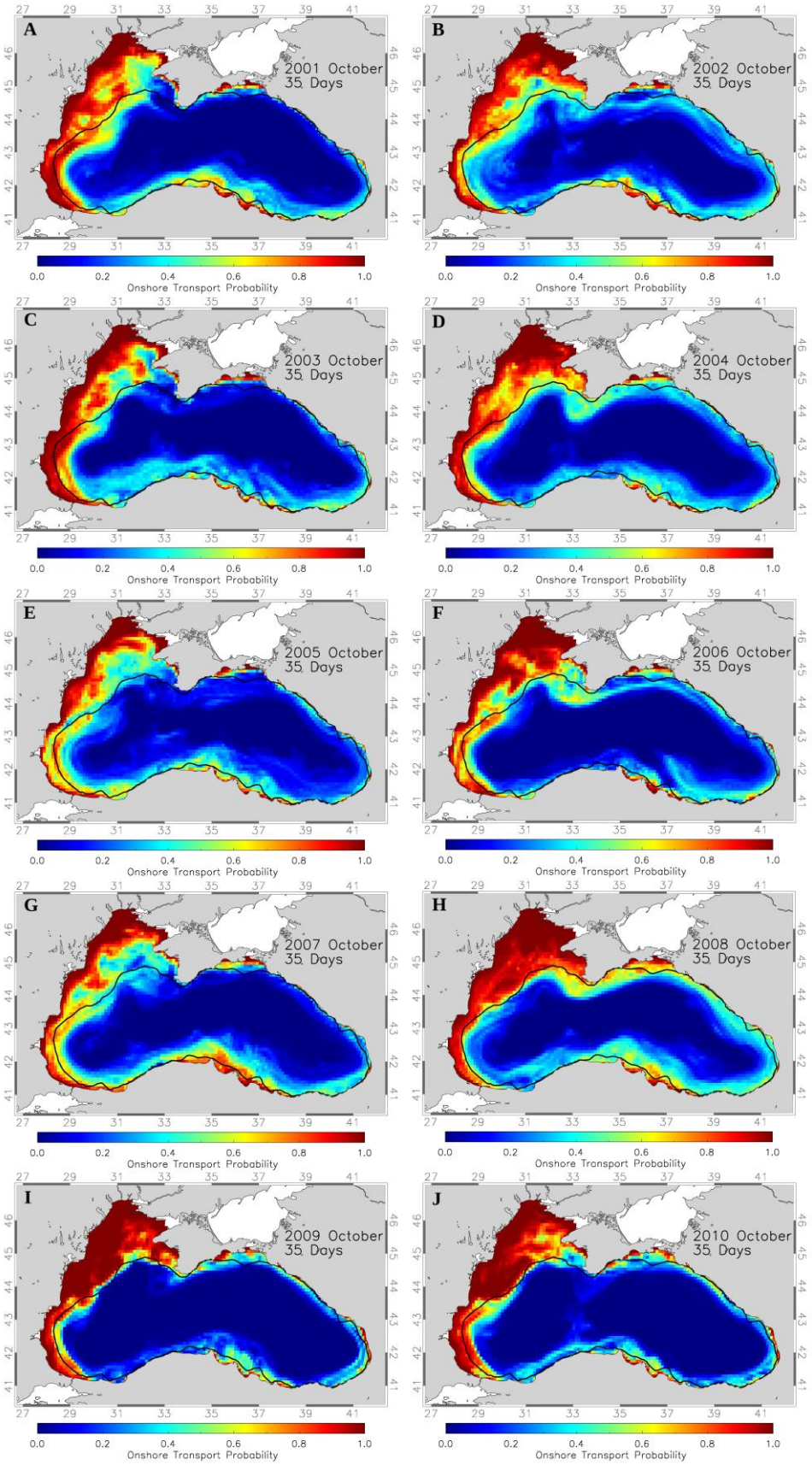

Appendix B 23: Simulation results of Onshore Transport Probability (ONTP) for simulations with October spawning times and 35 day Pelagic Larval Duration for A-J: 2001-2010.

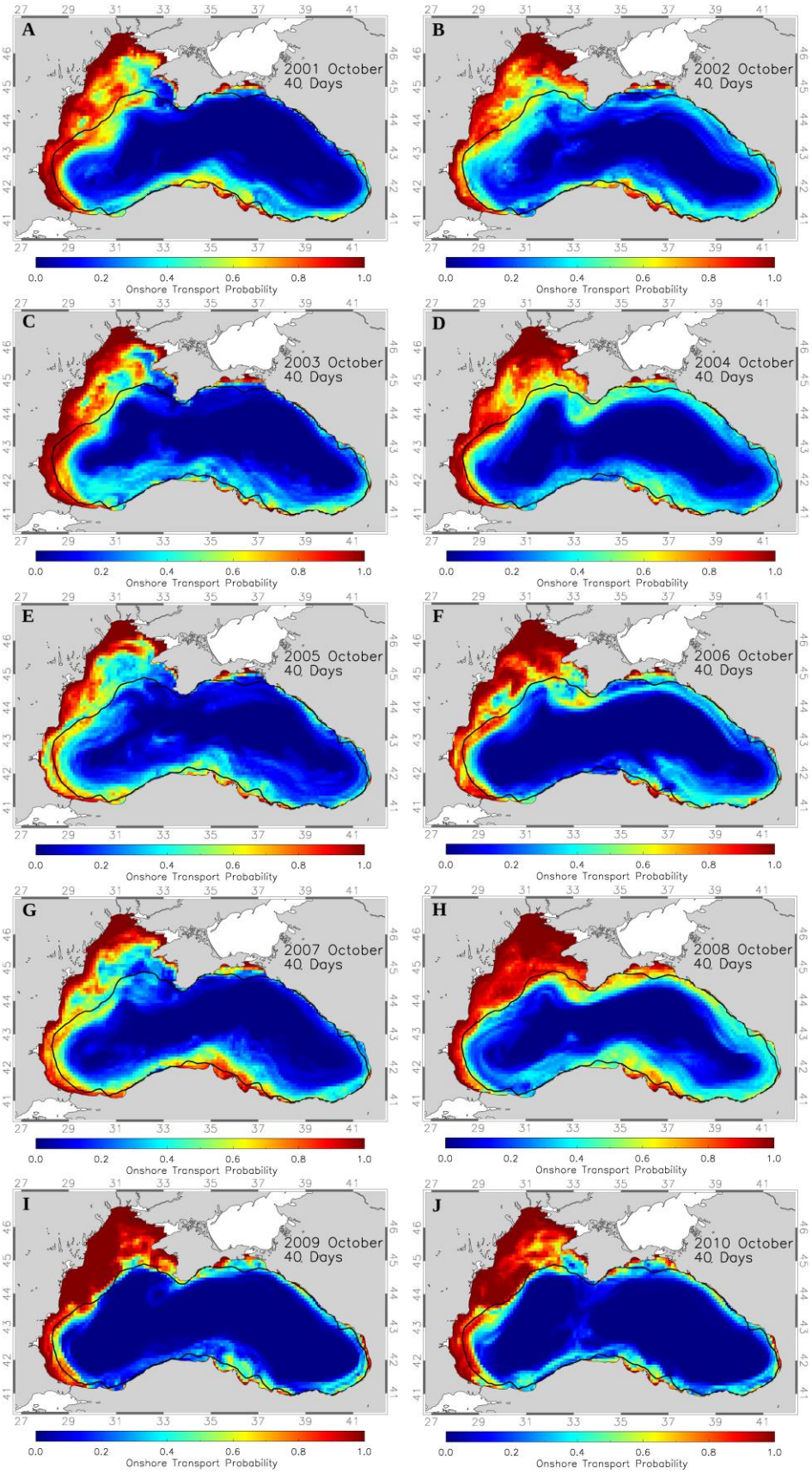

Appendix B 24: Simulation results of Onshore Transport Probability (ONTP) for simulations with October spawning times and 40 day Pelagic Larval Duration for A-J: 2001-2010.

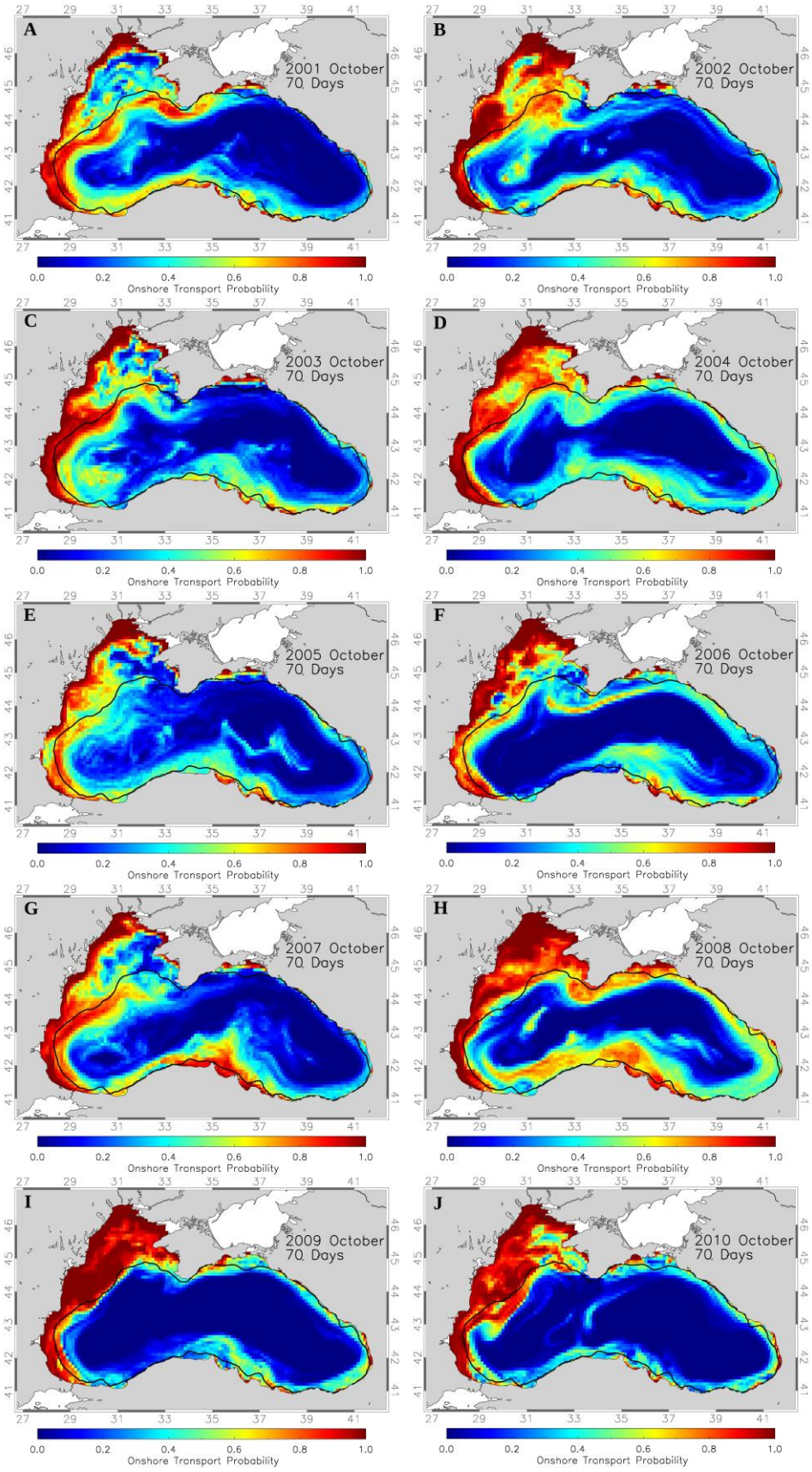

Appendix B 25: Simulation results of Onshore Transport Probability (ONTP) for simulations with October spawning times and 70 day Pelagic Larval Duration for A-J: 2001-2010.

Section C: Local Retention

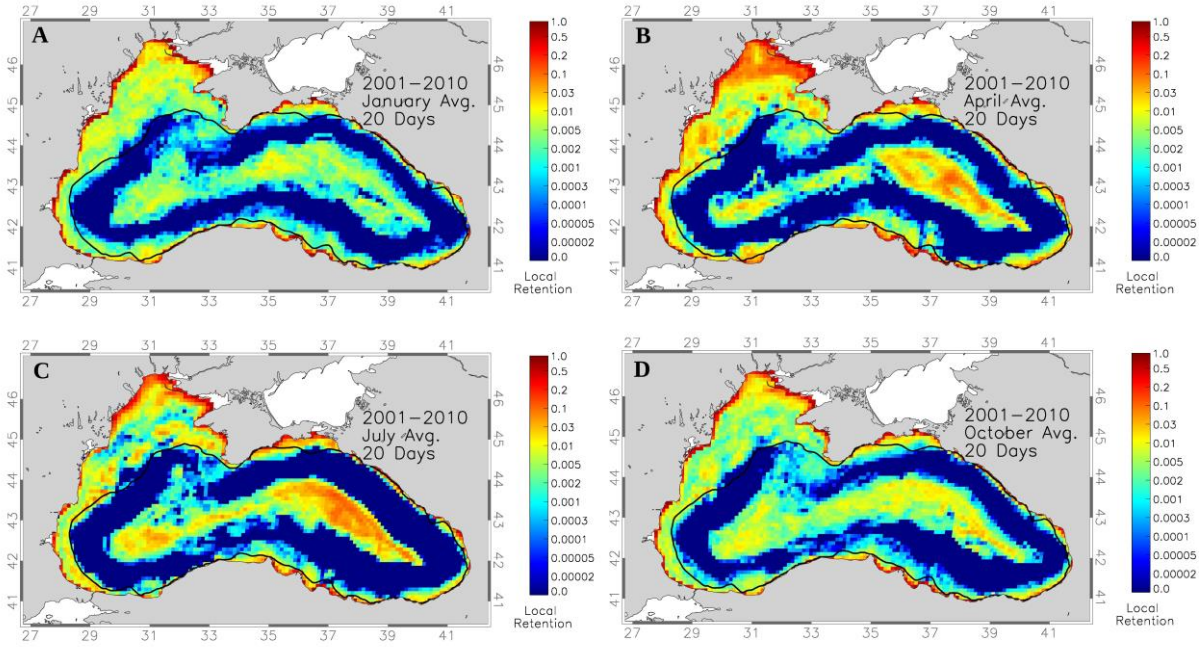

Appendix C 1: Simulation results of 10 years (2001-2010) averaged at 20 day Pelagic Larval Duration (PLD) to calculate the Local Retention (LR) for all seasonal averages. A: January average, B: April average, C: July average and D: October average.

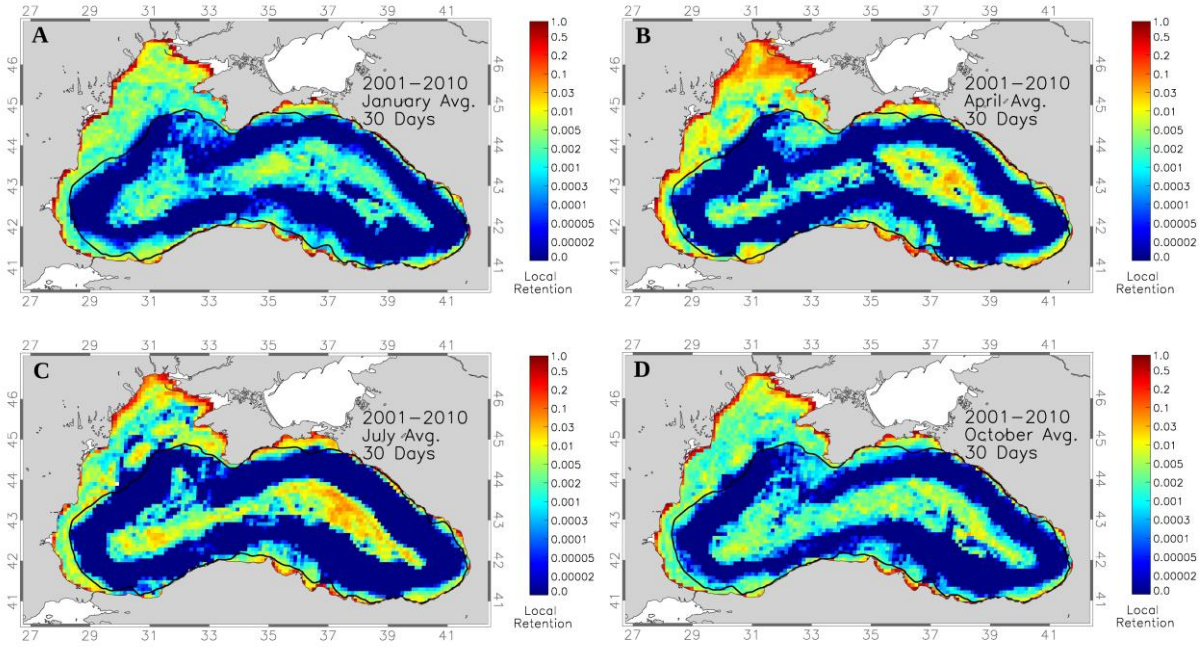

Appendix C 2: Simulation results of 10 years (2001-2010) averaged at 30 day Pelagic Larval Duration (PLD) to calculate the Local Retention (LR) for all seasonal averages. A: January average, B: April average, C: July average and D: October average.

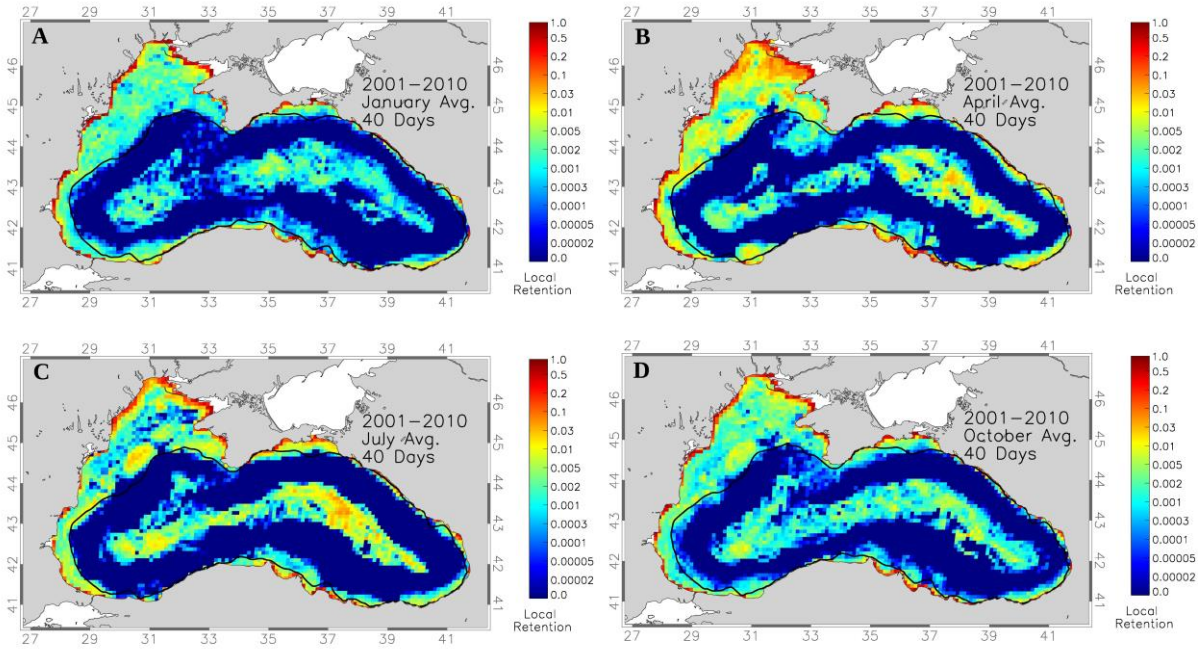

Appendix C 3: Simulation results of 10 years (2001-2010) averaged at 40 day Pelagic Larval Duration (PLD) to calculate the Local Retention (LR) for all seasonal averages. A: January average, B: April average, C: July average and D: October average.

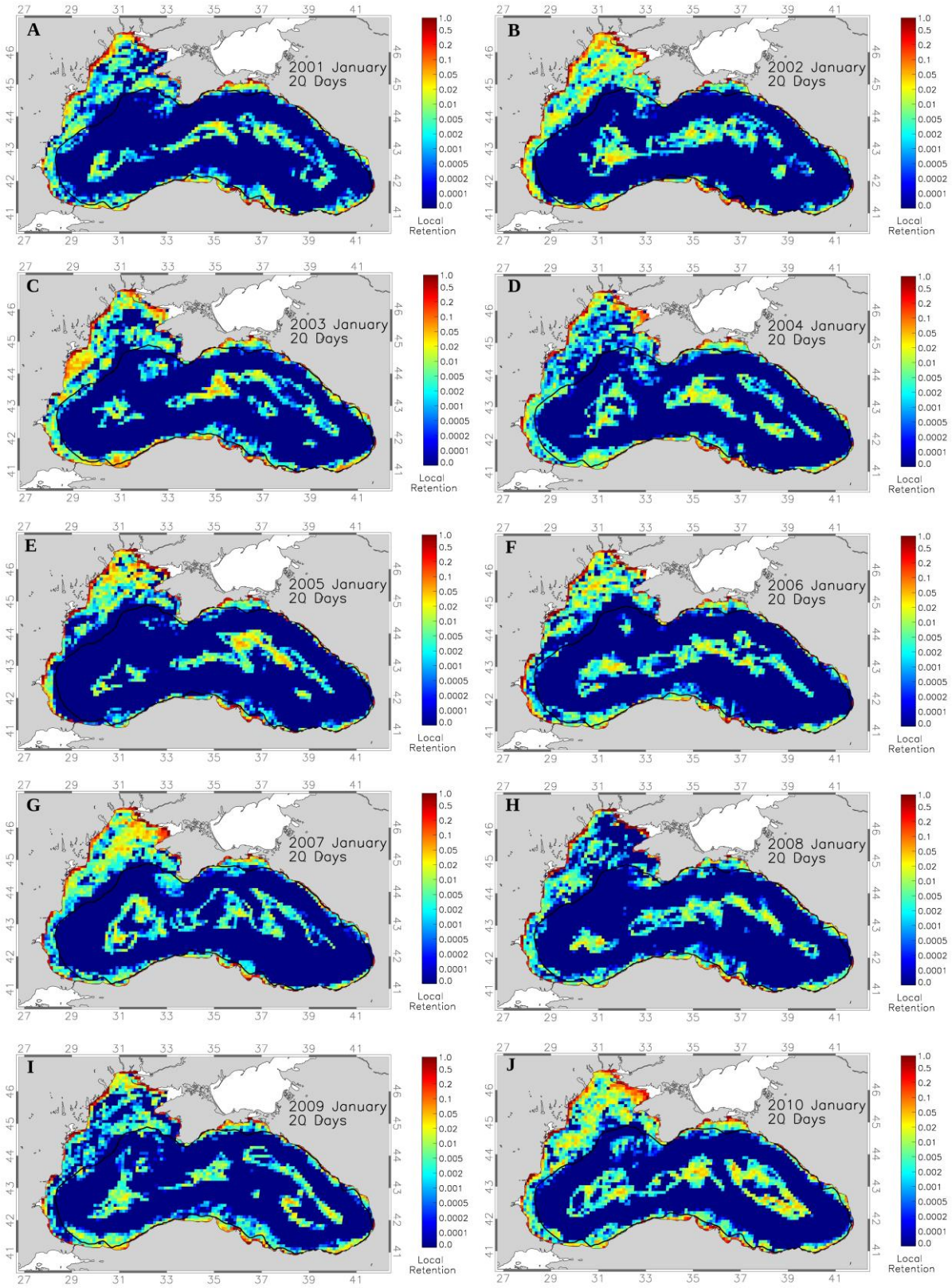

Appendix C 4: Simulation results of Local Retention (LR) using January spawning times and 20 day Pelagic Larval Duration (PLD) for A-J: 2001-2010.

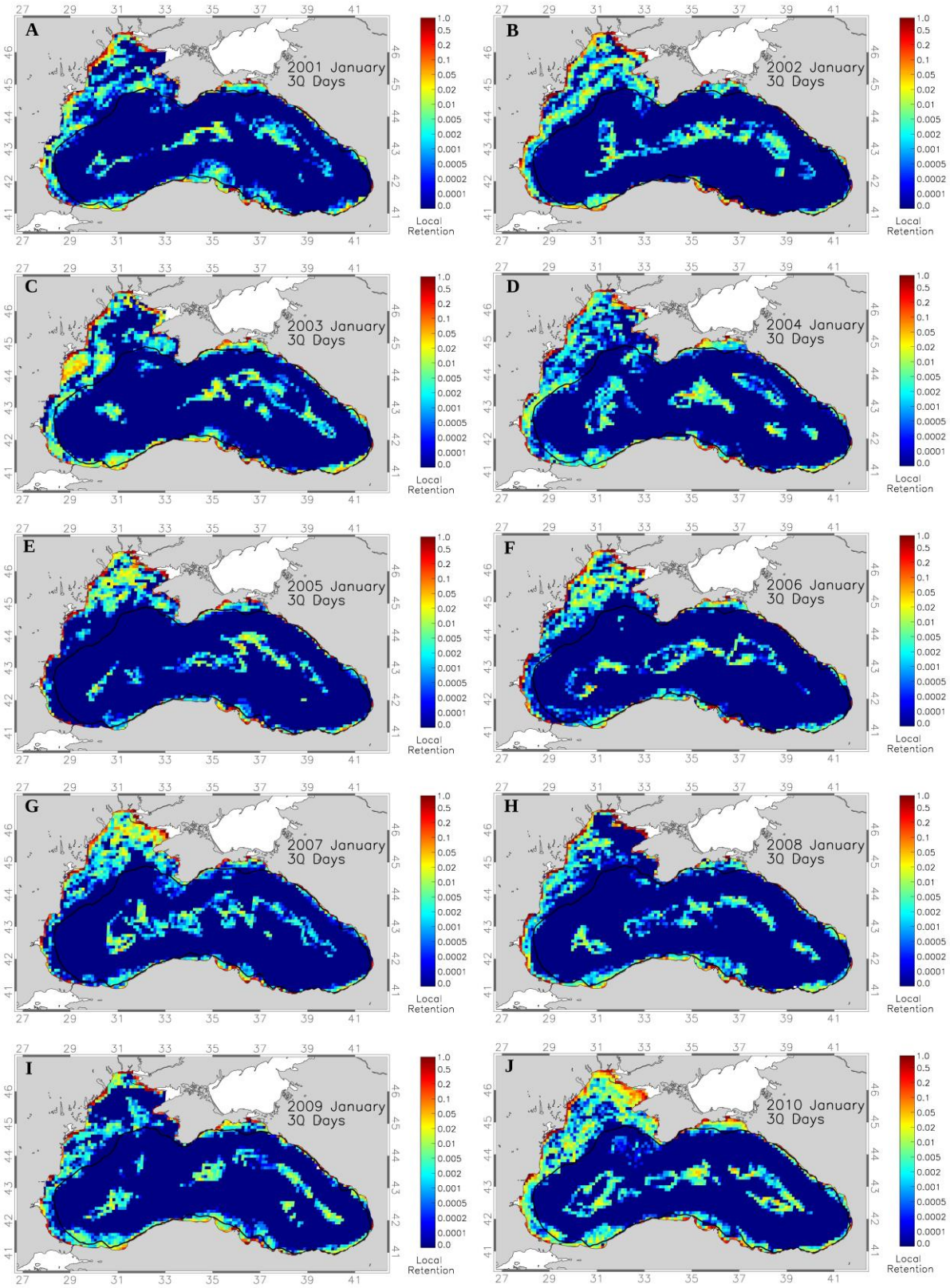

Appendix C 5: Simulation results of Local Retention (LR) using January spawning times and 30 day Pelagic Larval Duration (PLD) for A-J: 2001-2010.

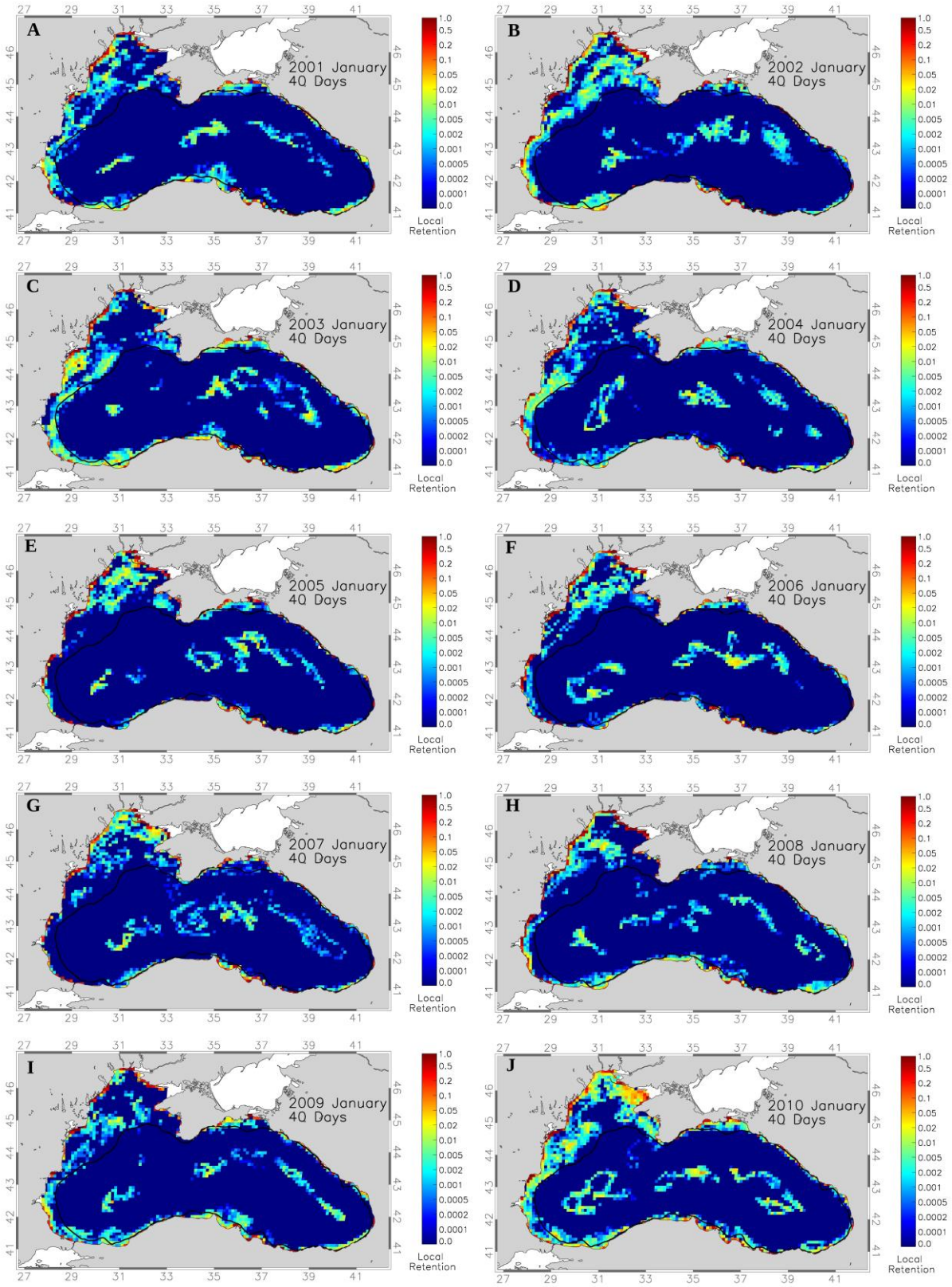

Appendix C 6: Simulation results of Local Retention (LR) using January spawning times and 40 day Pelagic Larval Duration (PLD) for A-J: 2001-2010.

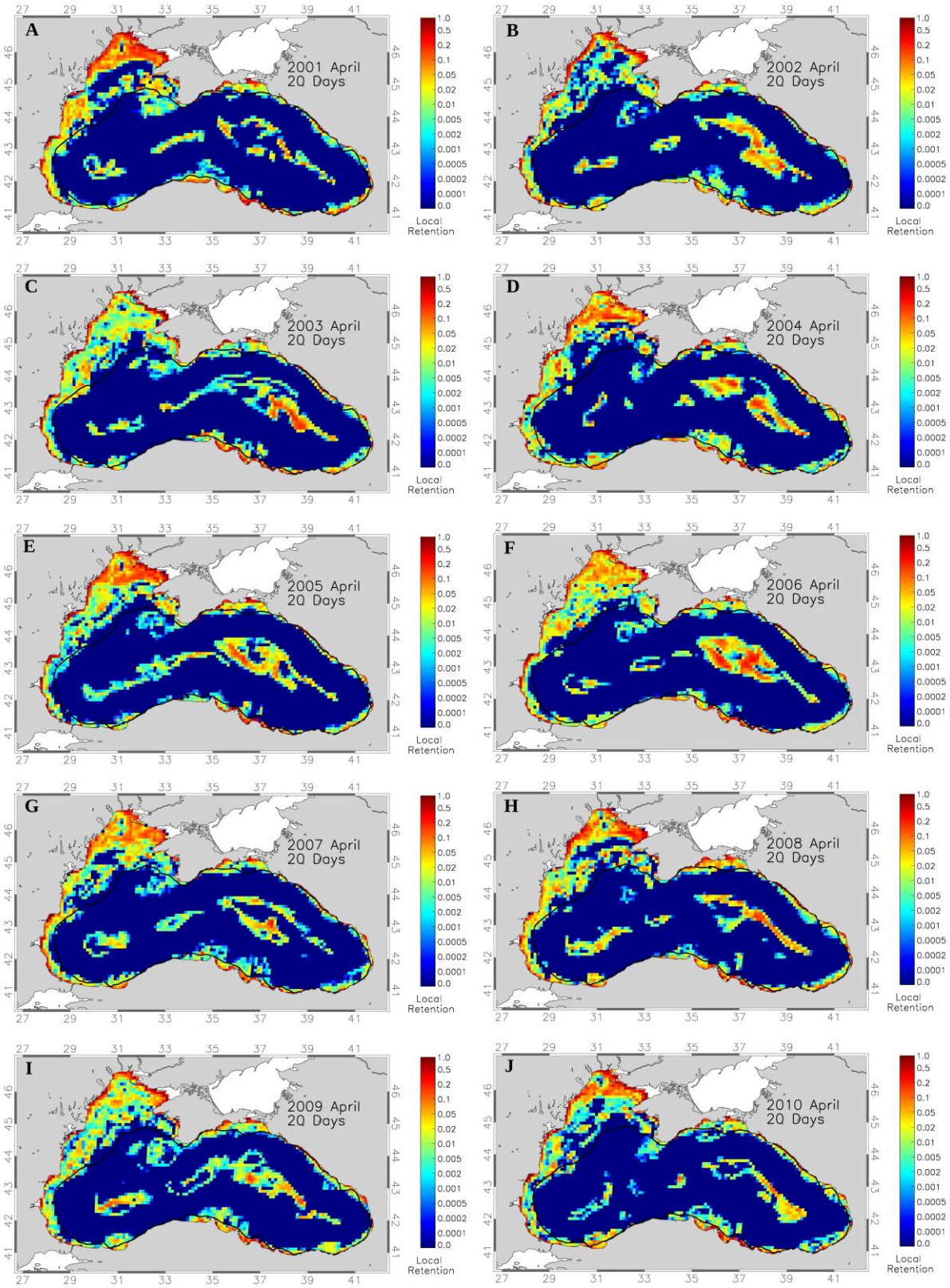

Appendix C 7: Simulation results of Local Retention (LR) using April spawning times and 20 day Pelagic Larval Duration (PLD) for A-J: 2001-2010.

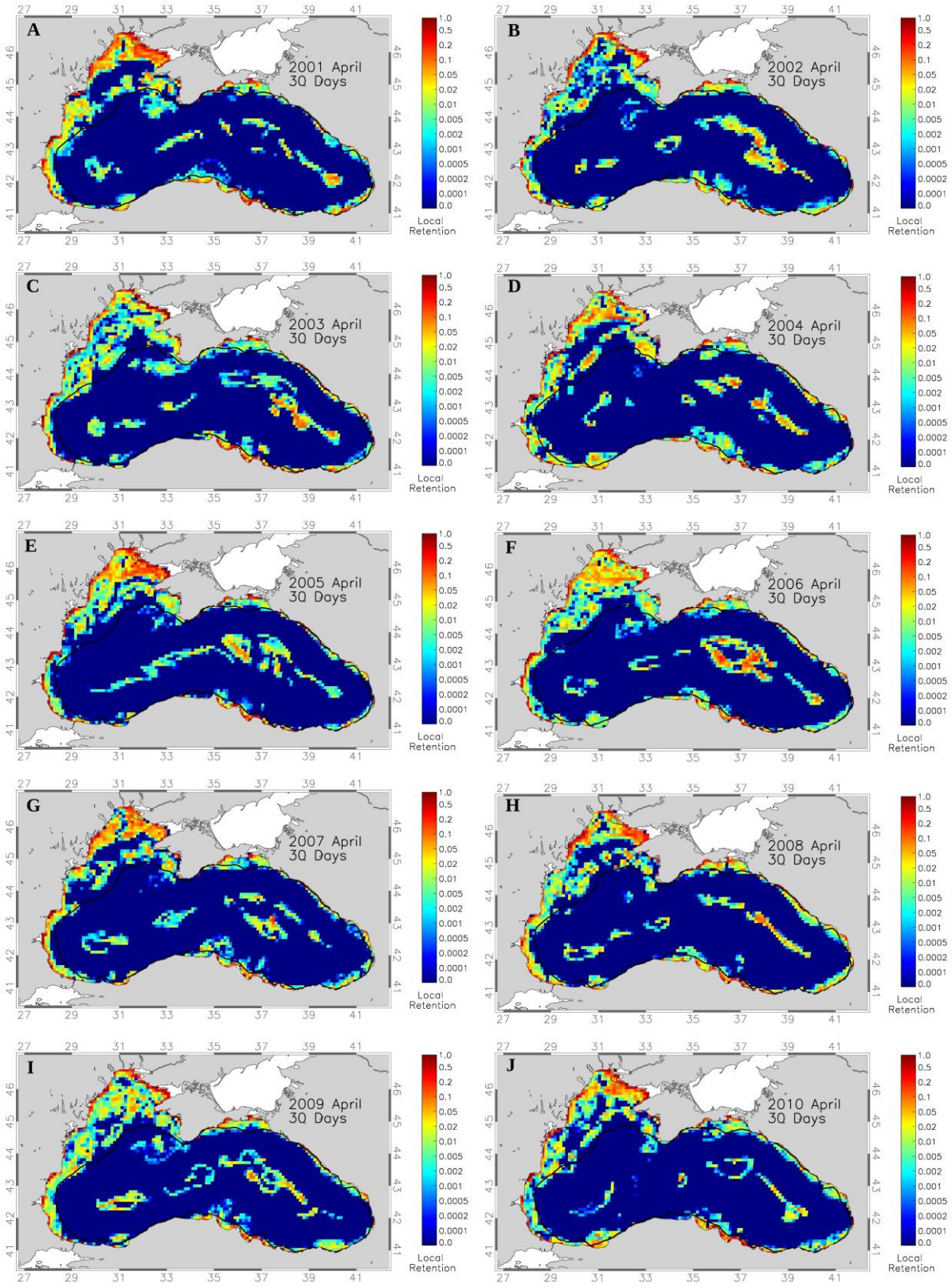

Appendix C 8: Simulation results of Local Retention (LR) using April spawning times and 30 day Pelagic Larval Duration (PLD) for A-J: 2001-2010.

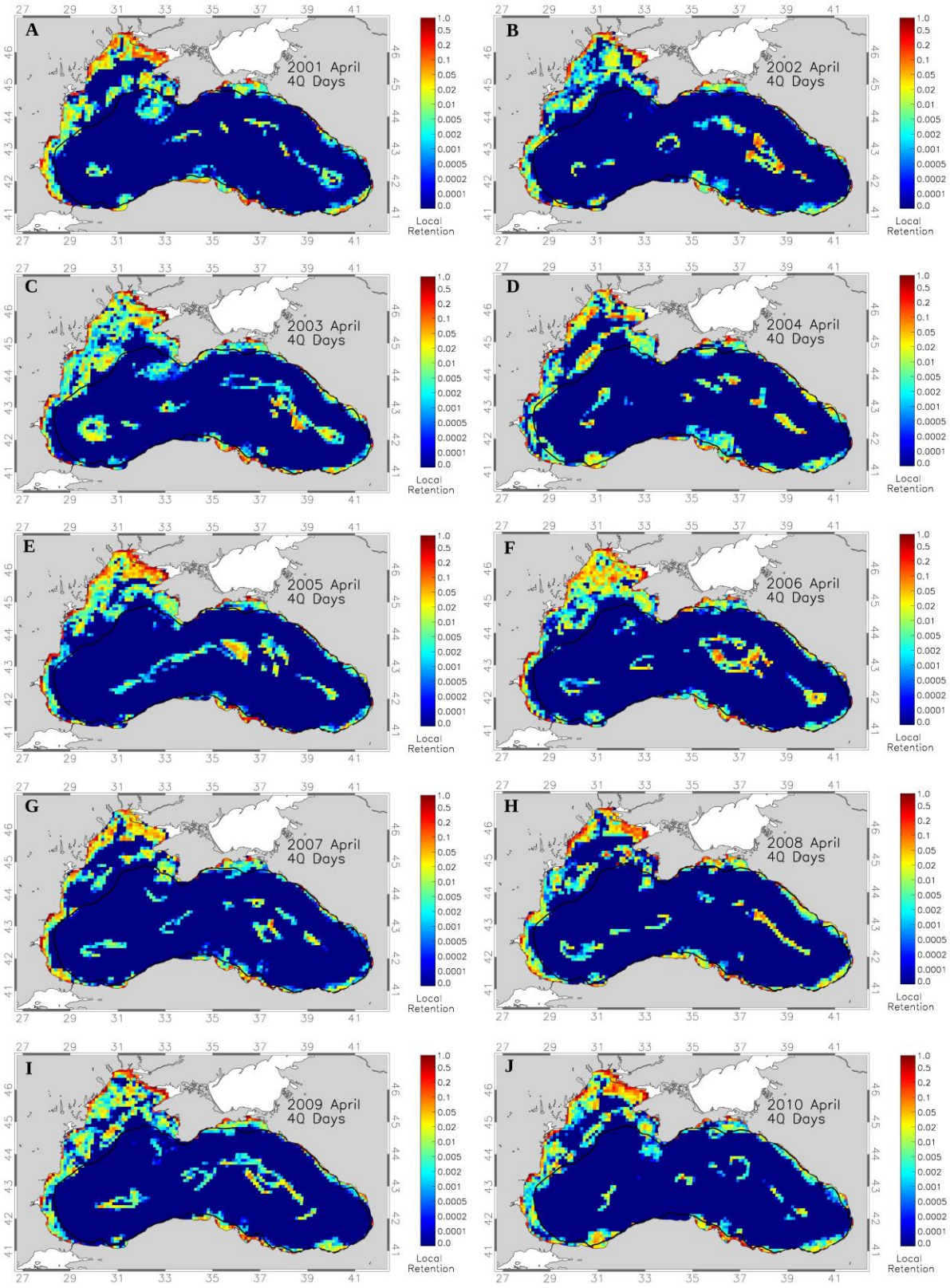

Appendix C 9: Simulation results of Local Retention (LR) using April spawning times and 40 day Pelagic Larval Duration (PLD) for A-J: 2001-2010.

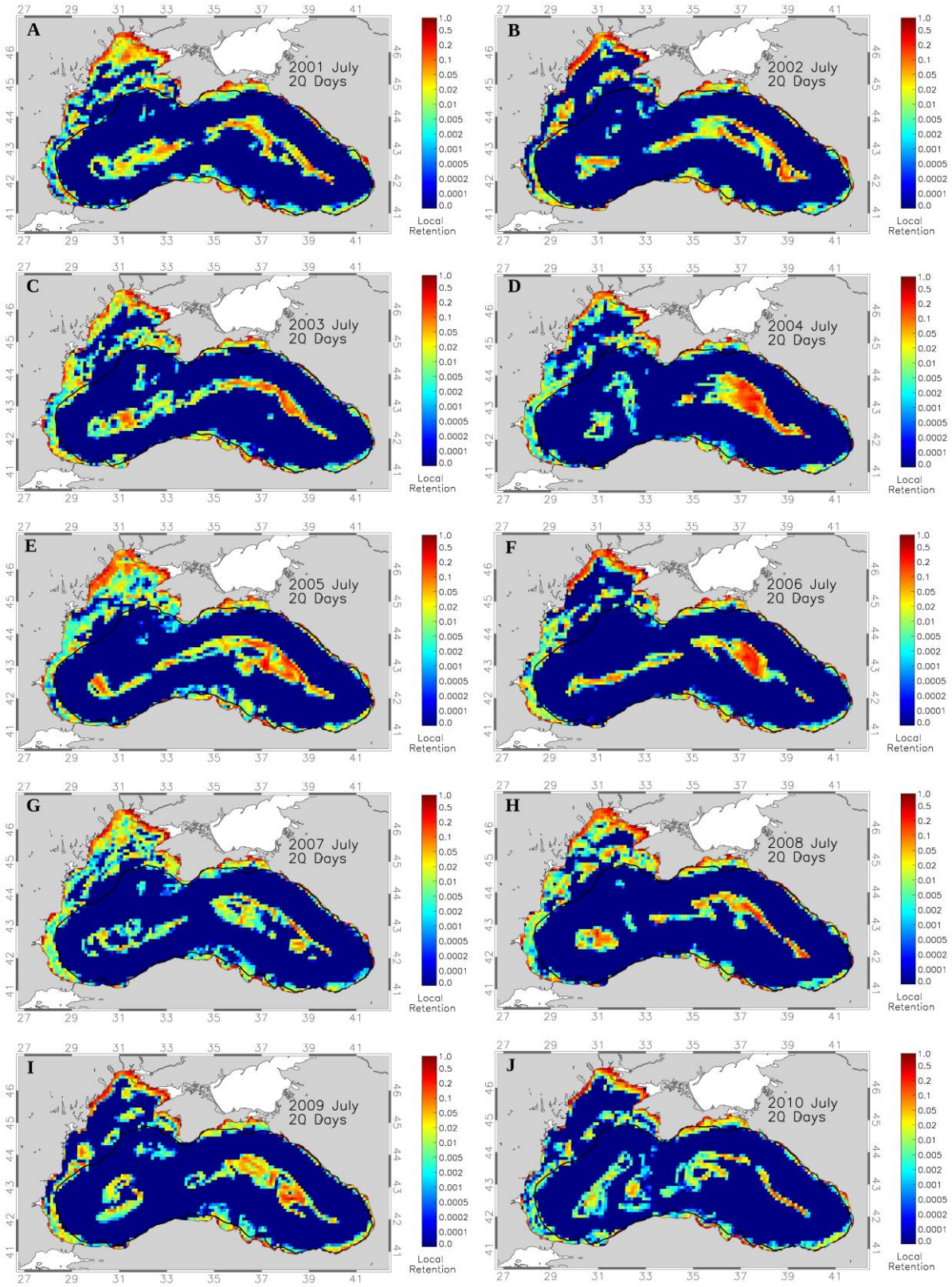

Appendix C 10: Simulation results of Local Retention (LR) using July spawning times and 20 day Pelagic Larval Duration (PLD) for A-J: 2001-2010.

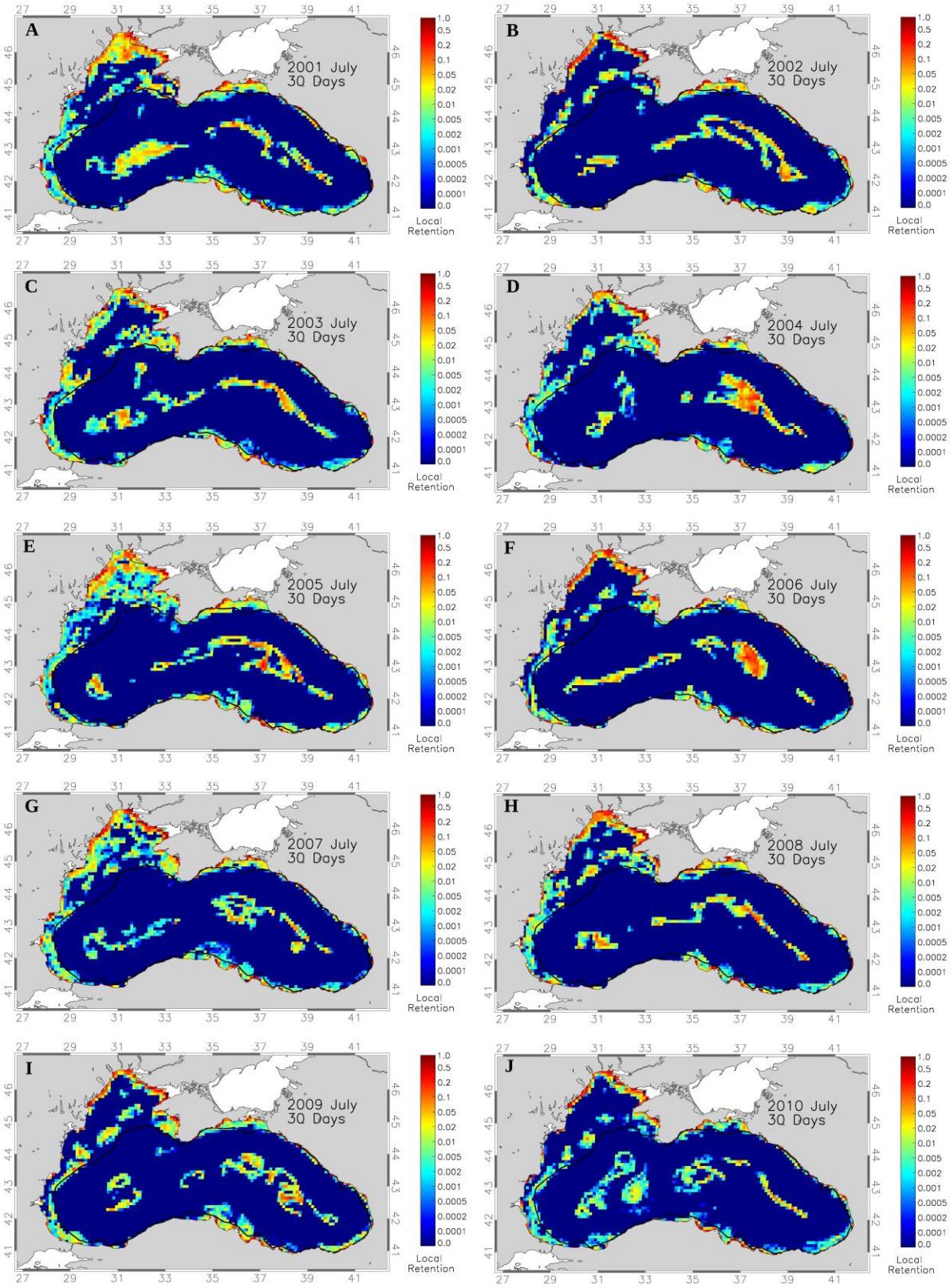

Appendix C 11: Simulation results of Local Retention (LR) using July spawning times and 30 day Pelagic Larval Duration (PLD) for A-J: 2001-2010.

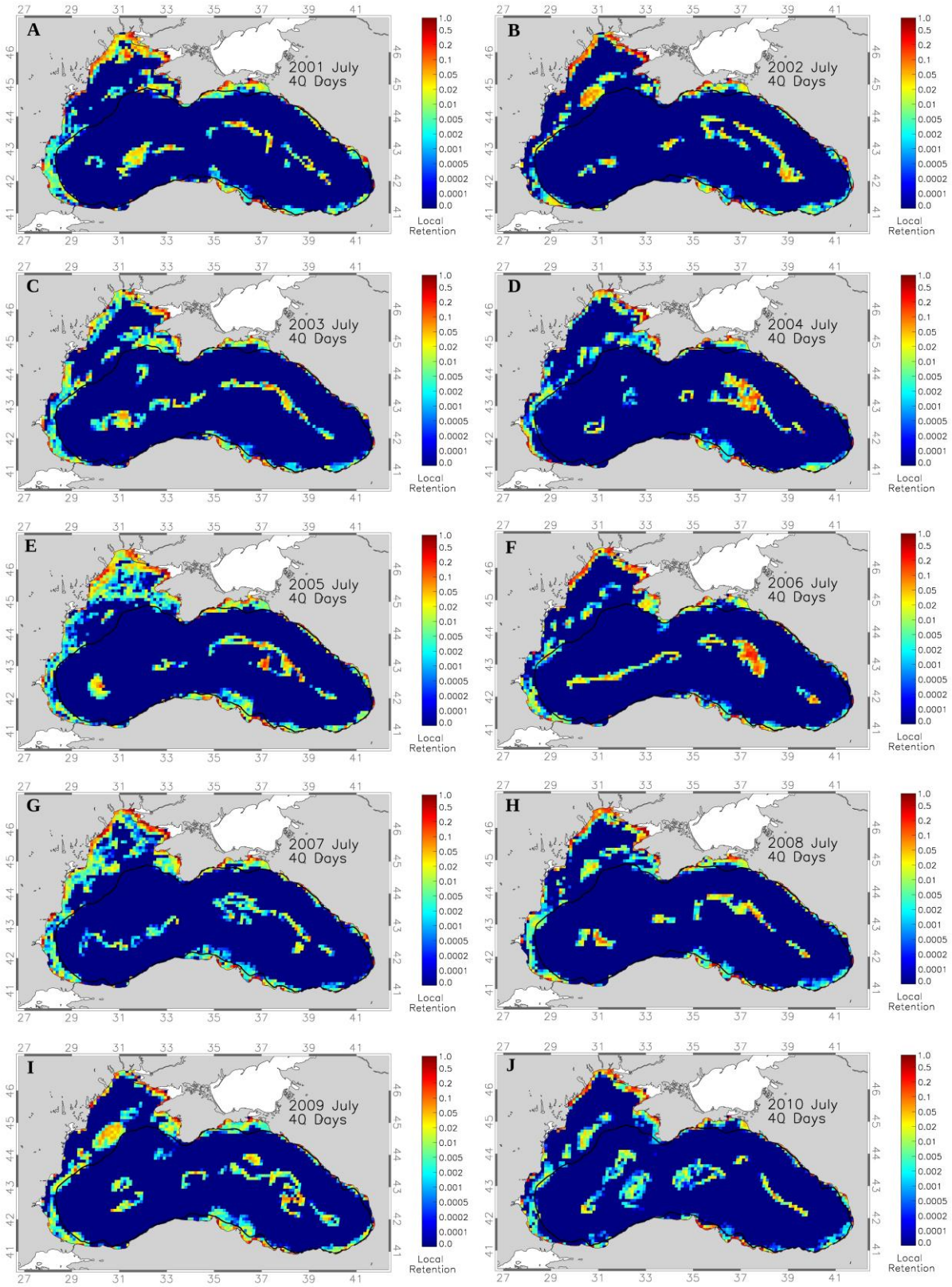

Appendix C 12: Simulation results of Local Retention (LR) using July spawning times and 40 day Pelagic Larval Duration (PLD) for A-J: 2001-2010.

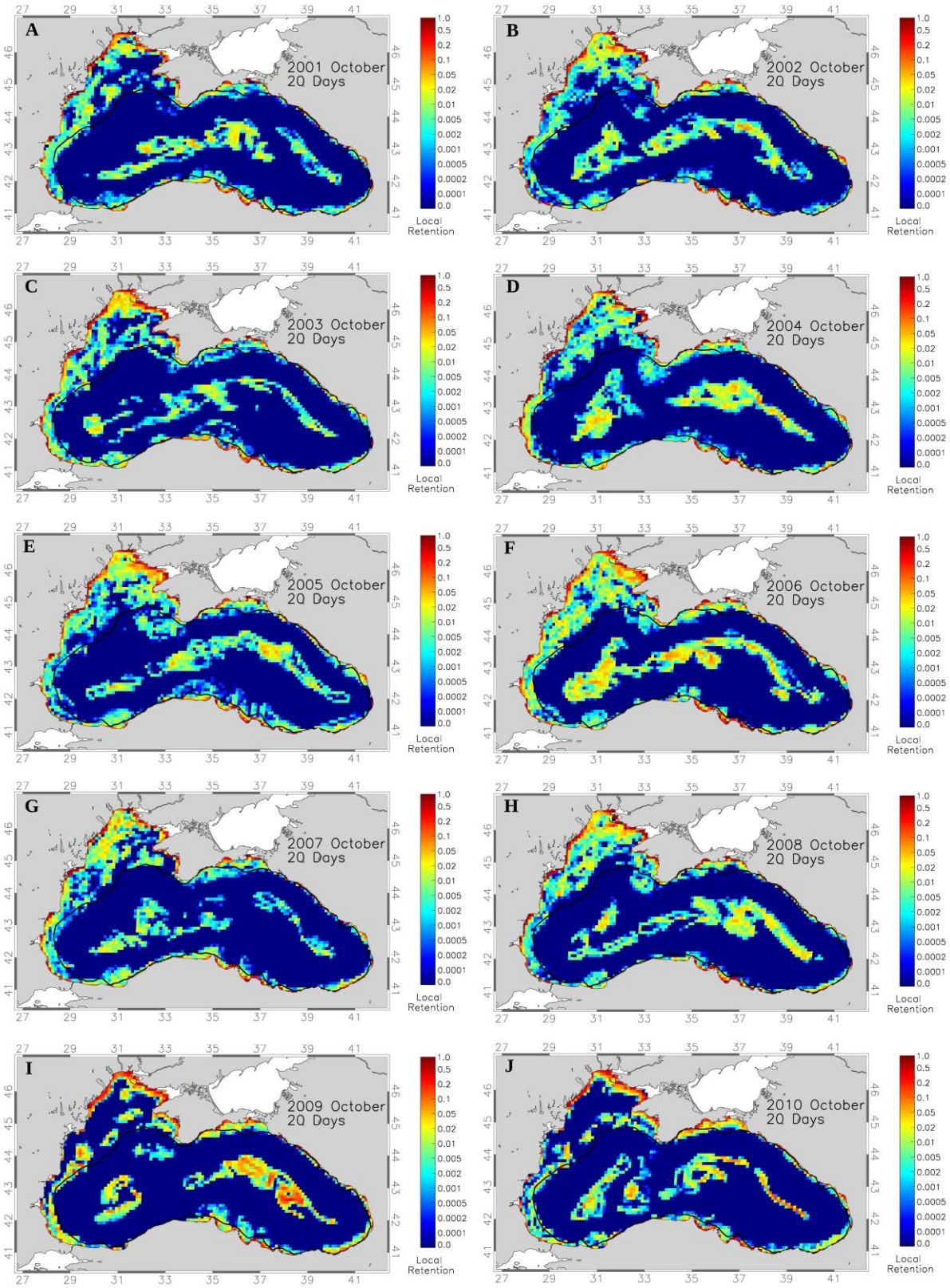

Appendix C 13: Simulation results of Local Retention (LR) using October spawning times and 20 day Pelagic Larval Duration (PLD) for A-J: 2001-2010.

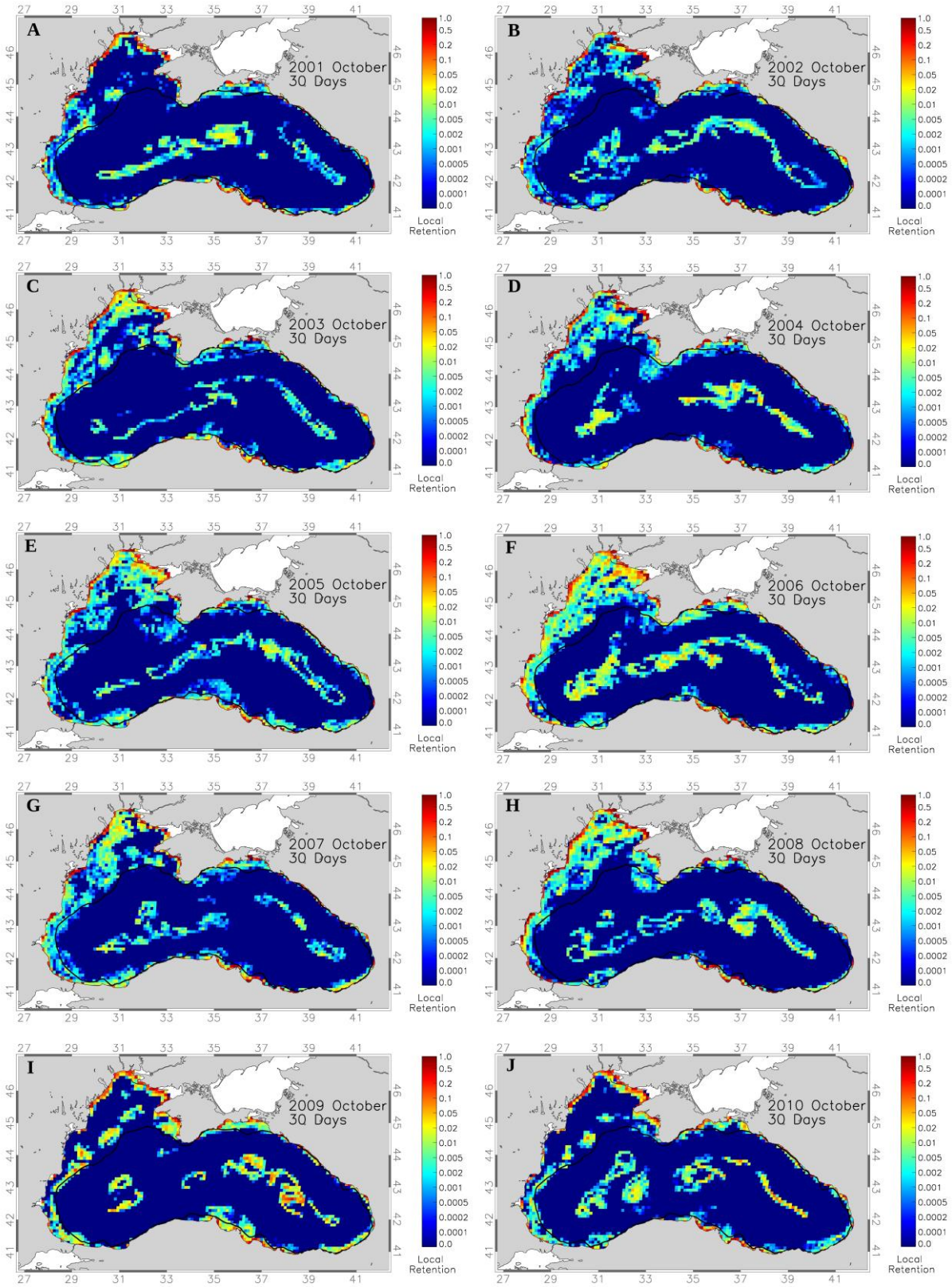

Appendix C 14: Simulation results of Local Retention (LR) using October spawning times and 30 day Pelagic Larval Duration (PLD) for A-J: 2001-2010.

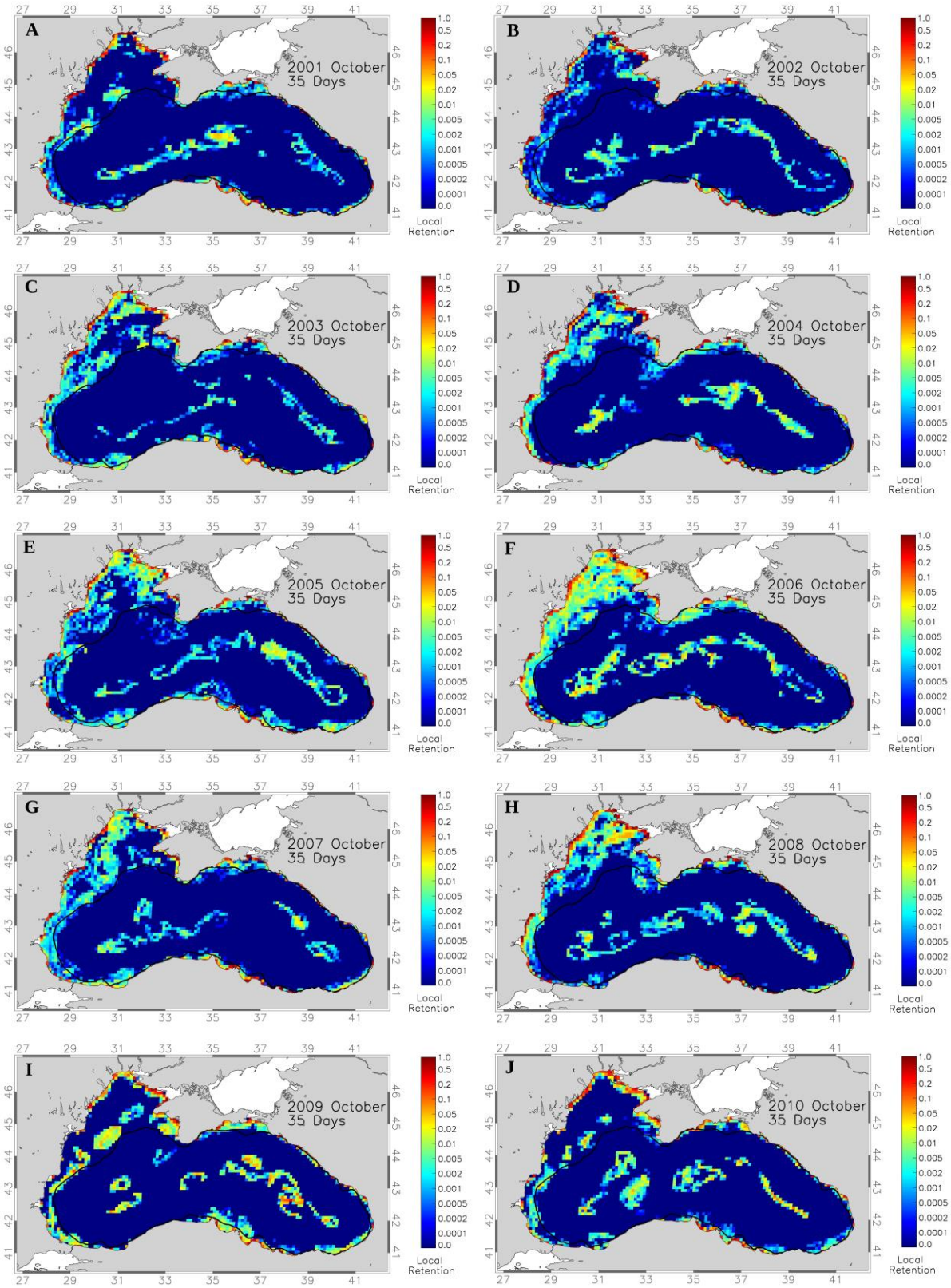

Appendix C 15: Simulation results of Local Retention (LR) using October spawning times and 35 day Pelagic Larval Duration (PLD) for A-J: 2001-2010.

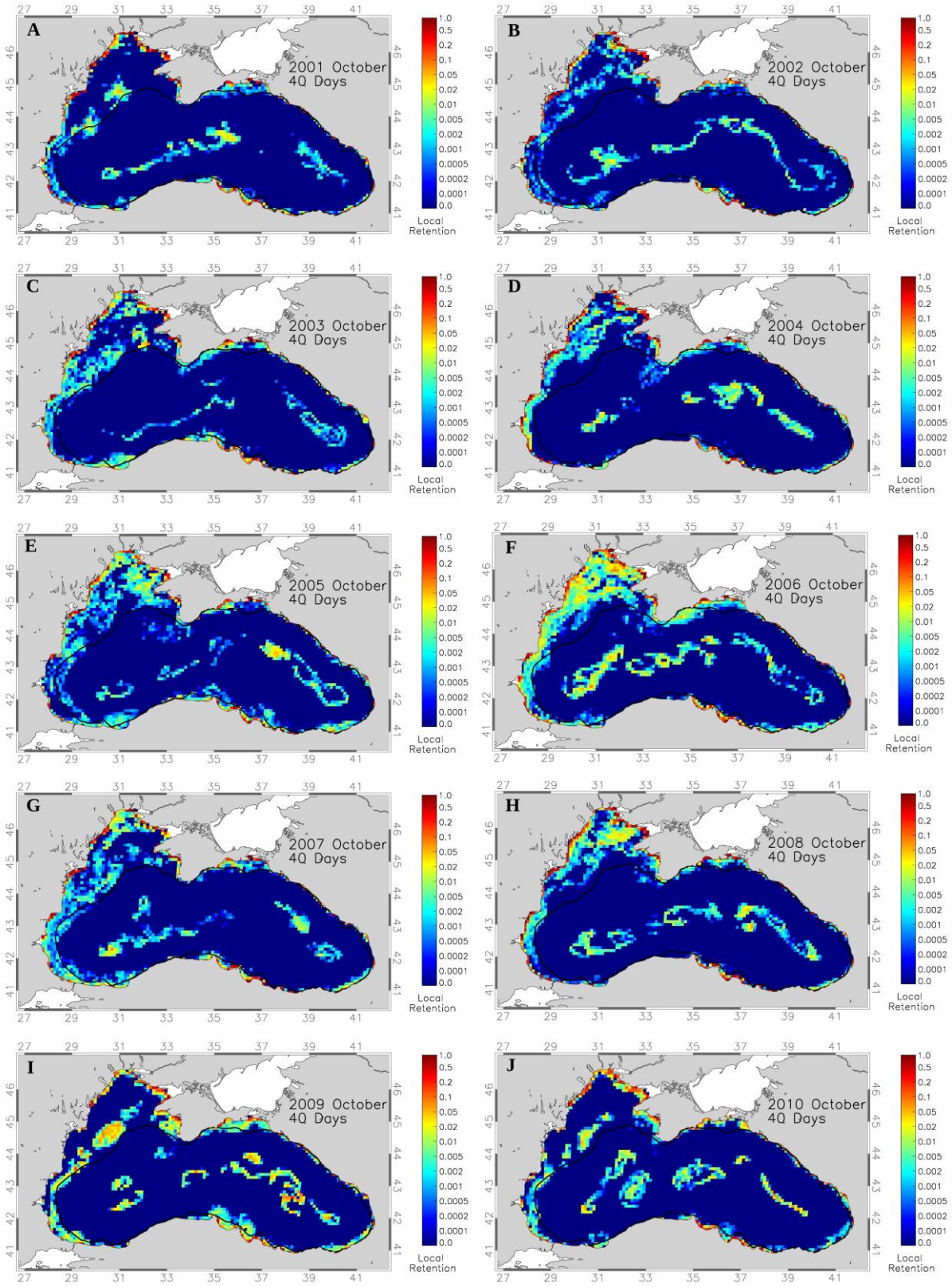

Appendix C 16: Simulation results of Local Retention (LR) using October spawning times and 40 day Pelagic Larval Duration (PLD) for A-J: 2001-2010.

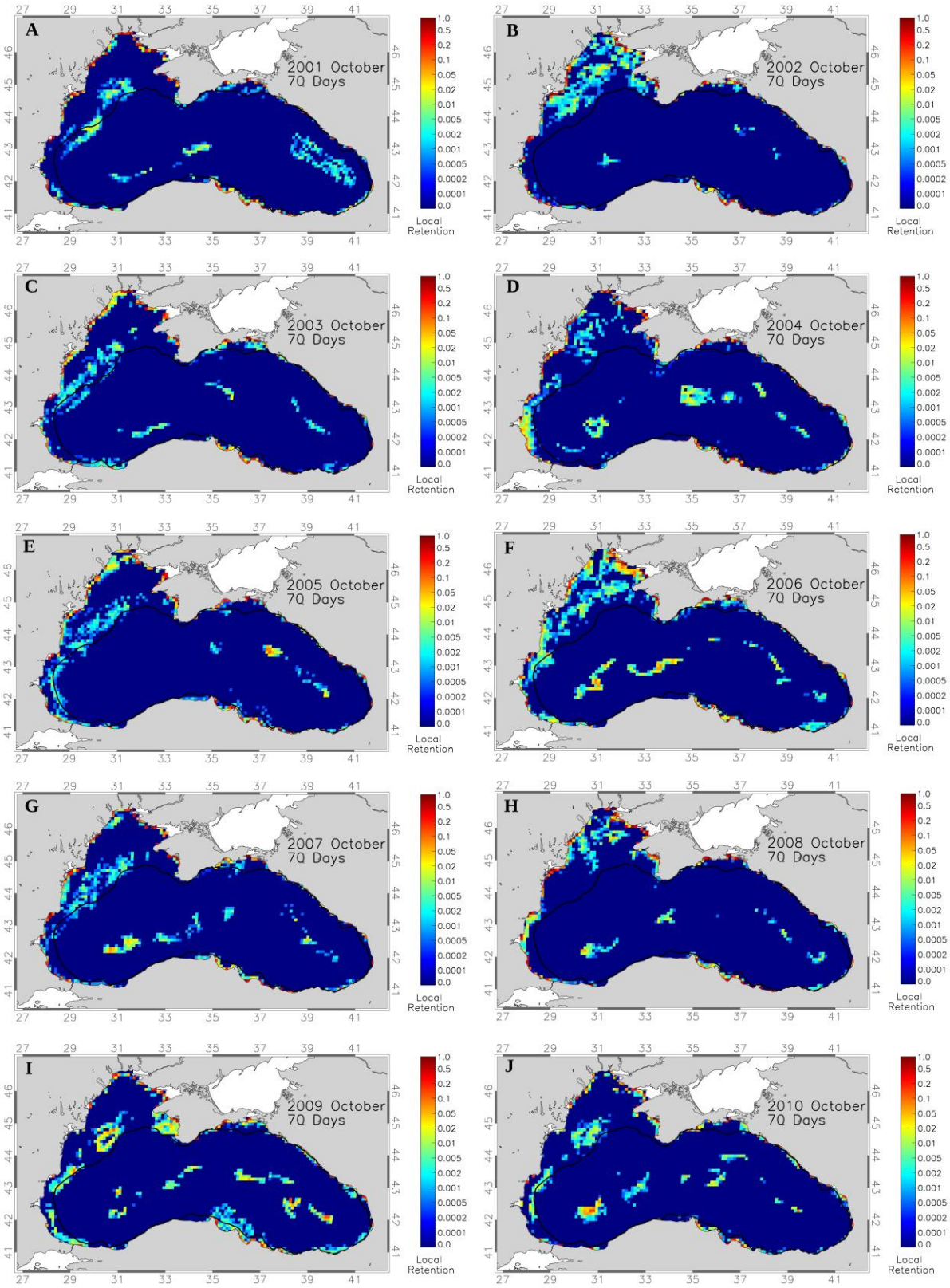

Appendix C 17: Simulation results of Local Retention (LR) using October spawning times and 70 day Pelagic Larval Duration (PLD) for A-J: 2001-2010.

Section D: Self Recruitment

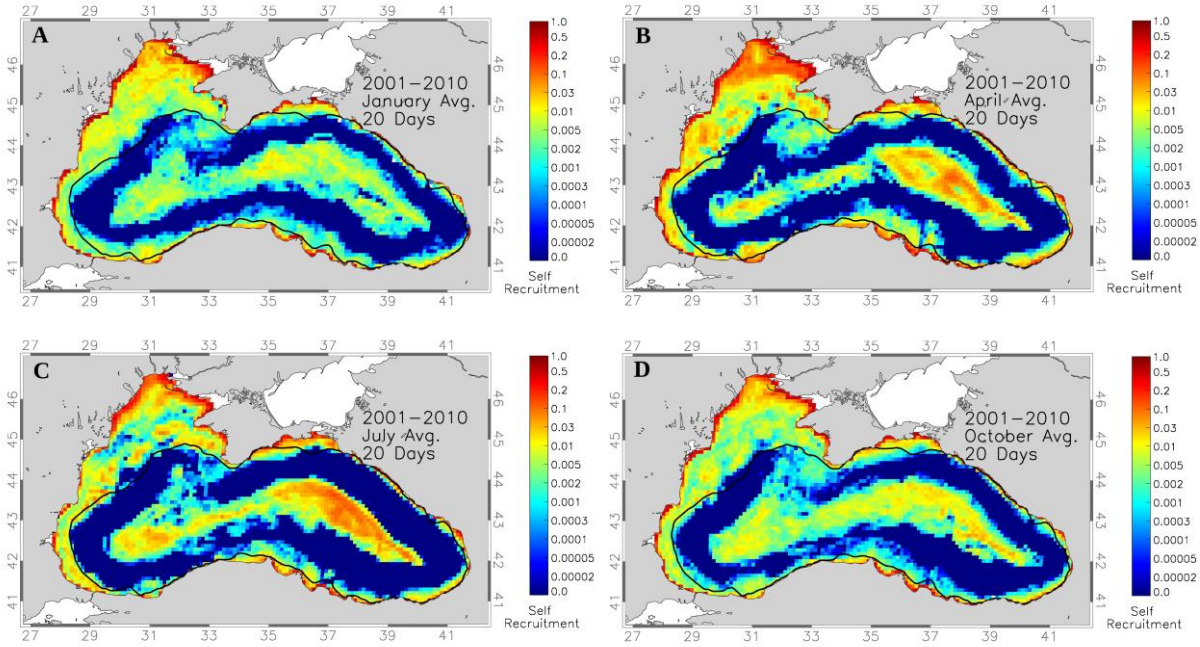

Appendix D 1: Simulation results of 10 years (2001-2010) averaged at 20 day Pelagic Larval Duration (PLD) to calculate the Local Retention (LR) for all seasonal averages. A: January average, B: April average, C: July average and D: October average.

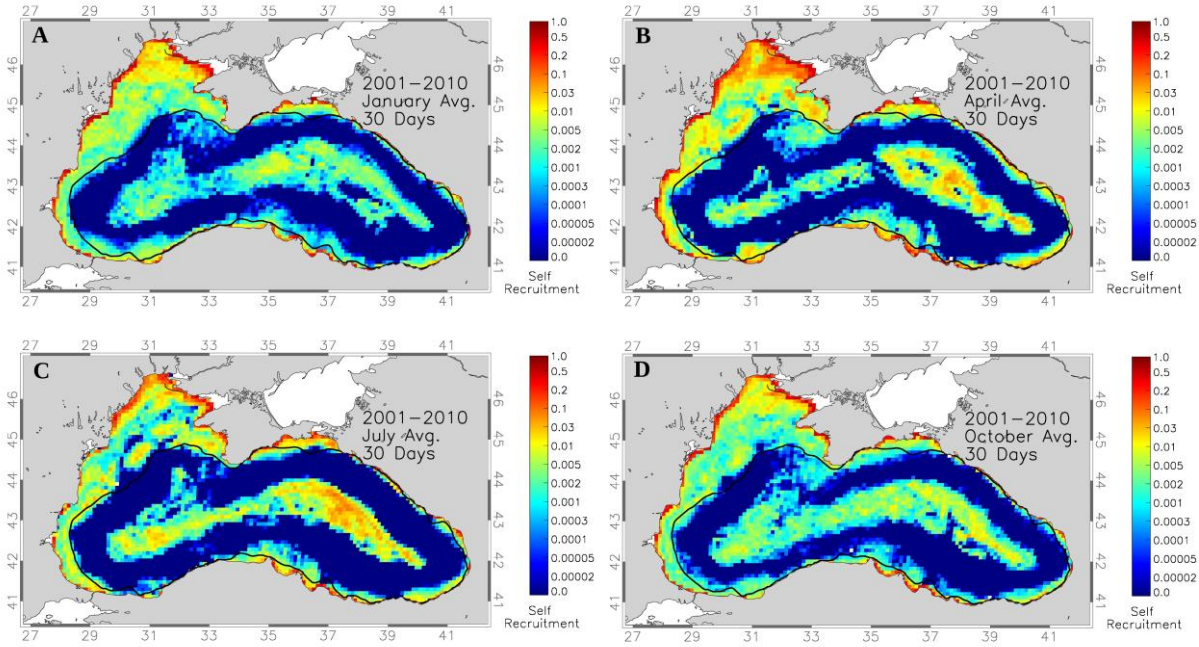

Appendix D 2: Simulation results of 10 years (2001-2010) averaged at 30 day Pelagic Larval Duration (PLD) to calculate the Local Retention (LR) for all seasonal averages. A: January average, B: April average, C: July average and D: October average.

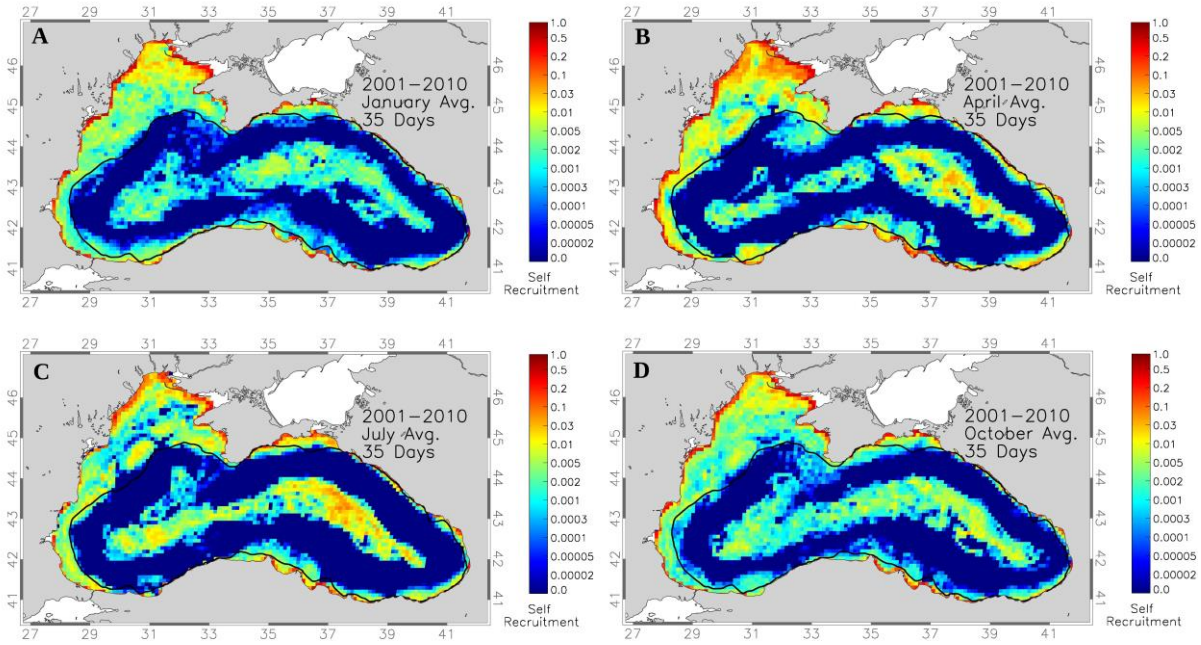

Appendix D 3: Simulation results of 10 years (2001-2010) averaged at 35 day Pelagic Larval Duration (PLD) to calculate the Local Retention (LR) for all seasonal averages. A: January average, B: April average, C: July average and D: October average.

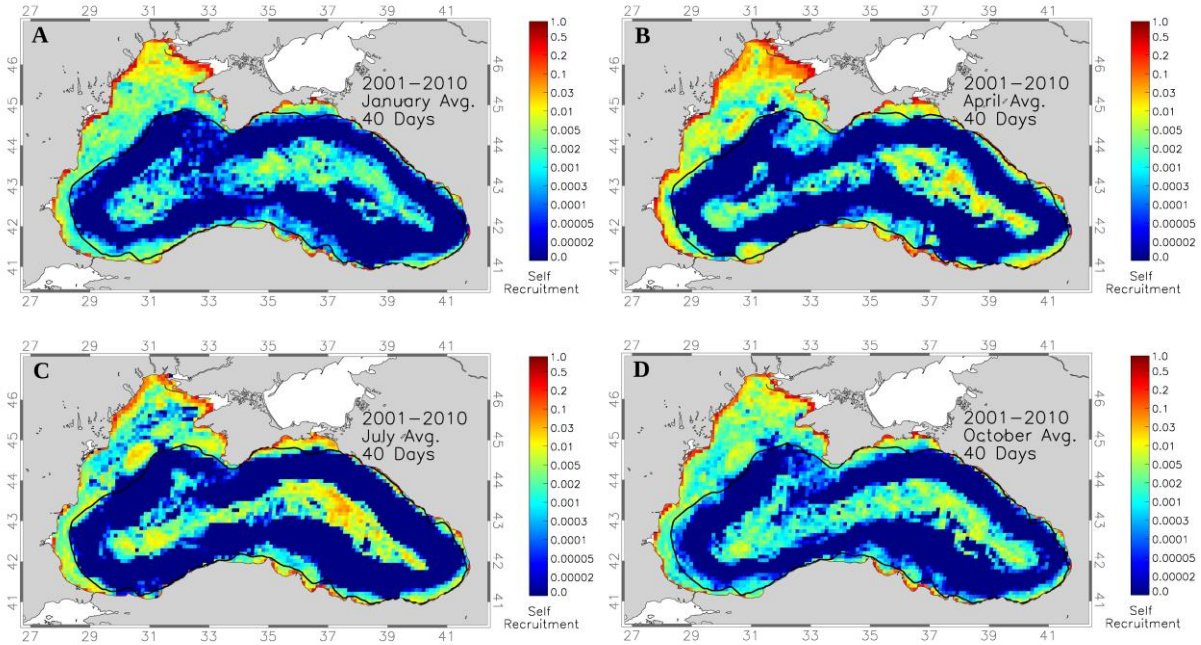

Appendix D 4: Simulation results of 10 years (2001-2010) averaged at 40 day Pelagic Larval Duration (PLD) to calculate the Local Retention (LR) for all seasonal averages. A: January average, B: April average, C: July average and D: October average.

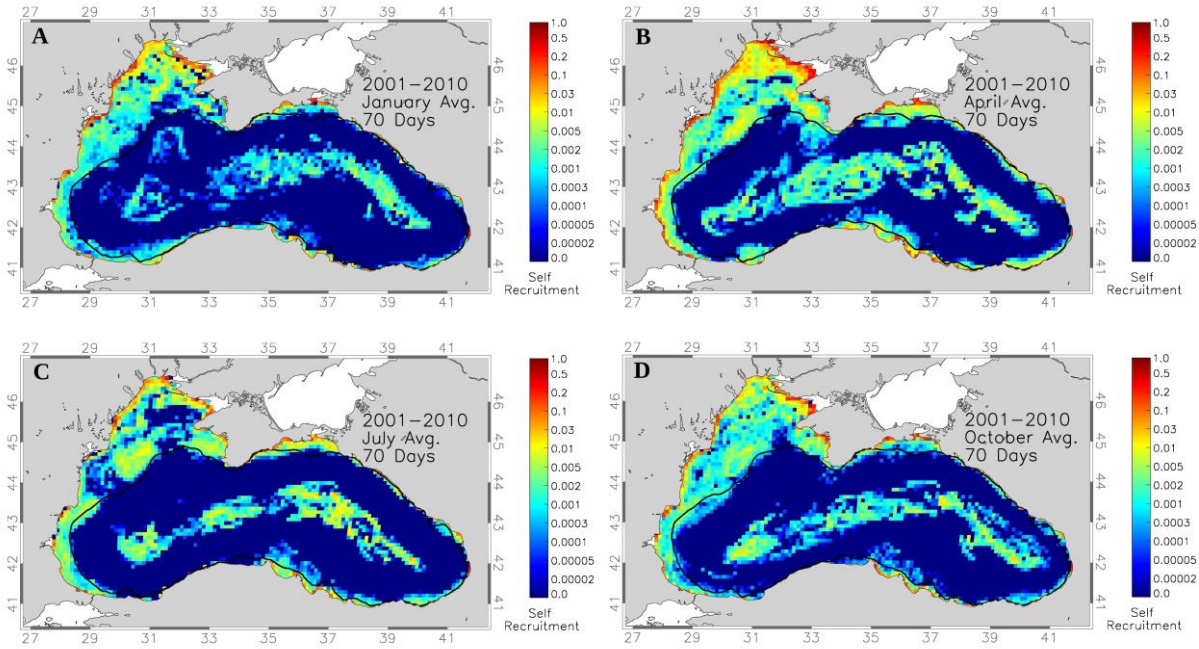

Appendix D 5: Simulation results of 10 years (2001-2010) averaged at 70 day Pelagic Larval Duration (PLD) to calculate the Local Retention (LR) for all seasonal averages. A: January average, B: April average, C: July average and D: October average.

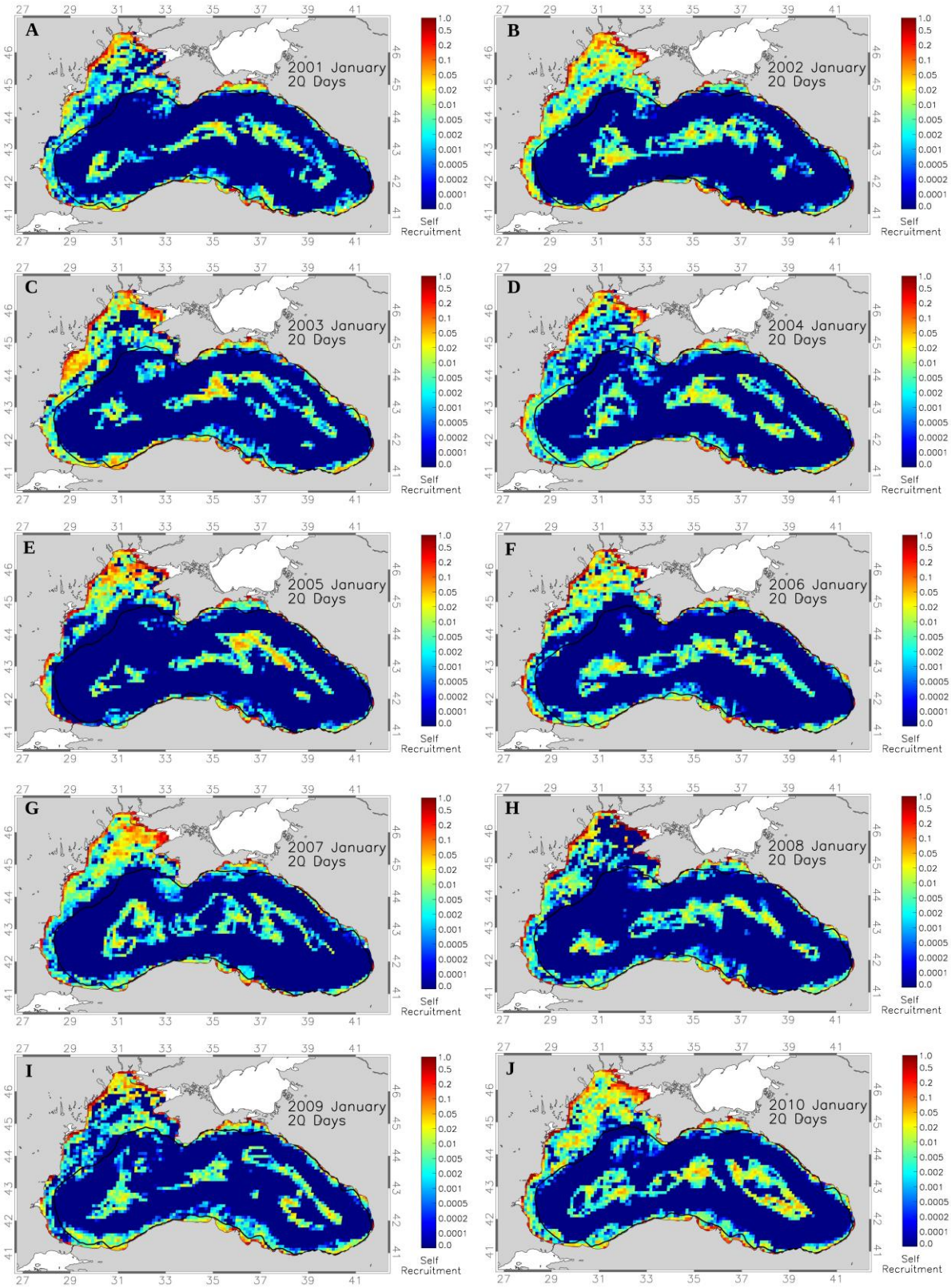

Appendix D 6: Simulation results of Self Recruitment (SR) using January spawning times and 20 day Pelagic Larval Duration (PLD) for A-J: 2001-2010.

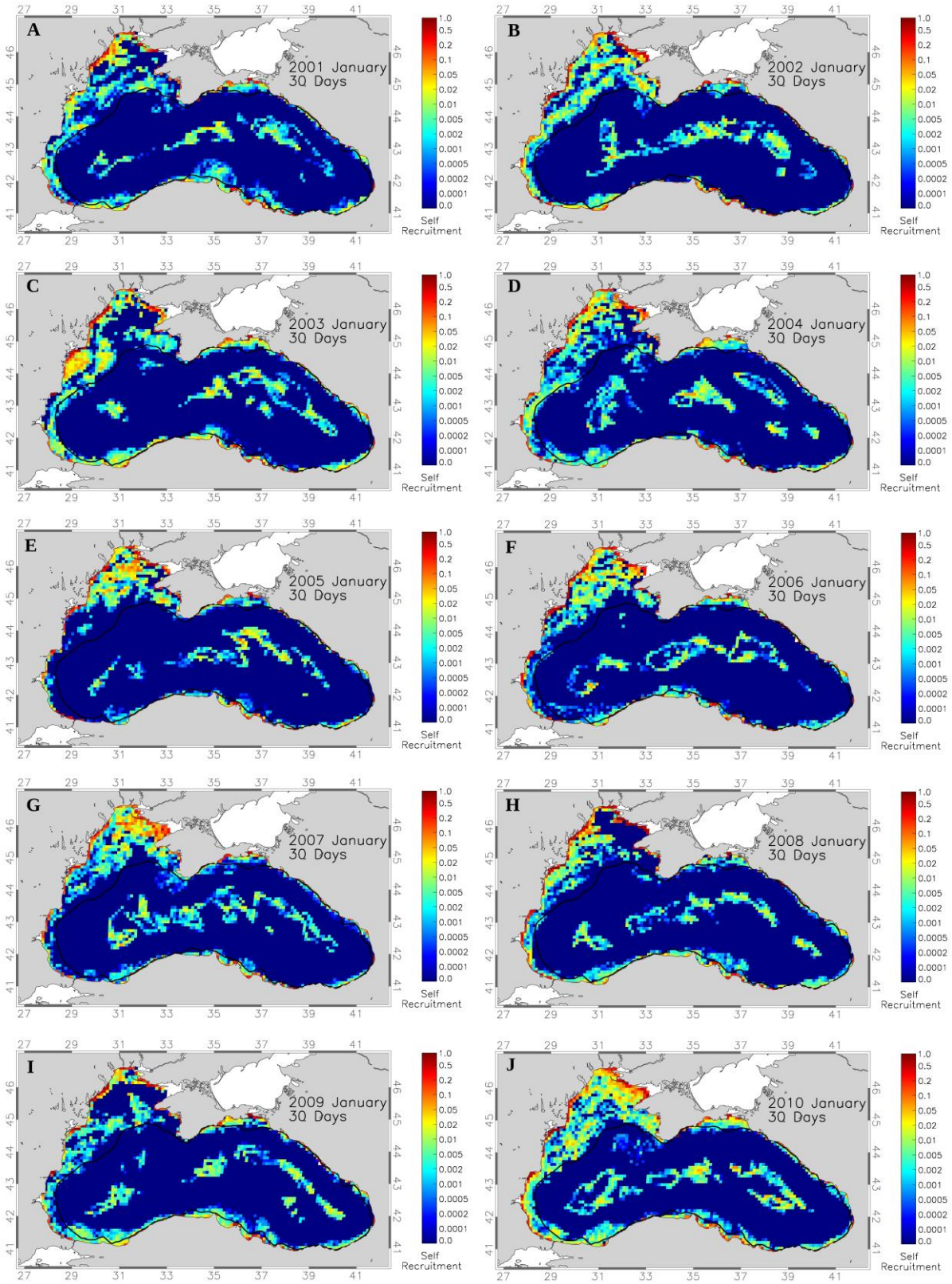

Appendix D 7: Simulation results of Self Recruitment (SR) using January spawning times and 30 day Pelagic Larval Duration (PLD) for A-J: 2001-2010.

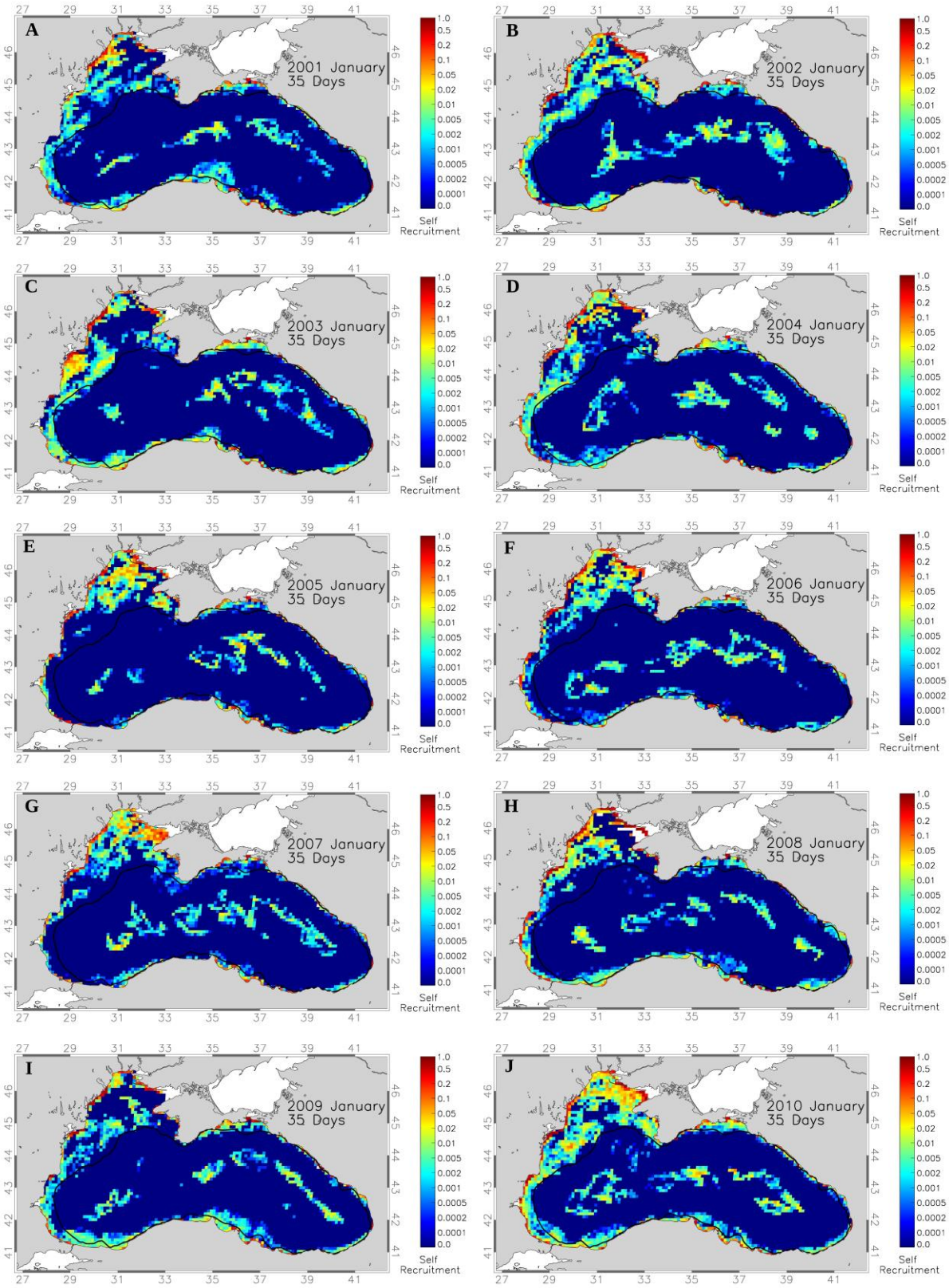

Appendix D 8: Simulation results of Self Recruitment (SR) using January spawning times and 35 day Pelagic Larval Duration (PLD) for A-J: 2001-2010.

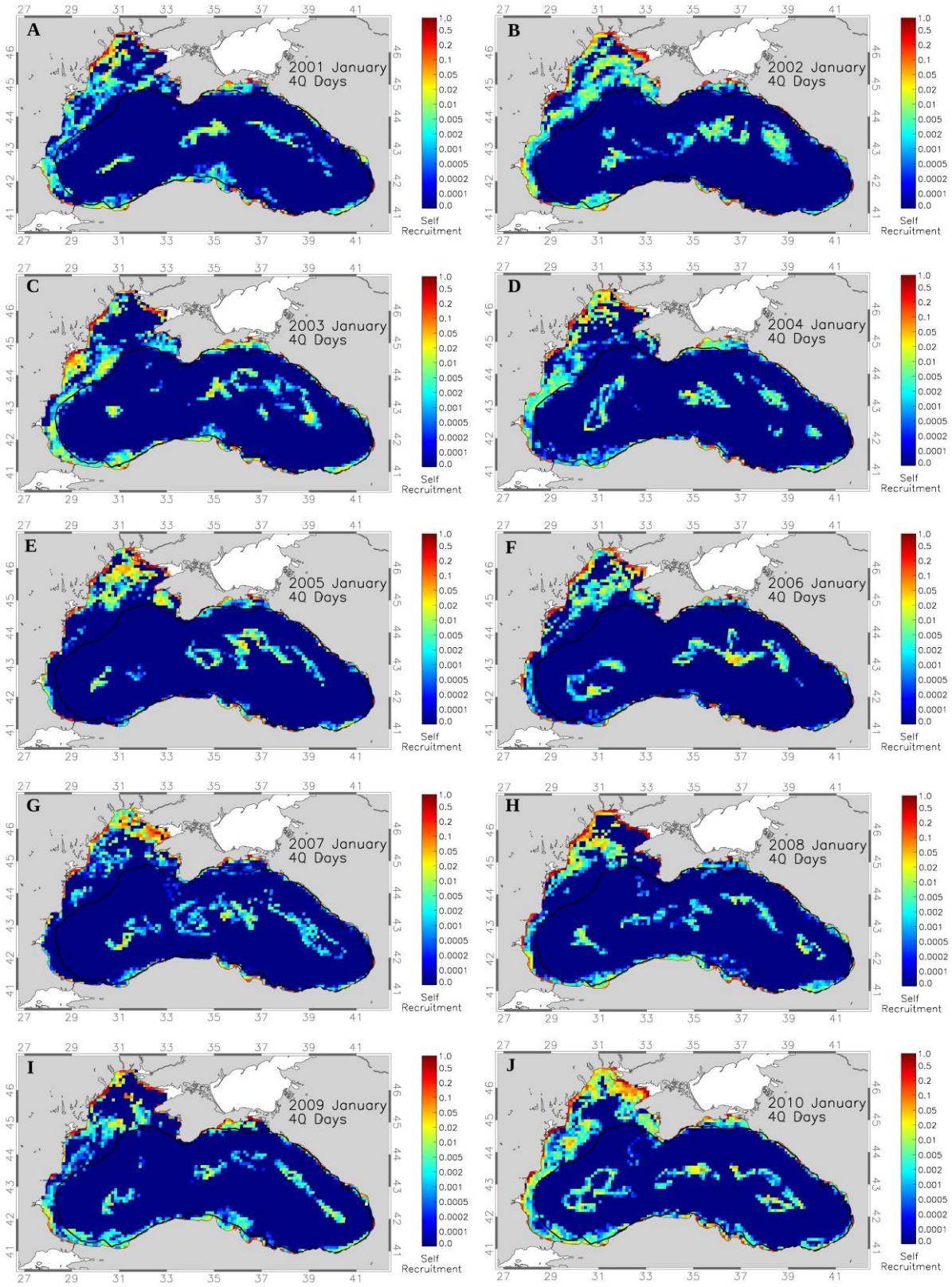

Appendix D 9: Simulation results of Self Recruitment (SR) using January spawning times and 40 day Pelagic Larval Duration (PLD) for A-J: 2001-2010.

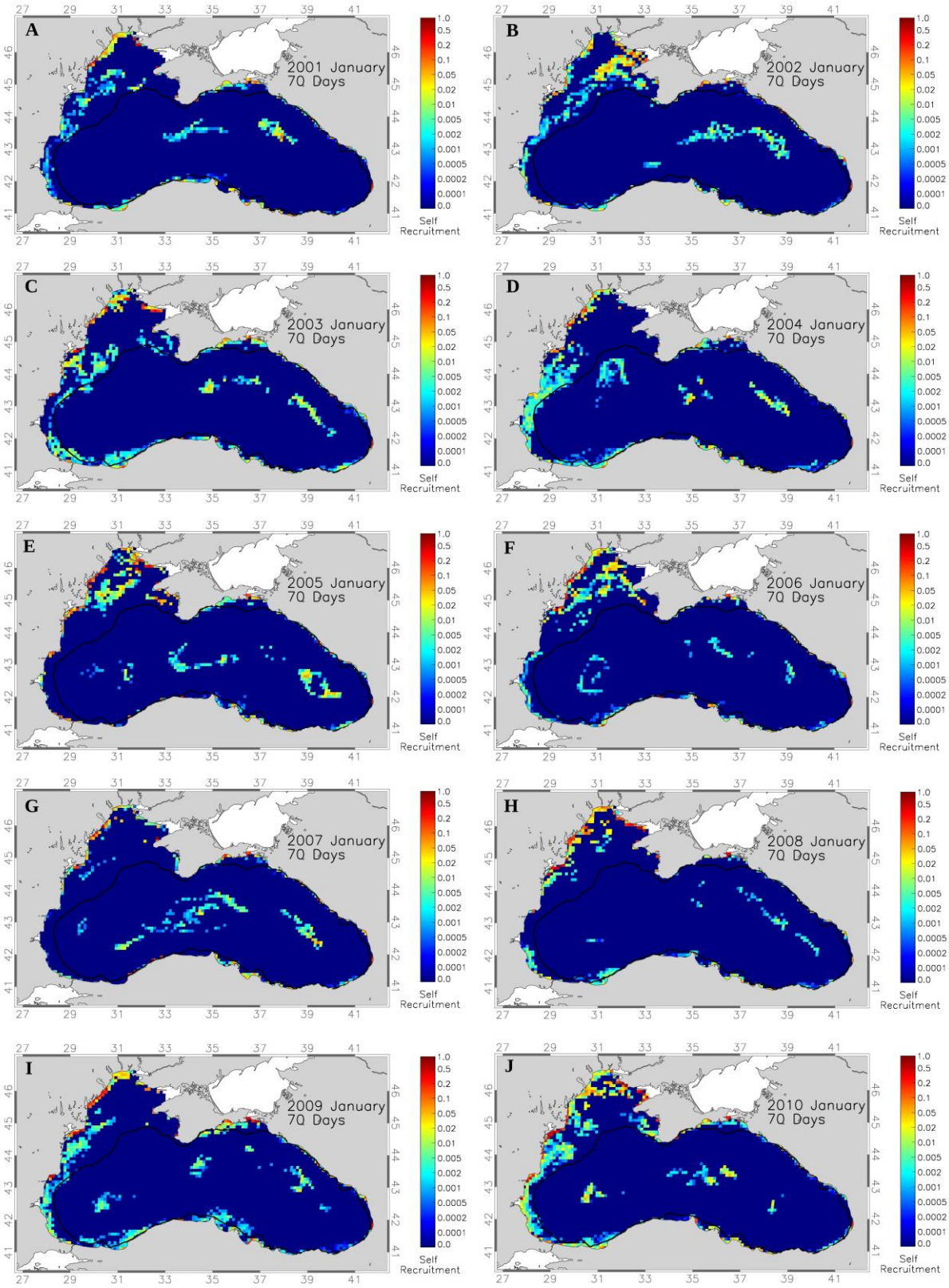

Appendix D 10: Simulation results of Self Recruitment (SR) using January spawning times and 70 day Pelagic Larval Duration (PLD) for A-J: 2001-2010.

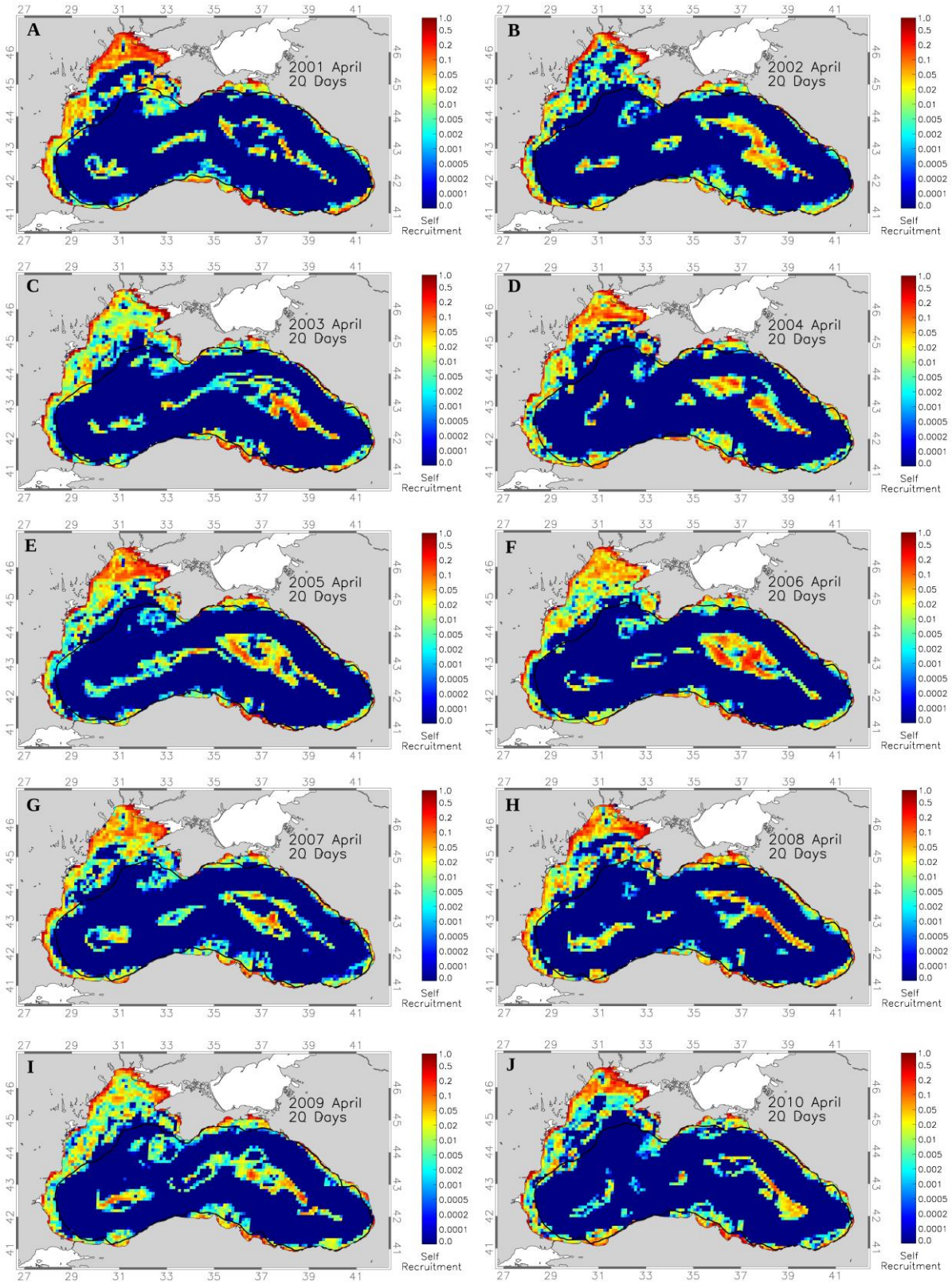

Appendix D 11: Simulation results of Self Recruitment (SR) using April spawning times and 20 day Pelagic Larval Duration (PLD) for A-J: 2001-2010.

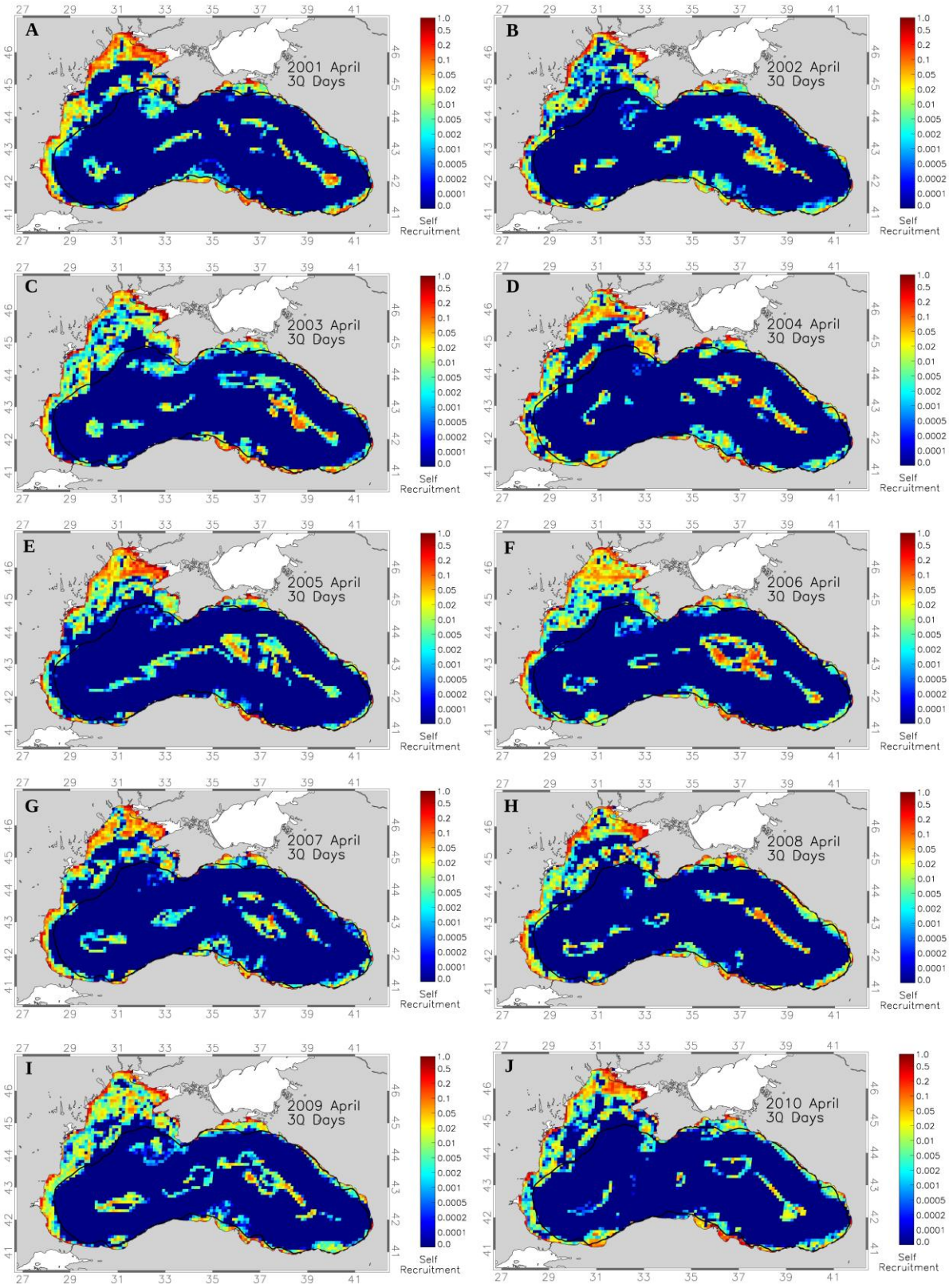

Appendix D 12: Simulation results of Self Recruitment (SR) using April spawning times and 30 day Pelagic Larval Duration (PLD) for A-J: 2001-2010.

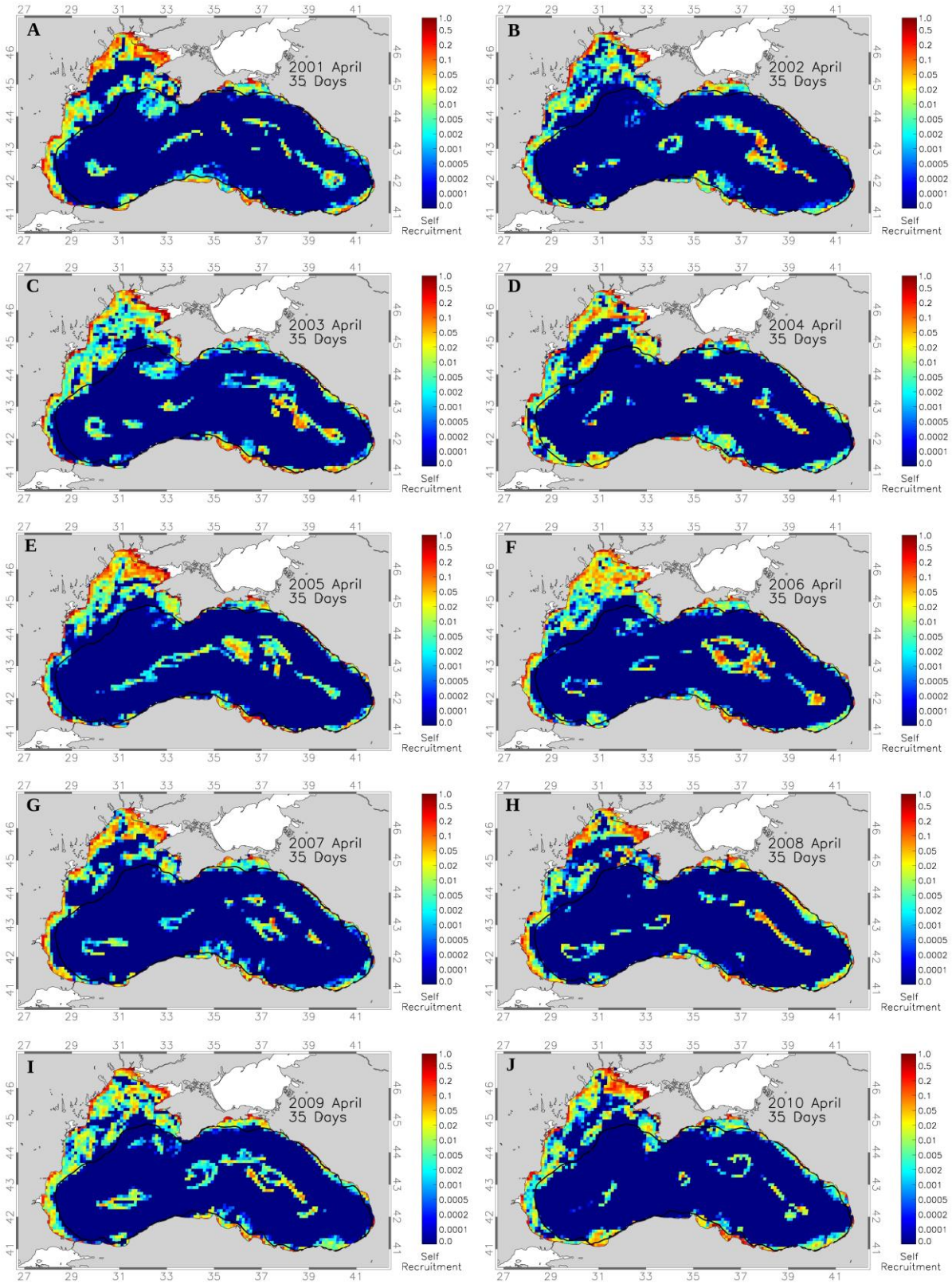

Appendix D 13: Simulation results of Self Recruitment (SR) using April spawning times and 35 day Pelagic Larval Duration (PLD) for A-J: 2001-2010.

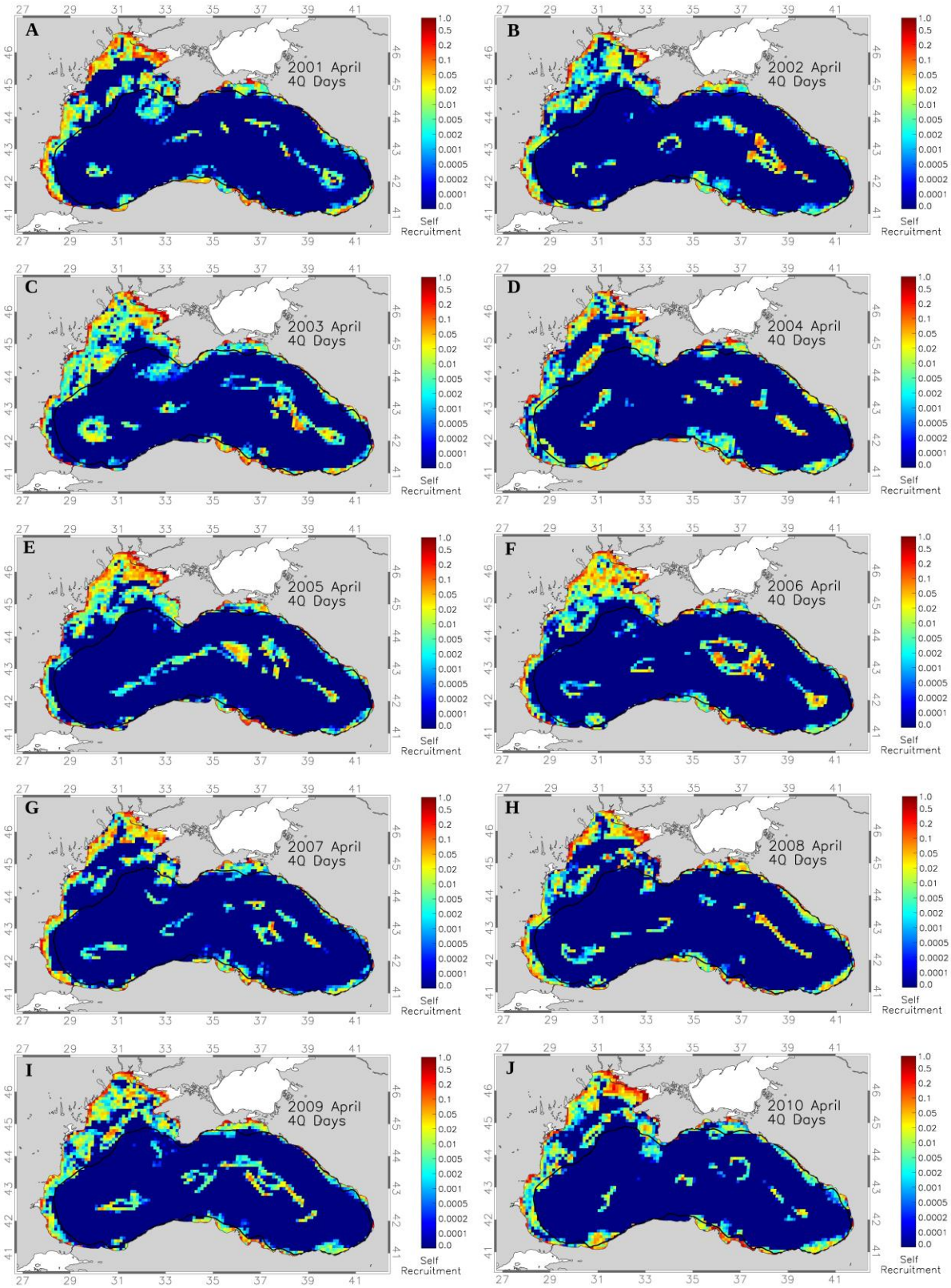

Appendix D 14: Simulation results of Self Recruitment (SR) using April spawning times and 40 day Pelagic Larval Duration (PLD) for A-J: 2001-2010.

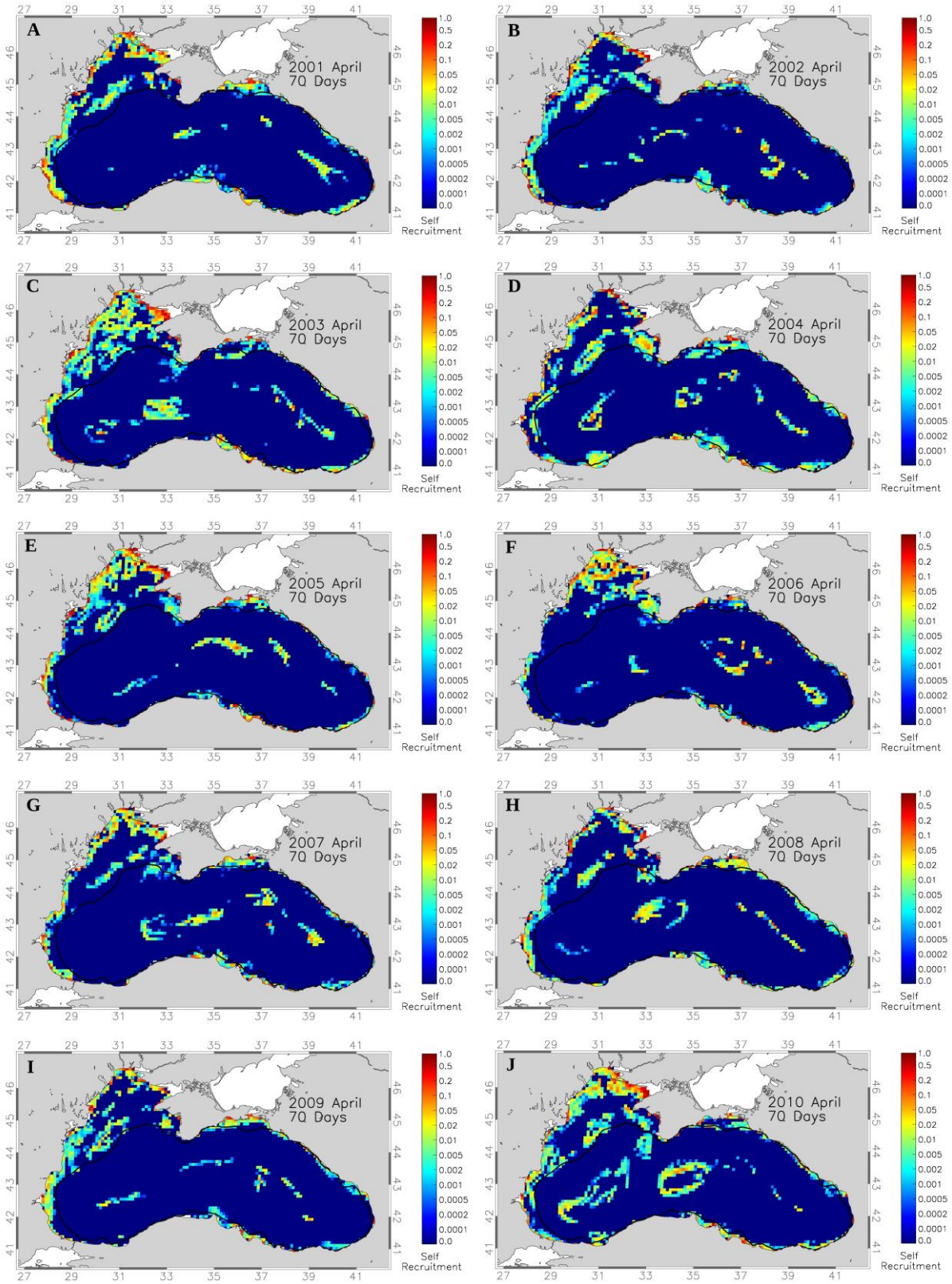

Appendix D 15: Simulation results of Self Recruitment (SR) using April spawning times and 70 day Pelagic Larval Duration (PLD) for A-J: 2001-2010.

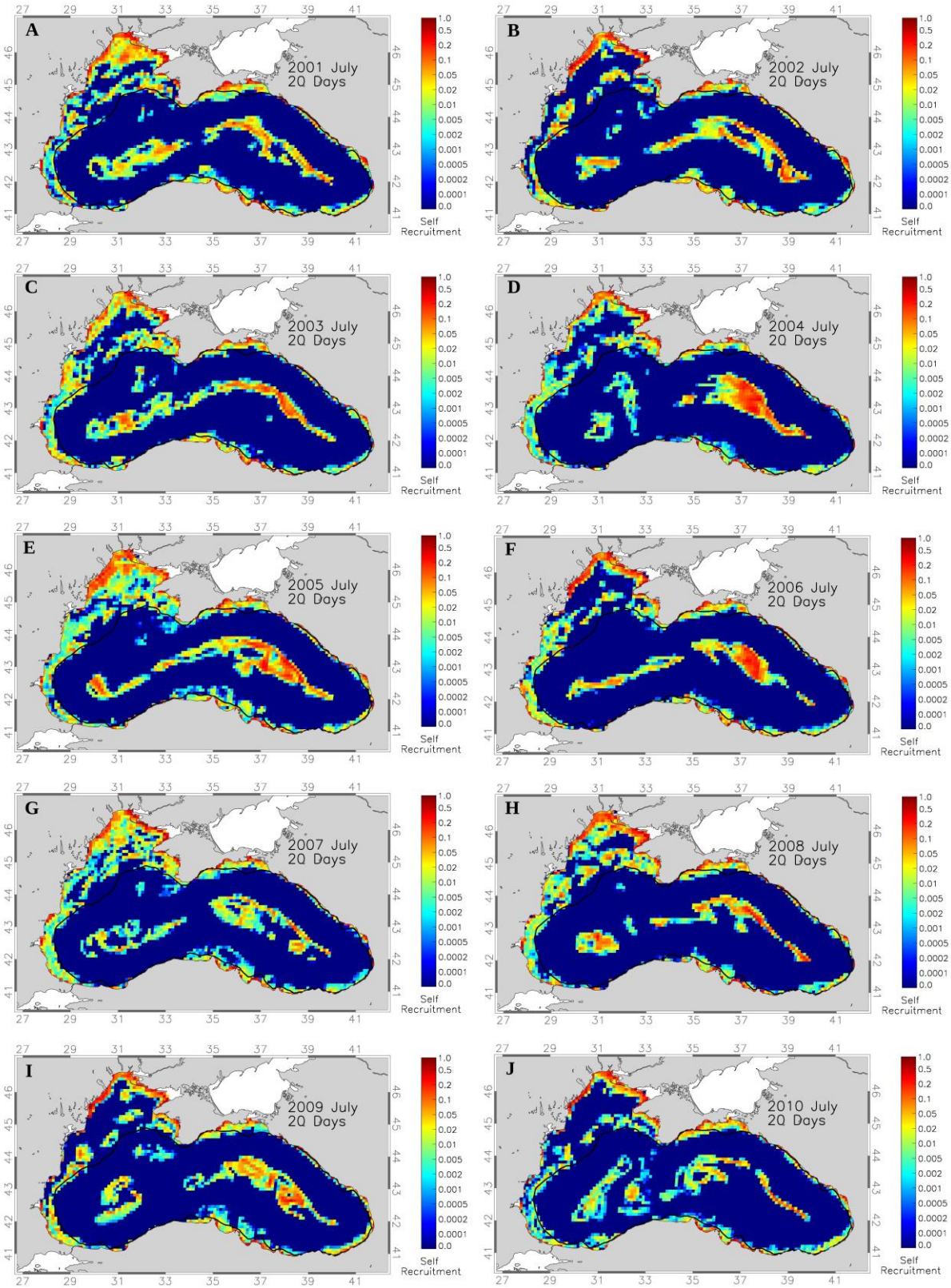

Appendix D 16: Simulation results of Self Recruitment (SR) using July spawning times and 20 day Pelagic Larval Duration (PLD) for A-J: 2001-2010.

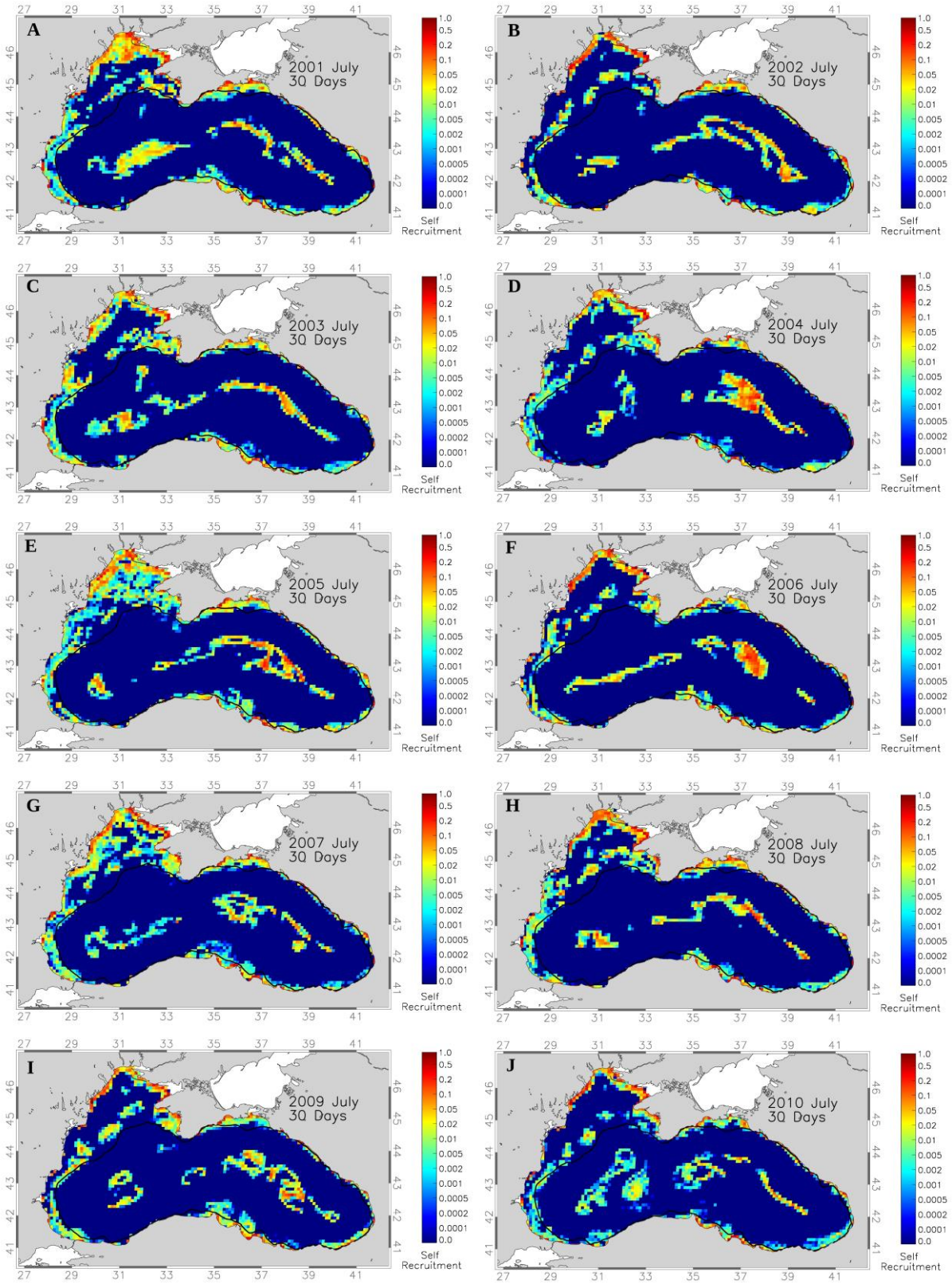

Appendix D 17: Simulation results of Self Recruitment (SR) using July spawning times and 30 day Pelagic Larval Duration (PLD) for A-J: 2001-2010.

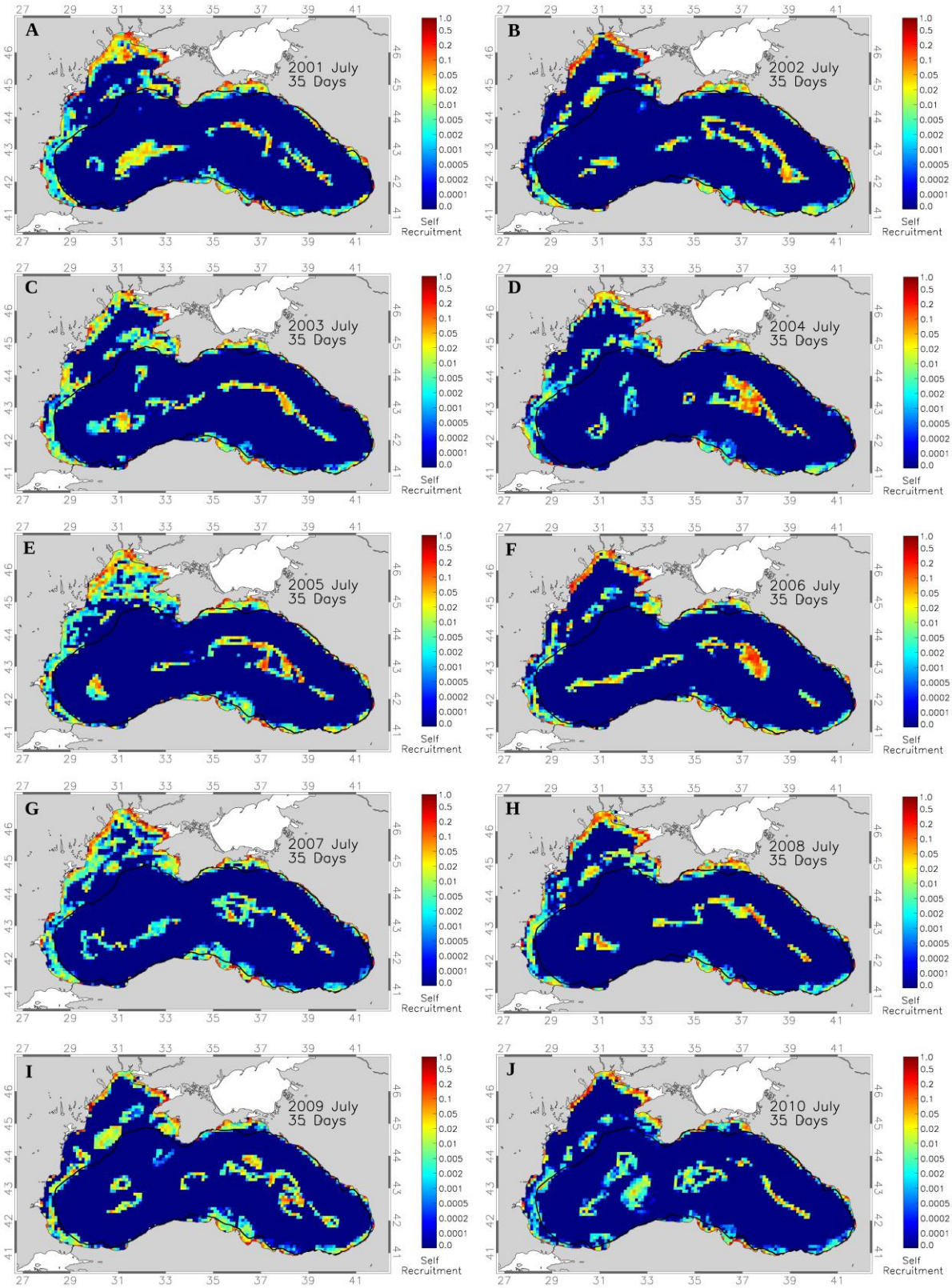

Appendix D 18: Simulation results of Self Recruitment (SR) using July spawning times and 35 day Pelagic Larval Duration (PLD) for A-J: 2001-2010.

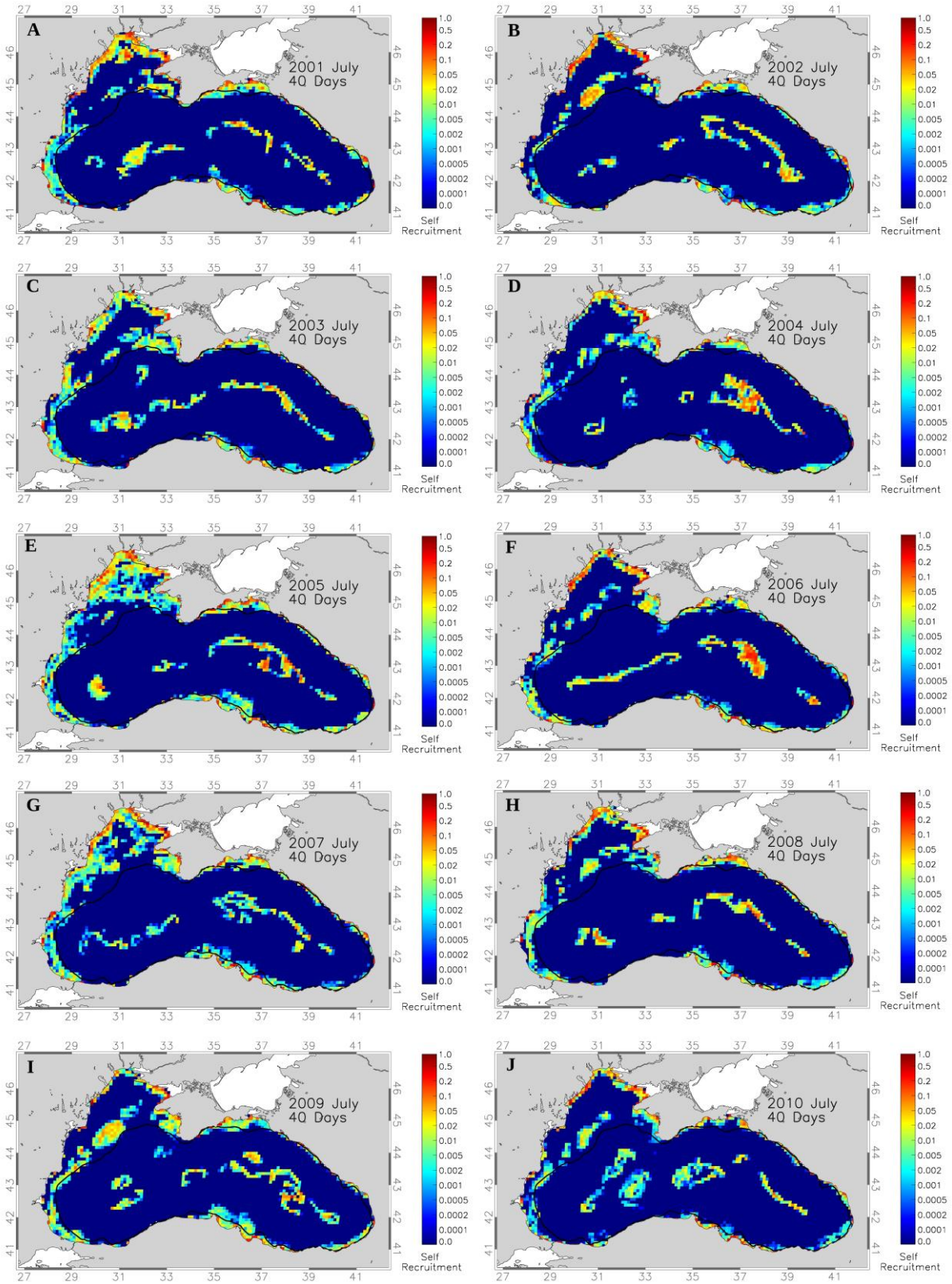

Appendix D 19: Simulation results of Self Recruitment (SR) using July spawning times and 40 day Pelagic Larval Duration (PLD) for A-J: 2001-2010.

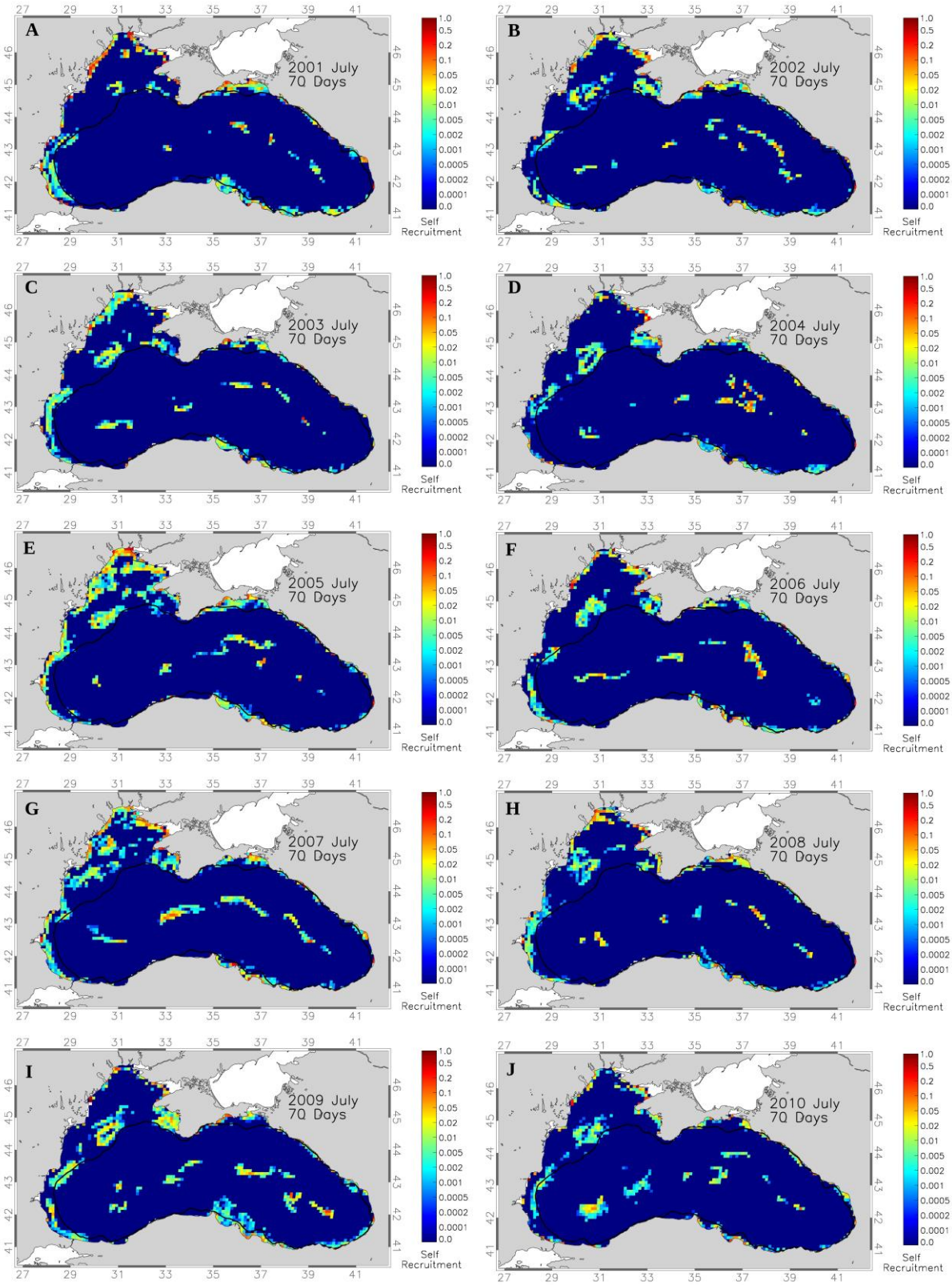

Appendix D 20: Simulation results of Self Recruitment (SR) using July spawning times and 70 day Pelagic Larval Duration (PLD) for A-J: 2001-2010.

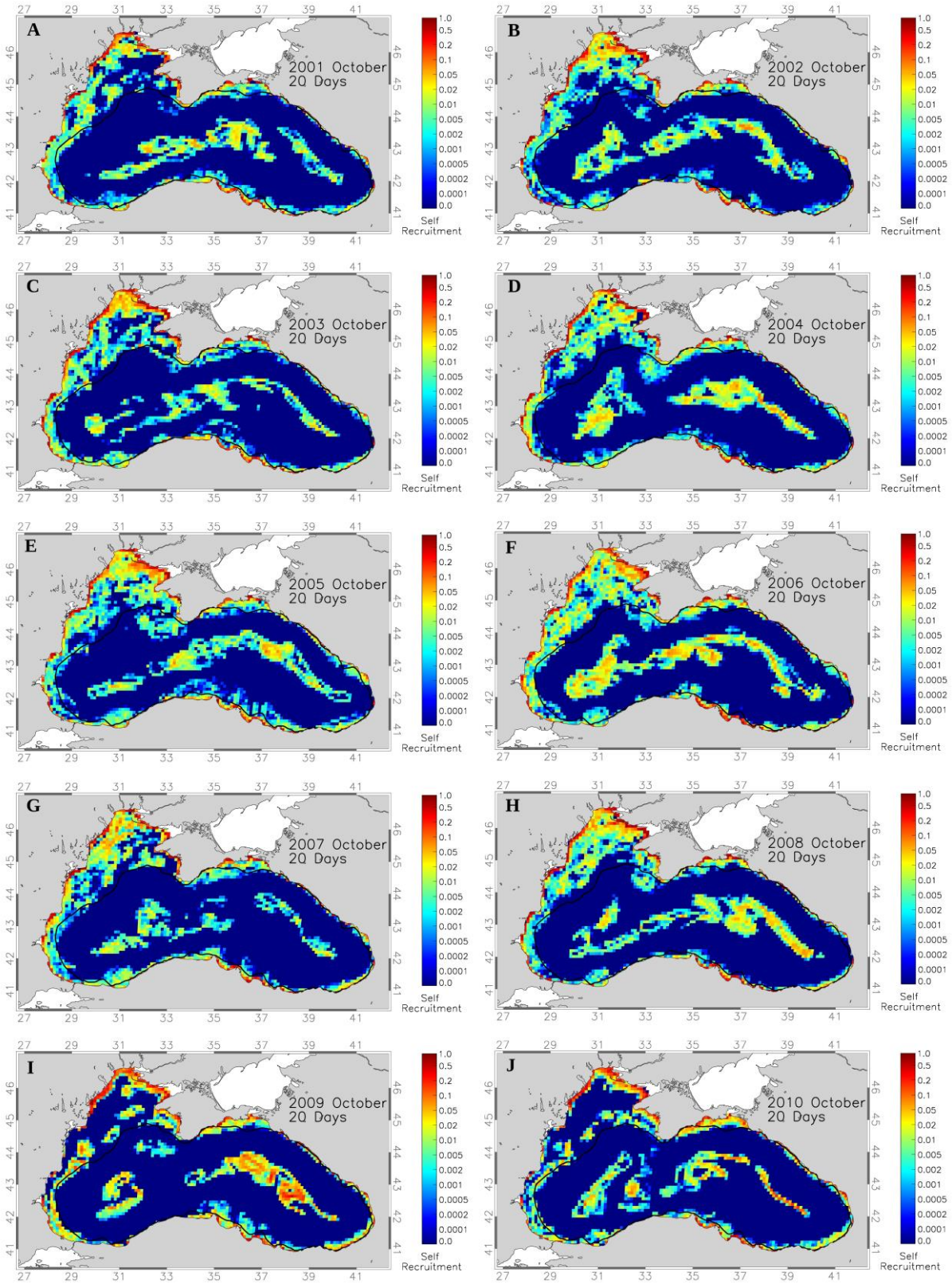

Appendix D 21: Simulation results of Self Recruitment (SR) using October spawning times and 20 day Pelagic Larval Duration (PLD) for A-J: 2001-2010.

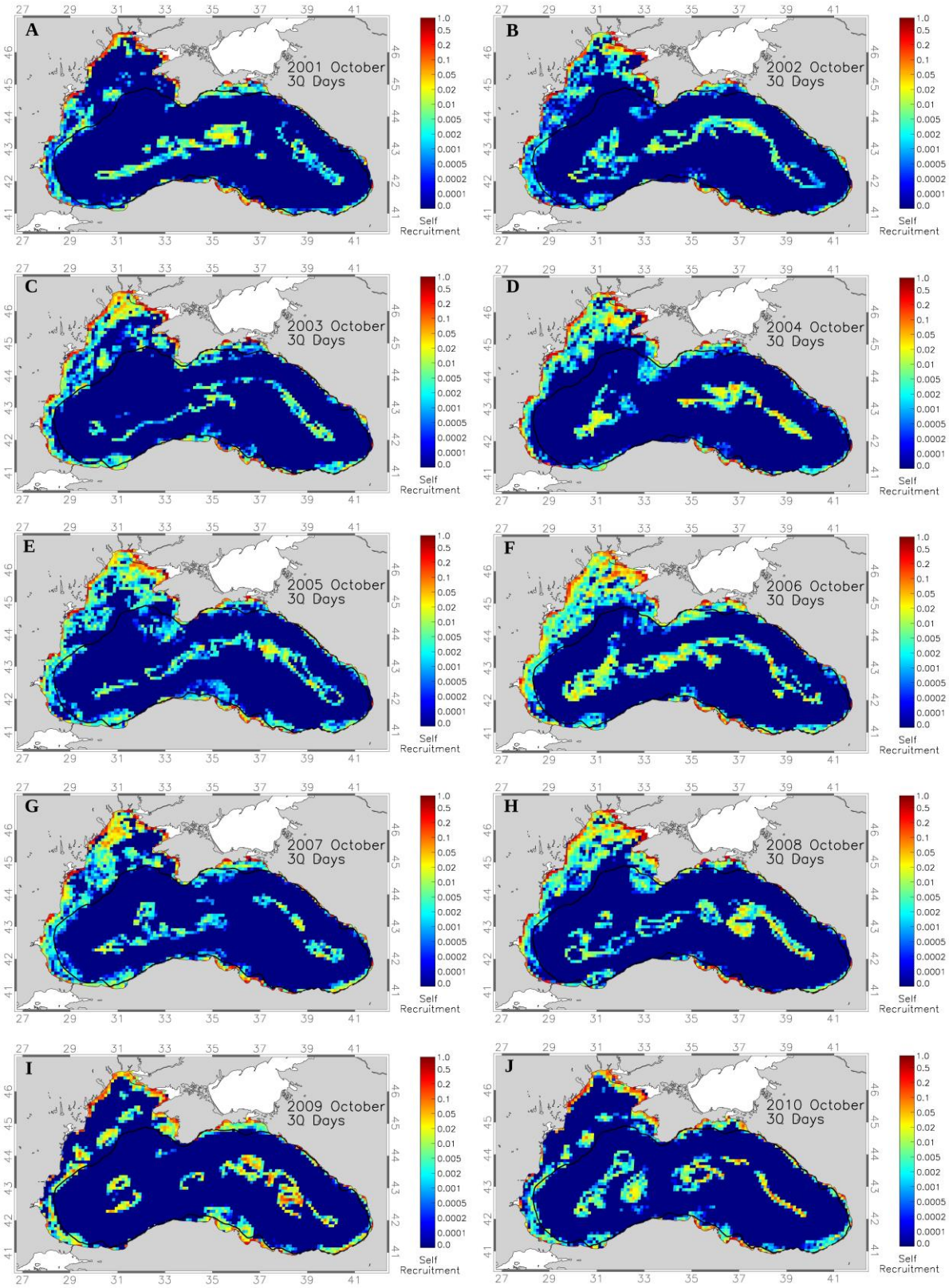

Appendix D 22: Simulation results of Self Recruitment (SR) using October spawning times and 30 day Pelagic Larval Duration (PLD) for A-J: 2001-2010.

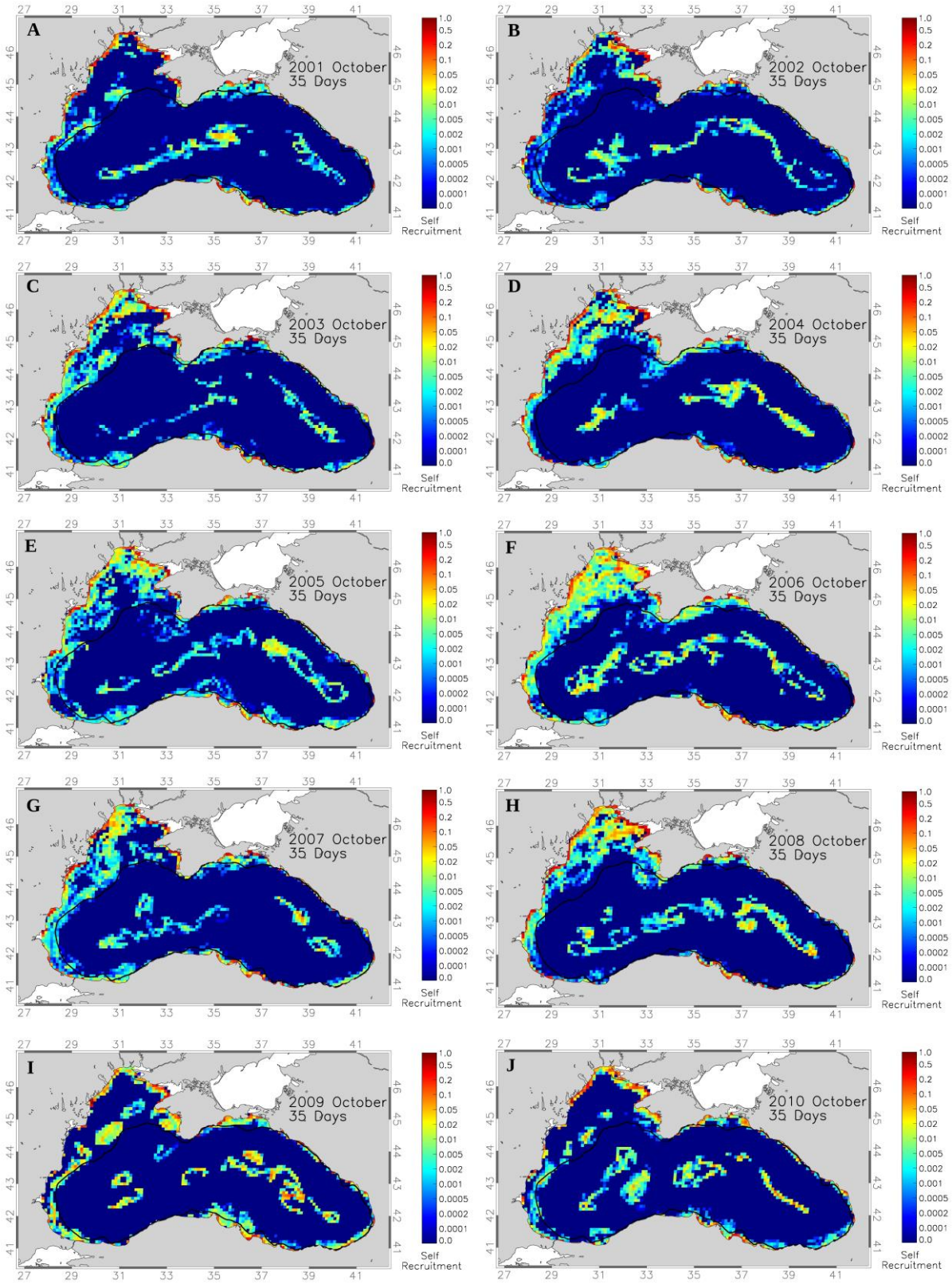

Appendix D 23: Simulation results of Self Recruitment (SR) using October spawning times and 35 day Pelagic Larval Duration (PLD) for A-J: 2001-2010.

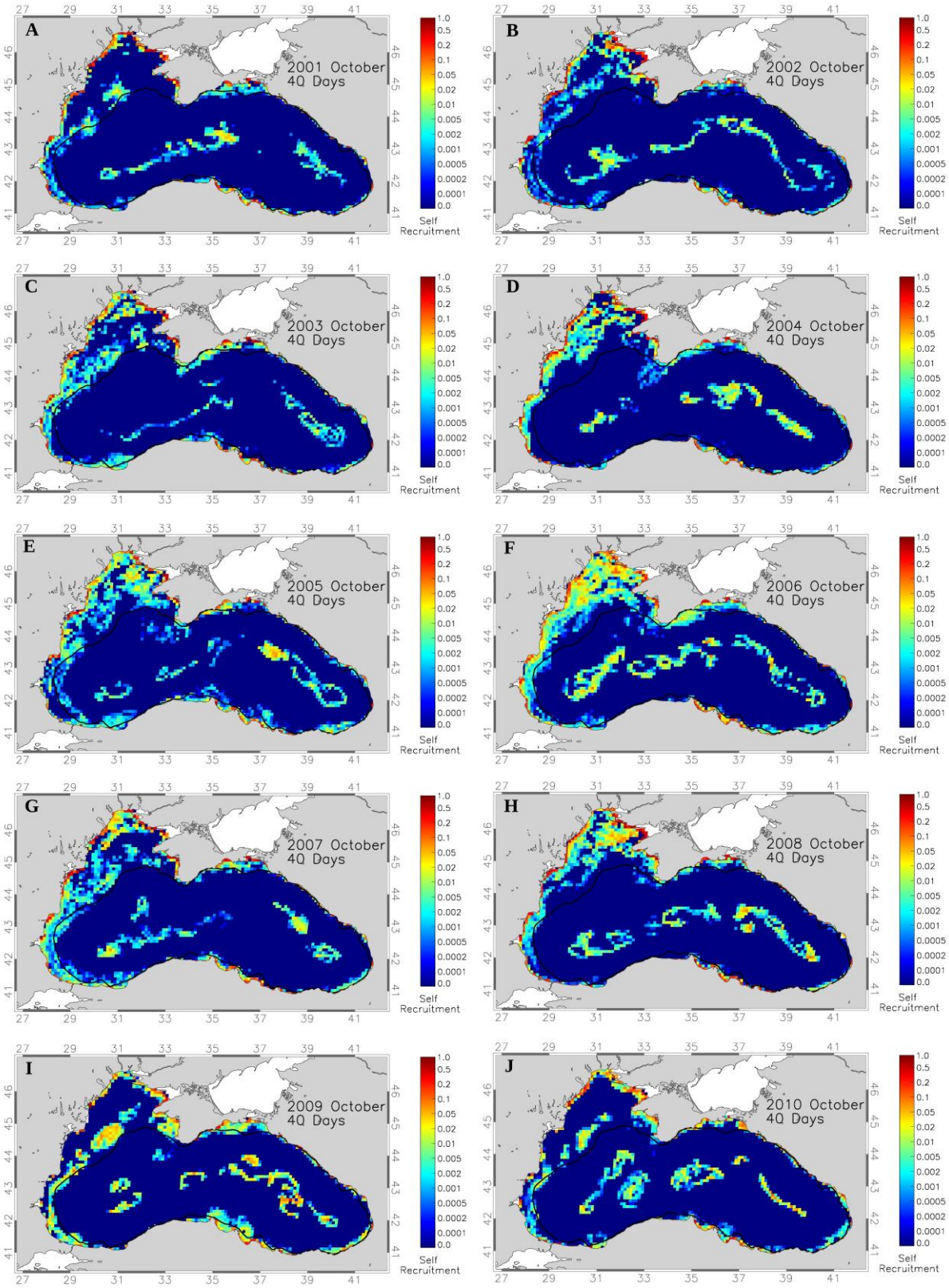

Appendix D 24: Simulation results of Self Recruitment (SR) using October spawning times and 40 day Pelagic Larval Duration (PLD) for A-J: 2001-2010.

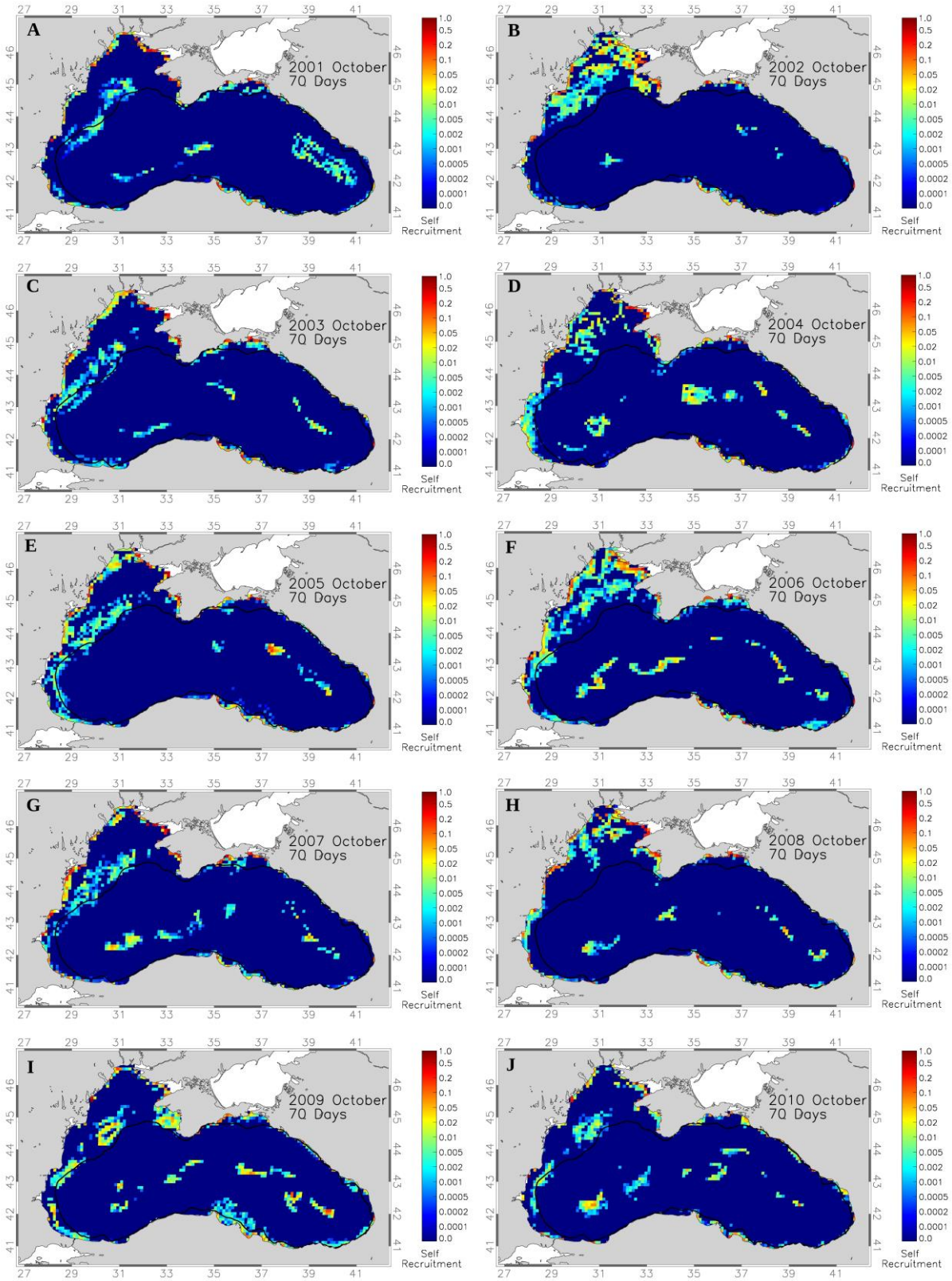

Appendix D 25: Simulation results of Self Recruitment (SR) using October spawning times and 70 day Pelagic Larval Duration (PLD) for A-J: 2001-2010.